2012

Mapping Deep-Sea Features in UK Waters For Use in Marine Protected Area Network Design

Davies, Jaime Selina

MAPPING DEEP-SEA FEATURES IN UK WATERS FOR USE IN MARINE PROTECTED AREA NETWORK DESIGN

JAIME SELINA DAVIES, B.Sc. (Hons.), MRes

A thesis submitted to the University of Plymouth

in partial fulfilment for the degree of

DOCTOR OF PHILOSOPHY

Faculty of Marine Science & Technology

School of Marine Science and Engineering

In collaboration with

British Geological Survey

National Oceanography Centre

Scottish Association for Marine Science

June 2012

AUTHOR'S DECLARATION

At no time during the registration for the degree of Doctor of Philosophy has the author been registered for any other University award without prior agreement of the Graduate Committee. This study was financed by the Joint Nature Conservation Committee (JNCC) and was carried out in collaboration with the British Geological Survey, the National Oceanography Centre and the Scottish Association for Marine Science. The work described in this thesis was conducted by the author, under the supervision of Dr. K. Howell, Prof. J. Spicer, H. Stewart, C. Jacobs and Dr. B. Narayanaswamy.

The data used within the thesis was collected by the author as part of collaborative research cruises funded by the JNCC. The processing and interpretation of the biological data within the thesis is completely the work of the author. Geological interpretation and production of substratum and geomorphology maps, from the two cruises, used in the thesis was undertaken by the British Geological Survey. Geological interpretation included in the thesis is taken from the cruise reports.

Relevant aspects of research training undertaken by the author include attendance on a PRIMER statistics course, ArcGIS and Fledermaus software training, and attendance on relevant video/image analysis workshops.

Conferences and workshops attended:

Oral presentations

Davies J. S., Howell K. L., Jacobs C., Narayanaswamy B. E., Stewart H. and Golding N. (2010). Mapping the benthic assemblages of Anton Dohrn Seamount. The 45th European Marine Biology Symposium. Edinburgh 2010.

Davies J. S., Howell K. L., Jacobs C., Narayanaswamy B. E., Stewart H. and Golding N. (2010). Mapping the benthic assemblages of Anton Dohrn Seamount. The 12th International Deep-sea Biology Symposium Reykjavik, Iceland 2010.

Davies J. S., Howell K. L., Stewart H., Guinan J. and Golding N. (2009). Investigating the use of geological and biological maps in designing a potential network of Marine Protected Areas for the UK's deep-sea. The 9th international marine geological and biological habitat mapping (GeoHab) symposium. Trondheim, Norway 2009.

Davies J. S, Howell H., Stewart H., Guinan J., Verling E., Golding N. (2008). Deep-water habitat mapping. Marine Biological Association Postgraduate conference, Aberystwyth 2008.

Poster presentations

Davies J., Howell K., Stewart H., Guinan J., Verling E. (2008). Biological communities of the South West Approaches (UK). The 8th international marine geological and biological habitat mapping (GeoHab) symposium. Sitka, Alaska 2008.

Conferences attended

Stakeholder participation and good decision making: MPAs and beyond, Exeter 2008.

Marine Policy: wider policy developments and the interaction with the marine bill, London, 2008.

Workshops attended

GeoHab video analysis workshop: Techniques for using video and stills as a tool for quantitative habitat description. Trondheim, Norway, 2009.

MBARI workshop: Classification and identification of marine organisms from images and video workshop (2009). MBARI, Monterey Bay.

Word count of main body of thesis: 48, 137

Signed …..……..

Date …..……

ABSTRACT

MAPPING DEEP-SEA FEATURES IN UK WATERS FOR USE IN MARINE PROTECTED AREA NETWORK DESIGN

JAIME SELINA DAVIES, B.Sc. (Hons.), MRes.

With an increase in demand on deep-sea resources comes a need for appropriate and effective management of this ecosystem. The establishment of a representative network of deep-sea Marine Protected Areas offers one tool with which to address the conservation needs of the deep sea. While a number of deep-sea habitats have been identified as vulnerable to anthropogenic activities (e.g. cold-water coral reefs and sponge aggregations), poor knowledge of the distribution of these habitats hinders conservation efforts and network planning, and thus we need habitat maps. With improvements in acoustic data resolution acquired from the deep sea, and the ability to cover large areas rapidly, the use of acoustic techniques in mapping biological habitats is growing. Multibeam bathymetry and its derived terrain variables can potentially provide important information that can aid in the delineation and characterisation of biological communities. A necessary prelude to mapping is therefore the definition of biological assemblages for use as mapping units.

Two megahabitat features (seamount and submarine canyons) were sampled using acoustic and ground-truthing to characterise and map the distribution of benthic assemblages. Species were identified as distinct morpho-types and catalogued, and still images quantitatively analysed. Standard multivariate community analysis was undertaken to define distinct faunal assemblage that may act as mapping units. Those

clusters identified by the SIMPROF routine were taken against a set of criteria to reject/accept as robust assemblages that may be used as mapping units. Twenty two benthic assemblages or biotopes were defined from multivariate analysis of quantitative species data, 11 from the SW Approaches and 11 from Anton Dohrn Seamount, and a further one from video observations (SW Approaches). Taken against current definitions, 11 of these were considered as Vulnerable Marine Ecosystems (VME). Diversity was measured to compliment the comprehensive description of biotopes. The use of multivariate diversity indices proved better for comparing diversity of biotopes as it captures a more than one aspect of diversity of the community. Two biotopes were common to both megahabitat features, cold-water coral reef habitats, and those from Anton Dohrn Seamount were more diverse than from the SW Approaches.

Modelling techniques were employed to test the relationship between biotopes and environmental and geophysical parameters, which may be used as surrogates to map VME. Generalised Additive Models of Vulnerable Marine Ecosystems revealed multibeam bathymetry and its derived parameters to be significant surrogate for mapping the distribution of some assemblages, particularly those that appear to be influenced by current regime; whilst not so well for those whose distribution is not so strongly current driven e.g. soft sediment communities. In terms of deep-sea mapping, the use of multibeam can prove a useful mapping tool if the resolution of the data is at an appropriate scale that will identify meso-scale geomorphological features, such as cliff-top mounds, that may act as proxies for occurrence of biotopes, but this relationship is still unclear. Surrogates were used to map VME across the seamount and submarine canyons, and full coverage maps were produced for all biotopes occurring on these megahabitat features.

ACKNOWLEDMENTS

I am profoundly grateful to my supervisory team, Kerry Howell, Heather Stewart, John Spicer, Colin Jacobs and Bhavani Narayanaswamy, who have been supportive throughout the PhD.

I am especially thankful to my mentor Kerry Howell, who has always believed in me and given me many opportunities to develop my career as a deep-sea ecologist. Heather Stewart has not only been a dedicated and supportive supervisor, but has taught me so much about geology and has been my mentor during research cruise work.

John Spicer has been a source of both wisdom and humour throughout this PhD, and has always been on hand to answer ‘random’ questions which I may have. I would also like to thank Andy Foggo for not only his advice regarding statistics but also his support. Prof. Robert Clarke has been of the utmost help regarding advice on statistical methods, and I am extremely grateful to him. I feel I have been very fortunate to have worked in such a friendly and supportive department as MBERC, and am grateful for the experience and friendships which I have formed.

My friends Kate de la Haye, Maria Campbell, Vale Lauria, Sam Patrick and Helen Saglam have been a rock for me, supported me when I needed it and even fed me frequently! I am very lucky to have you girls looking out for me. My family and friends have been very forgiving of my workaholic ways, and my all consumption by my PhD. Awantha, the person who knows me better than I know myself, and always seems to know what is best for me, thank you.

Lastly, I can never put into words how proud and grateful I am to have to such wonderful parents. They have supported my dream to be a marine biologist from a young age, and I would not be the person I am today without them. They never got frustrated when I had to work during visits home.

CONTENTS

(*contents continued*)

(*contents continued*)

(*contents continued*)

(*contents continued*)

LIST OF FIGURES

(*figures continued*)

(*figures continued*)

(*figures continued*)

(*figures continued*)

LIST OF TABLES

LIST OF ACRONYMS

BGS - British Geological Survey

BPI - Bathymetric Positioning Index

CBD - The Convention on Biological Diversity

CFP - Common Fisheries Policy

DGPS - Differential Global Positioning Systems

DTM - Digital Terrain Model

FAO - Food and Agriculture Organization of the United Nations

EEZ - Exclusive Economic Zone

EFZ - Exclusive Fisheries Zone

EUNIS - European Nature Information System

FSC - Faroe-Shetland Channel

GEBCO - General Bathymetric Chart of the Oceans

JNCC - Joint Nature Conservation Committee

MAR - Mid Atlantic Ridge

MESH - Mapping European Seabed Habitats

MPAs - Marine Protected Areas

NAC - North Atlantic Current

OSPAR - Oslo-Paris Convention

OTU - Operational Taxonomic Unit

RFMO - Regional Fisheries Management Organisations

ROV - Remotely Operated Vehicle

SAC - Special Areas of Conservation

SCI - Sites of Community Importance

SEA - Strategic Environmental Assessment

SIMPER - similarity percentage

(*acronyms continued*)

SIMPROF - similarity profile

SPA - Special Protected Areas

UKCS - United Kingdom Continental Shelf

UNCLOS - United Nations Convention of the Law of the Sea

UNGA - United Nations General Assembly

USBL - ultra-short baseline

VMEs - Vulnerable Marine Ecosystems

WTOW - Wyville Thomson Ridge Overflow Water

WTR - Wyville Thomson Ridge

CHAPTER 1

INTRODUCTION AND RESEARCH AIMS

The deep sea represents the largest ecosystem on earth. It is a vast area that is topographically complex, supporting a diverse range of habitats and species. Anthropogenic impacts on the deep sea are increasing. Fishing and oil and gas exploration and exploitation are moving progressively deeper (Rogers 1999; Glover and Smith 2003) and new potential threats continue to emerge, such as deep-sea mining (Halfar and Fujita 2007). With an increase in demand on deep-sea resources comes a need for appropriate and effective management of this ecosystem. While management of those industries operating in the deep sea are currently being addressed by relevant authorities e.g. the development of 'the mining code' by the International Seabed Authority and appropriate management of fisheries by Regional Fisheries Management Organisations (RFMOs), there is currently no ecosystem level approach to management of the deep sea.

The establishment of a representative network of deep-sea Marine Protected Areas offers one tool with which to address the conservation needs of the deep sea. The requirement for the establishment of such networks is driven by a number of international and national policies; and the challenge is now how to practically implement such networks given our limited understanding of the deep sea ecosystem. While a number of deep-sea habitats have been identified as vulnerable to anthropogenic activities (e.g. cold-water coral reefs and sponge aggregations) (FAO 2008), poor knowledge of the distribution of these habitats hinders conservation efforts and network planning. Additionally, it is difficult to use criteria (such as those set out by

the FAO) that have been developed for assessing habitat vulnerability (FAO 2008) as many deep-sea habitats have yet to be described, particularly in terms of their rarity, resistance, resilience and vulnerability. For example, although some habitats such as cold-water coral reefs are easily damaged from activities such as bottom trawling, it is not cold-water coral reefs that are subject to repeated trawling action in the way that some soft bottom deep-sea habitats are (Thrush *et al*. 2001).

Much research effort has been focused on hard bottomed habitats such as coral reefs, which has led to a misconception in terms of marine seafloor biodiversity (Thrush and Dayton 2002). Approximately 70% of the earth's seafloor is covered by soft sediment habitats (Wilson 1991), which can be highly heterogeneous and biodiverse (Etter and Grassle 1992, Thrush *et al*. 2001), but also vulnerable to fishing activities (Gage 2001). The physical effects on structuring organisms such as xenophyophores and glass sponges are severe from bottom trawling (Gage 2001) and can greatly reduce species diversity (Veale *et al*. 2000). In addition to the physical damage resulting from bottom trawling, the long term effects include the homogenization of the substratum (Veale *et al*. 2000) and re-suspension of sediments (Jones 1992; Pilskaln *et al*. 1998; Thrush *et al*. 2002). It is therefore important that our understanding of deep-sea habitats and their distributions are improved. One way to address this is through the use of habitat mapping.

1.1 Management and Policy Drivers

The United Nations Convention of the Law of the Sea (UNCLOS) is an international agreement that provides the legal basis for high seas[1] Marine Protected Areas (UNCLOS 1982). It came into force in 1994, and created 200 nautical mile wide

[1] The high seas are those waters outside of national jurisdiction.

Exclusive Economic Zones (EEZs) around all signatory states. The Convention on Biological Diversity (CBD) is an international legally binding treaty which includes within it a requirement for nations to establish a 'comprehensive, effectively managed and ecologically representative network of Marine Protected Areas by 2020' [(COP 10 Decision X/2) CBD 2010].

The Oslo-Paris Convention (OSPAR) is the current legal mechanism guiding international cooperation on the protection of the marine environments of the North-East Atlantic; the agreement is between 15 European countries and the European Commission. The OSPAR convention (The convention for the protection of the Marine Environment of the North East Atlantic) unified the original 1972 Oslo Convention against dumping and 1974 Paris Convention in 1992 and was adopted in 1998 and incorporated obligations under the CBD into the OSPAR framework. Annex V of the OSPAR convention lists a number of deep-sea habitats as 'threatened or declining', including: seamounts, *Lophelia pertusa* reefs, coral gardens, carbonate mounds, and sea pen and burrowing megafauna communities; and calls for nations to establish, "an ecologically coherent network of well managed Marine Protected Areas by 2020" for the protection of these listed habitats.

Within Europe, the main legislative power for managing fisheries and marine nature conservation are the Common Fisheries Policy and Habitats Directive (92/43/EEC). The Habitats Directive (conservation of the natural habitats of wild fauna and flora) is the first international tool to address the protection of selected habitats under Annex I as being important, and also protects listed species under Annex II. The Directive evolved from the 1979 Birds Directive, which was legally bound to establish a network of Special Protected Areas (SPAs) throughout the EC. The Habitats Directive requires

member states to designate and protect sites for their natural habitats or species present as Special Areas of Conservation (SACs). The 1992 Directive followed the same format as the Birds Directive, whereby member states were required to select and propose lists of Sites of Community Importance (SCIs) for the EC to evaluate. Subsequently, approved SCIs were designated by the member states as SACs. Initially, the Habitats Directive was drafted to include protection for offshore areas under Article 1, whereby areas within the member states jurisdiction/sovereignty Exclusive Fisheries Zone/ Exclusive Economic Zone (EFZ/EEZ) would be protected under the Directive – this was subsequently dropped and the final working directive was adopted in May 1992. This lack of protection for the UK's offshore waters was challenged by Greenpeace in 1999 (SSTI 2000). They took the UK Government to court to extend the applicability of the Habitats Directive from the 12nm limit to the 200nm limit, which was successful. These protected areas (SAC and SPA) together create the *Natura 2000* sites, which are a network of protected areas throughout the EC. Cold-water coral reefs, coral gardens and sponge dominated communities all come under the definition of Annex I listed 'reef' habitat.

The Common Fisheries Policy (CFP) began in 1970 with the establishment of a structural regulation for fisheries through defining regulations on access to fishing grounds, markets and structures (Regulation EEC, No 2141/70). Prior to this policy, fisheries were regulated primarily by international fisheries commissions and member states authorities. This changed in 1972 when the EC, under Article 102 of the Act of Accession of Denmark, Norway, Ireland and the UK, gained exclusive legislative rights to regulate fishing (EC 1972). Subsequently, the CFP went through many reforms to its current status (EC 2371/2002) which incorporates a component on the conservation and sustainable exploitation of fisheries resources, including emergency measures using the

precautionary approach to protecting living resources and ecosystems. This policy was used to close the Darwin Mounds: a carbonate mound area inhabited by the cold-water coral *Lophelia pertusa*. The emergency powers of the policy were used to impose an initial 6 month restriction on bottom trawling to protect the vulnerable coral habitat, which led to the subsequent closure of the Darwin Mounds to bottom trawling in 2003. This was the first instance where the CFP was used to conserve nature rather than fish stocks (De Santo and Jones 2007), although this is an exception rather than the rule as other attempts by the UK to use the CFP for wider marine conservation purposes have failed. In 2004 the UK put forward a proposal to ban sea bass pair-trawling in the English Channel. The use of this trawling method can result in the bycatch of cetaceans, thus under obligation of the Habitats Directive to protect cetacean species (listed in Annex IV) a proposal was put forward, but subsequently failed.

At a national level, a number of deep-sea habitats are listed as 'priority habitats' under the UK Biodiversity Action Plan (UKBAP): these are carbonate mounds, cold-water coral reefs (*Lophelia pertusa*), seamount communities, soft sediment habitats in deep waters and deep-sea sponge communities.

The 2006 United Nations General Assembly (UNGA) Resolution 61/105 calls for sustainable bottom fisheries and the protection of Vulnerable Marine Ecosystems (VMEs) from deep-sea fisheries in the high seas (UNGA 2006). Vulnerable Marine Ecosystems (VMEs) are defined as "any deep-sea ecosystem (ecotopes: finest scale units used for mapping ecosystems) which has very high vulnerability to one or more kinds of fishing activity" (FAO 2008). A number of VMEs have been identified from potential species groups, communities and habitat-forming species that have been documented or are considered sensitive and potentially vulnerable to deep-sea fisheries

[in the high-sea]: cold-water coral reefs, coral gardens, sponge dominated communities, seep and vent communities, and communities composed of epifauna that provide a structural habitat (e.g. xenophyophores and sea pens) for other associated species (FAO 2009). Topographical, hydrophysical or geological features that these VMEs may be associated with include: seeps and hydrothermal vents, submerged edges and slopes, summits and flanks of topographical features such as seamounts, guyots, banks, knolls, hills, canyons and trenches (FAO 2009).

1.2 Examples of 'listed' deep-sea habitats of conservation interest

1.2.1 *Lophelia pertusa* reefs

Deep-water corals have been of increased research interest (O'Hara *et al.* 2008) due to the widely documented high biodiversity associated with them (Bryan and Metaxas 2007; Henry and Roberts 2007). Deep-water coral reef/banks are widespread along the NE Atlantic margin, at shelf breaks and on the upper continental slope (De Mol *et al.* 2002). They are often found in areas of pronounced topographic relief such as the slopes of banks, submarine canyons, and seamounts due to the strong current regime (Genin *et al.* 1986; Frederiksen *et al.* 1992; MacIsaac *et al.* 2001) and hard substratum associated with the sloping areas (Freiwald *et al.* 1999; Bryan and Metaxas 2007). *Lophelia pertusa* reefs are listed as VMEs (FAO), Annex I habitat (Habitats Directive) and Annex V habitat (OSPAR).

Reef structures such as those composed of the scleractinian corals *Lophelia pertusa* and *Madrepora oculata* have been found on mound features (De Mol *et al.* 2002; Kenyon *et al.* 2003; Howell *et al.* 2007; Wienberg *et al.* 2008) and associated with topographical features (Roberts *et al.* 2006; Wheeler *et al.* 2007). The current theory of reef formation

suggests *L. pertusa* reef forms from an initial settlement of larvae on hard substrata. Subsequently, the coral develops and as the skeleton grows it becomes susceptible to bio-erosion (predominately from clionid sponges). As pieces of the reef break off they extend the extent of the reef and trap sediment, this process continues and thus establishes a reef complex (Roberts *et al.* 2006).

Lophelia pertusa is widely distributed in the North Atlantic, in oceanic waters at a temperatures of 4-12°C (Roberts *et al.* 2006) and is predominantly found at depths of 200-1000m but has been recorded shallower and deeper (Zibrowius 1980). It has been identified as occurring in areas subjected to fast currents such as carbonate mounds (De Mol *et al.* 2002), ridges and pinnacles (Howell *et al.* 2011).

Lophelia reefs have been described as having three distinct zones: 'live *Lophelia* zone' which is the main reef habitat found on the summit of the reef and consists of predominantly live *Lophelia pertusa* interspersed with areas of dead broken skeleton (Mortensen *et al*. 1995). 'Dead coral framework' zone that is characterised by suspension feeders including sponges, actinians, and other coral species (gorgonians) with smaller epifauna such as bryozoans, hydroids and barnacles (Mortensen *et al*. 1995; Roberts *et al*. 2009). This zone (*sensu* Mortensen *et al*. 1995) is known to be the most diverse area of a reef (Jensen and Frederiksen 1992; Mortensen *et al.* 1995). The '*Lophelia* rubble zone' is the outer 'apron' of the reef where the framework has been (bio)eroded and accumulates at the base of the reef, where the squat lobster *Munida sarsi* dominates (Mortensen *et al*. 1995).

1.2.2 Coral carbonate mounds

Carbonate mounds can form either directly from bioherms (Enachescu 2004) or subsequent to the formation of a mud volcano (through fluid expulsion) followed by authigenic carbonate formation (Kopf 2002). Another suggestion for the development of these mounds is from hydrocarbon seepage which encourages an initial bacterial community which precipitates authigenic carbonates thus providing a substratum for subsequent attachment of fauna (Naeth *et al.*, 2005).

Carbonate mounds which are comprised of coral are listed under annex V of OSPAR, and are defined as 'features which have formed by successive periods of coral reef development, sedimentation and (bio)erosion' (OSPAR 2010a) and are referred to as coral carbonate mounds. Coral carbonate mounds are thought to develop through inter-glacial periods, where the coral reef grows and produces layers of coral debris developing a mound structure. Then during glacial periods the coral dies and the coral debris is replaced by an ooze layer (Kenyon *et al.* 2003). During the next interglacial period, coral reef growth resumes. The subsequent formation of the coral carbonate mound occurs as interbedded growth layers following glacial cycles.

These mounds can form provinces and occur throughout the NE Atlantic region. They can be characterised by smaller mounds as in the case of the Darwin Mounds (northern Rockall Trough) or giant mounds as in the Porcupine Seabight (Roberts *et al.* 2006). The Darwin Mounds occur at ca. 1000m depth. They consist of numerous, small seabed mounds. These mounds have the cold-water coral *Lophelia pertusa* associated with them while the 'tails' of the mounds support dense populations of the xenophyophore *Syringammina fragilissima.* The corals associated with the mounds are not large reefs;

rather they comprise smaller patches of corals. Despite the patchiness of the coral, it still provides an important habitat for other fauna (Bett 2001).

Within the Porcupine Basin numerous areas of mound features exist: Hovland (725-900m) mounds, Magellan mounds and the Belgica (600-900m) mounds. It has been suggested that debris and live corals such as *L. pertusa* and *M. oculata* may have played a key role in the development of these mounds. Some of the mounds host impressive colonies of coral (live and dead), notably Belgica and Hovland mounds, corals are absent from the Magellan mounds, due to these mounds being sediment covered (De Mol *et al.* 2002).

1.3 Examples of 'listed' geomorphological features of conservation concern

1.3.1 *Seamounts*

Seamounts are listed under annex V of OSPAR and as features that may support VMEs (FAO 2009). In recent years seamount ecology and hydrography have received considerable research interest in an attempt to understand the ecology and functioning of seamount ecosystems (O'Hara 2007; Clark *et al.* 2010; Rowden *et al.* 2010; Shank 2010; Howell *et al.* 2010a). This has resulted in a number of previously held theories on seamounts being called into question.

Seamounts are large topographical features often characterised by complex hydrodynamic regimes. They exert an influence over ocean currents by interrupting the flow of water, this can cause tides to be amplified creating fast currents and producing eddies (Richardson 1980). These elevated currents have a functional role by increasing local food supply, eroding sediment, and in some cases exposing hard substratum for

faunal attachment thereby increasing larval supply and species recruitment; thus making seamounts diverse biological features (Rogers 1994). In some instances, eddies can get trapped over the seamount thereby creating a closed circulation system known as a Taylor column. These Taylor columns exert an influence on localised plankton densities by producing upwelling of nutrient-rich deep waters. It was assumed that Taylor column association with seamounts was a widespread phenomenon, but this view has recently been challenged as there appears little evidence to support the occurrence of Taylor columns at many of the seamounts investigated to date (McClain 2007). Additionally, for those seamounts where Taylor columns have been observed, it has been suggested that the column is not permanent, only lasting between less than 2 days to 6 weeks (Richardson 1980). However, Taylor columns do persist in some areas (Meredith *et al*. 2003) thus generalisations such as these may be inappropriate.

Seamounts are considered centres for high levels of biodiversity and endemism (Hubbs 1959; Rogers 1994; Parin *et al.* 1997; Richer de Forges *et al.* 2000), but while seamounts do support a diverse range of species, the theory that seamounts support high numbers of endemic species may not hold true. It has been suggested that the apparent high levels of endemism on seamounts is in fact a result of inadequate sampling in the deep sea (McClain 2007; O'Hara 2007). Although seamounts that are isolated from the continental margin may indeed show higher levels of endemism due to genetic isolation (McClain 2007), this apparent endemism may in some instances be a result of misidentification of species due to morphological differences induced in response to environmental conditions.

Increased species richness on seamounts (as compared to the surrounding seafloor) is suggested to be a result of high carbon inputs to these systems and the availability of

habitats. Seamounts were considered to support 'unique' habitats such as hard substrata, and biogenic habitats such as coral and sponge meadows, which in turn provide rich habitats for other associated fauna (Rogers 1994). However, this view has also been challenged in the last 5 years as not only do many seamounts not have these 'unique' habitats, but they are not unique to seamounts – they are found to occur on other topographical features (O'Hara 2007; Howell *et al.* 2010a). Despite this, some studies have found higher megabenthos biomass and species abundances on some seamounts in the SW Pacific and NW Pacific respectively (Rowden *et al*. 2010; McClain 2010). It is also likely that seamounts support a higher habitat diversity per unit area than the neighbouring continental shelf and thus can still be considered biodiversity hotspots.

The high carbon inputs to seamount systems are a result of the topography and hydrodynamics of seamounts. One theory to explain this relates to the diurnally migrating zooplankton layer that moves into surface waters at dusk. If prevailing currents carry the zooplankton over a seamount summit, when they descend at dawn, they become trapped by the seamount. This trapped layer provides a rich food resource for seamount inhabitants and an increased flux of detrital material to deeper waters (Vetter and Dayton 1998). Seamounts were considered to support and attract higher level predators including cetaceans (Rogers 1994; Morato *et al.* 2008). However this generalisation was made from sparse records and it is more likely that not all seamounts harbour such aggregations of higher predators (Morato *et al.* 2008).

Despite recent challenges to long held theories concerning seamount ecology, seamounts do support a rich fauna and may yet be important 'oases' in the oceans (Samadi *et al.* 2006) playing a significant role in species dispersal by acting as stepping stones (Hubbs 1959; Rogers 1994; Parin *et al.* 1997).

1.3.2 Submarine canyons

Submarine canyons are listed as an area that may support VMEs (FAO 2009). They are abrupt topographical features that incise much of the world's continental shelves and margins (Brodeur 2001). They can serve as sediment transport systems, moving sediment and organic matter from the shelf to the deep-sea floor (Shepard 1951; Heezen *et al.* 1955; Monaco *et al.* 1990; Vetter and Dayton 1999) and may be subject to some degree of physical disturbance (Rowe *et al.* 1982; Okey 1997; 2003). They are areas of high habitat heterogeneity (Schlacher *et al.* 2007; Tyler *et al.* 2009; Schlacher *et al.* 2010); and this coupled with the high productivity of these features results in enhanced benthic biodiversity (Rowe *et al.* 1982; Vetter and Dayton 1999). Canyons have been described as hotspots of biodiversity (De Leo *et al.* 2010). Despite the ubiquitous distribution of both seamount and submarine canyons, canyons are much more poorly sampled and thus much less well understood (De Leo *et al.* 2010).

1.4 Habitat mapping and classification

In order to take an ecosystem approach to managing the deep sea marine environment it is essential that we develop our understanding of the distribution and diversity of benthic habitats. What are required are habitat maps that will allow environmental managers to make informed decisions concerning the level of threat to habitats, and to take a strategic approach to MPA network design. Habitat mapping is the process of integrating geological characteristics and biological information (Todd *et al.* 1999). In the deep sea it is not feasible to use the same approaches as used for mapping shallow-water habitats. The vast area involved requires that a broad-scale approach is needed, although fine scale approaches may be nested within that. It is now possible, as a result of advancements in technology, to collect detailed bathymetry and seabed substratum

information, which when combined with georeferenced biological data and environmental data, may be used to produce biologically meaningful maps (Williams *et al.* 2007).

Habitat classification systems are prerequisite to mapping and understanding the marine environment (Cogan and Noji 2007). A range of marine habitat classification schemes that are applicable to the deep sea exist, and include those that are hierarchical, nested, and are focussed on biological components, such as EUNIS (European Nature Information System), and those that are top-down schemes and are more geologically based (Greene *et al.* 1999).

EUNIS is a hierarchical habitat classification system that is based on five levels covering terrestrial, marine, natural and artificial habitats. Within the marine category (level 1), the deep seabed is divided into zones at level 2 (A6). Level 3 and 4 are divided on the basis of substratum (level 3) and benthic assemblages (level 4). Topographical features such as seamounts and canyons are not related to seabed substratum or biological communities but are also included in level 3. EUNIS currently fails to provide as much detail for deep-water habitats (>200m) as it does for shallow-water habitats.

The scheme developed by Greene *et al*. (1999), incorporates geology, geophysics and biological observations. Those categories that apply directly to habitat interpretations from remote sensing data are divided on the basis of scale. At the largest scale, (kilometres to 10s of kilometres) megahabitats relate to large features such as seamounts, submarine canyons, banks and continental shelves that lie within major physiographic provinces e.g. continental shelf, slope and abyssal plain. Below this,

mesohabitats denote seabed features on a scale of tens of metres to 1 kilometre such as pinnacles, gullies and scarps; mesohabitat diversity may vary between megahabitats. Macrohabitats range in size from one to ten metres and include seafloor material and features such as boulders, bedrock outcrops and carbonate build-ups; mesohabitats can comprise several macrohabitats. Microhabitats are seafloor materials and features that are centimetres or smaller in size, these may be substratum or individual organisms.

Interestingly, within the Greene *et al*. (1999) scheme, megahabitat features such as seamounts and canyons are further divided into zones: seamount; top, flank and base and canyons; head (<100m depth), upper (100-300m depth), middle (300-500m depth) and lower (500-1000+m depth). Such divisions are lacking in the EUNIS scheme.

To implement ecologically representative networks within national waters, biologically meaningful maps are required to inform managers on the distribution and diversity of habitats. To adequately protect species and habitats, particularly those that are listed as being of conservation interest, the approach taken needs to be at a scale that is relevant to the biology. Taking a bottom-up approach, through first defining benthic assemblages that can then act as fine-scale mapping units, cannot only be used to inform the distribution of assemblages, but may also allow the inference of associations between biology and larger scale features (geomorphology), which may then enable these large scale features to be used for mapping across broad areas. To achieve an ecologically coherent network across regions, and globally, we need to be able to combine habitat maps originating from national and international programmes. To date deep-sea maps produced by different projects / countries are not able to be combined because of a lack of an agreed deep-sea classification system and recognised and agreed definitions of

mapping units. To overcome this, standardisation of mapping practices is necessary, with consistent terms used.

1.5 The study area: North East Atlantic

The North East Atlantic is defined by the OSPAR (Oslo and Paris) Convention as an area that extends from the North Pole to the straits of Gibraltar, and laterally from the coasts of mainland Europe to the Mid-Atlantic Ridge (MAR).

The NE Atlantic is a complex area of oceanic crust comprising a series of basins and ridges that are impinged by distinct topographical features such as seamounts, banks and oceanic islands, while the European continental shelf is incised by submarine canyon systems. The main ridge system that runs longitudinally down the Atlantic Ocean and divides the NE Atlantic from the NW Atlantic is the Mid Atlantic Ridge (MAR). The Reykjanes ridge is an extension of the MAR which extends in a southwest direction from Iceland to the MAR and separates the Irminger basin from the Iceland basin; and the Greenland-Scotland rise that extends from eastern Greenland to the Hebridean shelf and separates the Nordic Seas to the north of the ridge from the Atlantic Ocean to the south of the ridge. The area between the west of Scotland and Greenland were subject to compressional tectonic events and subsidence (Boldreel and Anderson 1993) which resulted in the basins (Irminger, Iceland, Hatton-Rockall Basins') having a NE-SW orientation, while the Porcupine Basin extends in a NW-SE direction. There are also vast expanses of relatively featureless deep water seabed such as deep channels (Norwegian Deep and Rockall Trough) and the Porcupine and Iberian Abyssal Plains.

Oceanographically, the NE Atlantic plays a vital role in global circulation. The movement of warmer saline water from the western Atlantic carried by the gulf stream crosses the Greenland-Scotland ridge while cold, fresher waters flows west across the

ridge and along the coast of Greenland – this exchange of water across the ridge provides a means for heat and salt exchange to northern Europe (Hansen and Østerhus 2000; van Aken 2000). Within the NE Atlantic, the hydrographic regime is complex with a counter-current flow of warm and cold water masses. The Iceland basin acts as the main route for the movement of the warm upper water mass from the North Atlantic Current (NAC) towards the Norwegian Sea and the counter current of cold waters entering the Northeast Atlantic Basin from the Nordic Seas (Hansen and Østerhus 2000).

The UK's deep-sea is largely found west and north of Scotland (NW Approaches); however there is a small area to the south west of England (SW Approaches). The NW Approaches incorporates part of two main basins, the Faroe Shetland Channel (north of Scotland) and the Rockall Trough (west of Scotland), which are separated by the Wyville Thomson Ridge (WTR). The Faroe-Shetland Channel (FSC) is a funnel-shaped basin that separates the Faroe Plateau from the West Shetland Shelf. To the North, the channel is connected to the Norwegian Sea, while at its Southern end it narrows from 175km to 90km wide and feeds into the Iceland Basin through the Faroe Bank Channel. The WTR is part of the Greenland-Scotland barrier which separates the Rockall Trough from the FSC. It extends in a NW direction from the Scottish continental shelf where it joins the Faroe Bank. Simplistically, either side of the WTR shares the same upper warm Atlantic water mass but the WTR acts as a barrier to the deeper cold Arctic waters preventing it from entering the RT (Turrell *et al.* 1999), thus creating a thermocline in the FSC between 400 and 600m (Bett 2001), although periodic overflow of the Wyville Thomson Overflow Water (WTOW) into the RT has been reported (Johnson *et al*. 2010).

The Rockall Trough extends from the WTR to the Porcupine Abyssal Plain which deepens with its southern extension. The trough incorporates the northern part of Rockall Bank, most of the Rockall-Hatton Basin, Hatton Bank, Anton Dohrn Seamount, Rosemary Bank Seamount, George Bligh Bank and Hebrides Terrace Seamount. The UK's offshore marine area (waters beyond 12nm, within the Exclusive Fisheries Zone limits and the seabed within the UK Continental Shelf limit) has a range of topographical features including seamounts, banks, submarine canyons, continental shelf and ridges; and is an ideal area for a case study mapping deep-sea topographical features.

1.6 Research aims and thesis outline

1.6.1 *Research aims*

The objective of this thesis is to address issues of conservation of deep-sea habitats, taking an applied approach and using the UK as a case study. There are two principle aims to this thesis. The first is to support international habitat mapping efforts through developing standardised descriptions of deep-sea biological assemblages, with a focus on assemblages that fit descriptions of 'listed' habitats, for use as functional and consistent mapping units (biotopes). The second is to investigate the feasibility of mapping large scale mega-habitat deep-sea features using defined mapping units (biotopes) and topographic data derived from multibeam bathymetry, again with a focus on habitats of conservation concern. These aims will be addressed through two case studies representing two types of 'listed' mega-habitat deep-sea features, the Anton Dohrn Seamount, and Dangaard and Explorer Canyons (part of the South West Approaches canyon system). The following questions form the basis of this study:

1) What epibenthic megafaunal assemblages are present on a seamount? 2) What epibenthic megafaunal assemblages are present in canyons? 3) Of these which could be classified as corresponding to 'listed habitats'? 4) Does the distribution of these 'listed' habitats show any relationship to seabed topography and geomorphology? 5) Is it possible to produce biotope maps of megahabitat features and what assumptions must be made in order to so?

These questions will be addressed through the following objectives:

1. *Use multivariate statistical methods to define deep-water benthic assemblages, using quantitative sample data from a seamount and submarine canyon, which may function as mapping units (Chapter 3 and 4).*
2. *Identify assemblages of conservation interest under international/national policy through comparison with existing published definitions.*
3. *Provide full descriptions of assemblages of conservation interest including characterising species, species densities, measures of diversity, and environmental characteristics.*
4. *Investigate the relationship between topographic variables (multibeam and its derived layers) and defined biological assemblages. (Chapter 5).*
5. *Produce full coverage maps of the distribution of biological assemblages across a canyon and seamount feature and critically examine the methods involved. (Chapter 5).*

1.6.2 *Thesis outline*

The thesis encompasses a range of topics that are relevant to mapping deep-sea features for use in MPA design, thus Chapter 1 aims to give: a general introduction and an overview of the policies that are driving the protection of the marine environment,

focusing on the UK; some ecological background to examples of listed deep-sea habitats that are dealt with in this thesis; and a brief introduction to habitat mapping.

Chapter 2 gives an overview of the equipment and methods used within the thesis, introducing acoustic and biological data acquisition and its uses in habitat mapping.

In Chapters 3 and 4, community analysis is used to group benthic assemblages and define fine scale biological mapping units from a seamount and submarine canyon respectively. To aid in the characterisation of biotopes, diversity is measured and compared between biotope. Newly described mapping units or 'biotopes' are related to interpreted geomorphological features, to expand knowledge of their spatial distribution. In these chapters the relationships between biotopes distribution and geomorphology will not be explicitly tested, but qualitative descriptions given; this will be addressed in chapter 5. Despite all benthic assemblages being defined, to aid in the flow of the thesis, these chapters focus on those habitats identified from the seamount and canyon features that are currently listed under policy. All other habitat descriptions are included as appendices.

Subsequent to defining benthic assemblages, Chapter 5 investigates how to map these across whole megahabitat features using modelling methods to determine the relationship between biotopes and mapping parameters. The application of multibeam bathymetry and its derived layers in mapping these assemblages is investigated in the context of the two different megahabitat features.

Chapter 6 discusses the overall findings of the thesis and what has been learnt about producing full coverage habitat maps in the deep sea and how these findings relate to,

and may be used in, mapping the deep sea, and designing and managing deep-sea / high sea MPA networks.

In the scope of the research undertaken within this thesis, I participated in two research cruises to collect the data. I contributed to the production of final reports from both cruises. These were delivered to the funding body the Joint Nature Conservation Committee. The reports illustrate the initial data analysis undertaken within the time constraints required by the funder. Subsequent to these reports, a more detailed interpretation of the data was undertaken for inclusion in the thesis. Although Rockall Bank was sampled and the data partially analysed for inclusion in the report it was not possible to fully analyse three megahabitat feature types within the duration of the PhD. For the purposes of the thesis it was decided that Anton Dohrn Seamount and the SW Approaches should be investigated as there has been little documented regarding these areas. In addition, seamounts and canyons are listed as potentially harbouring Vulnerable Marine Ecosystems (VMEs), and seamounts are also listed under OSPAR as 'threatened or declining' habitats. Rockall Bank is a shallower feature and has been more intensively sampled. In addition, full multibeam coverage of the bank was not achieved and thus a complete coverage map could not be produced, unlike the other two sites. Thus Rockall Bank was not included in the main body of the thesis. Geological interpretation to produce the substratum and geomorphology map used in this thesis was undertaken by experts at the British Geological Survey. I used this layers as base layers to map the two megahabitat features, but all further interpretation and habitat mapping was undertaken by myself.

CHAPTER 2

BENTHIC SURVEYS: EQUIPMENT AND METHODS

The purpose of this chapter is to introduce the equipment and methods used throughout this thesis to give a better understanding of them before commencing with the data chapters. The rationale behind the research surveys will be explained and a description of the survey areas given. Acoustic and biological data were acquired during each survey and are used in each data chapter, and it is thus important to introduce the principles and protocols of the acquisition and use of those data here.

2.1 Survey areas

The aims of the surveys were to (1) collect acoustic data within the areas of interest in order to better classify the geomorphological features, and (2) to help inform a comprehensive program of ground-truthing sites to characterise the ecology and seabed substratum of the study areas. Submarine canyons in the South West (SW) Approaches and a seamount (Anton Dohrn Seamount) were chosen as areas to survey, as they are distinct megahabitat features (*sensu* Greene *et al*. 1999) that are of conservation concern. Also, relatively little is currently known about the ecology of these features.

Over a five year period (2005-2009), three seabed surveys were undertaken within UK waters to assess the epifaunal assemblages and the distribution of seabed substratum types of Anton Dohrn Seamount (SEA7 survey in 2005; JNCC survey in 2009) and the SW Approaches (MESH survey in 2007)[2] (Fig. 2.1). Anton Dohrn Seamount is a dome-shaped seamount located in the central Rockall Trough between the UK continental shelf, west of Scotland, and a large shallow water shoal called Rockall Bank (Fig. 2.1).

The SW Approaches are characterised by a number of submarine canyons incised into the continental shelf of the Celtic Margin.

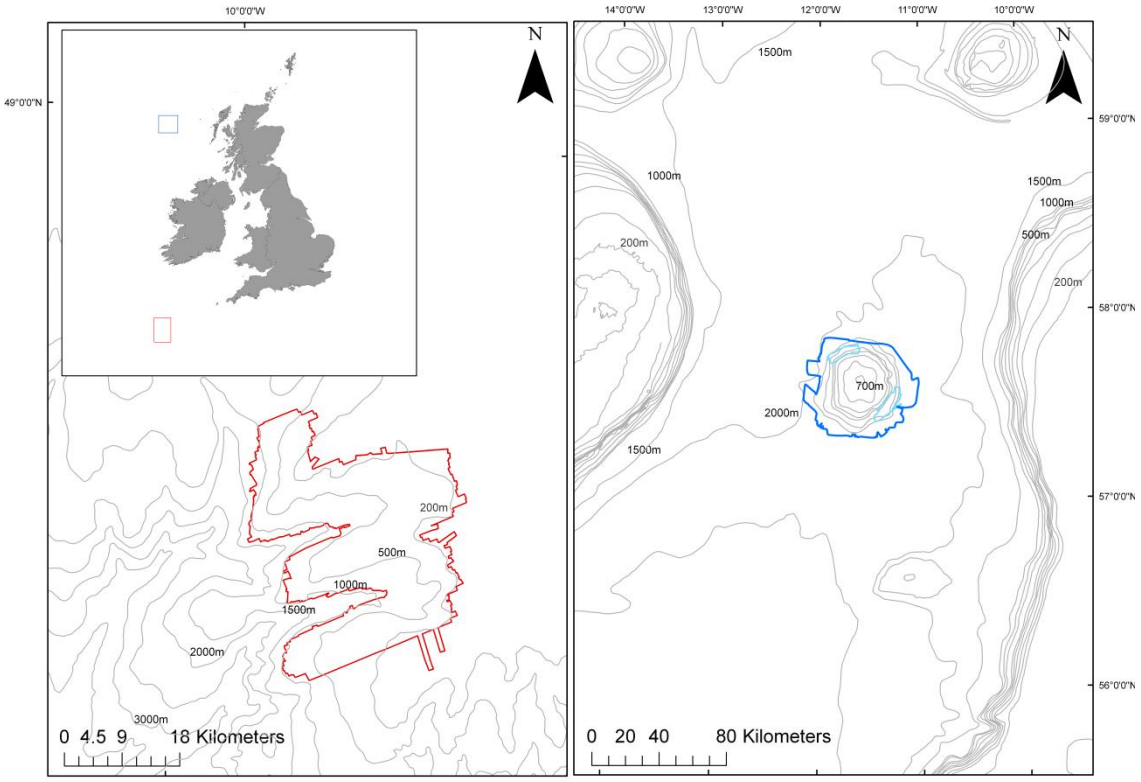

Fig. 2.1: The survey areas from the three research cruises. The insert map shows the survey locations in relation to the UK. The red area represents the 2007 SW Approaches survey and the dark blue the 2005 and light blue the 2009 Anton Dohrn Seamount surveys respectively.

2.2 Acoustic data acquisition

For the purposes of this thesis the term 'acoustic data' refers only to multibeam echosounder data, as described in detail below. Within geological and geophysical

[2]Strategic Environmental Assessment (SEA) surveys are undertaken in accordance with the European Strategic Environmental Assessment Directive (Directive 2001/42/EC) and are the process of appraisal through which environmental protection and sustainable development may be considered. SEA 7 covers a large area to the West of Scotland (www.offshore-sea.org.uk). Joint Nature Conservation Committee (JNCC). The principal purpose of the Mapping European Seabed Habitats (MESH) project is to harmonise the way in which habitat mapping initiatives are undertaken in northwest Europe (www.searchmesh.net).

disciplines the term also includes a host of vessel mounted and towed equipment which is used to acquire data to characterise the seabed and to penetrate the seabed to image the lithologies and structures within (Szuman *et al.* 2006).

Acoustic data collected during the course of this research were used to interpret the topography, and give an indication as to the seabed substratum type of the areas of interest. Multibeam echosounder data comprises two types of data. The first are high resolution bathymetric, or water depth, soundings which, once processed can be modelled to reveal the topography of the seabed. The second are backscatter intensity data that are acquired simultaneously with the bathymetric data and give an indication of the roughness and type of seabed substratum (McRea *et al.* 1999). Detailed bathymetric data are required to produce Digital Terrain Models (DTMs) from which terrain layers such as slope, aspect, rugosity and Bathymetric Positioning Index (BPI) can be derived and used to characterise the seabed (Wilson *et al*. 2007). These layers may also be used to produce biological habitat maps through investigation of relationships between combinations of these variables and faunal distributions (Wilson *et al*. 2007; Dolan *et al.* 2008; Buhl-Mortensen *et al.* 2009, Howell *et al*. 2011).

Multibeam echosounders are typically hull-mounted systems used to measure multiple water depths from one transducer array, although some systems can be pole mounted, Autonomous Underwater Vehicle (AUV) or Remotely Operated Vehicle (ROV) mounted. Multibeam echosounders measure water depths along a ‘swath’, fanning out from the transducer array. An acoustic signal (ping) is emitted from the transducer to the sea floor where it reflects off the sea floor and returns back to the transducer.

Multibeam echosounders are characterised by a number of parameters: a) frequency, where the lower the frequency the greater the working water depth, higher frequency systems are used to survey shallower seas and harbours; b) swath width, which typically ranges from 2 to 12 times water depth; c) beam width and; d) range resolution (Lekkerkerk *et al.* 2006). Accuracy generally degrades with the higher swath widths encountered in deeper water. When the emitted acoustic signal hits the seabed the area ensonified by each individual beam, making up the swath fanning out of the transducer, is referred to as its acoustic footprint. In deeper water the acoustic footprint of each beam increases, as does the distance between each beam and its neighbours, thereby reducing the resolution of the data. The term 'resolution', when referring to a gridded xyz dataset, is the cell size that the data are gridded to, i.e. the dimensions of the cells (pixel); the density of acoustic data within each cell determines the accuracy of the data. Simplistically, two datasets gridded at 100 m, which have a different number of pings per cell, result in different data accuracies. Figure 2.2 illustrates the difference between two datasets gridded to 100 m, and due to the variation in acoustic footprint have a different number of acoustic pings within each cell. If these data are subsequently re-gridded to a cell size of 25 m, the lower density dataset does not resolve the same level of detail as the higher density dataset due to the lack of pings in each cell. The data per cell is determined by averaging all the pings, thus the greater the number of pings per cell the less error is introduced to that cell. Gridding bathymetry data to a resolution lower than the number of pings per cell introduces errors and artefacts into the dataset. This is a particular problem when working in the deep sea, the number of pings per cell decreases with water depth and equipment type used, and needs to be taken into account when working with these data (see Fig. 2.3 for an example of the quality disparity between datasets that are gridded to a similar cell size) and datasets not taken beyond their capabilities.

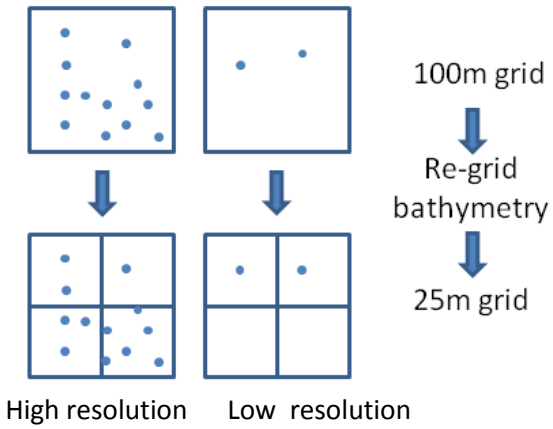

Fig. 2.2: Schematic of variation in the density of acoustic pings between high (left) and low (right) resolution acoustic data. At 100 m grid cell size both datasets contain depth sample data, but the mean depth for this cell produced from the dataset on the left will contain less error than the mean produced from the dataset on the right as the sample size is greater (12 depth soundings (pings) as opposed to 2). At 25 m grid cell size the dataset on the left still has data in each cell, however the dataset on the right contains cells with no data. The dataset on the right does not contain sufficient sample data to allow it to be gridded at 25 m.

It should be noted that each acoustic survey comprises high resolution geopositioning using accurate differential global positioning systems (DGPS), heave-pitch-roll sensors and a gyrocompass. In addition, time synchronisation between all equipment, sensors and logging software is essential. Prior to data acquisition a 'patch test' is undertaken to determine the fixed angular corrections for pitch and roll to be applied to the multibeam echosounder data to therefore account for any misalignment of the transducer with reference to the motion sensor. The vessel offsets between all pieces of equipment, sensors and the reference point of the vessel are also derived prior to operations. The velocity of sound in the water column affects both calculated depth and refraction paths of the acoustic signal and is therefore measured at intervals throughout the survey. In shallower water areas tidal corrections are required to adjust the data to the correct datum. In waters deeper than the continental shelf, tidal corrections are not required. All

of these parameters are measured and entered in the multibeam echosounder system and/or navigation system.

The acoustic data acquired over Anton Dohrn Seamount in 2005 were collected onboard the *SV Kommandor Jack* using a hull mounted Kongsberg EM120 system with an operating frequency of 12 kHz, capable of acquiring data in water depths up to 11,000 m. The processed multibeam bathymetry data were gridded to a spatial resolution of 20 m. The data collected during this cruise were not part of the work of the thesis but have been used as an additional data source and warrant introducing here.

The *RV Celtic Explorer* was used during the 2007 survey of the SW Approaches with acoustic data acquired using a hull mounted Kongsberg Simrad EM1002 system with an operating frequency of 98 kHz, capable of acquiring data in water depths up to 1000 m. The processed multibeam bathymetry and backscatter data were gridded to a spatial resolution of 25 m, although the data quality allowed subsequent re-gridding at finer resolutions.

In 2009, the *MV Franklin* was used to survey Anton Dohrn Seamount (see Chapter 3) which was fitted with a Kongsberg EM710 system with an operating frequency of 70-100 kHz, capable of collecting data in water depths up to 2000 m. The processed multibeam bathymetry and backscatter data were acquired from two survey areas, one from the North West flank of the seamount, the other from the south east flank. The high resolution acoustic data were acquired to complement the broader scale, lower resolution acoustic data acquired during the 2005 survey. The processed bathymetry data were gridded to a spatial resolution of 15 m.

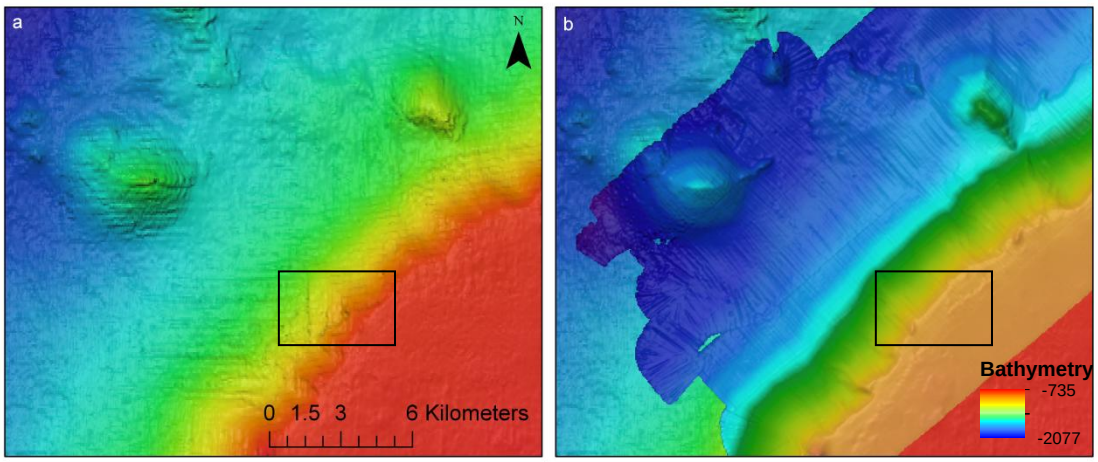

Fig. 2.3: Image of multibeam bathymetry acquired on the northwestern flank of Anton Dohrn Seamount during the 2005 (a) and 2009 (b) cruises. The low resolution data gridded at 20 m (a) and the higher resolution gridded at 15 m (b), and thus features are more clearly resolved in (b). This is illustrated by the edge of the seamount (as highlighted by the insert boxes), which is better resolved from the higher resolution dataset (b).

2.3. Biological sample design, data collection and analysis

2.3.1 *Sample design*

Video transects were undertaken over both megahabitat features and used to ground-truth the acoustic data. Transect length ranged between 0.5 km and 3.3 km, but were for the most part approximately 500 m long. Variations in transect length was either a result of poor sampling conditions (e.g. rough terrain, strong currents) or the desire to sample complete geomorphological features (e.g. a ridge). For the majority of transects, vessel speed was ~0.5 knots, with most transects lasting between 0.5-1.5 hrs. The drop frame was deployed from the starboard side of the vessel and towed in the water column 1-3 m above the seabed (dependent on substratum type, slope angle and currents) to capture the change in habitats, seabed substratum and larger conspicuous epifauna.

2.3.2 *Video/image collection*

A Seatronics drop-frame camera system (Fig. 2.4) was used during each survey to enable characterisation of deep-water benthic habitats and seabed substratum. Camera-transects were selected using the multibeam bathymetry and backscatter datasets to capture varying inferred sediment type (inferred from backscatter intensity), geomorphological features and water depth. To ensure comparability between datasets, the same standard setup was used for each survey, although position of lights and camera varied slightly from year to year, thus, highlighting the importance of calibrating the field of view of the camera for each survey.

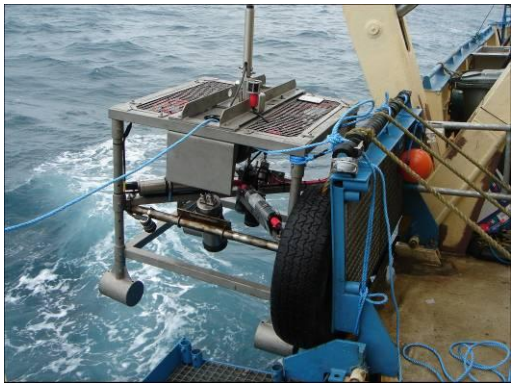

Fig. 2.4: The Seatronics drop frame camera system being deployed from the *MV Franklin*. Photograph taken by K. Howell.

The Seatronics drop-frame was fitted with a camera system, four lights set at oblique angles to the seabed to provide optimal illumination, and a flash unit to provide additional light for the collection of still images. The camera system comprised a DTS 6000 digital video telemetry system with a live feed to the surface, and a five megapixel Kongsberg Simrad digital stills camera (containing a Canon Powershot G5). The cameras were mounted opposite each other (with lights either side) at oblique angles to the seabed for optimal seabed coverage and to aid species identification. The frame was

also fitted with sensors to record depth, altitude and temperature, and an ultra-short baseline (USBL) beacon to collect accurate positional data for the frame.

Prior to data collection, the fields of view for both the stills and video cameras were calibrated by attaching a gridded quadrat of known dimensions to the camera frame which could be overlaid on stills images to allow quantitative analysis of fauna. Calibrations were made for 'on bottom' (drop frame sitting on the seabed; Fig. 2.5) and at 1 m, 2 m and 3 m elevation off the seabed. The calibration grid allowed measurements to be made of area cover of encrusting, colonial and lobose growth form organisms.

Fig. 2.5: Image of the calibration grid (on bottom) overlaid on a sample image from the 2009 survey. The grid cell size is 4.9 cm (vertical in figure) by 5.5 cm (horizontal in figure).

Following the MESH guidelines for data collection, a 2-5 min camera stabilisation period was undertaken at the beginning of each transect to ensure the camera was moving at a constant speed. Video footage was recorded along the entire transect, and at

approximately one minute intervals the drop-frame was landed and a stills image taken (sampling unit) which will be referred to here as a 'sample' image. Additional images were also taken to capture abrupt changes in substratum and to aid in species identification.

2.3.3 *Data analysis*

'Sample' images (those taken *approx*. every minute) and those that captured abrupt changes in substratum were examined to assess their quality for analysis, those which were designated 'of poor quality' (i.e. obscured by silt clouds, out of focus, or too high off the seabed to identify organisms) were not included in the analysis. Remaining sample images were quantitatively analysed using the calibration grid as a measure of area.

An inherent problem with working with deep-sea imagery data is that it is difficult and often impossible to identify organisms to species level without the use of physical samples, this is particularly true for poorly-sampled regions. However, observed organisms can be identified as distinct morphospecies [Operational Taxonomic Units (OTU)] which can correspond to species, genus, family or higher taxonomic levels. The use of OTU numbers, rather than taxonomic identifications, adds an extra level of resolution to the data, as functional groups can be used and it also allows the data to be revisited and identifications changed, enabling the dataset to be more readily combined with others.

All visible organisms >1 cm (at their widest point) were identified as distinct morphospecies (morphotypes) and assigned an OTU number (See electronic appendix for species catalogue). OTUs were identified to the lowest possible taxonomic level.

This work contributed towards the development of an image catalogue of deep-sea species, which is now available on the web for use by the wider deep-sea community [Howell and Davies (2010) http://www.marlin.ac.uk/deep-sea-species-image-catalogue/]. All individuals were counted, except in the case of encrusting, colonial and lobose forms, where area cover was recorded using the calibration grid overlain on the image as a quadrat (as described by Underwood and Chapman 2005). Image data were standardised to individuals/1 m^2 and percent cover/1 m^2 for each taxon.

A measurement scale that has been adopted to define littoral and sublittoral biotopes is the SACFOR scale (Connor and Hiscock 1996) where abundance estimates are based upon individual counts or the percentage cover of organisms. As the scale used is a ranked abundance scale it is only semi-quantitative and a level of resolution is lost in the data. Therefore, it was decided not to use the SACFOR scale for this study. The high resolution of the still images obtained (ability to identify species as small as 1cm) and the full calibration of the stills camera undertaken, meant that high resolution, quantitative biological data was attainable and using the SACFOR scale would not accurately reflect higher abundance, smaller species (Underwood and Chapman 2005). Additionally, full quantitative data was desired to use to measure diversity of the biotope, to aid in their characterisation.

To allow the combination of the two matrices for the cluster analysis and without losing partial resolution of the data by converting it to a semi-quantitative SACFOR scale, each matrix was standardised to the same scale (Stevens and Connolly 2004; Howell *et al.* 2010b). Count and cover data were treated independently prior to multivariate analysis, each were standardised to 1 m^2 (percent/1 m^2 for cover) and transformed according to the distribution of data. Standardisation per matrix was achieved by

dividing the matrix through itself and multiplying it by an appropriate factor to put the count and cover on relative scales (Prof. R. Clarke *pers. comm*).

2.4 Substratum classification

To enable definition of biological assemblages to use as mapping units to produce habitat maps, it is important for the classification of the substratum to be biologically meaningful; this is not always the case with existing classification systems. The Wentworth scale (Wentworth 1922) has eight grain size classes for sediment ranging from clay to boulder (Table 2.1), and while the Folk scale [(Folk 1954) see below for details] uses the Wentworth scale for grain size, it uses relative proportions of fractions of sediment to give more detailed sediment types, i.e. sandy mud, but does not distinguish between grain sizes greater than gravel (*sensu* Wentworth 1922). While both these classification schemes are widely-used they are unsuitable for defining mixed substrata.

The European Nature Information System (EUNIS) scheme is a pan-European hierarchical habitat classification scheme that was designed to facilitate and standardise data collection and description across Europe; which, in the context of producing habitat maps, is vital to allow continuity of data. All habitat types are covered within EUNIS, including terrestrial, freshwater and marine. Substrata are classified to level 3 for the deep sea (Table 2.2). The addition of bioherms and rock in this classification scheme are more biologically meaningful in terms of distinct communities that may use them as a habitat.

To produce a more coherent, biologically-meaningful substratum classification system, elements from both the Wentworth and EUNIS scheme were combined and, where

appropriate, modified. Grain size was recorded according to the Wentworth scale, but both primary (>50%) and secondary (<20%) substrata were recorded following the methods of Hixon *et al*. (1991). The EUNIS scheme does not sub-divide 'Bioherms' but many authors have reported different communities associated with different bioherm zones, thus a distinction was made between zones: mostly live coral (summit), or mostly dead framework and coral rubble as described by Mortensen *et al*. (1995), Pfannkuche *et al*. (2004), Wienberg *et al*. (2008), Roberts *et al*. (2009). For each 'sample' image substratum composition (type and percent cover) was classified according to the new classification scheme (Table 2.3). Due to the difficulty in classifying finer scale sediment (sand-gravel) from images, for those images inferred interpretation was cross-referenced with the expert interpretation which was undertaken by the British Geological Survey [(BGS), described below].

Systematic offshore survey work (geophysical and sampling) by the BGS began in 1966 and regional interpretations of the seabed sediments based in sieve analysis of samples obtained from Shipek grabs and sub-samples from the tops of gravity cores and vibrocores were produced (e.g. Graham 1990). Gravel percentage and sand to mud ratio maps were prepared and contoured at intervals corresponding to the divisions indicated on the modified Folk diagram (Graham 1990). In the deep water areas of the UK, beyond the continental shelf break, systematic seabed sediment maps such as Graham (1990) were not produced due to the sporadic distribution of seabed samples. The study areas covered in this thesis benefitted from the acquisition of multibeam echosounder and photographic ground-truthing data which, when used in conjunction with the existing BGS seabed samples, allowed systematic mapping of the seabed to take place.

For each digital stills image acquired, a seabed sediment classification was assigned, by marine geologists at the BGS, based on the modified Folk diagram utilised by Graham

(1990). These point classifications were used in conjunction with the existing BGS samples (discussed above) to ground-truth the multibeam echosounder data allowing a complete seabed substratum interpretation (polygon layer) to be created in an ArcGIS environment (Stewart 2011). The BGS seabed samples allowed the finer sediment fractions (mud and sand) visible in seabed photographs to be interpreted, even though the use of the calibration grid was not adequate for quantitative interpretation of the sand to mud boundary by visual means alone. It should be noted that backscatter data quality was not adequate to allow automated seabed sediment, or facies, classification although the backscatter was used to help aid delineation of boundaries where possible.

1

Particle size	Term
>256mm	Boulder
64-256mm	Cobble
4-64mm	Pebble
2-4mm	Gravel
0.0625-2mm	Sand
<0.0625mm	Mud
0.0625mm-2µm	Silt
<2µm	Clay

2

Level	Classification factor	Categories
Level 1	Habitat	Marine
Level 2	Depth zone	Deep-sea bed
Level 3	Substratum	Rock, mixed, sand, mud, muddy sand and bioherms
Level 4	Habitat	Various habitats

3

Substratum
Sand
Mud
Gravel
Mixed substratum: Pebbles
Mixed substratum: Cobbles
Mixed substratum: Pebbles & cobbles
Mixed substratum: Boulders and cobbles
Mixed substratum: Boulders
Rock: Bedrock
Bioherm: Biogenic gravel (coral rubble)
Bioherm: Live summit
Bioherm: low-lying coral (dead framework)

Tables 2: Table 2.1 is the Wentworth grain size scale, Table 2.2 is the EUNIS habitat classification scheme and Table 2.3 is the new substratum classification used in this study.

2.5 Characterisation of biotopes

2.5.1 Identification of biotopes

The production of habitat maps for use in Marine Protected Area network design requires the ability to map the biology at an appropriate level for use in planning, given the resolution of the underlying acoustic data. Due to the coarse resolution of acoustic data from the deep sea, mapping at a 'community' level is necessary to cover the vast area involved. To achieve this, biological assemblages or 'biotopes' are used as mapping units, where they represent distinct biological assemblages associated with certain environmental factors such as substratum and depth (Dahl 1908).

Biotopes were defined using multivariate analysis [PRIMER v. 6 (Clarke and Gorley 2006)] applied to quantitative morphospecies data derived from image analysis. Cluster analysis is a method for finding hierarchical grouping in multivariate datasets, and SIMPER [similarity percentage (Clarke 1993)] is a simple method for assessing which taxa are primarily responsible for an observed difference between groups of samples identified from the cluster analysis (Clarke 1993). SIMPER is not a statistical testing framework, but an exploratory analysis that indicates which species are principally responsible either for an observed clustering pattern, or for differences between sets of samples (Clarke and Warwick 2001). The ratio between the contribution each species makes to the average similarity within a group (sim) and the standard deviation (SD) of its contribution can be used to determine those species that typify a group; those species that are consistently abundant throughout, where the SD of its contribution is low, and the ratio between sim/SD is high is used to identify those species which characterise that cluster (Clarke 1993), additional species had to contribute > 5% to that clusters to be considered a characterising species. The SIMPROF [similarity profile (Clarke *et al*.

2008)] routine looks for statistically-significant evidence of genuine clustering in samples which are unstructured *a priori*.

As the purpose was to define benthic assemblages, highly mobile species such as fish were removed from the dataset prior to the analysis. Cluster analysis was used to identify significant clusters; the SIMPROF routine was undertaken on transformed, Bray-Curtis similarity matrices. Once significant clusters were identified, the SIMPER routine was used to determine which species were driving the clustering. Data were combined with available environmental data to define benthic assemblages.

Due to the nature of hierarchical analysis, samples may cluster together on the basis of a single, often abundant, species. The resulting cluster may not represent a distinct benthic assemblage that easily functions as a mapping unit. A number of criteria were used to accept / reject those clusters identified by SIMPROF, to remove outliers and to remove those which did not serve as coherent biological assemblages that could be used as mapping units:

1. Outlier clusters were taken at a 1% Bray-Curtis similarity level on the dendrogram and discarded.
2. Clusters that contained less than 7 images were deemed as not adequately representing a coherent assemblage and were also discarded.
3. Those clusters that have an average similarity (SIMPER) of less than 15% were defined as not being coherent.
4. In line with habitat classification, SIMPROF clusters can be split on the basis of substratum.
5. SIMPROF clusters can be combined at a lower similarity node on the dendrogram to produce more practical mapping units (appropriate scale).

Biotopes were defined as distinct benthic assemblages occurring on a specific substratum, or range of substrata, over a given depth, these definitions were used to biotope map the video footage.

An essential element of biotopes is that they are practical, mappable units that can be easily recognised visually and applied at an appropriate scale for management of SACs in order to allow cost effective, rapid assessment and monitoring of sites. With sparsity and issues relating to the acquisition of deep-sea data, it may not always be feasible to strictly adhere to statistical rigour, and thus additional criteria may need to be implemented – although this process needs to be transparent. Therefore following standard multivariate analysis, faunally distinct clusters (as assessed using the criteria described above) were assessed against a second set of criteria to determine their use as mapping units. Only those clusters that subsequently met these criteria were further analysed in terms of their faunal composition and diversity. To function as a mapping unit assemblages must 1) occur at a scale relevant to the resolution of the acoustic data and the scale of existing widely accepted benthic communities, such as cold water coral reefs (e.g. 10 m scale), and 2) be easily identified from video data.

To aid in the applied use of biotope, this requires a comprehensive description which can be recognised by others. Simply using species that typify a biotope identified by the SIMPER routine may not adequately reflect the assemblage. This is particularly true in instances where the sample size is too small to fully capture larger, conspicuous fauna, which in descriptive terms is necessary for the biotope to be recognised temporally and spatially. As biotopes need to be easily recognised from video data, in addition to using the results from the SIMPER analysis, those biotopes where the SIMPER analysis had not sufficiently identified the conspicuous taxa (i.e. due to sample size being too small)

names could be derived during video mapping. Coherent clusters that related to biotopes were given a code (for ease of interpretation) according to the characterising species (morpho-types), using a maximum of two, taking the first 3 letters of each. For example, if the chacterising species were *Lophelia pertusa* and *Madrepora oculata*, the code would be Lop.Mad. As biotopes are being described to produce standard terms to be used as mapping units, and thus recognisable, a full name was given that encapsulated the dominant taxa and associated substratum.

2.5.2 Assessing biotope diversity

The advantage of recording quantitative data gives a greater resolution for assessing diversity of communities. Species richness can be measured using diversity indices, species richness estimators or rarefaction curves. Diversity indices such as Margalef (1958), Shannon-Wiener (1963) and Simpson (1949) index are commonly used in ecology and can measure richness, dominance and evenness.

Simpson's Reciprocal index [1/D; where D represents λ] was chosen as a measure of dominance as it as it is less sensitive to sample size (Lande *et al*. 2000). It was measured using the DIVERSE routine in Primer v6 (Clarke and Gorley 2006) to give Simpson's diversity index (λ) and the reciprocal form taken by 1/D. To allow comparability between data chapters, untransformed, non standardised count (1 m^2) and cover (percent 1 m^2) data were used, hence count and cover data were not on comparable scales (as they had not gone through the standardisation process described in Sect 2.3.3). Simpson's Reciprocal Index of count and cover data were measured separately for each sample image and then averaged to give a single Simpson measure per image, and expressed as the mean Simpson's Reciprocal Index per biotope.

Species richness estimators attempt to use species accumulation curves to predict the asymptote as a measure of richness, and estimate the 'total species richness', including species not present in any sample. Due to the sensitivity of the relative weighting of count and cover data to each other when combined in a single dataset, in contrast to the more flexible ability of multivariate analysis (Prof. R. Clarke *pers. comm*), incidence-based species richness estimators were chosen.

First and second order Jackknife, ICE, Chao 2 and bootstrap estimators were run on the biotope incidence data. Jackknife is a non-parametric species richness estimator. Jackknife, by removing subsets of the data and re-calculating the estimator using the reduced samples, is a good technique for reducing bias (Gotelli and Colwell 2010; Smith and Pontius 2006). First order jackknife estimator of species richness is a function of the number of rare species in a community, where it calculates the number of species that occur in only one sample. Second order jackknife additionally calculates the number of species that occur only in 2 samples in a community (Hellmann and Fowler 1999). ICE (Incidence-based estimator) estimates the sample coverage, by the proportion of assemblage richness represented by the set of replicated incidence samples. That is, the proportion of all frequencies of infrequent species (found in 10 or fewer samples) which are not unique species. Chao 2 is an asymptote estimator of minimum richness (Gotelli and Colwell 2010). Bootstrap is a resampling procedure.

When comparing species richness between multiple sites, it is important to choose a test that can tolerate variation in sample size and/or effort. Rarefaction curves estimate expected species richness (Mao tau Sobs) for a sub-sample of the pooled total species richness, based on the species actually discovered (as opposed to estimators that estimate species richness including species not sampled) (Gotelli and Colwell 2010) and

allow interpolation at lower sample size. Rarefaction overcomes sampling bias and sampling differences (Ludwig and Reynolds, 1988).

A single diversity index is often not sufficient to allow adequate comparisons between assemblages (Hayek and Buzas, 1997), thus multiple indices were used to compare diversity of biotopes. To allow comparison between biotopes, raw, untransformed count and percent cover (standardised to 1 m^2) data were used for the Simpson diversity index, and incidence data for all others. Dominance (Simpson Index) and species richness (total number of species) was measured for all images belonging to each biotope and compared using an Analysis of Similarity (ANOSIM) test. Due to violations in the assumptions required to run a parametric 1-way Analysis of Variance (ANOVA), it was not plausible to use this test and ANOSIM was used instead. As these tests do not take into account variation in number of sample between biotopes, expected species richness (Sobs) derived from rarefactions curves and species richness estimators at a standardised sampling effort (EstimateS 8.2) were measured. A holistic approach was also undertaken, by using multivariate tests to compare diversity between biotopes. Simpson Index, Sobs, and species richness estimators (ICE, Jack 1 and 2, Chao 2, Bootstrap) were used for the multivariate test, and an ANOSIM run to compare diversity between biotopes.

2.6 Map production

2.6.1 *Substratum and geomorphology maps*

Seabed substratum and geomorphology were interpreted by the BGS and provided as polygon layers produced in ArcGIS 9.3. Seabed substratum were interpreted using multibeam bathymetry and backscatter data, ground-truthing data (still images) acquired

during surveys, and sub-bottom profiling data and sediment cores from the BGS regional mapping program (see sect. 2.4). The geomorphology of the study areas were interpreted using the same standards and techniques utilised to map 'landforms' onshore, including integration of all available datasets as per the seabed substratum interpretation. Individual features were identified to the best resolution of the data available. Terminology used was standard geological terms and definitions (e.g. Allaby and Allaby 1990). Refer to Stewart (2011) for full details of substratum and geomorphological interpretation.

2.7.2 *Biotope maps*

To aid in the interpretation and mapping of habitats, bathymetric terrain analysis was undertaken using the spatial analyst tool Benthic Terrain Modeler (Wright *et al.* 2005) and the Digital Elevation Models tool (Jenness 2010) in ArcGIS 9.3. Using multibeam echosounder data, derived layers of Bathymetric Positioning Index (BPI) (fine and broad), aspect, slope and rugosity were produced. Depth was derived from the multibeam echosounder data. These parameters can be used as surrogates to map the distribution of biotopes in the absence of biological data; this is discussed in more detail in Chapter 5.

Simplistically, statistical modelling can either be for explanatory or predictive purposes. Explanatory models measure the strength of the relationship between variables, thus testing causal theory, while predictive models are used to predict new or future observations (Shmueli, 2010). Generalized Additive models (GAMs) were used to measure the strength of relationships between the distribution of VME biotopes and physical parameters, to determine which variable (or combination) were significant surrogates to use for mapping of biotopes (Full descriptions are given in Chapter 5).

Video footage was reviewed and classified according to newly defined biotopes; change in seabed substratum using the new classification (Table 2.3) was also recorded. To produce biological distribution maps, geological layers of seabed substratum and geomorphology (produced by the BGS) were used in conjunction with bathymetric derived layers in the production of the final biotope maps. To achieve a full coverage map, a base layer is needed that can be further divided, in this instance, the substratum layers were used as base layers. Classified video data were imported into ArcGIS 9.3 and overlaid on all available data layers (bathymetric derivatives, substratum and geomorphology). The results of the modelling were used to inform relationships between VME biotopes and data layers, as to which layers to use for mapping the biotopes. VME biotopes were mapped across the survey areas using the results from the GAM to identify where substratum polygons could be further divided, or in instances where no relationship was found between VME biotopes and physical parameters, the base polygon which it occurred in was labelled with that biotope. To aid in the interpretation of the maps, a confidence map was also produced. This is important in terms of identifying the resolution of acoustic data and if ground truthing data was used to map a biotope in a given polygon. When mapping across large areas, using multiple resolution datasets, this is particularly important in terms of planning protected areas, as it allows a confidence to be assigned to the occurrence of a biotope. Once VME biotopes were mapped, all remaining biotopes were subsequently mapped across the survey area. This will be covered in more detail in Chapter 5.

Having covered all the methods and equipment used in the acquisition and analysis of the survey data presented in this thesis, the first data chapter follows, which is the definition of benthic assemblages from Anton Dohrn Seamount, and their distribution across the seamount, particularly in relation to geomorphology.

CHAPTER 3

BENTHIC ASSEMBLAGES OF THE ANTON DOHRN SEAMOUNT: DEFINING BIOTOPES TO SUPPORT HABITAT MAPPING EFFORTS

3.1 Introduction

With increased pressure on the marine realm, the need for better spatial management of our marine environment is growing globally; specifically, there is an impetus for the establishment of networks of Marine Protected Areas (MPAs) driven by global, European and national (within the UK) initiatives (92/43/EEC; CBD 2004; OSPAR Agreement 2008-6). One of the criteria by which MPAs are selected includes the protection of habitats and species that have been identified as rare, sensitive, functionally important, and threatened and / or declining (Convention on Biological Diversity (CBD) decision IX/20).

A number of habitats are listed under these various initiatives. Cold-water coral reefs, coral gardens, sponge dominated communities, seep and vent communities, and communities which are composed of epifauna that provide a structural habitat (e.g. xenophyophores and sea pens) for other associated species, are listed as Vulnerable Marine Ecosystems (VMEs) (FAO 2009). OSPAR lists a number of deep-sea habitats as 'threatened or declining', including: seamounts, *Lophelia pertusa* reefs, coral gardens, carbonate mounds, and sea pen and burrowing megafauna communities; while cold-water coral reefs, coral gardens and sponge dominated communities all come under the definition of Annex I listed 'reef' habitat under the Habitat Directive (92/43/EEC).

To date, a small number of MPAs have been established in the NE Atlantic deep-sea / high seas using one or more of these legal mechanisms. Existing MPAs have been designated on the basis of the known occurrence of *Lophelia pertusa* (e.g. NEAFC/EU fisheries closures and UK Government proposals for SCIs on Hatton Bank and Rockall Bank; (NEAFC 2007; EC 2008; NEAFC 2008) or are seamounts (e.g. NEAFC fisheries closures on the Mid Atlantic Ridge (MAR); (NEAFC 2009). The NEAFC fisheries closures on the MAR fall within a proposed OSPAR MPA (OSPAR ICG MPA, 2008) which encompasses a large area north and south of the Charlie-Gibbs Fracture Zone. To date there have been no closures made for other 'listed' habitats.

One of the principal difficulties in designating MPAs for the protection of 'listed' deep-sea habitats is a lack of detailed distribution data, e.g. maps. Mapping the distribution of deep-sea habitats is a necessity for governments if they are to adequately manage their offshore areas. Habitat mapping can be undertaken at different spatial scales, ranging from individual organisms up to ecosystems and landscapes (Buhl-Mortensen *et al.* 2009), and the method used often depends on the purpose for which the maps were created. To allow sustainable management of the marine environment, reliable habitat maps are required at a regional, and at a national level (Huang *et al.* 2011). Typically acoustic data (multibeam and/or sidescan sonar) is acquired, and interpreted to produce geomorphological / seabed substratum maps which may be ground-truthed. The use of large topographical features such as seamounts, banks and submarine canyons as a megahabitat landscape, (*sensu* Greene *et el.* 1999) at scales of kilometres to tens of kilometres has been used (Heap and Harris 2008), and proven useful for broad scale mapping over large areas. Whilst broad scale mapping may adequately represent some habitats, others are not distributed at the same spatial scale and thus require a different approach. To adequately represent the biology it is necessary to understand the

distribution of habitats at a data acquisition level, or fine-scale, which can be related to typically more generalised, broad scale maps which cover a wider geographic area.

Relationships between biological assemblages and geomorphological features at a mesohabitat scale (tens of metres to a kilometre; *sensu* Greene *et al*. 1999) have been reported, e.g. cold-water coral reefs associated with mound features (De Mol *et al.* 2002; Roberts *et al.* 2003; Henry and Roberts 2007). In general, a top down approach has been used whereby geomorphological units are mapped and then assumed to be biologically meaningful. However, a bottom up approach can be used where biological assemblages are described following community analysis (Howell *et al.* 2010b) and subsequently used as biological mapping units to generate habitat maps that are more ecologically meaningful (Shumchenia and King 2010); the relationship between biological assemblages and geomorphology at the meso-scale can then be investigated. Once the relationship between biological assemblages and geomorphology is understood, it may be possible to then 'scale it up' and relate biological assemblages to broad-scale geomorphological features which are inherently more easily mapped and can be used as a surrogate to predict the distribution of benthic habitats. This approach is particularly important in the deep sea and for habitats of conservation concern such as 'listed' habitats. The area covered by the deep sea is vast, and mapping efforts in this area are generally only likely to be at very broad scale and using readily available data such as biogeographical region, depth, and broad scale geomorphology (Harris and Whiteway 2009; Howell 2010).

A necessary prelude to mapping is therefore the identification and description of biological assemblages for use as mapping units. To allow comparability between maps from different areas / regions, which is essential for the implementation and

management of MPAs, it is important to use consistent terms for mapping units and to have adequate descriptions for these habitats so that these terms can be used across geographic regions (Greene *et al.* 1999; Howell 2010). In the deep sea there have been few attempts to produce descriptions of benthic assemblages for use in mapping (Le Danois 1948; Laubier and Monniot 1985; Howell *et al.* 2010b). Whilst some benthic assemblages are broadly recognised through the scientific literature, e.g. cold-water coral reefs, ostur (sponge communities), others have been described through the political process (e.g. coral gardens (OSPAR MASH 07/4 – Agenda item 4). Few 'listed' deep-sea habitats are supported by scientifically robust descriptions of community composition such that coherent mapping units can be described, and the relationship between 'listed' habitats and 'more easily mapped' geomorphological features remains unknown. As nearly all specifically 'listed' deep-sea habitats have been identified as occurring on seamounts, this study focuses on the Anton Dohrn Seamount, NE Atlantic.

The aims of this chapter are to:

1) *identify deep-sea benthic assemblages from Anton Dohrn Seamount that can serve as classification units in habitat mapping efforts.*
2) *identify biotopes of conservation interest under international/national policy and provide estimates of their biological diversity.*
3) *describe the distribution of biotopes of conservation interest in relation to the geomorphology of the seamount system.*

To address these aims, data acquired from transects collected using a drop-frame camera system will be analysed. Still images will be quantitatively analysed to

identify distinct morphospecies and community analysis undertaken to identify faunally distinct assemblages. Diversity will be measured for those clusters deemed as representing a coherent mapping unit (biotope) (as determined through assessment against pre-defined criteria). Described biotopes will be used to map the video data on either side of the seamount and to qualitatively assess the distribution of biotopes in relation to geomorphology. At a megahabitat scale, the possible hydrographical influence on faunal assemblages either side of the seamount will be tested using a PERMANOVA test.

3.2 Methods

3.2.1 *Study area*

Anton Dohrn Seamount (ADS) is a former volcano located to the west of Scotland in the northern Rockall Trough between the Hebrides Shelf and Rockall Bank within the UK's territorial waters (Fig. 3.1). Simplistically the feature is roughly circular in plan view, approximately 40 kilometres in diameter with a relatively flat summit at a depth of approximately 520 m below sea level with steep flanks. The seamount is encircled by a well-developed moat feature.

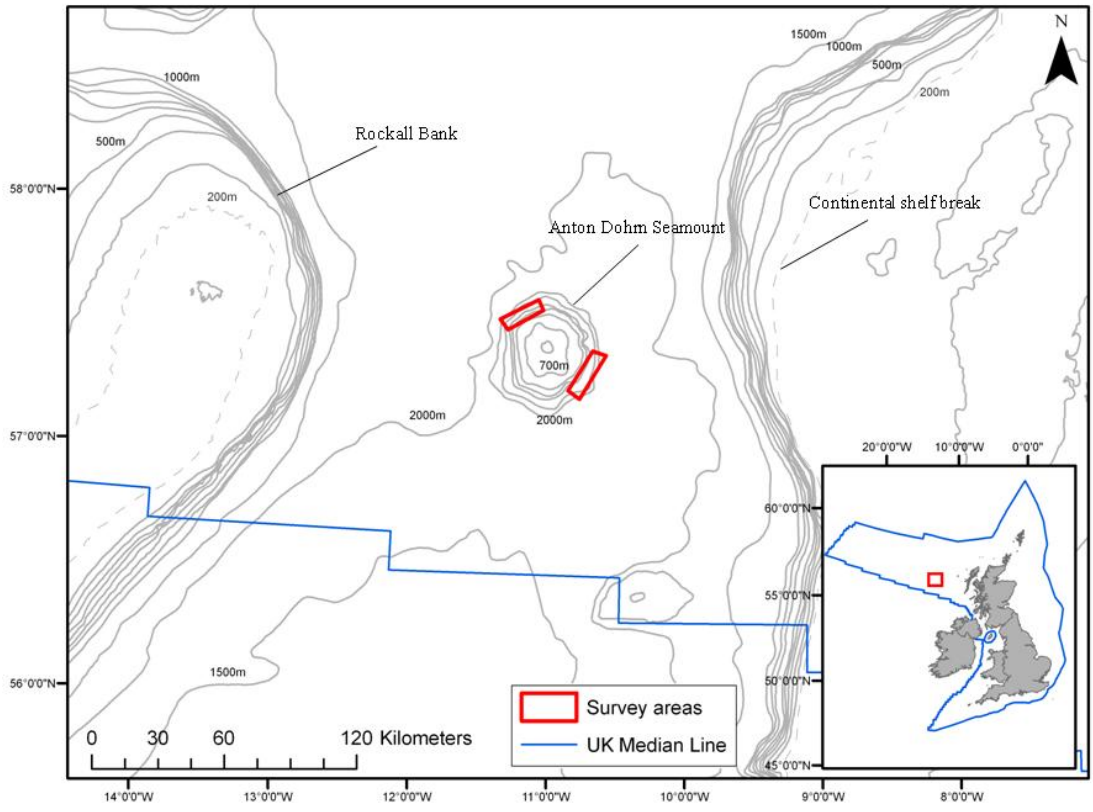

Fig. 3.1: The study area west of Scotland. The 2009 survey areas on the NW and SE sides of Anton Dohrn Seamount are marked. Bathymetric contours are provided by GEBCO, the 200 m depth contour (dashed line) marks the approximate position of the Continental shelf break. The UK median line corresponds to the UK Continental Shelf Limit.

The seamount is somewhat asymmetrical with the north-west (NW) side being shallower, with a shelf break at ~845 m water depth and flanks descending to a depth of ~2195 m in the moat, while the south-east (SE) has a shelf break at ~875 m water depth descending into the moat at 2300 m water depth. The bulk of the seamount probably comprises basaltic lavas (Jones *et al.* 1974; Jones *et al.* 1994; Stoker 2002) with a south-east thickening wedge of sediments on the top of the seamount identified on British Geological Survey seismic data.

The hydrographic activity within the Rockall Trough (RT) is complex and has been researched for many years. The Eastern North Atlantic Water (ENAW) flows along the continental slope and enters the southern part of the Rockall Trough and circulates in an anti-cyclonic direction and exits the trough to the NW (Lonsdale and Hollister, 1979). The slope current continues to transport warm, saline water along the shelf northwards across the WTR into the FSC (Ellett *et al.*, 1986). This ENAW has been found to occur to depths of approximately 750m overlaying Mediterranean Overflow Water (MOW) along the eastern flank of Porcupine Bank (De Mol *et al.*, 2002). The NW flank of ADS may be influenced by the Arctic waters that periodically overflow the WTR [Wyville Thomson Ridge Overflow Water (WTOW)] from the FSC, whilst it is unlikely that the SE side of ADS is influenced by this current (Johnson *et al*. 2010). To date, little has been documented about the pathways of this water into the RT. The biological communities from the contrasting warm and cold water masses are known to be strikingly different (Jones *et al*., 2007) and thus the periodic flushes of cold, nutrient rich waters into the Rockall Trough may have a significant influence on the distribution of species from the Arctic.

3.2.2 *Data acquisition*

In 2009, the NW and SE flanks of Anton Dohrn Seamount were surveyed using multibeam and video ground-truthing to identify VMEs (Fig. 3.2). Acoustic and biological data were collected from the survey areas over a four week period (July 2009) using the commercial research vessel *MV Franklin*. High resolution acoustic data were collected using a hull mounted Kongsberg EM710 multibeam echosounder system capable of operating in water depths up to 2000 m. Swath width was between 1.0-1.5 km and the operating frequency range for the system was 70-100 kHz. Data were processed on-board and gridded at a resolution of 15 m to allow detailed interpretation of meso-scale geomorphological features.

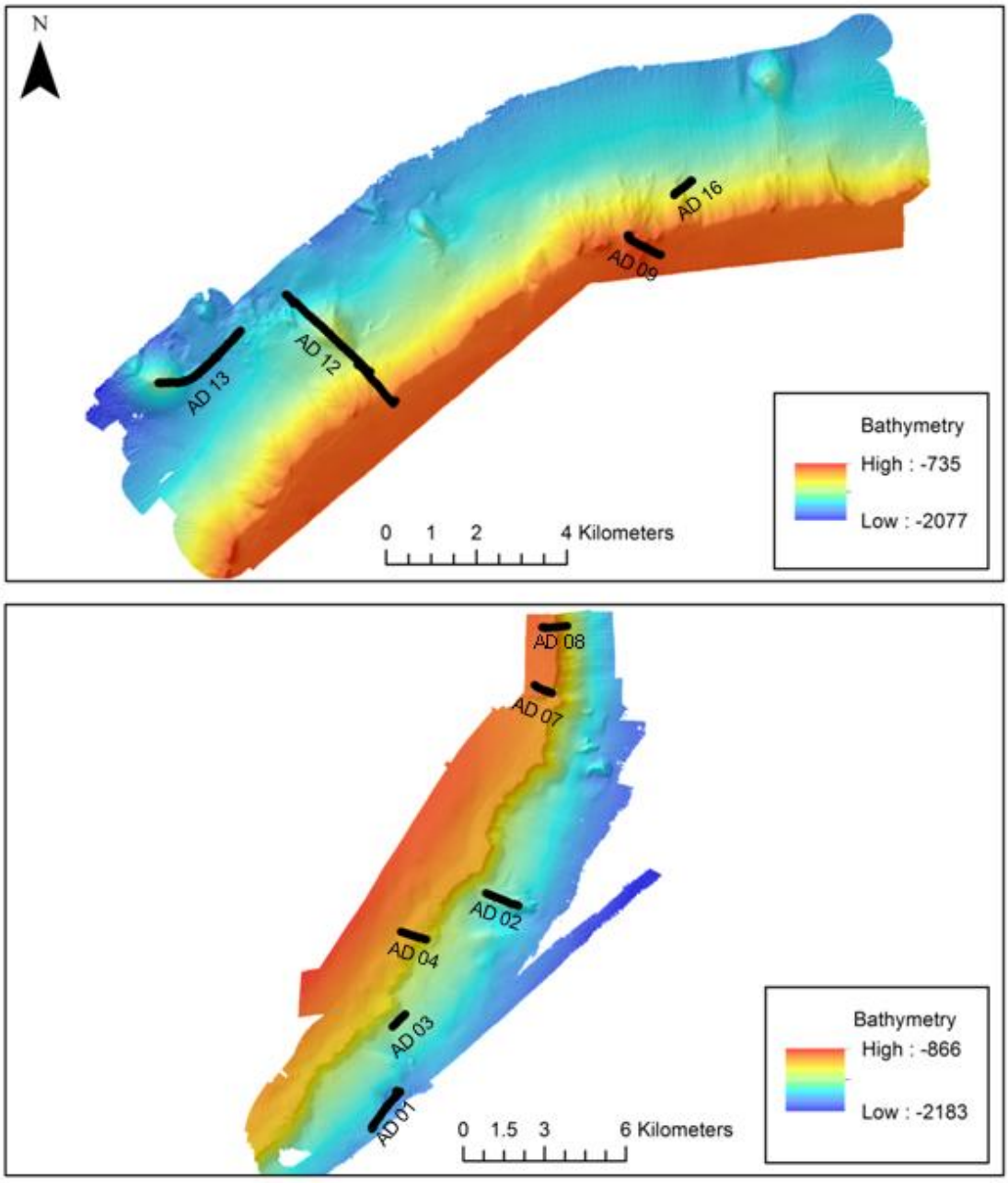

Fig. 3.2: Camera transects sampled from the NW (top) and SE (bottom) survey areas of Anton Dohrn Seamount overlaid on multibeam bathymetry.

Video and image data were collected from ten stations (four in the NW and six in the SE) using a drop-frame camera system. To achieve the main aim of the survey and characterise benthic assemblages of the seamount, transects were chosen to attempt to best capture the range of habitats on either side of the seamount. This was achieved by using the processed multibeam bathymetry and backscatter data to choose transects that represented different depths, interpreted geomorphology and seabed substratum

(inferred from backscatter data); where possible replicate sampling was undertaken both within and between the NW / SE survey areas. Orientation of transects was chosen, either to adequately sample a feature (i.e. to traverse the crest of a ridge), to maximise the depth range sampled, or simply on the basis of physical conditions, i.e. if it was safe to deploy the camera frame.

An initial calibration trial was undertaken to determine optimal camera setting for collection of high quality seabed images. Lighting was positioned for optimal illumination for video and image capture, and the stills camera was set on auto focus. Camera settings were optimised to produce seabed images of a high quality. The system comprised a 5 megapixel Kongsberg and Imenco digital stills camera and an integrated DTS 6000 digital video telemetry system. Optimal settings for the digital stills camera were established as auto focus, aperture F5.6, ISO 100, shutter speed 1/60sec and an image quality setting of 'superfine'. The drop-frame was also fitted with sensors to record depth, altitude above the seabed and temperature, and an ultra-short baseline (USBL) beacon, which is fully integrated with the vessel's digital geographic positioning system (DGPS), to collect accurate positional data for the camera frame (Stewart *et al.* 2009). Camera calibration and sampling protocols were undertaken as described in Sect. 2.3. Transect length varied between 0.5 km and 3.3 km over a depth range of 747-1887 m. The drop-frame was deployed from the starboard side of the vessel and towed 1-3 m above the seabed at a vessel speed of approx. 0.5 knots.

3.2.3 *Biological analysis*

3.2.3.i *Quantitative analysis of image data*

'Sample' images (defined in Sect. 2.3.2) and images taken to capture abrupt substratum changes were reviewed and poor quality images removed: e.g. too high off the ground,

obscured by silt clouds or blurred. The remaining samples were quantitatively analysed using the appropriate calibration grid as a measure of area. Identification of species from images is difficult, and in many cases impossible, without physical samples. This is an inherent problem when working in the deep sea, as a result of the lack of specimens from these regions and also the often poorly resolved taxonomy of many deep-sea species. However, observed organisms can be identified as distinct morphospecies (morphotypes); these can correspond to species, genus, family or higher taxonomic levels, depending on the group.

All visible organisms >1 cm (at widest point) were identified as distinct morphospecies and assigned an Operational Taxonomic Unit (OTU) number. OTUs were identified to the lowest possible taxonomic level (see electronic appendix for species catalogue). All individuals were counted except in the case of encrusting, colonial and lobose forms, where percentage area cover of the organism was used. Image data were expressed as either individuals/1 m^2 or percent cover/1 m^2. For each 'sample' substratum was assessed using the substratum classification described in Sect. 2.4 (Table 2.3). Interpreted image data were stored in an Access database prior to multivariate statistical analysis.

3.2.3.ii *Community analysis*

Standard multivariate community analysis techniques (Clarke and Gorley 2006) were used to identify faunally distinct benthic assemblages within the study area (described below).

Highly mobile species such as fish, which use multiple habitats and can thus confound the result of the cluster analysis, were removed prior to data analysis. Standardisation of

count and cover matrices was undertaken to place them on a common scale to allow a single combined analysis (Prof. R. Clarke *pers.comm*). The standardisation procedure is described in Sect 2.3.3. Each matrix was square root transformed, divided through itself and multiplied to put on a common scale of 0.006-0.76 (count * 200 and cover *100). Cluster analysis with group-averaged linkage was performed using a Bray-Curtis similarity matrix derived from transformed, combined species count and percent cover data. The SIMPROF routine [similarity profile (Clarke *et al.* 2008)] was used to identify significant clusters using a significance level of $p < 0.01$ and the SIMPER [similarity percentages (Clarke 1993)] routine used to identify those species that characterise significant clusters. Characterising species were defined as those species with a high sim/SD ratio (Clarke 1993), and contributed > 5% to that cluster similarity. Clusters identified by SIMPROF ($p < 0.01$) were assessed against the criteria set out in Sect. 2.5.1 and rejected or accepted as faunally distinct clusters.

3.2.4 *Characterising mapping units (biotopes)*

There is a discrepancy between the faunal assemblages identified using community analysis methods and what is required from a practically applicable mapping unit used in producing necessarily generalised maps of variation in the biological composition of the seabed. To characterise practical mapping units which can be mapped at a scale appropriate to that of the acoustic data, those clusters identified as faunally distinct (as assessed using the criteria described Sect. 2.5.1) using standard cluster analysis techniques were assessed against a second set of criteria to determine their use as mapping units. Only those clusters which met these criteria were further analysed in terms of their faunal composition and diversity. To function as a mapping unit assemblages must 1) occur at a scale relevant to the resolution of the acoustic data and

the scale of existing, widely accepted benthic communities such as cold water coral reefs (e.g. 10 m scale), and 2) be easily identified from video data.

Mapping units, hereinafter referred to as 'biotopes', were defined in terms of their characterising species, as determined by SIMPER analysis, together with the range of environmental conditions over which they occurred in this study. A 1-way Analysis of Similarity (ANOSIM) was undertaken on a normalised, Euclidean distance matrix of environment data (depth and temperature) to test if environmental conditions were different between biotopes.

To assess biotopes which could be considered of conservation concern, identified biotopes were compared with current definitions of OSPAR and the EC Habitats Directive listed habitats. To identify specifically those which are listed as VMEs, the guidelines of the FAO and current OSPAR definitions were used.

3.2.4.i *Diversity indices*

Diversity in terms of species richness and dominance were measured to compliment the characterisation of biotopes, and allow a more complete description of the assemblages. Simpson's Reciprocal Index [1/D] was measured using the DIVERSE routine in Primer v6 (Clarke and Gorley 2006) to give Simpson's diversity index (λ) and the reciprocal form taken by 1/D. Count and cover data were measured separately for each sample image and then averaged to give a single Simpson measure per image, and expressed as the mean Simpson's Reciprocal Index per biotope (as described in Sect.2.5.2).

Species richness was measured using two methods: firstly, simply by measuring species richness per sample image and expressing as mean species richness per biotope; and

secondly, due to variation in numbers of sample images (sample size) between the biotopes, standardised species richness was measured using rarefaction curves to calculate expected number of species (Mao tau Sobs) and incidence-based species richness estimators (ICE, Chao 2, Jackknife 1 and 2, and bootstrap) using EstimateS 8.3.

One-way Analysis of Similarity (ANOSIM) tests [Primer v6 (Clarke and Gorley 2006)] on Euclidean distance resemblance matrices were undertaken to test for significant differences in diversity between biotopes (H^o: no significant difference in diversity between biotope). Univariate ANOSIMs were undertaken to compare mean species richness and dominance between biotopes and a multivariate ANOSIM was also undertaken, using a suite of normalised diversity measures [Simpson's Reciprocal Index, expected species richness (Sobs) and the five incidence-based estimators] to give a holistic view of the diversity measure.

3.2.4.ii *Distribution of biotopes*

Megahabitat scale

Given the potential difference in the hydrographic conditions on NW and SE sides of the seamount, analysis was undertaken to test the difference between species assemblages from the NW and SE side of the seamount. A full factorial type I SS covariate PERMANOVA (PERmutational MANOVA, Anderson 2008) test was performed using the previously calculated Bray-Curtis similarity matrix, first testing for variance explained by the covariate depth, then for differences between 'locations' (fixed main effect), substratum (random factor nested within location) and finally the interactions.

Mesohabitat scale

Video transects were reviewed and visually classified (guided by the sample image analysis cluster output) using the newly defined biotopes, and changes of biotope type within a transect were mapped using ArcGIS 9.3. Biotope mapped video data were overlaid on an interpreted geomorphology (undertaken by H. Stewart, BGS) polygon layer in ArcGIS and used to qualitatively describe the distribution of biotopes in relation to meso-scale geomorphology, particularly focusing on those biotopes identified as VMEs. Abiotic data were also extracted from the mapped data to define the environmental range of the distribution of each biotope.

3.3 Results

3.3.1 *Geomorphology*

In total 215 line km of multibeam echosounder data were collected over the NW and SE survey areas on Anton Dohrn Seamount covering 220.5 km^2. Interpreted multibeam data was used to identify a number of geomorphological features (Fig. 3.3 and 3.4), and interpretation was undertaken by H. Stewart from the BGS (see sect. 2.6.1). The geomorphology of the seamount can broadly be divided into the summit and flank (megahabitat scale of kilometres to tens of kilometres; *sensu* Greene *et al*. 1999) with meso-scale features associated with each (Table 3.1).

Summit	**Flank**
Cliff-top mounds	Flute
Cliff edge	Escarpment
	Parasitic cone
	Radial ridge
	Landslide/Rockfall
	Furrow/moat

Table 3.1: Meso-scale geomorphological features identified from the summit and flank of Anton Dohrn Seamount. Interpretation undertaken by H. Stewart from the BGS.

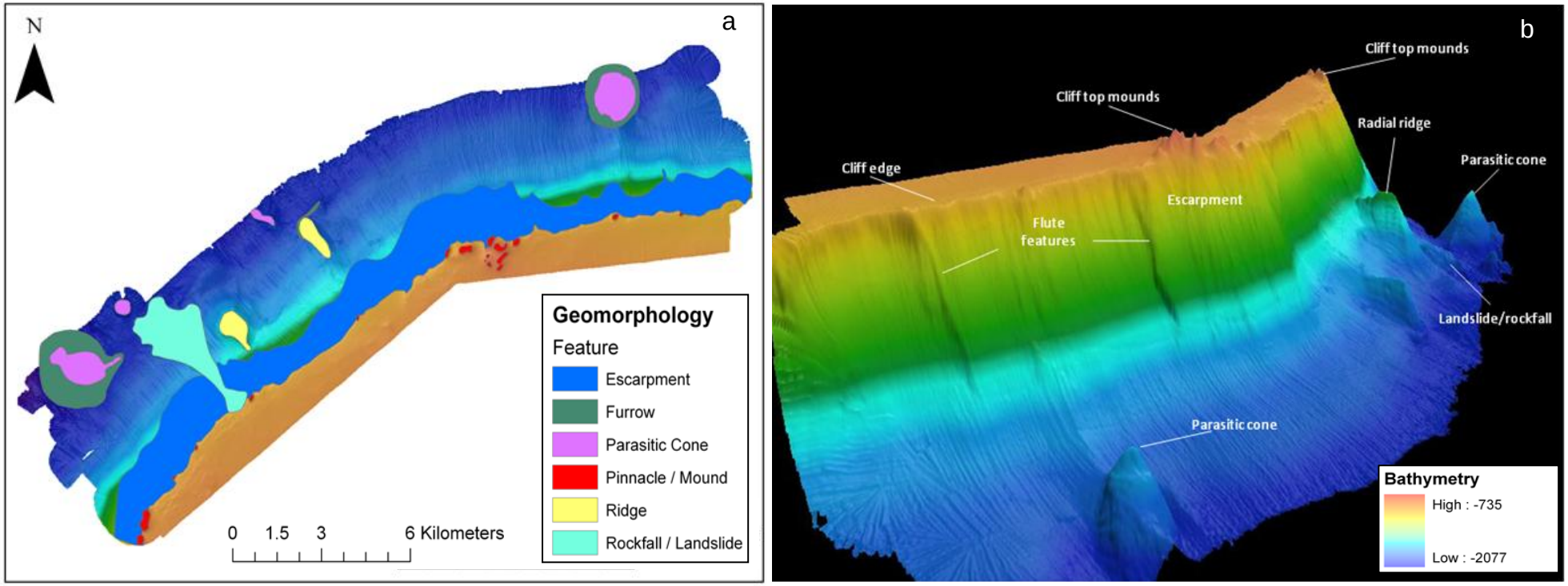

Fig. 3.3: Plan (a) and 3D perspective view (b) of multibeam bathymetry acquired over the NW flank of Anton Dohrn Seamount, meso-scale geomorphic features labelled. Fig 3.3a shows polygons of meso-scale geomorphological features interpreted by BGS. 3.3b is visualised in Fledermaus^{TM} software looking south, for scale of features see Fig. 3.3a and bathymetry colour bar see Fig. 3.3b.

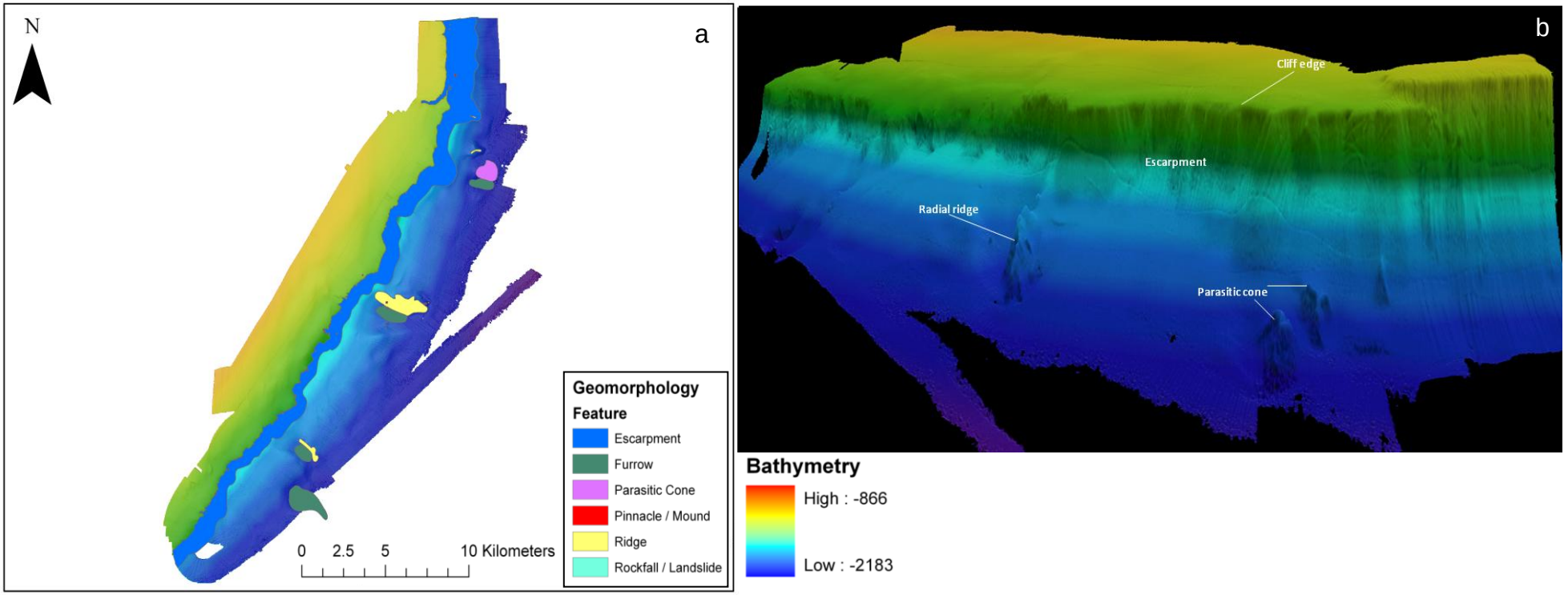

Fig 3.4: Plan (a) and 3D perspective view (b) of multibeam bathymetry acquired over the SE flank of Anton Dohrn Seamount, meso-scale geomorphic features labelled. Fig 3.4a shows polygons of meso-scale geomorphological features interpreted by BGS Fig 3.4b is visualised in Fledermaus™ software looking west, for scale of features see Fig. 3.4a and bathymetry colour bar see Fig.3.4b.

A prominent cliff edge encircles the whole seamount and was imaged in both survey areas, below which is a steep escarpment with slopes up to 40°. On the NW side of the seamount, almost vertical flute-like features, or ridges, were visible on the cliff face (flanks) (Fig. 3.3b). These flutes probably reflect variability in the erodability of the bedrock which may be due to the emplacement of igneous dykes in fissures extending from the Anton Dohrn igneous centre (Long *et al.* 2010). Radial ridges were imaged in both the NW and SE survey areas (Fig. 3.3 and Fig. 3.4); these radial ridges comprise extensive areas of rock and coarse material at seabed and are up to 100 m in height extending radially from the seamount. In the NW study area the largest radial ridge observed was almost 1 km long and ~ 0.5 km wide with slopes of up to 40°; and extending from 1260 m to 1550 m at its deepest point. A radial ridge on the SE side was similar in size and slope (almost 1.5 km long and 0.5 km wide with slope up to 42°) but occurred deeper at 1500 m at its shallowest point to almost 1800 m.

Cliff top mounds were identified from both study areas although these features were less significant in terms of their size [interpreted from the multibeam bathymetry data] on the SE flank compared to the NW flank. In the NW study area, cliff top mounds were visible along the cliff edge with each mound up to 50 m in height and 250 m wide (Fig. 3.3). In the SE study area cliff top mounds were less frequent and smaller being up to 20 m in height and 70 m wide. Parasitic cones had been identified on the lower flanks of Anton Dohrn Seamount from existing lower resolution multibeam echosounder data. Two previously identified features were located in the NW study area (Fig. 3.3), the largest of which was broadly conical in shape, ~400 m high and ~1300 m in diameter with slopes up to 45° and ranging from a depth of 1420 m to1750 m. These features have been interpreted as parasitic cones due to their shape and proximity to the Anton Dohrn igneous centre. Parasitic cones form from volcanic material erupting from lateral

fractures rather than the central, main vent of a volcano (Allaby and Allaby 1990). Moats have formed around the base of the parasitic cones in the NW study area, probably due to accelerated currents caused by the obstructive presence of the cones themselves (Long *et al.* 2010).

An area of uneven topography located at the base of the cliff at the western end of the NW study area has been identified as a submarine landslide or rockfall (Fig. 3.3) and appears to relate to a gully, or shute, on the cliff wall above. The distance from the headwall to the toe of the slide is 3.5 km and falls a height of 850 m. The clear evidence for this slide suggests that it is a young feature as it has not been reworked; however, the general uneven topography observed on the flanks suggests that there are multiple, probably small, slope failures (Stewart *et al.* 2009).

3.3.2 *Biological data*

Over 14 hours of video and 2745 still images were collected, of which 731 images were designated sample images (as described in Sect 2.3.2). Forty three sample images were omitted from the analysis due to poor quality, and 41 samples that captured abrupt changes in substratum were added to the analysis. Due to the taxonomic complexity of the images, time constraints did not allow for analysis of all sample images, thus every third sample (*approx.* 3 min intervals) was analysed (302 images). On the NW survey area transects were collected over a depth range of 747-1770 m with 7.1 line km of video acquired, and 6.4km of video over a depth range of 956-1889 m from the SE area.

3.3.2.i *Quantitative analysis of image data*

Three hundred and two still images (samples) were quantitatively analysed with 253 morphospecies identified and catalogued (see electronic appendix for species catalogue and raw data).

3.3.2.ii *Community analysis*

Thirty five clusters were identified by SIMPROF ($p < 0.01$) and using the criteria set out in Sect 2.5.1 outlier clusters (a-c) and those which contained less than 7 images (d-e, h-i, k-m, p, r-u, x-y, ac) were discarded. In addition one cluster was subjectively divided on the basis of substratum (bedrock and dead coral framework) in line with current habitat classification schemes [See Fig. 3.5, cluster (a)]. Five clusters [See Fig. 3.5, clusters labelled as (b)] were combined to give a coarser resolution cluster. Reasons for combining these clusters by moving up a node in the cluster analysis output are as follows: upon further examination of the underlying image data it was clear that the samples from the 5 clusters all occurred on the steep escarpment feature. The nature of the terrain affected how close the drop-frame camera could get to the seabed, thus making consistent sampling difficult. This was reflected in the samples, with varying sample sizes capturing fauna at different scales. These clusters were not deemed to be robust and were combined at a lower level of similarity. Given the problem with the changing size of field of view it could be argued that these data should be omitted. However, this would have resulted in no representation at all of the communities occurring on this type of terrain and seabed feature, which, given the aims of the study and the scarcity of data from seamounts, seemed the less favourable option. Thus, the data were retained but treated with a degree of caution.

The SIMPER routine was repeated to incorporate the modified clusters as described above, and results, along with environmental data, can be found in Table 3.2, and full SIMPER results in Appendix A3.1.

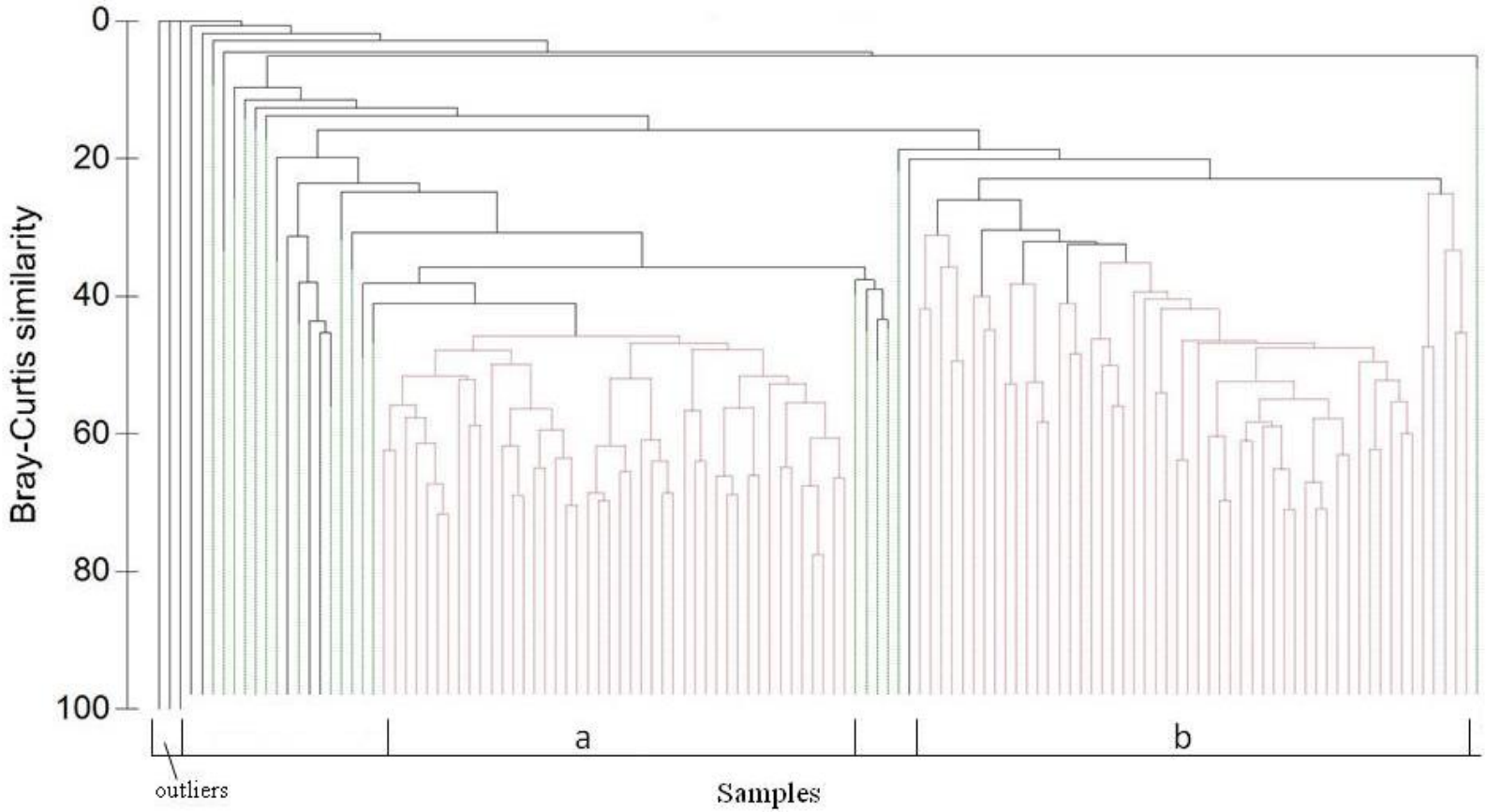

Fig. 3.5: Dendrogram of hierarchical cluster analysis of species data, clusters identified using the SIMPROF routine ($p < 0.01$), and outliers identified using a 1% Bray-Curtis slice across the dendrogram. Cluster (a) shows a SIMPROF cluster that was further divided on the basis of substratum (into bedrock and dead coral framework) and (b) shows 6 clusters that were combined at a lower similarity level. SIMPROF clusters are collapsed for ease of interpretation and are represented by green dashed lines. Grey lines represent SIMPROF identifying with no significant internal structure.

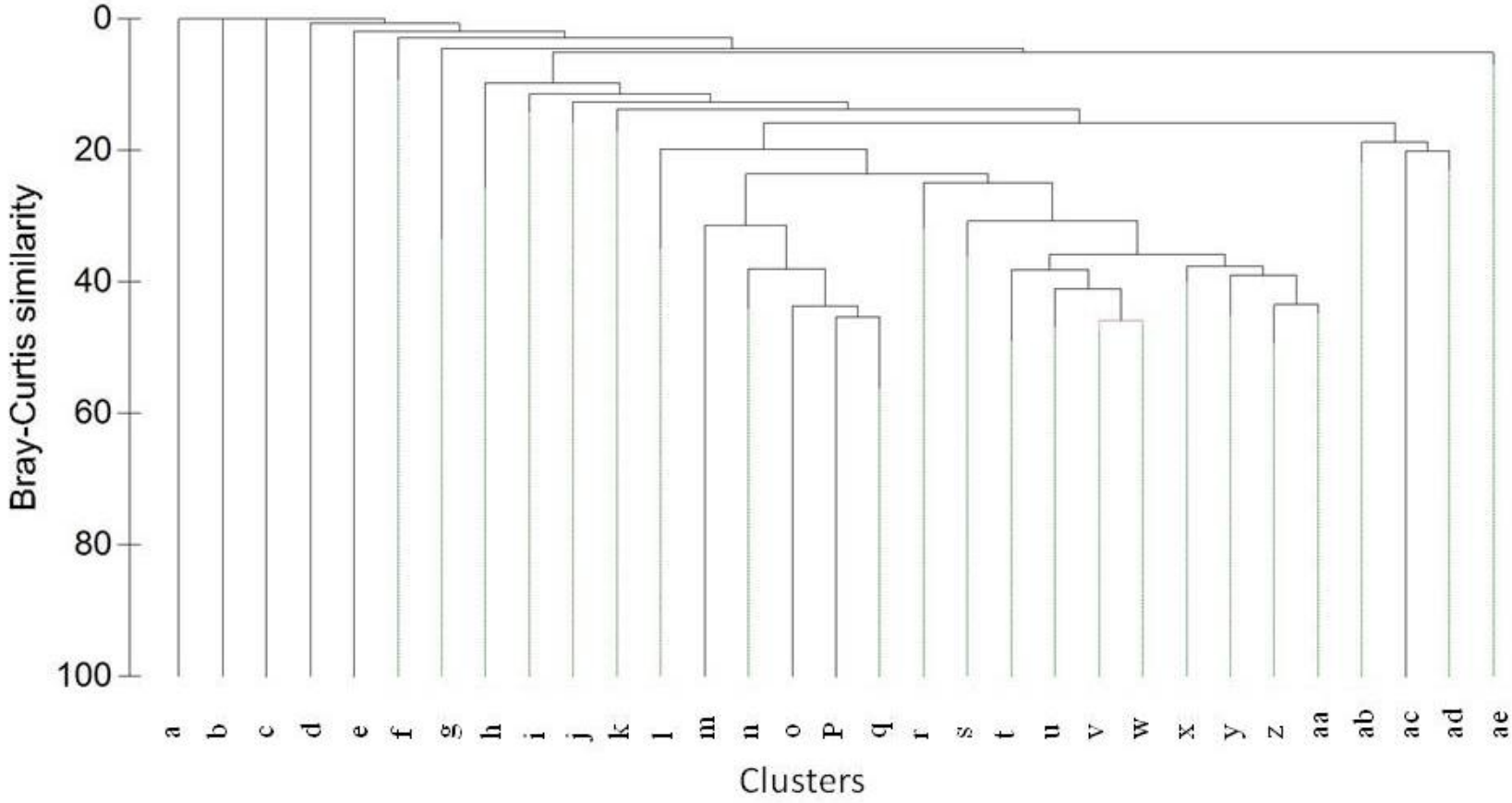

Fig 3.6: Dendrogram of hierarchical cluster analysis of species data, after cluster (a) and (b) from Fig. 3.5 were altered, to give clusters v and w (a) and ae (b) giving 31 clusters. All other clusters are those identified by the SIMPROF routine ($p < 0.01$) and collapsed for illustrative purposes.

Cluster	No. images	Useful mapping unit	SIMPER similarity level (%)	Temp range (°C)	Average Temp (SD)	Depth range (m)	Average Depth (SD)	Characterising species
a	1	N		3.894		1753		
b	1	N		3.76		1856		
c	1	N		5.5		1315		
d	1	N		5		1521		
e	1	N		7.8		1088		
f	16	Y	21.68	3.6-3.84	3.75 (0.05)	1794-1887	1847.8 (36.9)	*Ophiomusium lymani*, Unknown sp. 29, Crinoidea sp. 7
g	11	Y	19.54	3.9-9	4.92 (1.46)	810-1731	1477.7 (262.2)	*Lophelia pertusa*, *Caryophyllia* sp. 2, *Keratoisis* sp. 2, Porifera encrusting sp. 28, *Lepidisis* sp.
h	1	N		6.8	6.8	1152	1152	
i	3	N	20.38	4.4-8.8	6.04 (2.39)	854-1550	1309.7 (394)	Porifera encrusting sp. 1, Ophiuroidea sp. 2, Porifera encrusting sp. 26, Halcampoididae sp. 1, Porifera massive globose sp. 12, Porifera encrusting sp. 40
j	32	Y	24.27	3.7-5.38	4.18 (0.57)	1331-1885	1671.4 (167.8)	Ophiuroidea sp. 8, Caryophyllia sp. 2, Cnidaria sp. 1, Ophiuroidea sp. 2, *Syringammina fragillissima*, *Ophiactis balli*
k	6	N	22.70	5.6-9	7.31 (1.58)	901-1303	1116.9 (160.1)	Porifera encrusting sp. 22, Porifera encrusting sp. 1, *Lophelia pertusa* (dead structure), Porifera lamellate sp. 7, Crinoidea sp. 8
l	6	N	39.89	4.4-8.9	5.9 (2.08)	870-1534	1297.2 (277.4)	*Lophelia pertusa* (dead structure), *Lophelia pertusa*, Gorgonacea

m	1	N		9		750		
n	2	N	44.00	9-9.1	9.05 (0.07)	787-779	783.2 (5.37)	*Lophelia pertusa* (dead structure), *Protanthea simple*, *Madrepora oculata*, Cerianthidae sp. 1, Ophiuroidea sp. 2, Serpulidae sp. 1
o	1	N		9		794		
p	1	N		5.5		1316		
q	9	Y	61.70	8.8-9	8.91 (0.08)	749-790	769.4 (12.58)	*Lophelia pertusa* (dead structure), *Lophelia pertusa*, Decapoda sp. 5, *Madrepora oculata*, *Cidaris Cidaris*, Actiniaria sp.
r	4	N	35.38	8.02-8.21	8.16 (0.09)	972-1020	987.8 (22.36)	*Ophiactis abyssicola*, *Lophelia pertusa* (dead structure), Ophiuroidea sp. 6, *Psolus squamatus*
s	6	N	40.27	4.49-8.8	5.34 (1.69)	852-1570	1404.4 (271.8)	*Lophelia pertusa* (dead structure), Porifera encrusting sp. 28, Ophiuroidea sp. 8, *Ophiactis balli*, Porifera encrusting sp. 6
t	3	N	52.75	3.8-3.9	3.86 (0.05)	1701-1768	1740.7 (35.13)	*Ophiactis balli*, *Ophiactis abyssicola*, Ophiuroidea sp. 8, Ophiuroidea sp. 2, *Syringammina fragillissima*, , Cnidaria sp. 1
u	5	N	51.84	3.9-4.1	4 (0.07)	1620-1736	1688.98 (43.05)	*Ophiactis abyssicola*, *Lophelia pertusa* (dead structure), Ophiuroidea sp. 2, Ophiuroidea sp. 8
v	19	Y	51.77	3.8-4.75	4.34 (0.31)	1508-1737	1596.66 (70.31)	*Lophelia pertusa* (dead structure), Ophiuroidea sp. 2, Ophiuroidea sp. 8, *Lophelia pertusa*, Crinoidea sp. 1, *Caryophyllia* sp. 2
w	25	Y	50.48	3.8-4.74	4.20 (0.35)	1492-1766	1633.92 (105.88)	*Lophelia pertusa* (dead structure), Ophiuroidea sp. 2, *Ophiactis balli*, *Ophiactis abyssicola*, Ophiuroidea sp. 8, Porifera encrusting sp. 39

x	5	N	46.36	5.29-8.22	7.78 (1.10)	975-1361	1037.54 (143.27)	*Lophelia pertusa* (dead structure), *Ophiactis balli*, Ascidiacea sp. 2, *Ophiactis abyssicola*
y	2	N	45.00	4.7-5.2	4.95 (0.35)	1341-1420	1380.25 (56.07)	*Ophiactis abyssicola*, *Lophelia pertusa* (dead structure), *Ophiactis balli*, Ascidiacea sp. 2, Crinoidea sp. 1, Galatheidae sp. 1, *Pandalus borealis*
z	18	Y	53.60	4-5.5	4.48 (0.29)	1316-1644	1501.59 (76.03)	*Ophiactis balli*, *Lophelia pertusa* (dead structure), *Lophelia pertusa*, Ophiuroidea sp. 2, Gorgonacea sp. 6
aa	21	Y	53.71	4.6-9	5.48 (0.85)	789-1460	1323.99 (132.79)	*Ophiactis balli*, *Lophelia pertusa* (dead structure), *Ophiactis abyssicola*
ab	17	Y	28.91	4.4-9	7.568 (1.41)	819-1552	1080.24 (199.17)	Porifera encrusting sp. 1, Serpulidae sp. 1, *Psolus squamatus*, Porifera massive globose sp. 12, Porifera encrusting sp. 28, Ophiuroidea sp. 6, Majidae sp. 1, *Ophiactis abyssicola*
ac	1	N		6.63		1165		
ad	52	Y	34.06	5.2-9	7.135 (1.02)	851-1353	1124.34 (116.25)	*Psolus squamatus*, *Ophiactis balli*, Porifera encrusting sp. 22, Porifera encrusting sp. 28
ae	30	Y	15.21	3.68-9	6.30 (1.75)	820-1883	1275.88 (321.44)	Porifera encrusting sp. 1, *Syringammina fragillissima*, Serpulidae sp. 1, Ophiuroidea sp. 1

Table 3.2: Clusters identified from multivariate hierarchical analysis with associated environmental parameters, and SIMPER results identifying the taxa that characterise the clusters.

3.3.3 *Characterising mapping units (biotopes)*

In total 11 benthic assemblages were identified from the cluster analysis and related to available environmental data to describe distinct and useful mapping units [biotopes (see Fig. 3.7)]. Codes were allocated for those clusters that described biotopes; f (Oph. Unk), g (Lep.Ker), j (Syr.Car), q (Lop.Mad), v (Lop.Car), w (Lop.Por), z (Gor.Lop), aa (Lop.Oph), ab (Ser.Pso), ad (Por.Pso) and ae (Syr.Oph).

The 1-way ANOSIM test performed on the environmental data (depth and temperature) associated with each biotope revealed a significant difference in environmental conditions between biotopes (Global $R = 0.509$; $p < 0.01$). Thirty one tests were significant (Table 3.3) and Fig 3.8 illustrates an nMDS ordination plot of the separation of biotopes in relation to environmental condition. The data forms two groups that are clustered on the basis of depth. Biotopes aa, ab, ad and ae had an overall depth range of 819-1883 m (mean 1080-1323 m), while biotopes j, w, v and z have an overall range of 1316-1671 m (mean 1501-1671 m). Cluster g with a depth range of 810-1731 m sits in-between these apparent groups, and is only significantly different to biotope f, q, ab and ad. Biotopes f and q show the highest separation from the other biotopes and each other, as they are the deepest and shallowest biotopes, 1794-1847 m (mean 1847 m) and 749-790 m (769 m) respectively.

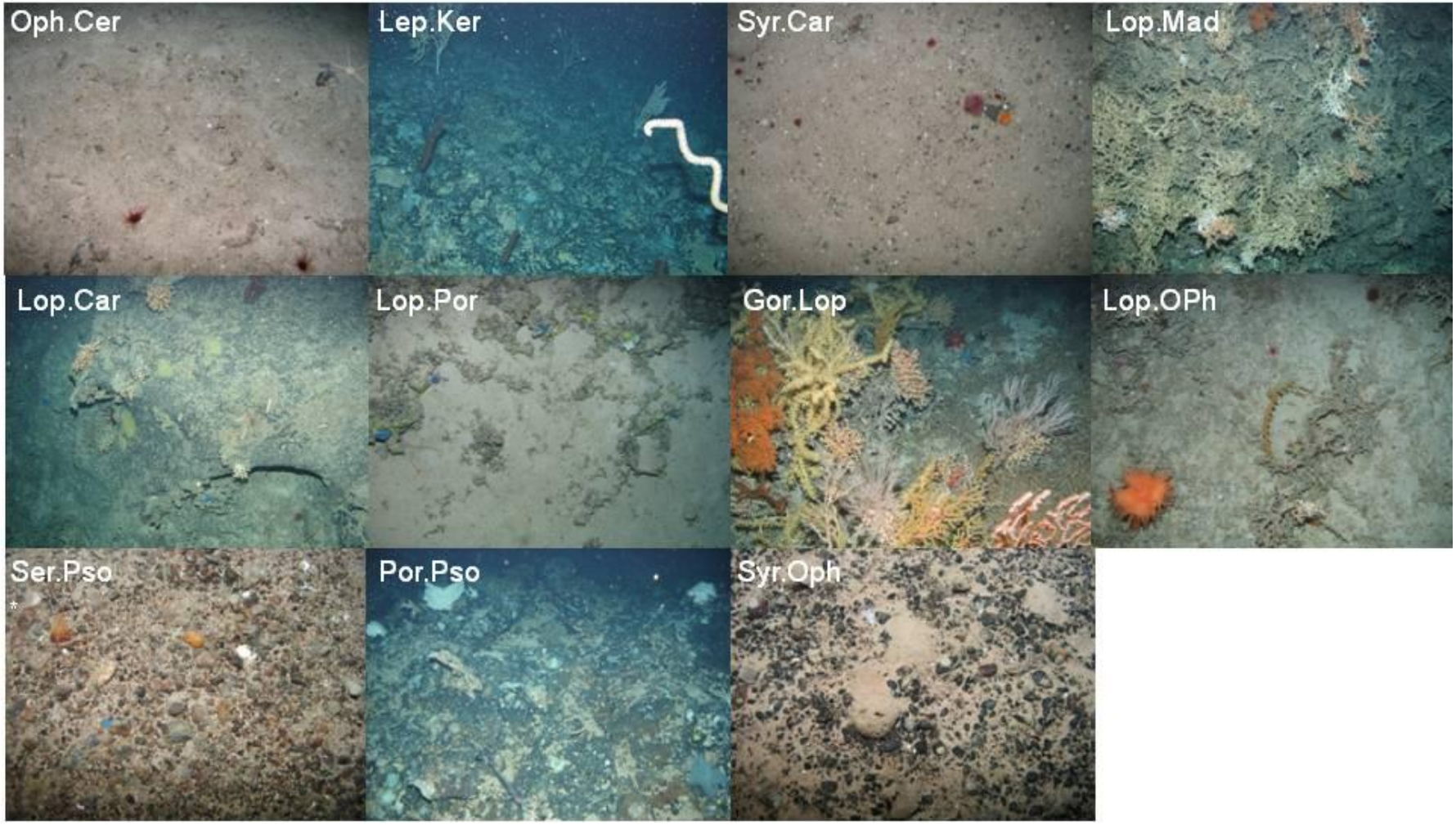

Fig. 3.7: Example images of biotopes identified from multivarite cluster analysis. Refer to Table 3.8 for biotope details. f (Oph.Unk), g (Lep.Ker), j (Syr.Car), q (Lop.Mad), v (Lop.Car), w (Lop.Por), z (Gor.Lop), aa (Lop.Oph), ab (Ser.Pso), ad (Por.Pso) and ae (Syr.Oph).

	g	j	q	v	w	z	aa	ab	ad	ae
f	**0.74 (0.1)**	0.136 (3)	**1 (0.1)**	**0.891 (0.1)**	**0.562 (0.1)**	**0.974 (0.1)**	**0.885 (0.1)**	**0.941 (0.1)**	**0.993 (0.1)**	0.386 (0.1)
g		0.206 (1.8)	**0.804 (0.1)**	0.18 (1.9)	0.173 (2.1)	0.248 (0.7)	0.479 (0.1)	**0.586 (0.1)**	**0.734 (0.1)**	0.064 (14.2)
j			**1 (0.1)**	0.165 (0.2)	0.087 (1.6)	0.321 (0.1)	**0.574 (0.1)**	**0.843 (0.2)**	**0.873 (0.1)**	0.36 (0.1)
q				**1 (0.1)**	**1 (0.1)**	**1 (0.1)**	**0.859 (0.1)**	**0.567 (0.1)**	**0.621 (0.1)**	0.356 (0.1)
v					0.073 (4.1)	0.205 (0.1)	**0.809 (0.1)**	**0.786 (0.1)**	**0.887 (0.1)**	0.236 (0.1)
w						0.269 (0.2)	**0.745 (0.1)**	**0.823 (0.1)**	**0.912 (0.1)**	0.328 (0.1)
z							**0.62 (0.1)**	**0.731 (0.1)**	**0.8 (0.1)**	0.183 (0.6)
aa								**0.612 (0.1)**	0.447 (0.1)	0.15 (0.6)
ab									0.197 (0.3)	0.108 (3.2)
ad										0.284 (0.1)

Table 3.3.: Pairwise results of the ANOISM test of environmental data for biotopes with R and P (%) values for each pair. Global R = 0.509 ($p < 0.01$). Significant pairwise tests are marked in bold. f (Oph. Unk), g (Lep.Ker), j (Syr.Car), q (Lop.Mad), v (Lop.Car), w (Lop.Por), z (Gor.Lop), aa (Lop.Oph), ab (Ser.Pso), ad (Por.Pso) and ae (Syr.Oph).

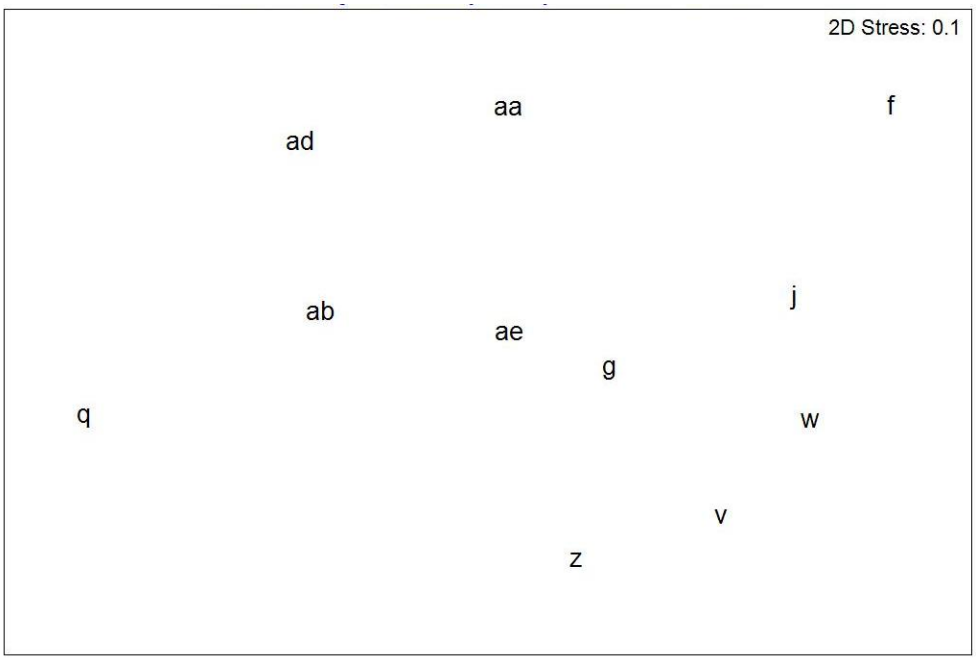

Fig. 3.8: nMDS ordination plot of pairwise ANOSIM test for depicting difference in environmental variables between biotopes.

3.3.3.i *Diversity indices*

The mean Simpson index and 95% confidence interals as seen in Fig. 3.9 (a) suggests there is a significant difference in diversity between some of the biotopes (see A3.2 for raw data). Biotope ad (Por.Pso) had the lowest variation around the mean (+/- 0.295), while biotope g (Lep.Ker) and q (Lop.Mad) had the highest (+/- 0.642 and +/- 0.709 respectively). A trend can be interpreted from Fig. 3.9 (a) using the mean Simpson Index giving three groups with varying diversity. A higher group with a Simpson Index of 3.7-4.1, consisting of biotopes ab (Ser.Pso) and q (Lop.Mad); a medium (2.3-3 Simpson Index) with five biotopes ad (Por.Pso), j (Syr.Car) , v (Lop.Car), f (Oph.Unk), w (Lop.Por), z (Gor.Lop); and a lower group (1.4-2 Simpson Index) with three biotopes aa (Lop.Oph), ae (Syr.Oph), g (Lep.Ker).

For mean species richness (see A3.2 for raw data), the distinction between biotopes is more apparent, with two groups clearly visible (with non overlap of 95% confidence intervals). Those biotopes with a high species richness of 13.6-19.44 [aa (Lop.Oph), ab (Ser.Pso), ad (Por.Pso), q (Lop.Mad), v (Lop.Car), w (Lop.Por), z (Gor.Lop)] and those with lower 4.1-4.9 [ae (Syr.Oph), f (Oph.Unk), g (Lep.Ker)]. Biotope j (Syr.Car) fall inbetween the two groups with a species richness of 8.4. Biotope ad (Por.Pso) had the lowest variation around the mean (+/- 1.13), while biotopes q (+/- 2.718) and g (+/- 2.459) had the highest.

Expected species richness (Sobs) interpolated from rarefaction curves followed the same general pattern observed for mean species richness. Using the mean Sobs alone, 3 groups can be classified, those with high Sobs of between 44-51[aa (Lop.Oph), ab (Ser.Pso), ad (Por.Pso), v (Lop.Car), w (Lop.Por), z (Gor.Lop); medium of between 33-38 [j (Syr.Car), q (Lop.Mad)] and low Sobs of 18-20 [ae (Syr.Oph), f (Oph.Unk), g

(Lep.Ker)]. It could also be interpreted using the 95% confidence intervals into 2 groups (the medium group is incorporated into the high) of 33-51 and 18-20. Biotope z had the highest variation around the mean (+/- 9.83) and e the lowest (+/- 4.6).

Rarefaction curves [Fig. 3.12-3.22 (see appendix A3.3)] of biotopes illustrate the species estimator curves in relation to the expected species richness curves (Sobs). Unique and duplicate species are also plotted as an indicator of estimator curve asymptote, when they cross, higher confidence can be taken from the estimators. Chao2 and ICE had the greatest SD across the estimators, as illustrated in Fig. 3.23-3.32 (see appendix A3.4).

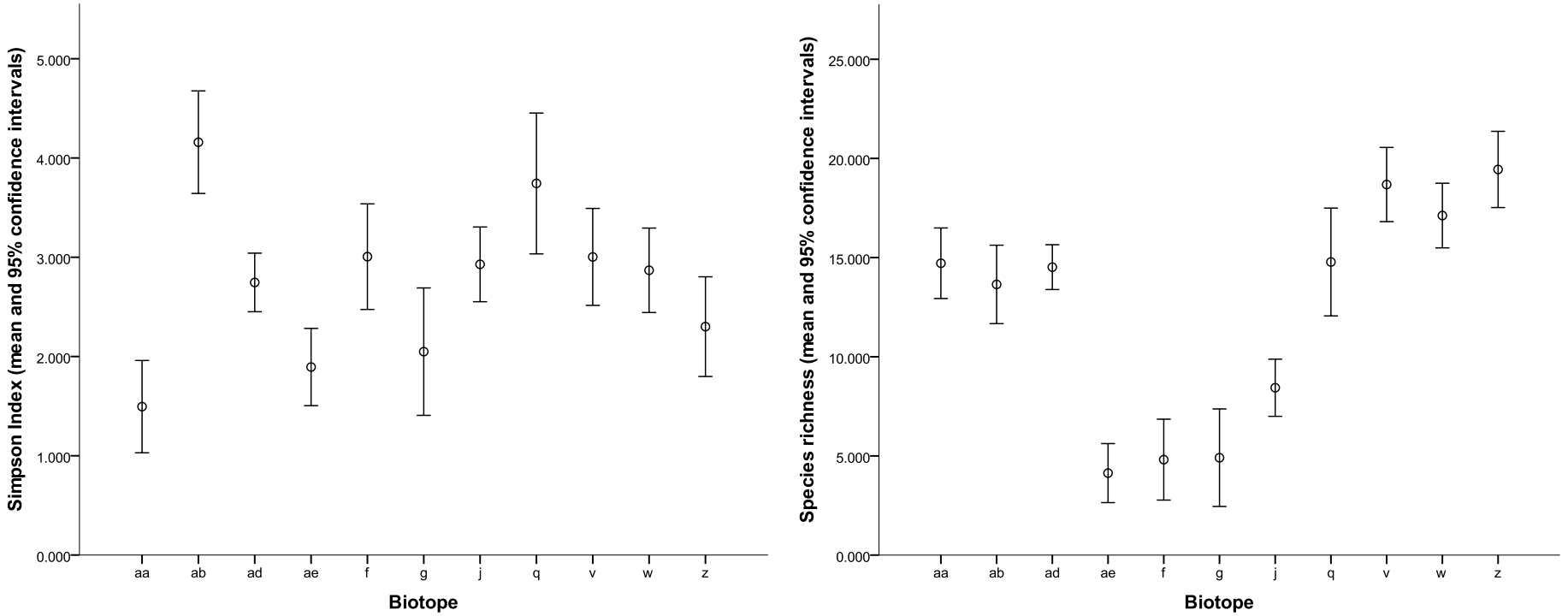

Fig. 3.9: (a) Mean Simpson index with 95% confidence interval for biotopes defined from cluster analysis, (b) mean species richness (derived per image) and 95% confidence intervals for each biotope. f (Oph. Unk), g (Lep.Ker), j (Syr.Car), q (Lop.Mad), v (Lop.Car), w (Lop.Por), z (Gor.Lop), aa (Lop.Oph), ab (Ser.Pso), ad (Por.Pso) and ae (Syr.Oph).

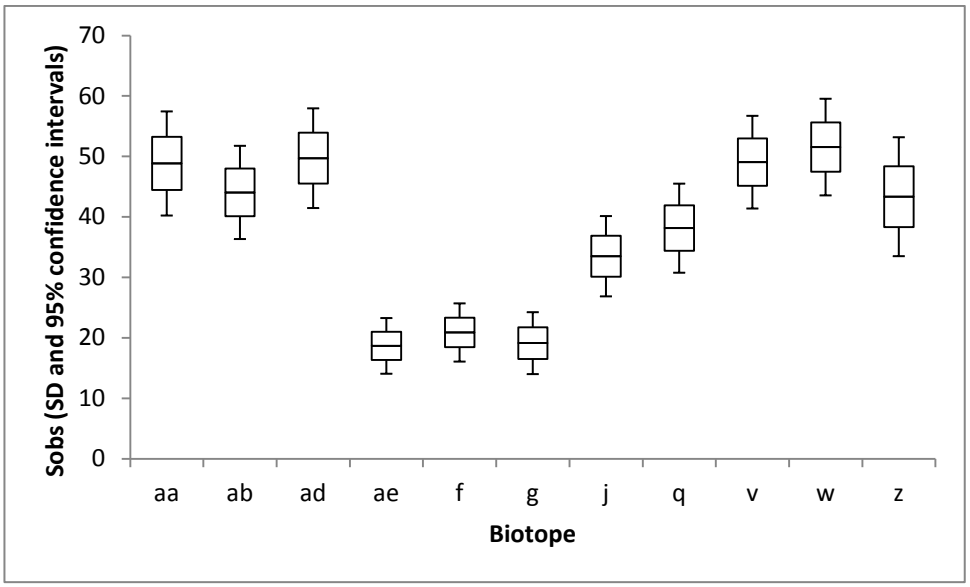

Fig. 3.10: Estimated species richness Sobs (Mao Tau) with standard deviation and 95% confidence intervals for each biotope at a standardised sample size of seven. f (Oph. Unk), g (Lep.Ker), j (Syr.Car), q (Lop.Mad), v (Lop.Car), w (Lop.Por), z (Gor.Lop), aa (Lop.Oph), ab (Ser.Pso), ad (Por.Pso) and ae (Syr.Oph).

All three ANOSIM tests were significant ($p < 0.01$) thus rejecting the H^o of no significant difference in diversity between biotopes. The multivariate ANOSIM [multiple diversity indices (Table 3.6)] had the highest global R (R= 0.499), followed by the univariate ANOSIM test for species richness (R= 0.373) then Simpson index (R= 0.155). Twenty seven pairwise tests were significantly different for the multivariate and univariate mean species richness ANOSIMs, and 25 for Simpson Index (Tables 3.4-3.6).

	g	j	q	v	w	z	aa	ab	ad	ae
f	-0.04 (72.4)	**0.173 (0.8)**	0.098 (8.9)	0.08 (3.9)	0.083 (5.9)	0.071 (4.2)	**0.335 (0.1)**	0.117 (2.3)	**0.164 (1.7)**	0.107 (5.3)
g		**0.196 (1.8)**	**0.356 (1.1)**	**0.175 (2.1)**	0.105 (7.4)	**0.207 (1)**	**0.269 (0.8)**	**0.238 (1.1)**	0.139 (6.1)	0.009 (38.5)
j			0.148 (6.2)	-0.026 (64.1)	-0.011 (56.1)	0.007 (35.1)	**0.473 (0.1)**	**0.212 (0.1)**	-0.005 (48.2)	**0.196 (0.1)**
q				0.101 (11.1)	0.109 (10.6)	**0.459 (0.1)**	**0.916 (0.1)**	-0.08 (87.2)	**0.216 (2)**	**0.496 (0.2)**
v					-0.039 (92.8)	0.053 (7.4)	**0.622 (0.1)**	0.105 (2.2)	-0.005 (50.7)	**0.214 (0.1)**
w						0.003 (33.9)	**0.417 (0.1)**	0.145 (1.1)	0.016 (30.1)	0.161 (0.2)
z							**0.52 (0.1)**	**0.335 (0.1)**	-0.081 (90.5)	0.057 (10.2)
aa								**0.665 (0.1)**	**0.271 (0.1)**	0.036 (14.1)
ab									**0.294 (0.2)**	**0.453 (0.1)**
ad										0.119 (0.6)

Table 3.4: Pairwise results of the ANOISM test for Simpson index of biotopes with R and P (%) values for each pair. Global R = 0.155, p < 0.01. Significant pairwise tests are marked in bold. f (Oph. Unk), g (Lep.Ker), j (Syr.Car), q (Lop.Mad), v (Lop.Car), w (Lop.Por), z (Gor.Lop), aa (Lop.Oph), ab (Ser.Pso), ad (Por.Pso) and ae (Syr.Oph).

	g	j	q	v	w	z	aa	ab	ad	ae
f	-0.042 (70.2)	0.149 (2.3)	**0.829 (0.1)**	**0.952 (0.1)**	**0.842 (0.1)**	**0.827 (0.1)**	**0.604 (0.1)**	**0.489 (0.1)**	**0.556 (0.1)**	0.097 (6.1)
g		0.126 (7)	**0.814 (0.1)**	**0.952 (0.1)**	**0.827 (0.1)**	**0.788 (0.1)**	**0.562 (0.1)**	**0.407 (0.1)**	**0.54 (0.1)**	0.059 (25.6)
j			**0.455 (0.1)**	**0.774 (0.1)**	**0.602 (0.1)**	**0.676 (0.1)**	**0.412 (0.1)**	0.212 (0.1)	0.275 (0.1)	**0.379 (0.1)**
q				0.135 (7.9)	-0.002 (43.3)	0.025 (30.6)	-0.082 (87.2)	-0.011 (47.6)	-0.076 (79.6)	**0.872 (0.1)**
v					0.001 (41.6)	0.01 (27.4)	0.049 (8.9)	0.346 (0.1)	0.074 (9.7)	**0.948 (0.1)**
w						0.061 (7.1)	0.015 (25)	0.209 (0.5)	0.008 (40.8)	**0.888 (0.1)**
z							0.072 (3.9)	0.2 (0.4)	0.155 (1.1)	**0.899 (0.1)**
aa								0.077 (5.9)	0.009 (38.7)	**0.745 (0.1)**
ab									0.057 (16.3)	**0.705 (0.1)**
ad										**0.659 (0.1)**

Table 3.5: Pairwise results of the ANOISM test for mean species richness of biotopes with R and P (%) values for each pair. Global R = 0.373 (p <0.01). Significant pairwise tests are marked in bold.

	g	j	q	v	w	z	aa	ab	ad	ae
f	0.145 (5)	**0.631 (0.7)**	0.392 (1)	0.485 (1.2)	**0.582 (0.8)**	**0.815 (0.8)**	**0.607 (0.2)**	**0.776 (0.2)**	**0.861 (0.2)**	-0.075 (83.5)
g		**0.987 (0.2)**	**0.717 (0.2)**	**0.651 (0.7)**	**0.946 (0.1)**	**1 (0.2)**	**0.662 (0.1)**	**0.981 (0.1)**	**0.992 (0.1)**	0.168 (5.9)
j			0.132 (7.2)	0.471 (0.1)	0.111 (10.5)	**0.669 (0.5)**	**0.711 (0.1)**	**0.545 (0.2)**	**0.695 (0.5)**	**0.707 (0.2)**
q				0.411 (1.3)	0.237 (3.7)	**0.599 (0.9)**	0.411 (1.4)	0.478 (0.4)	**0.518 (1.2)**	0.357 (1.3)
v					0.042 (23)	-0.032 (52.7)	0.265 (1.3)	0.172 (2.4)	0.372 (1)	**0.638 (0.8)**
w						0.145 (7.7)	0.343 (0.9)	0.078 (7.5)	0.406 (1.6)	**0.714 (0.2)**
z							0.13 (6.7)	0.25 (2.8)	0.308 (1.1)	**0.947 (0.1)**
aa								0.472 (0.2)	0.048 (20.8)	**0.648 (1)**
ab									0.434 (0.9)	**0.883 (0.1)**
ad										**0.937 (0.2)**

Table 3.6: Pairwise results of multivariate ANOISM test with R and P (%) values for each pair. Global R = 0.499 (p <0.01). Significant pairwise tests are marked in bold.

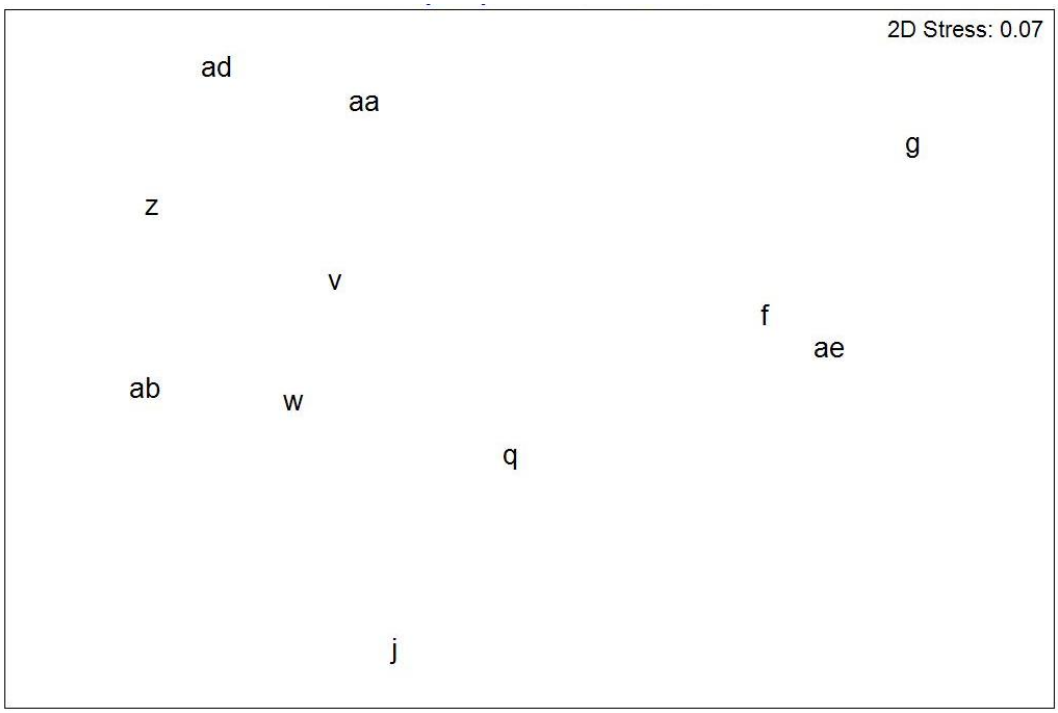

Fig 3.11: nMDS of multivariate diversity ANOSIM test. f (Oph.Unk), g (Lep.Ker), j (Syr.Car), q (Lop.Mad), v (Lop.Car), w (Lop.Por), z (Gor.Lop), aa (Lop.Oph), ab (Ser.Pso), ad (Por.Pso) and ae (Syr.Oph).

Broadly speaking, as illustrated by the nMDS (Fig.3.11) of the multivariate ANOSIM results (Table 3.6), there are two discernible groups on the basis of overall diversity. The box and whisker plots (Fig 3.23-3.32, see Appendix A3.4) illustrate the expected (Sob) and estimated (species richness estimator) contributions to the overall diversity. Biotopes aa (Lop.Oph), ab (Ser.Pso), ad (Por.Pso), v (Lop.Car), w (Lop.Por) and z (Gor.Lop) have a higher diversity than the lower group biotopes f (Oph.Unk), g (Lep.Ker, j (Syr.Car), q (Lop.Mad), and ae (Syr.Oph).

3.3.3.ii *Distribution of biotopes*

Megahabitat scale

The results of the covariate PERMANOVA (Table 3.7) test indicated there was a significant difference between the species assemblages from the NW and SE side of Anton Dohrn Seamount, but that this difference was attributable to the interactions between depth and the main effects, not the main effect of location in isolation. Thus, depth explained a significant ($P < 0.001$) portion of the variance within the model, whilst location did not, but the interactions between location, depth and substrate were highly significant ($P < 0.001$). To illustrate this, the data were filtered for only those corresponding to defined biotopes and plotted on an nMDS ordination plot (Fig. 3.12).

	df	SS	MS	Pseudo-F	P(perm)
Depth	1	59805	59305	13.47	0.001
Location	1	27498	27498	1.4122	0.15
Substrate (location)	15	2.2287E5	14858	5.7304	0.001
Depth x location	1	27465	27465	10.593	0.001
Depth x substrate (location)	15	88701	5913.4	2.2807	0.001
Error	273	7.0784E5	2592.8		
Total	306	1.1337E6			

Table 3.7: Results of Type I SS PERMANOVA test of assemblage data from NW and SE areas of ADS.

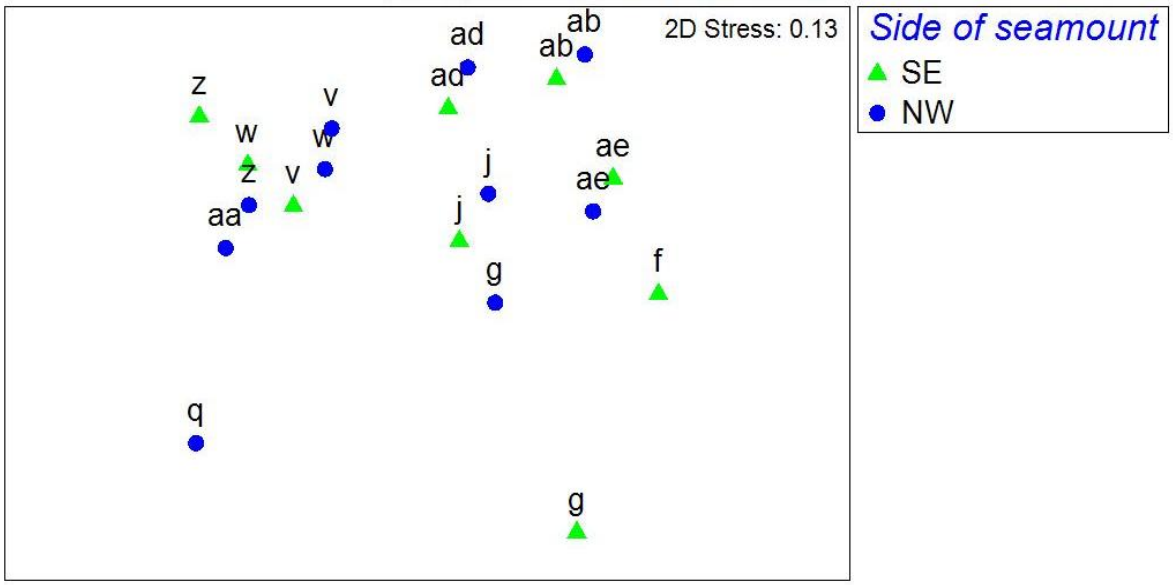

Fig. 3.12: nMDS ordination plot of differences between biological assemblages on the NW and SE side of Anton Dohrn Seamount.

Figure 3.12 illustrates that there is no difference between faunal assemblages between the NW and SE side of ADS, but that the significant interaction effect is a function of both depth and substratum.

Meso-scale geomorphology

Qualitative assessment of biotope distribution, determined from visually classified video transect data (Table 3.8) revealed the occurrence of biotopes either side of Anton Dohrn Seamount. Eleven biotopes were mapped from ADS, 10 from the NW side and 9 from the SE. Of those 11, nine fit the 'listed' habitats definition and can be classed as habitats of conservation interest. Seven can be identified as VMEs (3 coral reef, 2 coral gardens and 2 xenophyophore communities), and two as bedrock reef under the EC Habitats Directive.

Two coral gardens were identified and mapped on distinct meso-scale geomorphological features. The coral garden characterised by the conspicuous

gorgonian *Lepidisis* and *Keratoisis* on bedrock (Lep.Ker) occurred on a parasitic cone on the NW flank (1646-1753 m) and a radial ridge on the SE flank (1543-1567 m). While the second gorgonian dominated coral garden biotope Gor.Lop only occurred on the NW side of the seamount on a parasitic cone and radial ridge feature (1313-1634 m). *Lophelia pertusa* reef (Lop.Mad) occurred on two distinct meso-scale geomorphological features on the NW side of the seamount, namely a radial ridge on the flank, and the summit of cliff-top mounds on the edge of the summit. Predominantly dead coral framework (Pred.Oph) occurred off the summit of the cliff-top mounds (below the *Lophelia* reef) on the NW summit edge. It was also mapped on the radial ridge on both the NW and SE flank, the flute feature of the NW flank and on the summit edge on the SE side. The dead framework coral biotope with encrusting sponges (Lop.Por) only occurred on the NW side of the seamount on a radial ridge, parasitic cone and the landslide feature at the base of the flank. The xenophyophore biotopes occurred on both the NW and SE side of the seamount on the summit edge on the SE side (1104-1154 m) and on the flank on both sides, although only on one distinct meso-scale feature; a radial ridge on the NW and SE side flank.

Assemblage code	Cluster	Name of assemblage	Supporting evidence	Depth (m) & temperature (°C)	Associated geomorphic feature	Survey area	NW depth (m) & temperature (°C)	SE depth (m) & temperature (°C)
Oph.Unk	**f**	*Ophiomusium lymani* and cerianthid anemones on mixed substratum	Undescribed	1791-1889 3.7-3.9°C	Seamount flank	SE		1791-1889 3.7-3.9°C
Lep.Ker	**g**	Coral garden with bamboo corals and antipatharians on bedrock	Undescribed	1543-1567 3.57-4.59	Parasitic cone, radial ridge	NW & SE	1646-1753 3.57-4.02	1543-1567 4.51-4.59
Syr.Car	**j**	Xenophyophores and caryophyllids on gravelly sand and mixed substratum	Undescribed	1104-1770 3.8-7.23°C	Seamount flank, summit edge	NW & SE	1368-1770 3.9-5.29	1104-1154 6.79-7.23
Lop.Mad	**q**	*Lophelia pertusa* reef	Howell *et al*. (2010)	747-1337 5.2-9.1°C	Cliff-top mounds, radial ridge	NW	747-1337 5.2-9.1	
Lop.Car	**v**	*Lophelia pertusa* and encrusting sponges on bedrock	Howell *et al*. (2010)	1497-1742 3.87-4.72	Parasitic cone, radial ridge, landslide/rockfall	NW & SE	1704-1742 3.87-3.96	1497-1572 4.49-4.72
Lop.Por	**w**	Predominantly dead, low-lying coral framework with encrusting sponges	Undescribed	1267-1756 3.8-5.9°C	Radial ridge, parasitic cone, landslide/rockfall	NW & SE	1460-1754 3.76-4.45	1525-1572 4.48-4.64
Gor.Lop	**z**	Gorgonian dominated coral garden	Undescribed	1313-1634 4.03-5.52	Radial ridge, parasitic cone	NW	1313-1634 4.03-5.52	
Lop.Oph	**aa**	Predominantly dead, low-lying coral framework	Howell *et al*. (2010)	758-1445 4.49-8.9°C	Cliff edge, radial ridge, cliff-top mounds, flute	NW & SE	760-1445 4.49-8.9	975-980 8.1-8.2°C
Ser.Pso	**ab**	Serpulids, encrusting sponges and *Psolus* on mixed substratum	Undescribed	849-1037 8-9.1°C	Summit	NW & SE	849-1037 8.2-9.1°C	956-1016 8-8.3°C
Por.Pso	**ad**	*Psolus*, caryophyllids and lamellate sponges on mixed, boulder and bedrock	Undescribed	854-1345 5.1-9°C	Escarpment	NW & SE	854-1345 5.1-9°C	990-1232 6.2-8.2°C
Syr.Oph	**ae**	Xenophyophores and ophiuroids on mixed substratum	Undescribed	1076-1554 4.5-7.9°C	Flank, radial ridge	NW & SE	1076-1388 5.1-7.9°C	1100-1554 4.5-4.7°C

Table 3.8: Summary of biotope data mapped from video, giving depth and temperature range of biotopes from the NW and SE study areas and associated geomorphic feature.

3.4 Discussion

Seamounts are described as biodiversity hotspots and are listed as features of conservation interest, despite this there are few descriptions of biological assemblages from seamounts, particularly in the context of biotope mapping. Eleven biotopes were identified from Anton Dohrn Seamount and the results of the SIMPER analysis and descriptions are provided in Appendix A3.1 and A3.5. Biotopes were considered against current definition of VMEs and OSPAR habitats (OSPAR 2010; FAO 2008). Seven could be considered as VMEs and OSPAR habitats. Of these seven, three could be classified as cold-water coral reef, two as coral gardens, and two xenophyophore communities. Of the remaining four biotopes, two could be considered as bedrock/stony reef under the EC Habitats directive. The remaining assemblages, which are not listed habitats, will not be discussed here, however full descriptions can be found in Appendix A3.6.

3.4.1 *Descriptions of 'listed' habitats for use as mapping units*

4.3.1.i *Cold water coral reef*

Three biotopes were defined that could be considered as cold-water coral reef, one was characteristic of summit reef and the remaining two of dead framework structures.

Live biogenic coral reef (Lop.Mad) was characterised by the reef building corals *Lophelia pertusa* (live and dead) and *Madrepora oculata*, the pencil urchin *Cidaris cidaris,* anemones (Actiniaria sp.), decapods (Decapoda sp. 5) and the squat lobster *Munida sarsi*, gorgonian species and the antipatharian *Leiopathes* sp. (video footage). These findings broadly support those of previous studies. Freiwald *et al*. (2004) describe the summit regions of cold-water coral mounds and live reef areas as

supporting few permanently attached organisms, as the living corals are very successful in preventing fouling. Among those species that are permanently attached are the polychaete *Eunice norvegica*, the parasitic foraminiferan *Hyrrokkin sarcophagi*, and clusters of bivalves including *Delectopecten vitreus* and *Acesta excavata*. Howell *et al*. (2010b) describe an assemblage characterised by *L. pertusa*, *Madrepora oculata*, hydroids, anemones, decapods, cerianthid anemones and echinoderms (ophiuroids and echinoids) from Hatton Bank, George Bligh Bank, Rockall Bank and the Wyville Thomson Ridge.

Two dead coral framework biotopes were identified on Anton Dohrn Seamount and varied in their composition and associated fauna. Biotope Lop.Oph was characterised by dead *L. pertusa* coral framework and the ophiuroids *Ophiactis balli* and *Ophiactis* abyssicola; video footage revealed the large anemone *Phelliactus* sp. and the corkscrew antipatharian *Stichopathes* sp. to also be characterising species. While biotope Lop.Por was characterised by dead, low-lying *L. pertusa* framework, a number of ophiuroid species (Ophiuroidea sp.2, Ophiuroidea sp.8, *Ophiactis balli*, *Ophiactis abyssicola*) and green encrusting sponges, non sample images and video suggested caryophyllids and the soft coral *Anthomastus grandiflorus* may also be abundant.

While the Lop.Oph biotope had a wider depth range (758-1677 m), the dead framework with encrusting sponges (Lop.Por) was only observed deeper (1497-1742 m) on distinct meso-scale geomorphic features. The latter assemblage appears to be subject to increased sedimentation, which is possibly the reason for a significantly lower proportion of live *L. pertusa* polyps observed than from the former assemblage. This may explain the abundance of encrusting sponge species on the *Lophelia* framework, as live coral are known to be very capable of preventing fouling (Freiwald 2004).

Dead coral framework assemblages have been described by a number of authors. Wilson (1979) describes an assemblage that was associated with dead coral debris as supporting a diverse range of fauna including bryozoans, anemones, calcareous polychaetes, bivalves, asteroids and echinoids. Freiwald *et al*. (2004) list gorgonians, actinians and sponges as conspicuous and abundant megafauna within this habitat, while on a smaller scale hydrozoans, bivalves, brachiopods, bryozoans and barnacles are prevalent. Howell *et al*. (2010b) describe an assemblage characterised by dead *L. pertusa*, halcampoid anemones, encrusting bryozoans, encrusting sponges, squat lobsters, serpulid polychaetes, echinoderms (ophiuroids and asteroids), cup corals and ascidians. Dead coral framework is known to be more diverse than the living part of the reef (Jensen and Frederiksen 1992) and it has been suggested that the reason for this may be that live tissue prevents sessile epibiotic species from attaching to the framework (Buhl-Mortensen and Mortensen 2004). The hard coral skeleton provides a surface for attachment of associated fauna (Buhl-Mortensen *et al.* 2010).

3.4.1.ii *Xenophyophore communities*

Two different xenophyophore assemblages were identified from Anton Dohrn Seamount. The biotope xenophyophores and ophiuroids on mixed substratum (Syr.Oph) was characterised by the xenophyophore *Syringammina fragilissima*, an unidentified ophiuroid species (Ophiuroidea sp. 1), a white encrusting sponge (Porifera encrusting sp.1), and serpulid worms (Serpulidae sp. 1). This biotope occurred on mixed substratum (dominated by pebbles) on both sides of the seamount and was distributed over a depth of 1076-1554 m and a temperature of 4.5-7.9°C.

The biotope xenophyophores and caryophyllids on gravelly sand and mixed substratum (Syr.Car) was also characterised by xenophyophores (*Syringammina fragilissima*) but

was distinguishable from the previous biotope by the presence of various anthozoan species. It was distributed over a depth range of 1104-1770 m and a temperature of 3.8-7.23°C. Other characterising species associated with this biotope were a solitary coral species (Cnidaria sp. 1) unidentified ophiuroids (Ophiuroidea sp.8, Ophiuroidea sp.2), *Ophiactis balli.* Video observations suggested cerianthid anemones and pennatulids (*Pennatula phosphorea* and *Halipteris* sp.) may also be abundant throughout the biotope.

Large epifaunal xenophyophores increase habitat heterogeneity of deep-sea sediments and could serve the role of a structural habitat in providing: hard substratum for epifaunal species, refuge from predators, microhabitats for mating, reproduction and nursery functions, elevated positions for suspension feeders, and increased food availability to deposit feeders resulting from the deposition of fine particles (Levin *et al.* 1986; Levin 1991). They increase local biodiversity and represent a unique habitat on deep-sea soft sediments as many of the associated species do not occur on the surrounding seafloor where there are no xenophyophores (Buhl-Mortensen *et al.* 2010).

Whilst many authors have described the distribution of xenophyophore aggregations (Bett 2001; Hughes and Gooday 2002) there have been few descriptions of them in terms of an assemblage. The two xenophyophore assemblages identified on Anton Dohrn Seamount were found on gravelly sand or mixed substratum on the deep flanks of the seamount associated with, or proximal to, positive topographic features such as flutes on the cliff edge or cliff top mounds. These assemblages are similar to those described by Narayanaswamy *et al*. (2006) who identified xenophyophores and ophiuroids as being the dominant fauna between 980-1004 m on the Hebrides continental slope and between 798-835 m on Hatton Bank; and xenophyophores, sea

pens and solitary corals (probably *Flabellum* sp.) between 1739-1963 m on the NW flank of Anton Dohrn Seamount and xenophyophores, cerianthids and caryophyllids on George Bligh Bank (1112-1154 m).

3.4.1.iii *Coral gardens*

Coral gardens are listed under the OSPAR as 'threatened and/or declining species and habitats' (OSPAR Agreement 2008-6) and are defined as 'a habitat which has a relatively dense aggregation of individuals or colonies of one or more coral species which can occur on a wide range of soft and hard substrates' (OSPAR 2010b). In the context of hard substratum this habitat has been described as being dominated by gorgonian, stylasterid and/or antipatharian corals (ICES 2007) and can develop on exposed bedrock, boulders or cobbles (Roberts *et al.* 2009).

Coral garden with bamboo corals and antipatharians on bedrock

This coral garden biotope was characterised by the large bamboo corals *Lepidisis* sp. and *Keratoisis* sp. 2, small colonies of *Lophelia pertusa*, solitary cup corals (*Caryophyllia* sp. 2) and Porifera encrusting sp. 28.

Wienberg *et al*. (2008) describe a diverse 'discrete live coral colonies' assemblage from the Franken mound on western Rockall Bank associated with ridge features on the eastern and western flanks at a depth of 650-675 m. The assemblage is dominated by gorgonians (*Acanthogorgia armata*), antipatharian corals (including *Bathypathes* sp., *Stichopathes* cf. *gravieri*, *Leiopathes* sp. and *Parantipathes* sp.), a number of soft coral species (including *Anthomastus* and *Capnella glomerata*), stylasterid corals and associated megafauna. They noted that scleractinian corals were sparse with only *L. pertusa* observed. Another obvious difference is the presence/absence of stylasterid

corals and the relative abundance of *L. pertusa* which may be due to *L. pertusa* out-competing the stylasterid corals (Cairns 1992). It may be that the biotope observed from Anton Dohrn Seamount is a deeper version (1543-1567 m) of the assemblage described by Wienberg *et al*. (2008).

Gorgonian dominated coral garden

The second coral garden biotope observed on ADS (Gor.Lop) was characterised by dead *L. pertusa* framework, small growths of *L. pertusa* with an associated bamboo coral (*Keratoisis* sp 1), ophiuroids (*Ophiactis balli* and Ophiuroidea sp. 2) and Gorgonacea sp. 6. Non-sample images and video observation suggest other conspicuous fauna to include the antipatharians *Antipathes* sp., *Leiopathes* sp., *Stichopathes* sp. and the glass sponge *Aphrocallistes* sp., lamellate and cup sponges. The coral gardens appear to provide a suitable habitat for a diverse range of fish including the false boarfish *Neocyttus helgae, Lepidion eques,* and orange roughy (*Hoplostethus atlanticus*) all of which were observed on video in this biotope, however no quantitative analysis has been undertaken to assess any statistical relationships between fish and habitat; but interestingly orange roughy were only observed associated with this coral garden biotope, despite transects undertaken elsewhere on the seamount at comparable depths. The bathypelagic false boarfish is a good indicator species for coral habitats as they have a facultative relationship with fan and whip octocoral-dominated habitats (Moore *et al.* 2008). Their occurrence is thought to be indicative of a strong current regime (Pfannkuche *et al.* 2004).

Little has been documented regarding the distribution of coral garden habitats; many studies have identified the distribution of coral species which have the potential to form coral gardens, e.g. Bruntse and Tendal (2001) described the distribution of gorgonians

round the Faroe Islands and Grasshoff (Grasshoff 1972;1973;1977;1981a;1981b;1981c;1985) reported the distribution of gorgonians, antipatharians and pennatulids in the NE Atlantic; few authors have described coral garden assemblages. One of the most diverse coral garden habitats reported to date is from the Aleutian Islands and is dominated by gorgonians and stylasterid corals (Heifetz *et al.* 2005). A review by OSPAR (OSPAR 2010b) summarised the occurrence/potential of coral garden habitats in the NE Atlantic. These include seamounts in the Azores which were dominated by large gorgonians and antipatharian corals, Le Danois Bank (Spain) which was characterised by the large gorgonian *Callogorgia verticillata*, and the Mid-Atlantic Ridge (Mortensen *et al.* 2008). Buhl-Mortensen *et al*. (2010) refer to shallow (200 m) coral gardens characterised by *Paragorgia arborea* and *Primnoa resedaeformis* off Norway. Durán Muñoz *et al*. (2009) identified areas of bedrock outcrop on the western flank of Hatton Bank from multibeam echosounder data, and results from dredge samples suggested that these outcrops provide suitable substratum for cold-water corals which may be potential coral gardens. Additional longline survey data identified a number of species associated with these areas as *L. pertusa*, *Madrepora oculata*, seafans, bamboo corals (*Acanella* sp.), antipatharians, stylasterids corals and glass sponges.

The coral gardens found on Anton Dohrn Seamount are the first to be described from UK waters. The difference between the two coral garden biotopes is the presence of large conspicuous gorgonian corals in the Lep.Ker coral garden, and lower abundance of *Lophelia pertusa*, while the gorgonian-dominated coral garden had, in areas, higher proportions of dead *L. pertusa* framework. It may be that the hydrodynamic conditions and substratum availability influence the distribution of these two biotopes. It appears that the dead framework in the later biotope is acting as a substratum for the

colonisation of other coral species, while the former is using bedrock as a point of attachment.

3.4.1.iv *Other 'reef' habitat under EU Habitats Directive*

Two biotopes were identified as potential bedrock 'reef' habitat under the EU Habitats Directive.

Lophelia pertusa and encrusting sponges on bedrock

This biotope was characterised by small colonies of *L. pertusa*, a number of ophiuroids species (Ophiuroidea sp. 2, Ophiuroidea sp. 8), crinoids (Crinoidea sp. 1) and *Caryophyllia* sp. 2. The SIMPROF routine included this biotope with the dead framework and encrusting sponges biotope (Lop.Por), but separated it on the basis of substratum, in line with current habitat classification systems. Despite the same characterising species being present, it is important from a conservation perspective to know if it is a coral 'reef' or an area of bedrock with reef-like fauna. Video observation also suggested this biotope to be characterised by the antipatharian *Bathypathes* and encrusting sponges. It occurred on distinct geomorphology (parasitic cone, radial ridge and landslide/rockfall) on the NW and SE side of ADS over a depth of 1497-1742 m.

This biotope is similar to that described by Howell *et al*. (2010b) as 'discrete coral (*Lophelia pertusa*) colonies on hard substratum' from the Wyville Thomson Ridge and Hatton Bank at an average depth of 637 m. This assemblage differs to that described by Wienberg *et al*. (2008) in terms of the relative proportion of corals species; with a lower abundance of conspicuous gorgonians and antipatharians which are replaced by small growths of *L. pertusa*.

*Psolu*s, caryophyllids and lamellate sponges on mixed, boulder and bedrock substratum

The second 'reef' biotope identified (Por.Pso) has not been described previously from the deep sea but is similar to that observed along the bedrock escarpment on Rockall Bank (~350-600 m) and appears to be a deeper version occurring along the steep break of the slope. The assemblage on Rockall Bank is characterised by large lobose sponges, stylasterid corals, encrusting sponges and the pencil urchin *Cidaris cidaris*, whilst the newly described assemblage from Anton Dohrn Seamount is characterised by large conspicuous coral (antipatharians), caryophyllids, small growth of *L. pertusa* and encrusting and lamellate sponges. The main difference between these assemblages is the absence of stylasterid corals associated with the assemblage from Anton Dohrn Seamount, and may be because they are being out-competed by scleractinians that are more able to adapt to variable conditions (Cairns 1992).

3.4.2 *Diversity of biotopes*

The overall diversity captured by undertaking a multivariate diversity ANOSIM test shows there to be differences in diversity between the biotopes. The xenophyophore biotope Syr.Oph is comparable with the deep biotope Oph.Unk and bamboo and antipatharians coral garden (Lep.Ker). While the bedrock reef biotopes (Por.Pso and Lop.Car) are closer in their levels of diversity to the dead framework biotopes (Lop.Oph and Lop.Por), coral garden (Gor.Lop) and the mixed substratum biotope (Ser.Pso). The *L.pertusa* reef biotope (Lop.Mad) is only significantly different to Gor.Lop, Por.Pso and Lep.Ker.

Measuring and comparing diversity in this way may expand the current, but limited, definitions of biological communities, particularly VMEs. The diversity of the VMEs

described from Anton Dohrn Seamount differ, this is particularly interesting in terms of the coral garden biotopes and xenophyophore community. The diversity of the Lep.Ker coral garden is lower than that found for the Gor.Lop, this may be due to the addition of dead framework in the later biotope. The presence of this structural complexity may be increasing the diversity. The diversity of the two xenophyophore biotopes is significantly different, with Syr.Cer having the higher diversity. The overall diversity results support previous reports that the dead framework zones of reefs are more diverse than the live summits (Jensen and Frederiksen 1992; Mortensen *et al.* 1995), although the Simpson Index shows the reverse of this, with the reef having the highest diversity.

The results of the diversity tests highlight how dependent the interpretation is upon the test used, and illustrate that caution is needed when measuring diversity. As each diversity index measures a different component of the community, using a multivariate approach gives a more holistic view of that diversity, allowing a greater understanding of the community which can be used in the implementation of conservation measures.

3.4.3 *Relationship between 'biotopes of conservation interest and meso-scale geomorphological features*

3.4.3.i *Cold-water coral reef*

In this study *L. pertusa* reef was associated with cliff top mounds, radial ridges and parasitic cone features on the NW side of Anton Dohrn Seamount over a depth and temperature range of 747-1337 m and 5.5-9.1°C respectively. These findings support those of earlier studies which found that the largest reefs occur in depths between 500-1200 m (Frederiksen *et al.* 1992; Wheeler *et al.* 2007) and may be associated with topographic features such as ridges (Sula Ridge), escarpments (Pelagia Mounds) and channels (Hovland Mounds) (Howell *et al.* 2007; Wheeler *et al.* 2007; Howell *et al.*

submitted). This relationship most likely reflects both the substratum and hydrodynamic requirements of reef habitat development. Reef habitat forms in areas of enhanced turbidity, within a narrow density envelope, with high current velocities that prevent local sedimentation but provide enhanced encounter rates with food particles (Thiem *et al.* 2006; Miensis *et al.* 2007; Dullo *et al.* 2008). These conditions must be stable over long periods of time to allow reef development (Thiem *et al.* 2006).

3.4.3.ii *Xenophyophore communities*

The xenophyophore assemblages observed on Anton Dohrn Seamount were either associated with geomorphic features [flank, cliff edge (edge of seamount summit) and radial ridges)] or were in close proximity (< 100 m) to geomorphic features (between cliff edge and flute feature, between parasitic cone and landslide). Previous studies have shown they are often found in areas with enhanced organic carbon fluxes, such as beneath highly productive surface waters, on sloped topography, or near certain topographic features such as caldera walls, basalt outcrops, or on the sides of sediment mounds and small ridges (Tendal 1972; Levin and Thomas 1988; Levin 1994; Hughes and Gooday 2004). Rogers (1994) suggested that this may be a result of topographically-enhanced currents or high concentrations of suspended matter associated with these regions, which provide an increased food supply for suspension feeding organisms such as xenophyophores.

3.4.3.iii *Coral gardens*

The OSPAR definition of coral gardens is very broad, and the habitat in terms of biodiversity and densities of associated species can vary with region, hydrography, topography, substratum and depth (OSPAR 2010b). For these reasons OSPAR states that a more precise description within regional seas is needed as is the need to establish

relationships with features, substratum and depth which can be used as proxies for identifying and mapping these vulnerable habitats.

The coral gardens observed on Anton Dohrn Seamount occur on distinct topographical features along the crest of the parasitic cones and radial ridges on the NW and SE flank. The gorgonian dominated coral garden (Gor.Lop) occurred on the crest of a radial ridge and parasitic cone on the NW flank, while the other coral garden biotope (Lep.Ker) occurred deeper on the same parasitic cone and was absent from the NW radial ridge but occurred on the SE radial ridge.

The occurrence of these assemblages is most likely a result of the presence of favourable hydrodynamic conditions and suitable substratum in these areas. Gorgonians settle on hard substrata, and availability of hard substratum can be a limiting factor to their distribution (Kinzie 1973). Water motion is also one of the primary factors influencing the distribution of gorgonians (Barham and Davies 1968; Kinzie 1973) because of its role in delivering food (Carpine and Grasshoff 1975), removing CO_2 (Stoddart 1969), and preventing sedimentation. The elevated position provided by raised topographical features, in this case parasitic cones and radial ridges, provide optimal conditions for gorgonian settlement and growth.

In terms of conserving representative habitats it is important to understand the hydrography and the affect this may have on the distribution of species. A PERMANOVA routine was undertaken to investigate which environmental factors affect the biology on the NW/SE side of ADS. The results showed a significant difference in species either side of the seamount, but this difference could not solely be explained by location, but rather an interaction between location, depth and substrate.

This may possibly be an effect of sampling bias in relation to targeted depth and substratum either side of the seamount. From the results we cannot conclude that communities on the NW and SE side of ADS are different as a result of the influence of different water masses, but we can infer that they are subject to varying hydrodynamic activity. The NW side appears to be subject to faster currents, suggested by the well-formed moats at the base of the parasitic cones and less marine snow observed at the seabed on the NW compared to SE side.

3.4.4 *Conclusions*

Anton Dohrn Seamount hosts a diverse range of biotopes, some of which have been described from other megahabitat features, such as banks and submarine canyons. Sampling of distinct geomorphological features identified nine biotopes that fit with current definitions of those of conservation concern under FAO, OSPAR and EC Habitats Directive; seven of these are identified as VMEs.

This work not only provides much needed descriptions of deep-sea biotopes, which is particularly important for the protection of VMEs, but also provides new insights into their potential associations with meso-scale geomorphic features which may be used to map these habitats across broad areas. Listed habitats such as coral gardens, *Lophelia pertusa* reef and bedrock reef habitats were found on distinct topographical features including cliff-top mounds, parasitic cones and radial ridges; and xenophyophore assemblages were found either on geomorphic features or in close proximity (< 100m). There are therefore indications that some biotopes of conservation concern may show some relationship to meso-scale geomorphological features however, further work is needed to test this relationship.

CHAPTER 4

BENTHIC ASSEMBLAGES OF SUBMARINE CANYON SYSTEMS: DEFINING BIOTOPES TO SUPPORT HABITAT MAPPING EFFORTS.

4.1 Introduction

The identification and designation of Marine Protected Areas in the deep sea / high seas is reaching a crucial stage with imminent deadlines (2020 for OSPAR; 2012 for EC Habitats Directive) by which time nations must have implemented a strategy for the protection of species and habitats.

For nations to fulfil their legal requirements to conserve deep-sea habitats they require maps that inform them of the spatial distribution of species and habitats. In light of the vast area covered by the deep sea, numerous approaches have been adopted to mapping, with a view to preserving deep-sea habitats (Harris and Whiteway 2009; Howell 2010). Mapping at a landscape scale (megahabitat scale of kilometres to tens of kilometres; *sensu* Greene *et al*. 1999), using large topographic features such as submarine canyons and seamounts, allows large areas to be covered using lower resolution data, and is thus both cost and time effective. Whilst mapping at this scale may be appropriate for regional level conservation efforts, to adequately protect habitats within national waters it may be more appropriate to map at finer resolutions (< 1 km). In order to achieve finer scale mapping it is necessary to understand the biology of these megahabitat features. In recent years significant research effort has been focused on seamount features, adding much to our understanding of these systems (Clark *et al.* 2010; Rowden *et al.* 2010; Shank 2010; Howell *et al.* 2010a). However, contrastingly, submarine canyons are more poorly sampled, and thus less well understood (De Leo *et al.* 2010).

Submarine canyons are topographically complex features (Yoklavich *et al.* 2000) found incised into many of the world's continental slopes (Hickey 1995; Brodeur 2001). Canyons have been reported as containing diverse bottom types (Kottke *et al.* 2003), have been described as areas of high habitat heterogeneity (Schlacher *et al.* 2007), and are suggested to enhance biodiversity on landscape scales (Vetter *et al.* 2010). The presence of submarine canyons on the continental shelf can significantly alter the hydrodynamic regime of the region, thus canyons may be highly unstable environments subject to periodically intense currents, debris transport, sediment slumps and turbidity flows (Shepard and Marshall 1973; Inman *et al.* 1976; Gardner 1989).

Canyons may act as conduits, transporting sediment and organic matter from the continental shelf to the deep sea (Shepard 1951; Heezen *et al.* 1955; Monaco *et al.* 1990), and can be areas of enhanced production as a result of accumulation of organic matter and/or upwelling. Those with near-shore heads may accumulate drift macrophyte material which may be transported deep into the canyon system (Emery and Hülsemann 1963), a process that has been widely documented from canyons globally (Houston and Haedrich 1984; Flach and Heip 1996; Harrold *et al.* 1998; Vetter and Dayton 1998;1999; Allen *et al.* 2001; Duineveld *et al.* 2001; Okey 2003). Upwelling of nutrient rich deeper waters within canyons provide a nutrient source which leads to enhanced species diversity and biological productivity (Hickey 1995).

Submarine canyons have been suggested to play a role in generating areas of high megabenthic biodiversity due to their complex topographies (Schlacher *et al.* 2007). Canyon fauna flourish as a result of suspension feeding organisms benefiting from accelerated currents within canyons (Rowe 1971) as well as increased secondary production (Vetter *et al.* 2010) through the exploitation of localised increase in

zooplankton during vertical migration (Greene *et al.* 1988). In addition, detritivores benefit from enhanced sedimentation rates and accumulated macrophytic detritus (Vetter 1994; Harrold *et al.* 1998). However, a high incidence of disturbance through sediment transport by intense tidal currents, turbidity currents and detrital flows may be unfavourable to sessile invertebrate megafauna while favouring highly motile species (Rowe 1971; Vetter and Dayton 1999).

Little is known about canyon fauna. Studies of the megabenthos have reported increased, (Rowe 1971; Headrich *et al.* 1975; Rowe *et al.* 1982; Hecker *et al.* 1988; Cartes *et al.* 1994; Sardà *et al.* 1994; Gage *et al.* 1995; Vetter and Dayton 1998), lower, (Maurer *et al.* 1994) or similar, density or biomass (Houston and Haedrich 1984) in canyons compared with equivalent depths on the surrounding shelf and slope. Typical megabenthic filter feeders such as sea whips, sponges, basket stars, anemones and corals have been found in high densities inside canyons (Rowe 1971; Brodeur 2001; Ramirez-Llodra *et al.* 2008) and appear to benefit from the greater availability of hard substratum and the enhanced currents within the canyons (Hecker *et al.* 1988; Ramirez-Llodra *et al.* 2008). Deposit feeding echinoderms such as ophiuroids, holothurians and urchins have been found in greater abundance (urchins, Dume Submarine Canyon) and density (urchins, La Merenguera, western Mediterranean), lower abundance [urchins, Scripps and La Jolla Canyons (Vetter and Dayton 1999); ophiuroids, Hatteras Canyon (Rowe 1971)] and similar abundance [holothurians, Whittard Canyon (Duineveld *et al.* 2001)] in canyons as compared to the neighbouring continental slope.

Topographic features such as canyons, which provide enhanced food supply, diverse habitats, and alter hydrodynamic activity have been described as ‘Keystone structures’ (Vetter *et al.* 2010). Keystone structures are defined as “distinct spatial structures

providing resources, shelter or 'goods and services' crucial for other species" (Tews *et al.* 2004). Those canyons which act as keystone structures, and may be described as biodiversity hotspots, merit special attention in management (Smith *et al.* 2008). The inclusion of canyons as examples of topographical features that may potentially support Vulnerable Marine Ecosystems (FAO 2009) reflects this.

Within the current pan European habitat classification system (EUNIS), canyons are classified at level 4 (A6.8) within the class "A6.81: Canyons, channels, slope failures and slumps on the continental slope". Level 5 further divides these features into: active downslope channels, inactive downslope channels, alongslope channels and turbidites and fans. The EUNIS classes reflect physical processes within these deep-sea features and are not adequate for use in conservation planning since they have no clear relationship to biological assemblages; which is partly because they are still very much at the megahabitat (landscape, *sensu* Greene *et al.* 1999) scale. Fine scale biotope level classes are lacking.

There are few descriptions of benthic assemblages from canyon systems, and none in the context of defining units for use in habitat mapping, or assessing the potential conservation value of canyons. Consequently, the aims of this study are to:

1) *Characterise deep-sea benthic assemblages from submarine canyon features that can serve as classification units (biotopes) in habitat mapping efforts.*

2) Identify biotopes of conservation interest under international/national policy and provide estimates of their biological diversity.

3) *Describe the distribution of biotopes of conservation interest in relation to the geomorphology of the canyons systems.*

To achieve these aims, quantitative analysis of still images (that represent ‘samples’) using identified morphospecies will be undertaken to use in community analysis to identify distinct faunal groups. Criteria to accept/reject clusters as practical ‘mapping units’ will be applied to produce final biotopes. Associated environmental data will be used to characterise defined biotopes, and species data from sample images used to assess and compare diversity between biotopes. Video data will be classified using newly defined biotopes and visualised in ArcGIS 9.3 to describe the distribution of biotopes in terms of environmental factors, canyon, and occurrence on meso-scale geomorphology.

4.2 Methods

4.2.1 *Survey area*

The South West (SW) Approaches study area is located on the Celtic Margin and is an area characterised by a number of submarine canyons (Fig. 4.1). The shelf break, which marks the boundary between the near horizontal sea floor of the continental shelf and the steeper continental slope, occurs between 180 and 250 m water depth with steep flanks reaching the canyon floor.

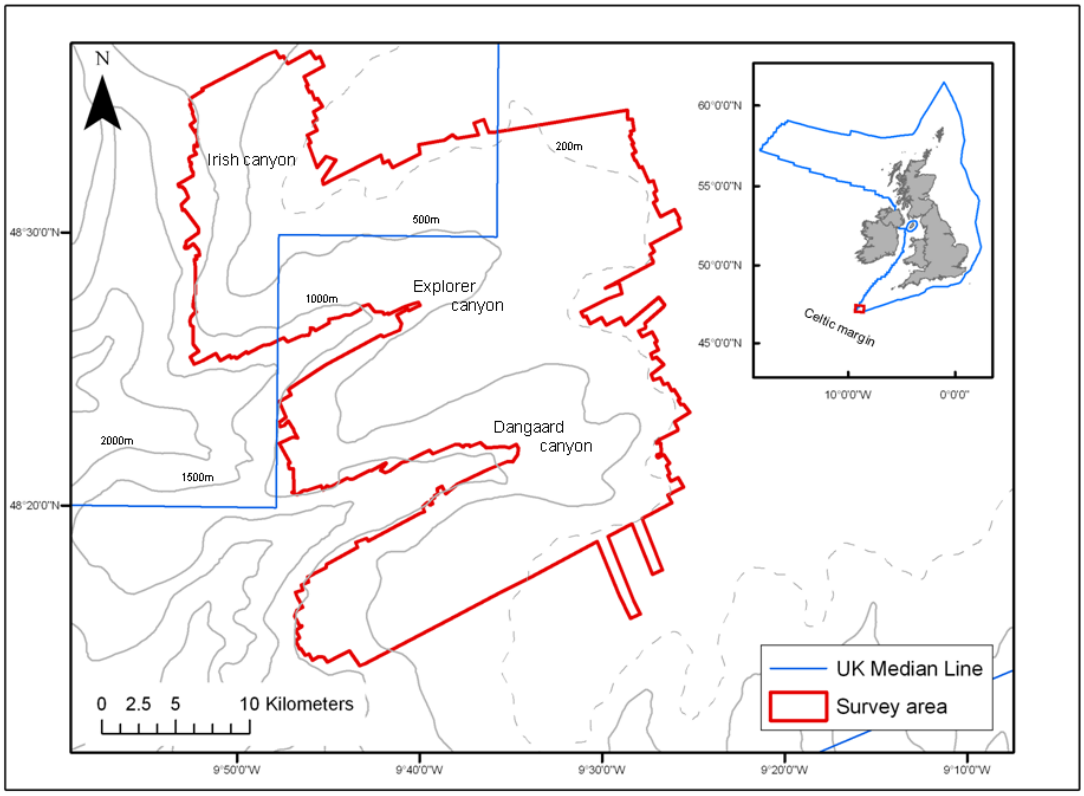

Fig. 4.1: The study area on the Celtic Margin encompassing Dangaard and Explorer canyons and the eastern flank of a third canyon in Irish waters. Bathymetric contours are provided by GEBCO, the 200 m depth contour (dashed line) marks the approximate position of the continental shelf break. The UK median line corresponds to the UK continental shelf limit.

4.2.2 *Data acquisition*

In June 2007 two submarine canyons (Dangaard and Explorer canyons) and a flank of a third canyon (located in Irish waters) in the SW Approaches were surveyed over a thirteen day period onboard the *RV Celtic Explorer* (The Marine Institute, Ireland). High resolution multibeam echosounder data were acquired (Fig. 4.2) over the survey area using a hull mounted Kongsberg Simrad EM1002 system capable of collecting swath bathymetry to ~1000 m water depth. A fixed swath width of 660 m was employed throughout the survey and the operating frequency range for the system was 93-95 kHz. Data were processed onboard and gridded at a resolution of 25 m to allow detailed interpretation of substratum and meso-scale geomorphological features (undertaken by H. Stewart at the BGS).

Video and image data were collected from 44 stations using a drop-frame camera system (Fig. 4.2 see Sect. 2.3.2 for details). Transects were chosen using the processed multibeam bathymetry and backscatter data to cover variations in depth, interpreted geomorphology, seabed substratum (inferred from backscatter data); and where possible, replicate sampling was undertaken within and between all canyons. Seabed type was interpreted in the simplest of terms, to differentiate between hard and soft substratum, principally, as one of the aims of the cruise was to survey bedrock reef habitats. Transect position and orientation was chosen dependent on the terrain, on the steep areas of the canyon flank it was decided that it was safer for the towed camera to travel down- rather than along- slope.

An initial calibration trial was undertaken to determine optimal camera setting for collection of high quality seabed images. Lighting was positioned for optimal illumination for video and image capture, and the stills camera was set on auto focus.

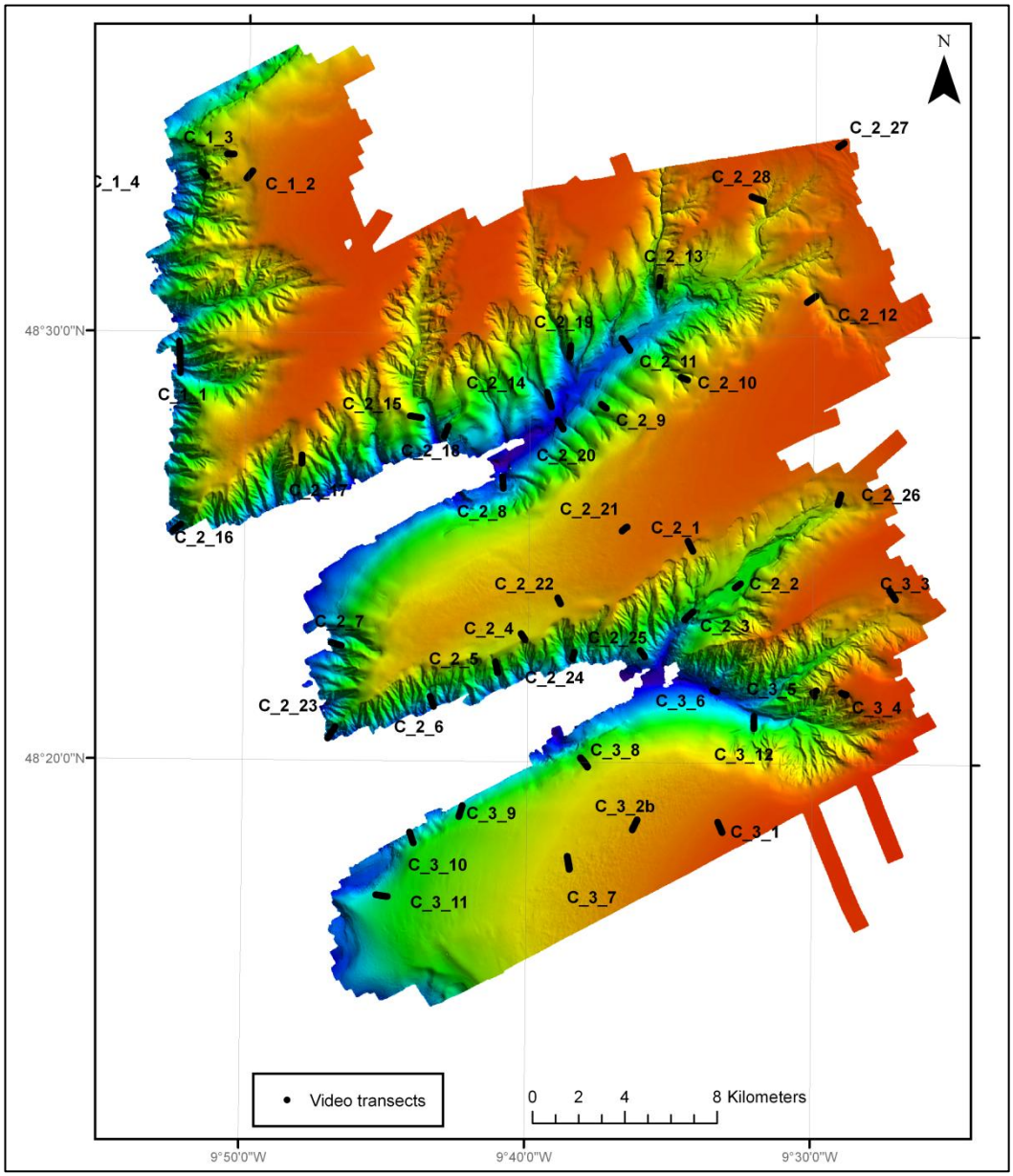

Fig. 4.2: Multibeam bathymetry data and video transects acquired over the SW Approaches survey area. Black dots represent video transects and are labelled with transect names.

The drop-frame was also fitted with sensors to record depth, altitude above the seabed and temperature, and an ultra-short baseline (USBL) beacon, which was fully-integrated with the vessel's digital geographic positioning system (DGPS), was used to collect accurate positional data for the camera frame (Stewart and Davies 2007). Eight days into data acquisition the USBL for the drop-frame camera system suffered a malfunction, from this point onwards the vessel position was utilised for all drop-frame

work. A comparison between vessel position and USBL position on previous transects (in ArcGIS) revealed a high degree of confidence for the vessel position being sufficiently accurate for use with all transects, and was achieved by overlaying both the vessel position and the USBL beacon position on the multibeam echosounder data. The accuracy of the vessel position was sufficient enough [within 30 m of the USBL (Stewart and Davies 2007) to suffice for the remaining 30 camera tows completed during operations.

Camera calibration and sampling protocols were undertaken as described in Sect. 2.3.2. Transect lengths were *approx*. 500 m over a depth range of 184-1094 m. The drop-frame was deployed from the starboard side of the vessel and towed 1-3 m above the seabed at a vessel speed of *approx*. 0.5 knots (min 0.3 and max 0.7) with tows lasting between 0.5-1.5 hrs.

4.2.3 *Biological data analysis*

4.2.3.i *Quantitative analysis of image data*

'Sample' images (defined in Sect. 2.3.2) and those taken at abrupt changes in substratum were reviewed and poor quality images removed, predominantly due to silt clouds obscuring the image or the image being out of focus. The remaining images were quantitatively analysed using image area (derived from the calibration grids). An inherent problem with working in the deep sea is the lack of specimens to aid in identification, and without physical samples it is difficult, and in many cases impossible, to identify organisms to species level from image data; however, observed organisms can be identified as distinct morphospecies (morphotypes).

All visible organisms >1 cm (at their widest point) were identified as distinct morphospecies and assigned an Operational Taxonomic Unit (OTU) number. OTUs were identified to the lowest possible taxonomic level which can correspond to species, genus, family or higher taxonomic levels depending on the group. All individuals were enumerated except in the case of encrusting, colonial and lobose forms where area cover was used. Count data were expressed as taxa/1 m^2 and area cover as percentage cover/1 m^2. To allow combined analysis of cover and percent cover data, a standardisation function was employed (see Sect. 4.2.3.ii).

Seabed substratum composition was assigned to each 'sample' image using the substratum classification described in Sect. 2.4 (see Table 2.3). Image data were stored in an Access database prior to multivariate statistical analysis (see electronic appendix).

4.2.3.ii Community analysis

Standard multivariate community analysis techniques were used to identify faunally distinct benthic assemblages within the study area (described below).

Highly mobile species such as fish, which use multiple habitats and can thus confound the result of the cluster analysis, were removed prior to data analysis. Standardisation of count and cover matrices was undertaken to place them on a common scale to allow a single combined analysis (Prof. R. Clarke *pers.comm*). Each matrix was transformed separately according to distribution of data and the requirement for transformation. Count data were square root transformed, divided through the matrix and multiplied by 200; cover data were 4^{th} root transformed, divided through the matrix and multiplied by 100, to put on a scale of 0.01-1.019. The matrices were combined and then hierarchical cluster analysis undertaken.

Cluster analysis with group-averaged linkage was performed using a Bray-Curtis similarity matrix derived from transformed, combined species count and percent cover data. The SIMPROF routine [similarity profile (Clarke *et al.* 2008)] was used to identify significant clusters using a significance level of $p < 0.01$ and the SIMPER [similarity percentages (Clarke 1993)] routine used to identify those species that characterise those clusters. Characterising species were defined as those species with a high sim/SD ratio (Clarke 1993), and contributed > 5% to that cluster similarity. Clusters identified by SIMPROF ($p < 0.01$) were assessed against the criteria set out in Sect. 2.5.1 and rejected or accepted as faunally distinct clusters on that basis.

4.2.4 *Characterising mapping units (biotopes)*

There is a discrepancy between the faunal assemblages identified using community analysis methods and what is required from a practically applicable mapping unit used in producing necessarily generalised maps of variation in the biological composition of the seabed. Therefore following standard multivariate analysis, faunally distinct clusters (as assessed using the criteria described Sect. 2.5.1) were assessed against a second set of criteria to determine their use as mapping units. Only those clusters that subsequently met these criteria were further analysed in terms of their faunal composition and diversity. To function as a mapping unit assemblages must 1) occur at a scale relevant to the resolution of the acoustic data and the scale of existing widely accepted benthic communities such as cold water coral reefs (e.g. 10 m scale), and 2) be easily identified from video data.

Only those clusters identified by SIMPROF, which contained > 7 images and those which conformed to that of a ‘mapping unit’ criteria (as described above) were considered further.

Mapping units, hereinafter referred to as 'biotopes', were defined in terms of their characterising species, as determined by SIMPER analysis, together with the range of environmental conditions over which they occurred in this study, and named according to the dominant species, in accordance with the EUNIS classification system. A potential pitfall of the sampling method used meant that larger conspicuous fauna may have been mis-represented in the analysed images, thus additional descriptive elements were added from video observations. A 1-way Analysis of Similarity (ANOSIM) on normalised depth and temperature, Euclidean distance matrix was undertaken to test if biotopes were different in term of environmental factors.

To assess those biotopes which could considered of conservation concern, identified biotopes were compared with current definitions of OSPAR and the EC Habitats Directive. Specifically, to identify those which are VMEs, the guidelines of the FAO and current OSPAR definitions were used.

4.2.4.i *Diversity indices*

To assess the diversity of biotopes, species richness and dominance were measured. Mean species richness (total number of species per image) and mean dominance (Simpson's Reciprocal Index per image) were measured for each biotope using all samples defined by the SIMPROF routine as belonging to each biotope. EstimateS 8.3 was used to calculate expected number of species (Mao tau Sobs) interpolated from rarefaction curves, and incidence-based species richness estimators (ICE, Chao 2, Jackknife 1 and 2, and bootstrap) for each biotope, at a standardised sampling effort (the minimum number of samples in a biotope). 1-way Analysis of Similarity (ANOSIM) tests using Primer (v6) were undertaken on a Euclidean distance matrix to test for significant differences in diversity between biotopes (H^o: no significant difference in diversity between biotope). Univariate ANOSIMs were undertaken to compare mean

species richness and dominance between biotopes. A multivariate ANOSIM was also undertaken, using a suite of normalised diversity measures (Simpson Index, expected species richness (Sobs) and incidence-based estimators) to give a holistic view of the diversity measure.

4.2.4.ii *Distribution of biotopes*

Video transects were reviewed and visually classified (guided by the sample image classification) using the newly defined biotopes, and changes of biotope type within a transect were mapped using ArcGIS 9.3. Biotope mapped video data were overlaid on an interpreted geomorphology (undertaken by H. Stewart, BGS) polygon layer in ArcGIS and used to qualitatively describe the distribution of biotopes in relation to geomorphology. Abiotic data were also extracted from the mapped data to define the environmental range of the distribution of each biotope.

4.3 Results

4.3.1 *Geomorphology*

In total 1106 km^2 of multibeam data were acquired over a depth range of 137-1167 m. The multibeam echosounder data revealed the complex morphology of the canyons characterised by amphitheatre rims, slides and headwall scars (Fig. 4.3). The Explorer and Dangaard canyons were incised in the Pleistocene (approximately 1.8 million – 10,000 years ago) during episodic periods of low sea level (Evans 1990). Times of lower sea level caused intensified wave and tidal action initiating cutting of the canyons where previous topographic depressions in the seabed existed or were sites of older buried canyons (Evans 1990). There is no evidence to suggest that canyon cutting is ongoing at the present time, although active headwall erosion has occurred since the last period of low sea level (last glacial maximum) (Evans and Hughes 1984; Cunningham *et al.* 2005). The canyons were classified into the following geomorphological types at the mesohabitat scale (Table 4.1) by H. Stewart at BGS.

Interfluves	**Canyon heads**	**Flank**	**Floor**
Mini-mounds	Tributary gullies	Amphitheatre rims	
	Amphitheatre rims	Tributary networks	
	Incised channels	Tributary gullies	
		Flutes	

Table 4.1: Broad scale division of the canyons system into interfluve, canyon head, flank and canyon floor, with meso-scale geomorphological features identified.

The Dangaard and Explorer canyons are separated by smooth interfluves, which are areas of un-dissected continental shelf and slope. These interfluves host a number of mini-mound features with individual mounds between 2-4 m high and 50-150 m in diameter. These mini-mounds yielded a distinct mottled, or patchy, backscatter response. In the canyon heads, distinct channels are visible and are thought to be

drainage basins in which the catchments area is fed by a network of tributaries (Belderson and Kenyon 1976; Cunningham *et al.* 2005). Amphitheatre rim features were also dominant features in the canyon heads and along the edge of the flanks. Distinct incised channels were visible from the canyon heads to the canyon floor, the steep flanks of the canyons varied from smooth to those with intricate features, such as tributary networks, gullies and flutes. The data also showed that the area was characterised by a number of erosional features such as slumps, slides and slump scars.

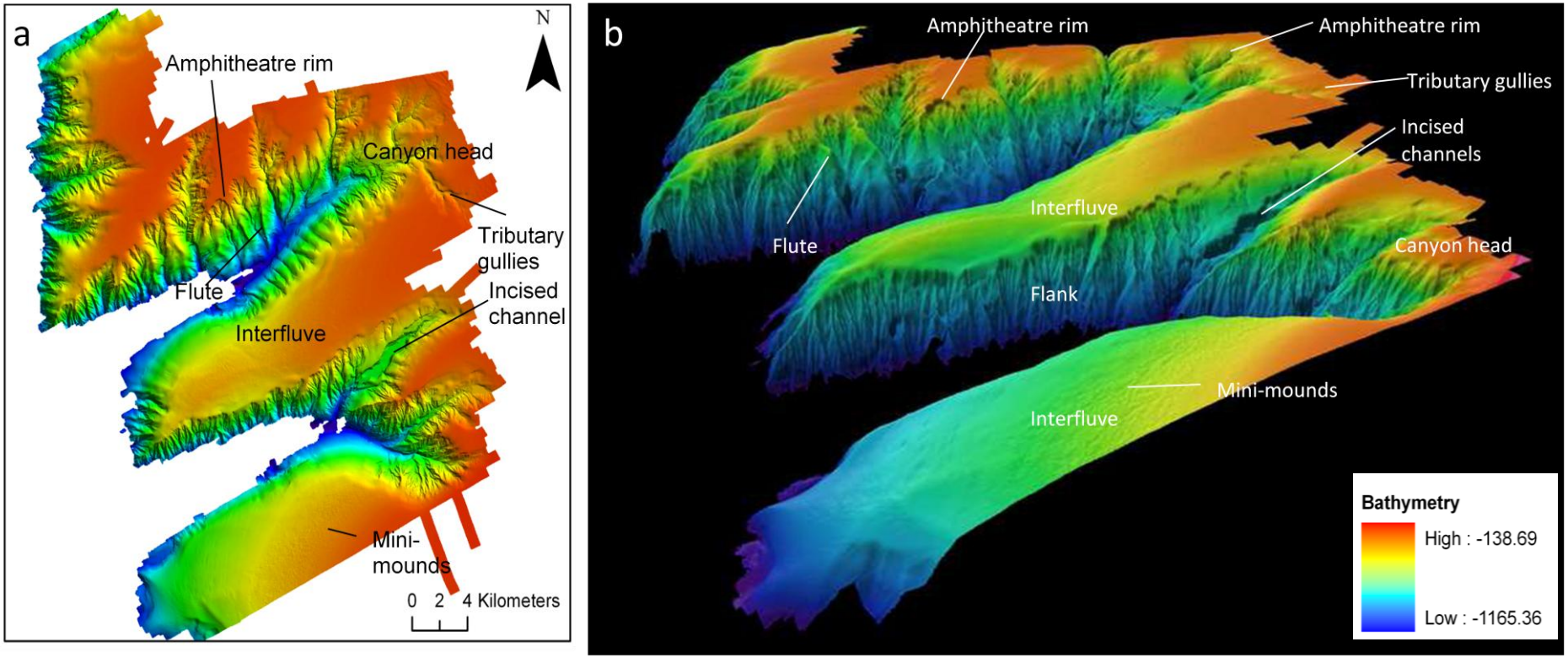

Fig. 4.3: Plan (a) and 3D view (b) of multibeam bathymetry acquired over the survey area, meso-scale geomorphology (*sensu* Greene *et al*. 1999) is labelled. Fig. 4.3b is visualised in Fledermaus™ software, for scale of features see Fig. 4.3a.

4.3.2 *Biological data*

Over 23 hours of video footage and 5000 still images were collected over the survey area. Of these images, 1073 were 'sample' images (those taken at *approx*. 1 minute intervals); upon inspection 199 were discarded due to poor quality (as defined in Sect. 2.3.3).

4.3.2.i *Quantitative analysis of image data*

Eight hundred and seventy four 'samples' were quantitatively analysed (see electronic appendix for raw data) with 161 morphospecies identified and catalogued (see electronic appendix for species catalogue). Those samples where no fauna were recorded were removed prior to the multivariate analysis. Cluster analysis was performed on the remaining 746 samples.

4.3.2.ii Community analysis

The SIMPROF routine identified 43 clusters ($p < 0.01$) (see Table 4.2 for statistical results of clusters). Using the criteria described in Sect. 2.5.1, outlier clusters were removed (cluster a-q) and those that did not act as coherent units for mapping discarded. The following identifies the specific reasons for discarding of specific clusters: less than 7 samples (clusters t-w, aa-ab, ad-ag, ai, ak and an), had a within group SIMPER similarity of < 15% (cluster s) and not recognisable from video (cluster z). The remaining 11 clusters were accepted as practically applicable mapping units. Results from the cluster analysis of still image "samples", including SIMPER analysis and a description of the environmental characteristics associated with each cluster are shown in Table 4.2 (see appendix A4.1 for SIMPER results).

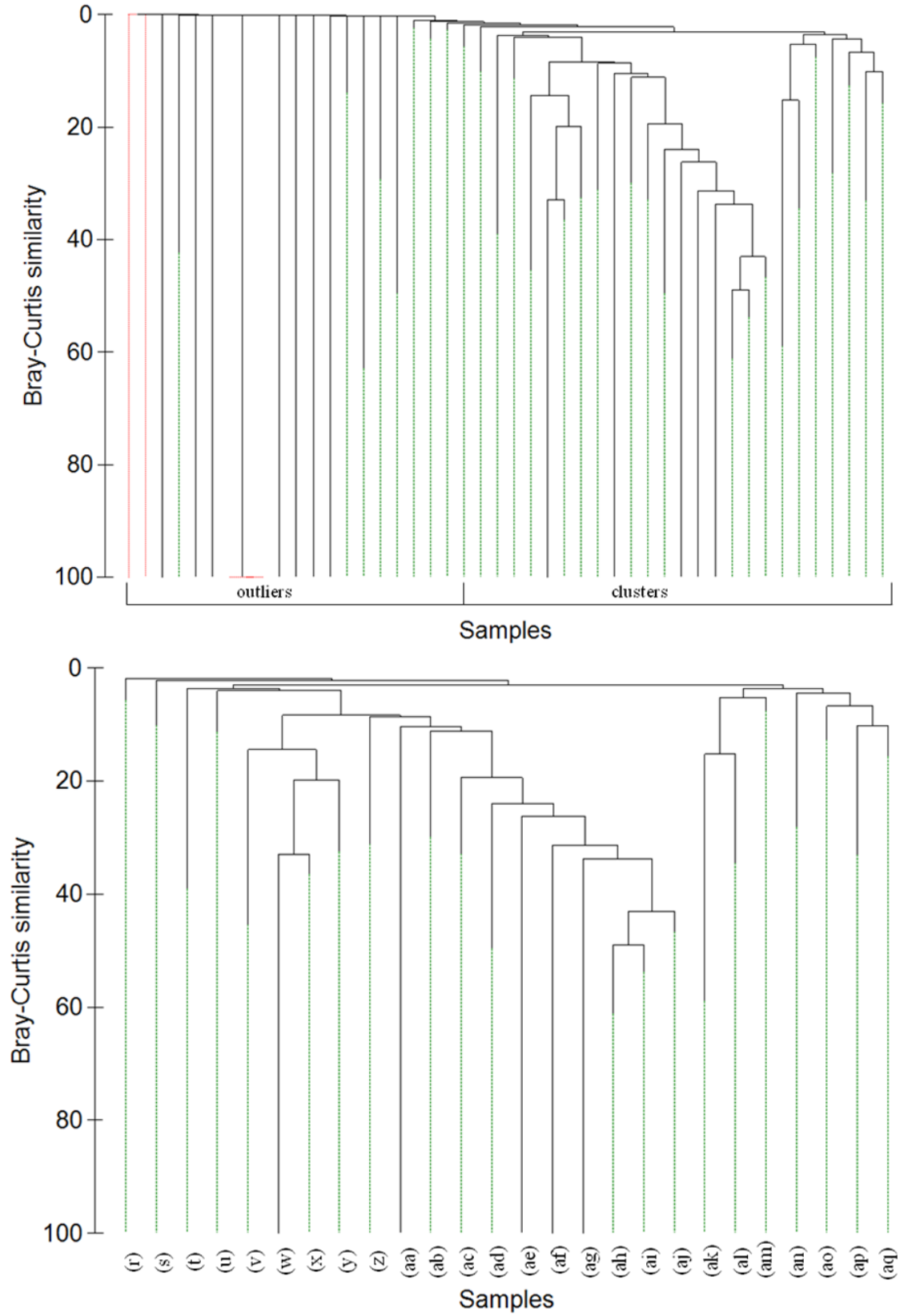

Fig.4.4 Dendrogram of hierarchical cluster analysis of species data, clusters identified using the SIMPROF routine ($p < 0.01$). Dendrogram (a) shows those clusters identified as outliers at a 1% Bray Curtis similarity level and (b) remaining clusters for rejection/acceptance process. SIMPROF clusters have been collapsed for illustrative purposes.

Cluster	No. images	Useful mapping unit	SIMPER similarity level (%)	Temp range (°C)	Average Temp (SD)	Depth range (m)	Average Depth (SD)	Characterising species
a	2	N	0	9.6-11.3	10.487 (1.21)	316-840	578 (370.5)	
b	1	N		11.546	11.546	256	256	
c	2	N	42.26	10.4-11.7	11.118 (0.90)	210-695	452.5 (342.9)	Sabellidae sp. 1
d	1	N		9.252	9.252	850	850	
e	1	N		11.496	11.496	309	309	
f	3	N	100	9.0-10.4	9.951 (0.80)	508-866	694.3 (151.3)	*Benthogone* sp.
g	1	N		11.497	11.497	311	311	
h	1	N		11.542	11.542	256	256	
i	1	N		10.007	10.007	788	788	
j	1	N		9.91	9.91	762	762	
k	3	N	25.93	9.7-10.4	9.970 (0.38)	602-755	695.6 (82.1)	*Protoptilum* sp., *Pseudarchaster* sp.
l	4	N	68.45	11.22-11.74	11.388 (0.23)	212-401	342.5 (88.6)	Edwardsiidae sp. 1
m	3	N	44.15	8.8-9.1	9.02 (0.12)	885-1006	947.3 (60.5)	Halcampoididae sp. 3, Unknown sp. 13
n	2	N	49.42	11.549	11.549	321-323	322 (1.4)	Unknown sp. 15

o	16	N	50.48	9.3-10.2	9.732 (0.24)	714-928	800.6 (51.7)	Sagartiidae sp. 3
p	6	N	18.04	8.9-11.1	10.499 (0.83)	331-1059	596.5 (249.7)	Actiniaria sp. 14, Cerianthidae sp. 3
q	11	N	10.73	7.7-11.6	10.465 (1.24)	185-1009	543 (305.4)	*Caryophyllia* sp. 2, Porifera encrusting sp. 1, Hydrozoa (flat branched)
r	7	Y	25.07	8.9-11.6	10.062 (1.32)	190-909	625.7 (341.4)	cf. *Bathylasma* sp., Hydrozoa (bushy)
s	9	N	14.78	10.3-11.4	11.11 (0.47)	238-800	407 (222.8)	Terebellidae sp. 1, Actiniaria sp. 17
t	2	N	38.99	9.2-9.7	9.745 (0.03)	729-782	755.5 (37.4)	Amphipoda sp. 1
u	4	N	20.08	8.1-10.1	9.379 (0.94)	741-1015	852.5 (122.6)	*Colus* sp. 2
v	3	N	49.37	10.5-11.3	11.026 (0.43)	378-601	452.6 (128.4)	*Pachycerianthus multiplicatus*, Cerianthidae sp. 1
w	1	N		11.174	11.174	333	333	
x	49	Y	54.39	9.0-11.5	9.922 (0.59)	308-954	738.6 (164.7)	Cerianthidae sp. 1
y	39	Y	49.80	9.1-10.3	9.544 (0.29)	609-953	836.7 (89.3)	*Kophobelemnon stelliferum*, Cerianthidae sp. 1
z	23	N	41.11	8.0-11.5	10.31 (1.20)	295-1054	615.6 (288.2)	*Ophiactis balli*
aa	1	N		9.599	9.599	938	938	
ab	3	N	31.57	8.0-9.8	9.207 (1.01)	781-1012	869 (124.9)	Sabellidae sp. 2
ac	46	Y	47.47	7.7-10.7	9.294 (0.82)	316-1048	829.7 (166.7)	Unknown sp. 26, Cerianthidae sp. 1

ad	6	N	59.02	9.0-11.7	9.517 (1.06)	184-942	778.8 (294.2)	*Lophelia pertusa* (dead structure)
ae	1	N		9.763	9.763	699	699	
af	1	N		9.878	9.878	798	798	
ag	1	N		9.011	9.011	874	874	
ah	30	Y	66.25	9.5-9.9	9.780 (0.09)	797-938	860.9 (43.7)	*Lophelia pertusa* (dead structure), *Lophelia pertusa*, *Madrepora oculata*, Unknown sp. 26, Actiniaria sp. 13
ai	3	N	61.28	9.5-9.7	9.646 (0.08)	914-936	922.3 (11.9)	Unknown sp. 26, *Lophelia pertusa* (dead structure), *Madrepora oculata*
aj	7	Y	54.00	9.0-9.8	9.377 (0.39)	816-942	894.6 (55.6)	*Lophelia pertusa* (dead structure), Halcampoididae sp. 1, *Lophelia pertusa* Cerianthidae sp. 1
ak	3	N	66.33	9.7-11.3	10.523 (1.09)	417-782	640.3 (195.7)	Halcampoididae sp. 5
al	71	Y	53.22	7.6-11.5	10.163 (0.98)	254-1008	654.3 (218.9)	Amphiuridae sp. 1, Cerianthidae sp. 1
am	276	Y	47.39	8.9-11.8	10.803 (0.64)	205-1021	477.3 (195.37)	Ophiuroidea sp. 1
an	6	N	49.67	10.5-11.4	10.988 (0.38)	257-600	433.1 (159.6)	Crinoidea sp. 5, *Stichopathes* cf. *gravieri*
ao	24	Y	27.51	9.4-11.8	10.943 (0.68)	189-803	464.1 (214.9)	Serpulidae sp. 1, Brachiopoda sp. 1, *Munida sarsi*
ap	20	Y	41.38	9.6-11.6	10.926 (0.73)	252-791	423.9 (212.9)	Ophiuroidea sp. 5, *Munida sarsi*
aq	51	Y	31.11	9.0-11.7	11.303 (0.40)	192-825	326.4 (124.0)	*Munida sarsi*, *Leptometra celtica*

Table 4.2: Clusters identified using the SIMPROF routine, SIMPER similarity, environmental variables and characterising species for each cluster identified.

4.3.3 *Characterising mapping units (biotopes)*

In total 11 mapping units (biotopes) were identified from the cluster analysis (Fig. 4.5) and related to available environmental data to describe distinct mapping units [(biotopes) see Table 4.2 for details]. A 1-way ANOSIM test of environmental data (depth and temperature) for the 11 biotopes defined from image data revealed a significant difference in environmental conditions between biotopes (Global $R = 0.265$, $p < 0.01$). Thirty one pairwise tests were significant (Table 4.3) and Fig. 4.6 illustrates an nMDS plot showing a variation of biotopes relating to environmental conditions. Two groups are apparent and appear to be related to depth zones, one on the left comprising of 5 biotopes (x, y, al, ac and aj) a deeper zone (654-894 m average depth of biotopes) and the other having 4 biotopes (am, aq, ap and ao) at shallower depths (326-477m average depth of biotopes). Biotope r and ah are most dissimilar, although appear not to be strongly related to either of the main groups observed in Fig. 4.6.

Fig. 4.5: Example images of biotopes showing fauna characteristic of each assemblage. Codes given to biotopes correspond to SIMPROF clusters in brackets: Bat.Hyd (r), Amp.Cer (ae), Kop.Cer (y), Unk.Cer (ac), Lop.Cri (not defined from cluster analysis), Lop.Hal (aj), Lop.Mad (ah), Cer (x), Oph (am), Ser.Bra (ao), Mun.Lep (aq), Oph.Mun (ap). Lop.Cri was not identified from the cluster analysis, but described from the video.

	x	y	ac	ah	aj	al	am	ao	ap	aq
r	**0.395 (0.3)**	**0.545 (0.1)**	**0.299 (1.9)**	**0.948 (0.1)**	0.143 (10.7)	0.187 (0.5)	**0.379 (0.1)**	**0.297 (0.7)**	**0.326 (1.2)**	**0.494 (0.2)**
x		0.028 (8.2)	0.045 (0.3)	0.106 (1)	-0.004 (45.9)	0.006 (32.3)	**0.314 (0.1)**	**0.402 (0.l)**	**0.461 (0.1)**	**0.755 (0.1)**
y			0.031 (4.7)	**0.32 (0.1)**	0.108 (17.4)	0.074 (0.074)	**0.481 (0.1)**	**0.705 (0.1)**	**0.732 (0.1)**	**0.939 (0.1)**
ac				0.09 (2.4)	-0.148 (92.2)	0.091 (0.5)	**0.494 (0.1)**	**0.499 (0.1)**	**0.543 (0.1)**	**0.845 (0.1)**
ah					**0.535 (0.2)**	0.041 (14.2)	**0.45 (0.1)**	**0.768 (0.1)**	**0.796 (0.1)**	**0.936 (0.1)**
aj						0.03 (34.2)	**0.574 (0.1)**	**0.579 (0.1)**	**0.69 (0.1)**	**0.943 (0.1)**
al							0.199 (0.1)	0.076 (3)	0.109 (0.9)	**0.349 (0.1)**
am								0.029 (24)	0.005 (44.8)	-0.042 (89.3)
ao									0.028 (13.2)	0.242 (0.2)
ap										0.064 (15.7)

Table 4.3: Pairwise results of the ANOISM test of environmental data for biotopes with R and P (%) values for each pair. Global R = 0.265, P = < 0.01. Significant pairwise tests are marked in bold.

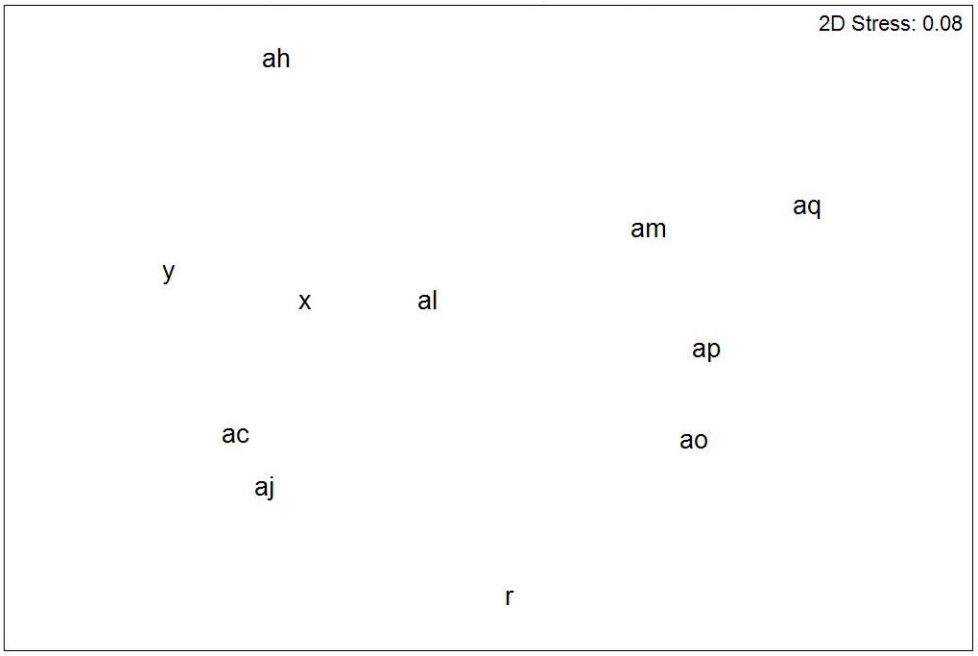

Fig. 4.6: nMDS ordination plot of pairwise ANOSIM test for depicting difference in environmental variables between biotopes. Cluster letters correspond to biotope codes: r (Bat.Hyd), ae (Amp.Cer), y (Kop.Cer), ac (Unk.Cer), aj (Lop.Hal), ah (Lop.Mad), x (Cer), am (Oph), ao (Ser.Bra), aq (Mun.Lep), ap (Oph.Mun).

4.3.3.i *Diversity indices*

The mean Simpson Index and 95% confidence intervals per biotope as seen in Fig. 4.7a indicate a significant difference in diversity between some biotopes (data from figures 4.7 are in Appendix A4.2). Biotopes aq [Mun.Lep (+/- 0.135)] and r [Bat.Hyd (+/- 0.68) showed the largest variation around the mean, while biotope am [Oph (+/- 0.074)] had the lowest. The *Lophelia pertusa* reef biotope ah (Lop.Mad) had the highest Simpson Index, and the soft sediment ophiuroids biotope am (Oph) had the lowest Simpson Index.

Interestingly, Fig 4.7b indicates a clear difference in species richness (averaged for images), with biotopes falling into three groups. A higher species richness [ah (Lop.Mad)] of 8.9, medium [ac (Unk.Cer), aj (Lop.Hal)] of 4.4–5, and lower [al (Amp.Cer), am (Oph), ao (Ser.Bra), ap (Oph.Mun), aq (Mun.Lep), r (Bat.Hyd), x (Cer), y (Kop.Cer)] of 1.8–3.1. Contrary to this, the expected number of species (Sobs) extracted from rarefaction curves (see Appendix A4.3) for a standardised sampling effort show two less clearly defined bands (Fig. 4.8b). Those biotopes with higher Sobs of between 12–17.7 [r (Bat.Hyd), ac (Unk.Cer), ah (Lop.Mad), aj (Lop.Hal), ap (Oph.Mun) and lower with a range of 6.4–9.7 [x (Cer), y (Kop.Cer), al (Amp.Cer), am (Oph), ao (Ser.Bra), aq (Mun.Lep)]. Note that two of the biotopes with lower species richness (r and aj) in Fig. 4.7b can be classed in the higher Sobs band on Fig. 4.8.

Rarefactions curves [Fig. 4.9-4.19 (see appendix A4.3)] of biotopes illustrate the species estimator curves in relation to the Sobs. Unique and duplicate species are also plotted as an indicator of estimator curve asymptote, when they cross, higher confidence can be taken from the estimators. Chao2 and ICE had the greatest SD across the estimators, as illustrated in Fig. 4.20-4.30 (see appendix A4.4).

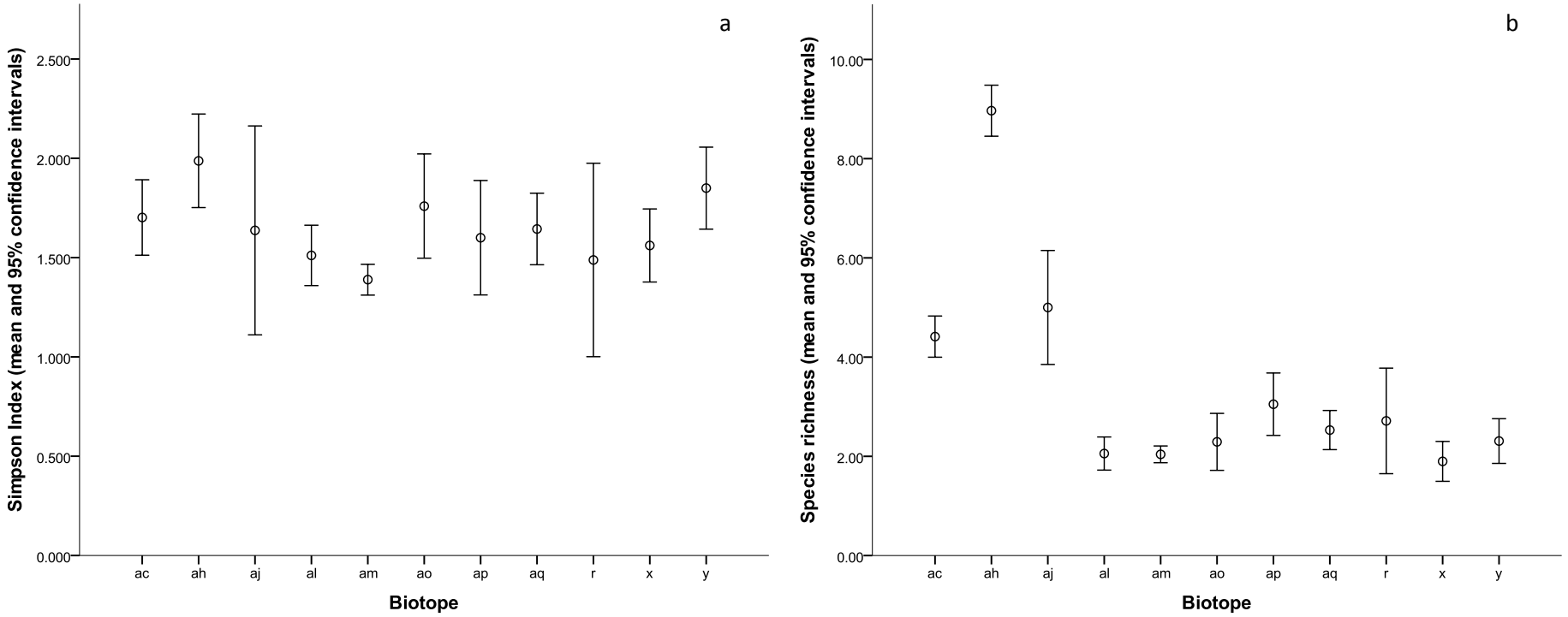

Fig. 4.7: (a) Mean Simpson index with 95% confidence interval for biotopes defined from cluster analysis, (b) mean species richness (derived per image) and 95% confidence intervals for each biotope. r (Bat.Hyd), ae (Amp.Cer), y (Kop.Cer), ac (Unk.Cer), aj (Lop.Hal), ah (Lop.Mad), x (Cer), am (Oph), ao (Ser.Bra), aq (Mun.Lep), ap (Oph.Mun).

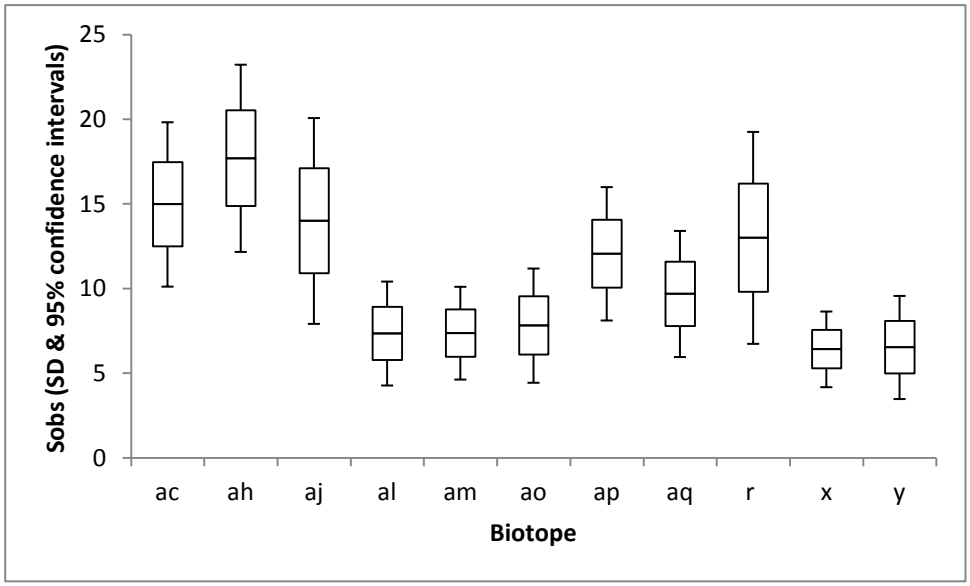

Fig. 4.8: Estimated species richness Sobs (Mao Tau) with standard deviation and 95% confidence intervals for each biotope at a standardised sample size of seven. r (Bat.Hyd), ae (Amp.Cer), y (Kop.Cer), ac (Unk.Cer), aj (Lop.Hal), ah (Lop.Mad), x (Cer), am (Oph), ao (Ser.Bra), aq (Mun.Lep), ap (Oph.Mun).

Diversity in terms of estimated species richness (Sobs) increases with habitat complexity (Fig. 4.7). With soft sediment biotopes [x (Cer), Y (Kop.Cer), al (Amp.Cer), am (Oph) having the lowest mean Sobs, and with the mixed substratum biotope ao (Ser.Bra) having marginally higher Sobs, followed by the biogenic gravel biotopes [aq (Mun.Lep), ap (Oph,Mun)], bedrock [r (Bat.Hyd), aj (Lop.Hal)], with Lop.Mad (ah) (ah) and Unk.Cer (ac) having the highest Sobs. Dominance (Simpson Index) of biotopes was lowest for all soft sediment biotopes, with the exception of the sea pen biotope Kop.Cer which had the second highest Simpson Index.

All three ANOSIM tests were significant at $P < 0.01$, thus rejecting the H^o of no significant difference in diversity between biotopes. The multivariate ANOSIM (multiple diversity indices) (Table 4.6) had the highest global R (R= 0.403), followed by the univariate ANOSIM test for species richness (R= 0.22) then Simpson index (R= 0.161). Thirty one pairwise tests were significant for the multivariate ANOSIM, 21 for

species richness, and 11 for Simpson Index (Tables 4.4 - 4.6). Overall, Lop.Mad had the highest diversity, in terms of Simpson Index, and was significantly different ($P < 0.01$) to all biotopes except y (Kop.Cer), ac (Unk.Cer) and aq (Oph.Mun); species richness was significantly different to all biotopes; and multivariate diversity measure was significantly different to all except ac (Unk.Cer) and aq (Oph.Mun).

Comparing diversity using one diversity measure only provides one aspect of the diversity of that assemblage. Taking a more holistic approach (multivariate) captures other aspects of diversity that genuinely exist. Each index captures a different aspect of diversity, thus, strengthening the comparative tests between biotopes. The higher global R from the multivariate ANOSIM illustrates the benefit of using a suite of diversity indices to compare diversity between assemblages. The performance of species richness estimators can vary greatly (as observed by the variation observed in Fig. 4.20-4.30, A4.4), thus using several estimators for comparing diversity provides statistical rigour and allows for improved confidence in findings of assemblage diversity.

	x	y	ac	ah	aj	al	am	ao	ap	aq
r	-0.011 (52.3%)	0.169 (3.4%)	0.023 (38.2%)	**0.519 (0.1%)**	-0.009 (43%)	-0.012 (50.6%)	0.053 (29.7%)	-0.07 (69.7%)	-0.029 (51.2%)	-0.01 (48%)
x		0.154 (0.1%)	0.085 (0.1%)	**0.296 (0.1%)**	0.051 (28.9%)	0.013 (21.7%)	0.053 (12.9%)	0.046 (14.9%)	0.034 (24.7%)	0.037 (2.6%)
y			0.081 (0.6%)	-0.005 (48%)	-0.013 (52%)	0.141 (0.1)	**0.282 (0.1%)**	0.087 (1.9%)	0.124 (1.1)	0.048 (3.1%)
ac				0.131 (0.2%)	-0.026 (51.6%)	0.042 (6.2%)	**0.193 (0.1%)**	0.061 (10.1%)	-0.007 (46.2%)	-0.001 (39%)
ah					**0.212 (6%)**	**0.231 (0.1%)**	**0.393 (0.1%)**	**0.24 (0.1%)**	**0.341 (0.1%)**	0.109 (0.5%)
aj						0.05 (28.3%)	**0.182 (8.8%)**	-0.092 (74.8%)	-0.008 (44.8%)	-0.056 (63.2%)
al							0.065 (5.5%)	0.079 (8.5%)	0.014 (33.8%)	0.02 (12.8%)
am								**0.173 (0.7%)**	0.134 (3.9%)	0.149 (0.1%)
ao									-0.012 (54%)	0.028 (24.2%)
ap										-0.013 (52.9%)

Table 4.4: Pairwise results of the ANOISM test for Simpson index of biotopes with R and P (%) values for each pair. Global R = 0.161 (p <0.01). Significant pairwise tests are marked in bold. r (Bat.Hyd), ae (Amp.Cer), y (Kop.Cer), ac (Unk.Cer), aj (Lop.Hal), ah (Lop.Mad), x (Cer), am (Oph), ao (Ser.Bra), aq (Mun.Lep), ap (Oph.Mun).

	x	y	ac	ah	aj	al	am	ao	ap	aq
r	0.198 (1.3%)	**0.269 (0.27%)**	0.019 (35.3%)	**0.828 (0.1%)**	0.093 (13.9%)	0.218 (1.4%)	0.195 (4.6%)	0.084 (16.6%)	0.001 (40.3%)	0.118 (6.7%)
x		0.053 (1.5%)	**0.299 (0.1%)**	**0.958 (0.1%)**	**0.57 (0.1%)**	-0.001 (42%)	-0.015 (63.9%)	0.041 (14.7%)	0.216 (0.4%)	0.054 (1%)
y			0.174 (0.1%)	**0.95 (0.1%)**	**0.518 (0.2%)**	0.002 (40%)	0.023 (27.6%)	0.041 (9.7%)	0.16 (0.3%)	-0.019 (90.4%)
ac				**0.536 (0.1%)**	0.005 (45.3%)	**0.333 (0.1%)**	**0.435 (0.1%)**	0.098 (2.3%)	-0.019 (63.4%)	0.168 (0.1%)
ah					**0.49 (0.1%)**	**0.965 (0.1%)**	**0.946 (0.1%)**	**0.903 (0.1%)**	**0.827 (0.1%)**	**0.93 (0.1%)**
aj						**0.552 (0.1%)**	**0.537 (0.1%)**	**0.415 (0.3%)**	0.205 (6.6%)	**0.405 (0.2%)**
al							-0.004 (52%)	0.041 (15.5%)	0.208 (0.1%)	0.041 (3%)
am								0.056 (15.5%)	**0.226 (0.1%)**	0.091 (1.1%)
ao									0.053 (6.9%)	0 (43.6%)
ap										0.063 (7.8%)

Table 4.5: Pairwise results of ANOISM test for mean species richness of biotopes. Global R = 0.22(p < 0.01). Significant pairwise test are marked in bold. r (Bat.Hyd), ae (Amp.Cer), y (Kop.Cer), ac (Unk.Cer), aj (Lop.Hal), ah (Lop.Mad), x (Cer), am (Oph), ao (Ser.Bra), aq (Mun.Lep), ap (Oph.Mun).

	x	y	ac	ah	aj	al	am	ao	ap	aq
r	0.007 (35.6%)	0.304 (0.6%)	**0.815 (0.1%)**	**0.641 (0.9%)**	0.01 (38.9%)	0.141 (5.3%)	-0.097 (92%)	0.02 (36%)	**0.427 (1.2%)**	0.247 (3.8%)
x		0.148 (4.4%)	**0.9 (0.1%)**	**0.786 (0.4%)**	0.259 (4.6%)	-0.004 (40.7%)	-0.039 (68%)	0.113 (7.8%)	**0.729 (0.1%)**	**0.558 (0.8%)**
y			**0.801 (0.1%)**	**0.746 (0.2%)**	0.381 (1.5%)	**0.455 (0.2%)**	0.206 (2.7%)	**0.459 (0.1%)**	**0.642 (0.5%)**	**0.623 (0.1%)**
ac				-0.105 (98.9%)	**0.684 (0.2%)**	**0.957 (0.2%)**	**0.797 (0.3%)**	**0.851 (0.3%)**	**0.481 (0.7%)**	**0.546 (0.7%)**
ah					**0.518 (1.6%)**	**0.813 (0.3%)**	**0.638 (0.2%)**	**0.729 (0.2%)**	**0.475 (0.7%)**	0.464 (0.9%)
aj						**0.453 (0.6%)**	0.11 (11.9%)	0.297 (3.1%)	0.199 (5.6%)	-0.032 (52.6%)
al							0.08 (9.9%)	0.288 (1.5%)	**0.834 (0.4%)**	**0.75 (0.1%)**
am								-0.019 (55.3%)	**0.484 (0.7%)**	0.356 (1.4%)
ao									**0.565 (0.7%)**	**0.485 (0.6%)**
ap										0.033 (28%)

Table 4.6: Pairwise results of ANOISM test for multivariate diversity test of biotopes, standardised for sample size (7 samples). Global R = 0.403 ($p < 0.01$). Significant tests are marked in bold. r (Bat.Hyd), ae (Amp.Cer), y (Kop.Cer), ac (Unk.Cer), aj (Lop.Hal), ah (Lop.Mad), x (Cer), am (Oph), ao (Ser.Bra), aq (Mun.Lep), ap (Oph.Mun).

4.3.3.ii *Distribution of biotopes*

Visual classification of video data according to the newly defined biotopes revealed an assemblage that did not fit with any of those defined. Upon reviewing the data, it was apparent that image sample data had failed to capture this assemblage (due to limited areas of bedrock captured by the still images). Based on visual assessment of the assemblage it appears similar to assemblages described by Weinberg *et al*. (2008) and Howell *et al*. (2010b) and was therefore classified as such. In the interests of fully characterising the Canyons region, and given that this previously described biotope is of particular conservation importance due to the occurrence of listed species (*L. pertusa*), as well as being the only bedrock community observed in the canyons that may be classed as Annex I bedrock reef (under the EC Habitats Directive), its distribution within the canyon system is also considered here.

Qualitative assessment of biotope distribution, determined from visually classified video transect data, (Table 4.7) revealed that six of the 12 biotopes were observed in all 3 canyons, 4 soft sediment biotopes (Kop.Cer, Cer, Amp.Cer and Oph), a mixed substratum (shell hash) biotope (Mun.Lep) and Lop.Cri on bedrock. Five biotopes fit with the 'listed habitats' definition. The sea pen biotope Kop.Cer was observed in all three canyons on the flank and incised channels over a depth of 463-1059 m. The bedrock associated biotope, Lop.Cri, was also observed in all canyons, occurring on incised channels, tributary gullies, flank and amphitheatre rims features over a depth of 253-1022 m. The *Lophelia pertusa* reef biotope Lop.Mad was only observed once in Explorer canyon on flute features 795-940 m, while the dead framework biotope Lop.Hal was observed in both Explorer and Dangaard on the flanks and flute features (697-927 m). The coral rubble biotope Oph.Mun was observed in Explorer and Dangaard canyons on incised channel and mini-mound features over a depth of 303-1017 m.

Assemblage code	Cluster	Assemblage name	Depth	Temperature	Geomorphological Feature	Substratum	Canyon
Bat.Hyd	r	cf. *Bathylasma* sp. and hydroid assemblage on bedrock	902-912 m	8.99-9°C	Incised channel	Bedrock	Explorer
Kop.Cer	y	*Kophobelemnon stelliferum* and cerianthid assemblage on mud/muddy sand	463-1059 m	8.87-10.85°C	Flank and incised channel (canyon head)	Mud and muddy sand	Explorer, Irish and Dangaard
Cer	x	Cerianthids on sediment draped bedrock	360-1064 m	8.98-11.3°C	Canyon head, amphitheatre rims, incised channels, flank	Bedrock with sand veneer	Explorer, Irish and Dangaard
Unk.Cer	ac	Annelids, hydroids and cerianthids on bedrock ledges	238-1070 m	8.36-11.51°C	Canyon head and incised channels (canyon floor)	Bedrock and bedrock with sand veneer	Explorer and Dangaard
Lop.Mad	ah	*Lophelia pertusa* reef	795-940 m	9.41-9.92°C	Flute feature	Coral framework	Explorer
Lop.Hal	aj	Predominantly dead low-lying coral framework	697-927 m	8.97-9.77°C	Flank and flute feature (end of interfluves)	Coral rubble, bedrock and bedrock with sand	Explorer and Dangaard
Amp.Cer	al	Amphiuridae ophiuroids and cerianthid anemones on bioturbated mud/sand	184-943 m	9.59-11.69°C	Flank, canyon head and continental shelf	Mud and sand	Explorer, Irish and Dangaard
Oph	am	Burrowing (*Amphiura* sp.) and surface dwelling ophiuroids on mud/sand	184-1094 m	7.67-11.69°C	Flank, tributary gullies, amphitheatre rims	Mud and sand	Explorer, Irish and Dangaard
Ser.Bra	ao	Serpulids and brachiopods on mixed substratum	691-764 m	10.1-10.5°C	Flank	Mixed	Dangaard
Oph.Mun	ap	Ophiuroids and *Munida sarsi* associated with coral rubble	303-1017 m	7.98-11.5°C	Incised channels and mini-mounds	Biogenic gravel (coral rubble)	Explorer and Dangaard
Mun.Lep	aq	*Munida sarsi* and *Leptometra celtica* on mixed substratum	183-792 m	9.79-11.79°C	Interfluves and canyon head	Mixed, biogenic gravel (shell hash)	Explorer, Irish and Dangaard
Lop.Cri	*	*L. pertusa* and crinoids on bedrock	253-1022 m	7.93-11.42°C	Incised channels, tributary gullies, flank, amphitheatre rims	Bedrock	Explorer, Irish and Dangaard

Table 4.7: Summary of mapped biotope data, abiotic data extracted from video metadata, geomorphology and substratum extracted from ArcGIS 9.3 layers.* refers to the biotope described from the video footage.

4.4 Discussion

Submarine canyons are considered to be potential biodiversity hotspots, however, to date there is very little data on canyon community composition of these features, or measures of diversity to assess their potential importance as features of conservation interest. Eleven biotopes were identified using traditional multivariate cluster analysis methods, and a further from my video observation from the SW Approaches submarine canyons (Fig. 4.5) and full descriptions with the SIMPER results are provided in Appendix A4.1 and A4.5. Five of the biotopes could be considered of conservation interest. Of these five, only four come under the definition of VMEs, three could be classified as cold-water coral reefs under the EC Habitats Directive and OSPAR Convention, whist the fourth could be classed as 'Sea pen and burrowing megafauna communities' under the current OSPAR definition. The fifth could be considered bedrock reef under the EC Habitats Directive. Seven biotopes were soft sediment communities or faunally-sparse and thus, have little or no perceived conservation interest; of these, three have been previously described by a number of authors while four are new descriptions (see Appendix A4.5 for descriptions). Those habitats that are listed under policy (OSPAR and EC Habitats Directive) will be discussed in terms of a description of the new biotopes defined within this chapter and related to other research, those which are not 'listed' habitats will not be discussed; however full descriptions for each are given in Appendix A4.6. A comparison of diversity of biotopes, followed by the occurrence of biotopes on meso-scale geomorphological features will also be discussed.

4.4.1 *Descriptions of 'listed' habitats for use as mapping units*

4.4.1.i Cold-water coral reef

Three biotopes were defined that could be considered as cold-water coral reef, these communities represent distinct reef zones (*sensu* Mortensen *et al*. 1995) or macrohabitats (*sensu* Greene *et al*. 1999) each with different associated fauna forming distinct communities.

Lophelia pertusa reef

This biotope (Lop.Mad, cluster ah) was characterised by dead *Lophelia pertusa* framework and live patches of *L. pertusa* and *Madrepora oculata* which provide a structural habitat for associated species. Other characterising species (as identified by SIMPER) were small anemones (Actiniaria sp.13) and an unidentified species (Unknown sp.26) which were associated with the *Lophelia*. Additional species identified from qualitative video observations were *Pandalus borealis* and the echinoid *Cidaris cidaris*; halcampoid anemones (Halcampoididae sp.1) inhabited the interspersed sediment patches in the reef. Other conspicuous fauna observed from the image and video data were large cerianthid anemones, the decapod *Bathynectes* sp. and the fish *Lepidion eques*. This assemblage was observed on steep flute features on the flank of Explorer canyon over a depth of 795-940 m and temperature of 9.41-9.92°C.

This assemblage corresponds to the 'live *Lophelia* zone' as described by Mortensen *et al*. (1995) which is the main reef habitat found on the summit of the reef and consists of predominantly live *Lophelia pertusa* interspersed with areas of dead broken skeleton.

Lophelia pertusa is widely distributed in the North Atlantic, in oceanic waters at temperatures of 4-12°C (Roberts *et al.* 2006) and is predominantly found at depths of

200-1000 m but has been recorded shallower and deeper (Zibrowius 1980). *L. pertusa* has been identified as occurring in areas subjected to fast currents such as carbonate mounds (De Mol *et al.* 2002), ridges and pinnacles (Howell *et al.* 2007). Pfannkuche *et al*. (2004) observed *L. pertusa* reef on the slopes of the Castor mound in the Belgica mound province (Porcupine Seabight) from 950-1036 m depth, and describe complete cover of live and dead coral colonies of *Lophelia pertusa* and *Madrepora oculata* with antipatharians, actinians and hexactinellid sponges present. Howell *et al*. (2010b) described a similar *L. pertusa* reef from various locations within UK waters as being characterised by the reef-forming corals *L. pertusa* and *M. oculata*, hydroids, anemones, decapods, cerianthids and echinoderms (ophiuroids and echinoids); whilst a similar assemblage was observed from Anton Dohrn Seamount (see Chapter 3) consisting of *L. pertusa* (dead and live), *M. oculata*, *Cidaris cidaris* and anemones.

Whilst the assemblage defined from the SW Approaches canyons has some of the same associated species as described previously from reef habitat, the canyon assemblage appears to be subject to increased sedimentation which is clearly visible from the image and video data; although an analysis of sedimentation rates has not been carried out. Canyons are likely to experience increased rates of sediment transport as a result of hydrodynamic regime (Vetter and Dayton 1998). The interpreted higher level of sedimentation in the study area may result in a lower proportion of live *Lophelia pertusa* colonies and fewer suspension feeders; however, a full comparative analysis would be required to test this.

Predominantly dead low-lying coral framework

The assemblage identified as Lop.Hal (cluster aj) was characterised by small live colonies of *Lophelia pertusa* and dead *Lophelia* framework with sediment infill, the

sediment areas provided microhabitats for soft sediment dwelling organisms such as cerianthid (Cerianthidae sp. 1) and halcampoid (Halcampoididae sp.1) anemones. Fauna associated with the dead framework were small growths of live *Madrepora*, the bamboo coral *Acanella*, ascidians and crinoids. This assemblage was observed from the Explorer and Dangaard canyons on the flanks, and on a flute feature over a depth of 697-927 m and temperature of 8.97-9.77°C.

Mortensen *et al*. (1995) and Roberts *et al*. (2009) describe a 'Dead coral framework' zone that is characterised by suspension feeders including sponges, actinians, and other coral species (gorgonians) with smaller epifauna such as bryozoans, hydroids and barnacles. Similar assemblages have also been described from Rockall Bank (Wilson 1979; Howell *et al.* 2010b), Hatton Bank (Howell *et al.* 2010b) and Anton Dohrn Seamount (defined in Chapter 3). The 'Dead coral framework' zone (*sensu* Mortensen *et al*. 1995) is known to be the most diverse area of a reef (Jensen and Frederiksen 1992; Mortensen *et al.* 1995). Whilst the assemblage described by the present study may be functionally similar to the dead framework assemblages of Wilson (1979), Mortensen *et al*. (1995) Roberts *et al*. (2009) and Howell *et al*. (2010b), based on their descriptions it would appear this assemblage is more sediment in-filled, as there are more sediment dwelling organisms associated with this biotope. A similar assemblage has been reported on the upper slope and summit of Erik mound in the Belgica province from 818-855 m depth. Coral rubble with isolated live patches of *L. pertusa* and *M. oculata* and a low abundance of associated fauna (antipatharians and *Aphrocallistes* sp.) was described with muddy sand areas between the rubble inhabited by *Cerianthus* sp. (Pfannkuche *et al.* 2004).

Ophiuroids and *Munida sarsi* associated with coral rubble

Biotope Oph.Mun (cluster ap) was identified as a typical reef rubble habitat which was characterised by coral fragments in the form of rubble/biogenic gravel. The rubble was acting as a habitat for the squat lobster *Munida sarsi* and the ophiuroid Ophiuroidea sp.5. The assemblage was found associated with incised channels and mini-mound features on the interfluves in Explorer and Dangaard canyons over a depth range of 303-1017 m and a temperature of 7.98-11.5°C.

Oph.Mun biotope corresponds to 'the *Lophelia* rubble zone' described by Mortensen *et al*. (1995) which is the outer 'apron' of the reef where the framework has been (bio)eroded and accumulates at the base of the reef, the squat lobster *Munida sarsi* dominates this zone.

4.4.1.ii Sea pen and burrowing megafauna communities

Kophobelemnon stelliferum and cerianthids on mud/sand

The assemblage Kop.Cer (cluster y) was associated with mud and muddy sand substratum and was characterised by the sea pen *Kophobelemnon stelliferum* and cerianthid anemone. Other conspicuous fauna associated with this assemblage were the large *Bolocera*-like anemones (Sagartiidae sp. 3), sea pens *Halipteris* sp., a number of echinoderm species including the asteroid *Pseudarchaster* sp., the crinoid *Pentametrocrinus atlanticus* (sediment dwelling) and the holothurian *Benthogone* sp. Video observations revealed the bamboo coral *Acanella* sp. to be more abundant than suggested from the image analysis. Kop.Cer biotope was observed most frequently and was widespread throughout the canyons. The assemblage was observed from all three canyon flanks, and from an incised channel in Explorer Canyon, over a depth range of 463-1059 m and a temperature of 8.87-10.85°C.

Kophobelemnon stelliferum is an upper bathyal species (Rice *et al.* 1992) and is known to be a deeper sea pen species (López-González and Williams 2009) widely distributed at depth from 400-2500 m in the north Atlantic and Pacific oceans (Rice *et al.* 1992). Rowe (1971) reported the occurrence of a *K. stelliferum* from Hatteras canyon between 1440-2060 m and considered this species to be a 'canyon indicator' as it was not found away from the canyon. Whether this assemblage is unique to the canyon system here is unknown as no comparable data are available from the neighbouring continental slope.

The sea pen assemblage has not been described from the deep sea but is similar to the shallower EUNIS 'Sea pen and burrowing megafauna in circalittoral mud' biotope. A xenophyophore biotope with an abundance of sea pens has also been described from Anton Dohrn Seamount (see Chapter 3), although this community is distinct from that observed on Anton Dohrn Seamount.

Sea pens are known to increase local biodiversity through increased habitat heterogeneity (Buhl-Mortensen *et al.* 2010). Sea pens are protected under the UK Biodiversity Action Plan (UKBAP) as 'Mud habitats in deep water' which corresponds to the OSPAR 'Threatened and/or Declining Habitat' 'Sea pen and burrowing megafauna communities' (OSPAR Agreement 2008-6). The newly described assemblage could also be considered both a Vulnerable Marine Ecosystem (VME) (FAO 2009) and a 'coral garden' habitat (OSPAR 2010b).

4.4.1.iii Other reef habitat under EC Habitats Directive

<u>*L. pertusa* and crinoids on bedrock</u>

As this biotope was described from the video, characterising species were assessed visually. Small growths of *Lophelia* (live & dead), the holothurian *Psolus squamatus*

and Holothuroidea sp.4; the corkscrew antipatharian *Stichopathes* and crinoids were identified as characterising species from video. The assemblage was associated with bedrock and was observed from Dangaard, Explorer and Irish canyon associated with incised channels, amphitheatre rims, tributary gullies (canyons heads) and the flanks over a depth of 253-1022 m and temperature range of 7.93-11.42°C.

The assemblage appears to be a highly sedimented version of the 'Discrete coral' biotope described by Weinberg *et al*. (2008) and Howell *et al*. (2010b). The assemblage described by Weinberg *et al*. (2008) was associated with ridge features on the flanks of Rockall Bank between 650-675 m dominated by a diverse range of corals (gorgonians, antipatharians, soft corals and stylasterids); whilst Howell *et al*. (2010b) describe a modified version of this assemblage with a lower proportion of gorgonians and antipatharians but with the addition of *L. pertusa*.

4.4.2 *Diversity of biotopes*

The *Lophelia pertusa* reef biotope (Lop.Mad) was the most diverse assemblage described from the SW Approaches in terms of dominance (Simpson Index), mean species richness and estimated species richness (Sobs). The reef framework provides a complex structure, thereby providing a habitat for associated species. While others have reported dead framework to be more diverse than the live part of the reef (Jensen and Frederiksen 1992; Mortensen *et al.* 1995), this was not the case in the SW Approaches. A plausible explanation is that the reef and dead framework biotopes in the SW Approaches are more typical of canyon environments. This may be inferred from the visually higher sedimentation observed on reef habitats on seamount and banks in UK waters (Howell *et al*. 2007), as higher sedimentation is known to lower diversity (Rogers 1990; Stafford-Smith 1993. Interestingly, reef / dead framework assemblages observed in the SW

Approaches had a higher proportion of live *M. oculata* than those reefs observed on Hatton and Rockall Bank (Howell *et al*. 2010). This may be attributed to a tolerance difference of *L. pertusa* and *M. oculata* to higher sedimentation levels, but this has not been previously documented. The sea pen biotope Kop.Cer was comparable to the reef biotope in terms of dominance (Simpson Index), but not in terms of expected species richness (Sobs) and mean species richness, and may be attributed to the lower structural complexity, despite this, this biotope was more diverse than the other soft sediment biotopes described. The least diverse biotopes in terms of Sobs, mean species richness and dominance were soft sediment assemblages [(am (Oph), al (Amp.Cer), x (Cer)].

In terms of comparing diversity between biotopes, these results highlight the diversity of biotopes in canyon systems, but these results need to be interpreted in the context of the methods used. These methods are comparing epibenthic fauna, but soft sediment habitats are known to harbour high infaunal diversity (Etter and Grassle 1992) and thus may also be of conservation concern. In addition, it is important to remember to compare like with like, a coral reef is not the same 'habitat' as a soft sediment habitat, their ecological worth in terms of ecosystem function are not equivalent, therefore comparisons of levels of diversity between biotopes as a means to assess their conservation importance should not be taken alone.

When comparing diversity, caution needs to be taken regarding which indices are used. Simply averaging species richness across samples can be misleading, as observed in Fig. 4.6b, as no standardisation for sampling effort is made. Diversity indices, such as the Simpson index, are less sensitive to sampling bias than others (Lande *et al*. 2000), and this criterion should be taken into consideration. To measure species richness, standardisation for sampling effort should be undertaken using rarefactions curves.

Additionally, the use of estimators can add greater insight into the diversity of assemblages, particularly in the context of taking a multivariate approach.

4.4.3 *Relationship between Vulnerable Marine Ecosystems (VMEs) and meso-scale geomorphological features*

4.4.3.i *Lophelia pertusa* reef

In this study, *Lophelia pertusa* reef, consisting of *Lophelia pertusa* framework and live patches of *L. pertusa* and *Madrepora oculata* was only observed on a steep flute feature on the canyon flanks and canyon floor (at the end of the interfluve) at 795-940 m depth and 9.41-9.92°C. As observed in Chapter 3, these findings support those of earlier studies which found that the largest reefs occur in depths between 500-1200 m (Frederiksen *et al.* 1992; Wheeler *et al.* 2007) and may be associated with topographic features such as ridges (Sula Ridge), escarpments (Pelagia Mounds) and channels (Hovland Mounds) (Howell *et al.* 2007; Wheeler *et al.* 2007; Howell *et al.* 2011) that provide suitable substratum and hydrodynamic conditions for reef habitat development (Thiem *et al.* 2006; Miensis *et al.* 2007; Dullo *et al.* 2008).

However, despite repeat sampling of high slope 'flute' features, *Lophelia pertusa* reef was only observed in one area. It was also highly sediment draped in that area. This relative rarity and condition of the reef habitat in the canyons region may be attributed to high sedimentation within the canyons. Sedimentation is a controlling factor in reef development and high species diversity is normally limited to areas with low sedimentation rates, i.e. < 10-20 mg cm^{-2} d^{-1} (Rogers 1990; Stafford-Smith 1993). This suggests that although the canyon flanks may provide appropriate substratum and current regimes for the development of reef, the apparent high sedimentation rates may limit the amount of suitable habitat within the canyons for reef development. In turn this

suggests that the use of meso-scale geomorphological features as surrogates for biological assemblages may only be achievable if taken in the context of megahabitat features i.e. 'canyon flank' as a geomorphological unit may not represent the same faunas as 'seamount flank' (see Chapter 5).

Whilst an intact biogenic reef was not observed on the interfluve areas, the reef rubble habitat 'Ophiuroids and *Munida sarsi* associated with coral rubble' was observed associated with mini-mound features 2-4 m in height and 50-150 m in diameter. The extent of coverage of rubble suggested that this assemblage was not typical 'rubble apron' associated with live reef areas, but was once an area that hosted live *L. pertusa* colonies that has been damaged, most probably by fishing activity, which is known to be intensive in this area (CEFAS *pers.comm*).

The mini-mounds with which the *Lophelia pertusa* reef is associated are similar to the Macnas mounds in the Porcupine Seabight, which are between 50 and 100 m in diameter and 5m high (Wilson *et al.* 2007); and the Darwin mounds which are typically 75 m in diameter and 5m high (Masson *et al.* 2003). Mini-mounds with associated *Lophelia pertusa* rubble have also been reported on the interfluve (Odet Spur) of the Guilvinec Canyon (Bay of Biscay) at a depth of 260-350 m (De Mol *et al.* 2010). From the acoustic data it could be suggested that the mini-mounds from the SW Approaches may be carbonate in origin, and thus could be classified as carbonate mounds under the OSPAR definition (OSPAR 2010a).

The association between mound features and *Lophelia pertusa* reef is well established (De Mol *et al.* 2002; Roberts *et al.* 2003; Henry and Roberts 2007). Large cold-water coral covered carbonate mounds (up to 190 m high) are located in the Porcupine

Seabight (De Mol *et al*. 2002) and giant (up to 350 m high) mounds can be found along the eastern and western Rockall Trough margin (Kenyon *et al.* 2003).

4.4.3.ii *Sea pen and burrowing megafauna communities*

The Kop.Cer biotope predominantly occurred on the lower part of the canyon flanks. From the high number of observations of this biotope on the flanks, it suggests that 'canyon flank' may act as a useful geomorphological indicator for this biotope, this requires statistical testing, and will be addressed in Chapter 5. It has been suggested that the sea pen *Kophobelemnon stelliferum* is an indicator species of increased near-bed currents and re-suspended organic matter (Rice *et al.* 1992), thus, the distribution of this biotope within the canyons may be related in part to hydrodynamic activity.

Sea pens are known to provide structural heterogeneity which leads to increased habitat biodiversity (Buhl-Mortensen *et al.* 2010) and are vulnerable to disturbance from fishing activity (Dinmore *et al.* 2003) thus, the improved understanding of their distribution is a conservation priority.

4.4.4 *Conclusion*

Submarine canyons harbour a range of biological assemblages, some of which correspond to those described from other megahabitat features, such as seamounts or the continental shelf. Other assemblages may be unique to canyons, but this is merely speculative as there is no compatible data. Canyons harbour assemblages of conservation concern, including three *L. pertusa* biotopes, one sea pen and burrowing megafauna biotope, and one bedrock reef. Meso-scale geomorphology appears to show some relationships, but is unlikely to be useful on its own, and thus there is the need to include other variables using a statistical framework.

The findings of this work have extended our knowledge of submarine canyons by providing much needed, comprehensive descriptions of biological assemblages and associated biodiversity, and suggested that canyons may harbour modified versions of assemblages observed on other megahabitat features. The mapping of these communities, in terms of depth and geomorphology, allows for regional comparisons to be made.

CHAPTER 5

THE USE OF MULTIBEAM AND ITS DERIVED LAYERS IN MAPPING THE DISTRIBUTION OF BENTHIC ASSEMBLAGES, WITH A FOCUS ON VULNERABLE MARINE ECOSYSTEMS, ON SEAMOUNT AND CANYON FEATURES

5.1 Introduction

With national and international obligation of governments to implement Marine Protected Areas (MPAs), there is an urgent need for regional and national habitat maps for offshore waters (Huang *et al.* 2011). It is necessary to have an understanding of the range and diversity of habitats to allow representative protection of habitats and species; which is one of the criteria for MPA selection (Convention on Biological Diversity (CBD) decision IX/20). The use of computer based tools, such as Marxan, for priority setting and reserve design to identify potential network sites that would meet conservation objectives is growing (Ball *et al*. 2009; Leslie 2005). Marxan has been used for both terrestrial and marine solutions for protected areas / spatial planning (Richardson *et al.*, 2006; Douvere and Ehler 2007). While Marxan is an effective tool, and allows the use of multiple layers, such that additional data may be added to compliment the biological data, continuous spatial layers are needed.

Due to the constraints of working in the deep sea, it is not feasible to collect complete coverage biological data (Diaz *et al.* 2004) and the use of photo-imagery is growing as a method of sampling the benthos, as these systems can be used for rapid assessment of habitats (Kostylev *et al.* 2001; Mortensen and Buhl-Mortensen 2005). With improvements in acoustic data resolution acquired from the deep sea, and the ability to

cover large areas rapidly, the use of acoustic techniques in mapping biological habitats is growing (Rooper and Zimmermann 2007; Dolan *et al.* 2008; Holmes *et al.* 2008; Post 2008; Huang *et al.* 2011), but there are inherent problems associated with this method. There is often a disparity between the resolution of the acoustic data and the biological data (Diaz *et al.* 2004), which is particularly true for ship-borne multibeam echosounder systems (Dolan *et al.* 2008). To enable production of habitat maps, which can be used for marine management, it is important to understand the physical properties of the seabed and water column at a scale that is relevant to the distribution and variability of seabed biota (Post 2008).

Whilst broad, low resolution datasets can be used to define topography and seabed substratum (Diaz *et al.* 2004), which are useful in habitat mapping, the previously common practice of using substratum alone to map the distribution of biological communities does not account for important environmental factors such as hydrodynamics (Kostylev *et al.* 2001; Diaz *et al.* 2004; Hewitt *et al.* 2004).

It is generally recognised that organisms show a particular affinity for certain types of topographical features or terrain (Džeroski and Drumm 2003; Roberts *et al.* 2003) and multibeam bathymetry and derived terrain variables can potentially provide important information that can aid in the delineation and characterisation of biological communities (Wilson *et al.* 2007). Within the deep sea environment many environmental parameters vary with depth, such as temperature (Haedrich *et al.* 1975), pressure (Siebenaller and Somero 1978), and food supply (Cartes and Sardá 1993), and as such, the multibeam bathymetry or depth layer can be used as an indirect surrogate for these parameters (Harris and Whiteway 2009; Howell 2010). In addition, derived terrain variables can act as surrogates for a number of other environmental variables

such as bottom current speed, direction, and variability of the substratum (rugosity), that influence the fine scale distribution of species.

Typically, surrogates used in habitat mapping are parameters that can be derived directly from the acoustic multibeam data, such as slope, aspect, rugosity and Bathymetric Position Index (BPI). Slope is a measure of the average change in bathymetry over a particular scale (pixel) and is a widely used surrogate because of its potential influence on benthic communities. Areas with steeper slope angles tend to support different communities to flatter areas (Lundblad *et al.* 2006). In some instances, higher slope angles can contribute to the acceleration of currents (Mohn and Beckmann 2002) which can increase the local food supply. This has been widely documented for suspension feeders, such as corals, which have been associated with areas with higher slope angles (Genin *et al.* 1986; Frederiksen *et al.* 1992; Thiem *et al.* 2006).

Aspect (orientation) is a measure of the direction the steepest slope faces (0-360°), and thus reflects the orientation of the seabed at a given location. This parameter is particularly relevant in relation to the orientation of the seabed to prevailing currents, and thus the potential to host suspension feeders. Rugosity is the ratio of the surface area to planar area which essentially gives an indication of the variability of the seabed. BPI is a measure of the relative position of a pixel in relation to the neighbouring ones, and identifies positive and negative features such as ridges and furrows (Lundblad *et al.* 2006; Wilson *et al* 2007).

There are a number of approaches that can be taken when habitat mapping: a top-down approach, which defines the abiotic/geophysical variables independent of the biological information (Hewitt *et al.* 2004); a bottom-up approach which first defines the patterns

of biodiversity and then relates this to the abiotic/geophysical variables (Eastwood *et al.* 2006; Rooper and Zimmermann 2007); and where patterns in biodiversity and abiotic/geophysical variables are defined together (Shumchenia and King 2010).

With a top-down approach, it may be that there is little relationship between the scale and distribution of the biological communities and the abiotic/geophysical variables, and thus using this approach for prediction may prove difficult (Williams *et al.* 2009). The advantage of a bottom-up approach is that ecological knowledge can be applied in the mapping process. Defining the patterns in biodiversity and abiotic/geophysical variables together may give insight into what is driving the distribution of habitats.

The disparity between the resolution of ship-borne acoustic data and the scale at which biological data are collected means that mapping the fine scale distribution of fauna on the coarser resolution of the acoustic data is often not feasible. In these instances, it may be possible to relate the biological habitats to larger geological features (mesohabitats with dimensions of tens of metres to a kilometre; *sensu* Greene *et al*. 1999) which are easily mapped from the acoustic data; this has proven successful when mapping cold-water coral reefs associated with pinnacles and carbonate mounds (De Mol *et al.* 2002).

The use of broad scale topography (megahabitats with dimensions from a kilometre to tens of kilometres or more; *sensu* Greene *et al*. 1999) is relevant to the distribution and composition of megafauna, but mapping at a mesohabitat (*sensu* Greene *et al*. 1999) scale using finer resolution biological data allows differentiation between biological habitats (Buhl-Mortensen *et al.* 2009). This may be an appropriate approach to mapping Vulnerable Marine Ecosystems (VMEs) such as coral gardens and *Lophelia pertusa* reef. Coral VMEs are likely to be found associated with broad scale topographical

features such as the summits and flanks of seamounts, canyons and banks (FAO 2009), and relationships between biological assemblages and geomorphological features at a mesohabitat scale (tens of meters to a kilometre; *sensu* Greene *et al*. 1999) have been reported, such as cold-water coral reefs associated with mound features (De Mol *et al.* 2002; Roberts *et al.* 2003; Henry and Roberts 2007).

The aim of this chapter is to produce full coverage, biologically meaningful habitat maps for two megahabitat features (*sensu* Greene *et al*. 1999), submarine canyons and a seamount, that may be used in designing and monitoring MPA. Taking a bottom-up approach to establish the relationship between biological assemblages and terrain parameters derived from multibeam data, geomorphology and substratum, focusing on those identified as VMEs. To achieve this, biotope level data (described in Chapters 3 and 4) will be used to investigate the use of acoustic derivatives in mapping the distribution of biological assemblages to address:

1) *Does the distribution of 'listed' habitats show any relationship to seabed topography and geomorphology?*

To address this aim, Anton Dohrn Seamount and the submarine canyons of the South West (SW) Approaches, will be used as case studies to investigate how to map the spatial distribution of biotopes across these megahabitats (*sensu* Greene *et al*. 1999). Seabed substratum and geomorphology layers, which were interpreted from acoustic data by H Stewart from the BGS (see Sect. 2.6.1 for details), will be examined in conjunction with derived acoustic data layers to investigate relationships between the biotopes and parameters using Generalized additive models (GAMs) (see Sect. 5.2.2) to determine if and how such data can be used to map biotopes (those defined in Chapters

3 and 4). Examples will be given on the process of habitat mapping, highlighting the use of surrogates, and particularly the use of meso-scale geomorphological features where possible, to delineate biological boundaries. In order to focus the text, specific examples of habitats that have been identified as VMEs will be used to investigate these aims. However, the final maps produced and the final discussion will take a more general view.

5.2 Methods

Multibeam echosounder data and video / image ground-truthing data acquired during the Strategic Environmental Assessment area 7 (2005) and Joint Nature Conservation Committee (2009) cruises to Anton Dohrn Seamount, and the MESH (Mapping European Seabed Habitats) (2007) cruise to the SW Approaches (see Chapter 2 for more details) were used during this study.

5.2.1 *Data layers*

Multibeam echosounder data were acquired and processed from Anton Dohrn Seamount and the SW Approaches as described in Sect. 2.2. Processed xyz bathymetry data were gridded in Fledermaus™ to produce Digital Terrain Models (DTMs). The grid size of a dataset is referred to as the resolution, which is the dimension of the cells (pixel). A DTM is commonly a uniformly gridded surface that represents the discrete sampled function z = f(x, y), where z is the elevation above the datum at the locations given by the coordinates (x, y) (Ali 2009). Surface grids were exported from Fledermaus™ in ASCII format and were converted into rasters in ArcGIS and geo-referenced to WGS84 UTM zone 29N (World Geodetic System 1984, Universal Transverse Mercator). Rasters are digital images that are made up of rows and columns of cells, with each cell (pixel) storing a single value. They are used to undertake terrain analysis.

5.2.1.i. *Seabed substratum and geomorphology*

Seabed substratum and geomorphology for both study areas were interpreted by the British Geological Survey (BGS), both under contract to the UK Government and as part of their ongoing regional mapping programme. Seabed substratum were interpreted using multibeam bathymetry and backscatter data, ground-truthing data (still images)

acquired during the seabed surveys, combined with existing sub-bottom profiling data and sediment cores acquired by the BGS.

For Anton Dohrn Seamount, the 2005 acoustic dataset was gridded at 20 m and provided full coverage of the entire seamount at relatively low resolution (few 'pings' per cell, see Chapter 2 for explanation). The higher resolution 2009 acoustic dataset (many 'pings' per cell), gridded at 15 m, covered two smaller areas from the north west (NW) and south east (SE) sides of the Seamount (Fig. 5.1; see Sect. 2.1 and 2.2 for details). These data were collectively interpreted by H. Stewart from the BGS to produce polygon layers of seabed substratum and geomorphology for the whole seamount (Fig. 5.2). However, a more detailed interpretation was possible from the higher resolution dataset (2009), which is nested within the lower resolution (2005) dataset.

The interpreted polygon layers (by H. Stewart from the BGS) for the SW Approaches (Fig. 5.3) were produced using a single acoustic dataset gridded at 25 m (see Sect. 2.2 for details). The ground-truthing data (stills images) were analysed to determine the composition of the seabed, and were classified using the Folk (1954) scale (see Sect 2.4 for details). The results from the image analysis were plotted in ArcGIS and overlaid on the acoustic data and existing BGS sediment samples.

For Anton Dohrn Seamount the final seabed substratum layer was classified using the modified Folk (1954) scale whereas the SW Approaches seabed substratum layer was classified using the pan European EUNIS (European Nature Information System) scheme, the difference was due to varying objectives given under contract for each of the surveys. EUNIS is less detailed than the categories used for the Folk scale.

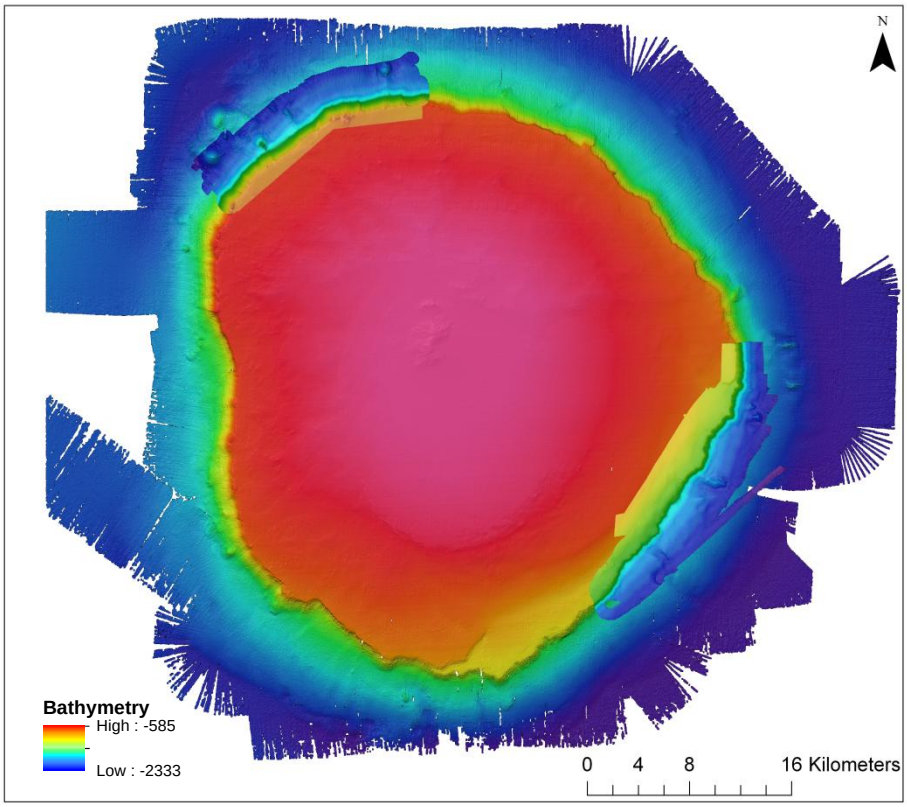

Fig. 5.1: Multibeam echosounder data over Anton Dohrn Seamount. The dataset that covers the entire seamount is gridded at 20 m (2005 low resolution dataset), and the higher resolution datasets covering areas from the NW and SE flanks is gridded at 15 m. For location of Anton Dohrn Seamount see Fig. 2.1.

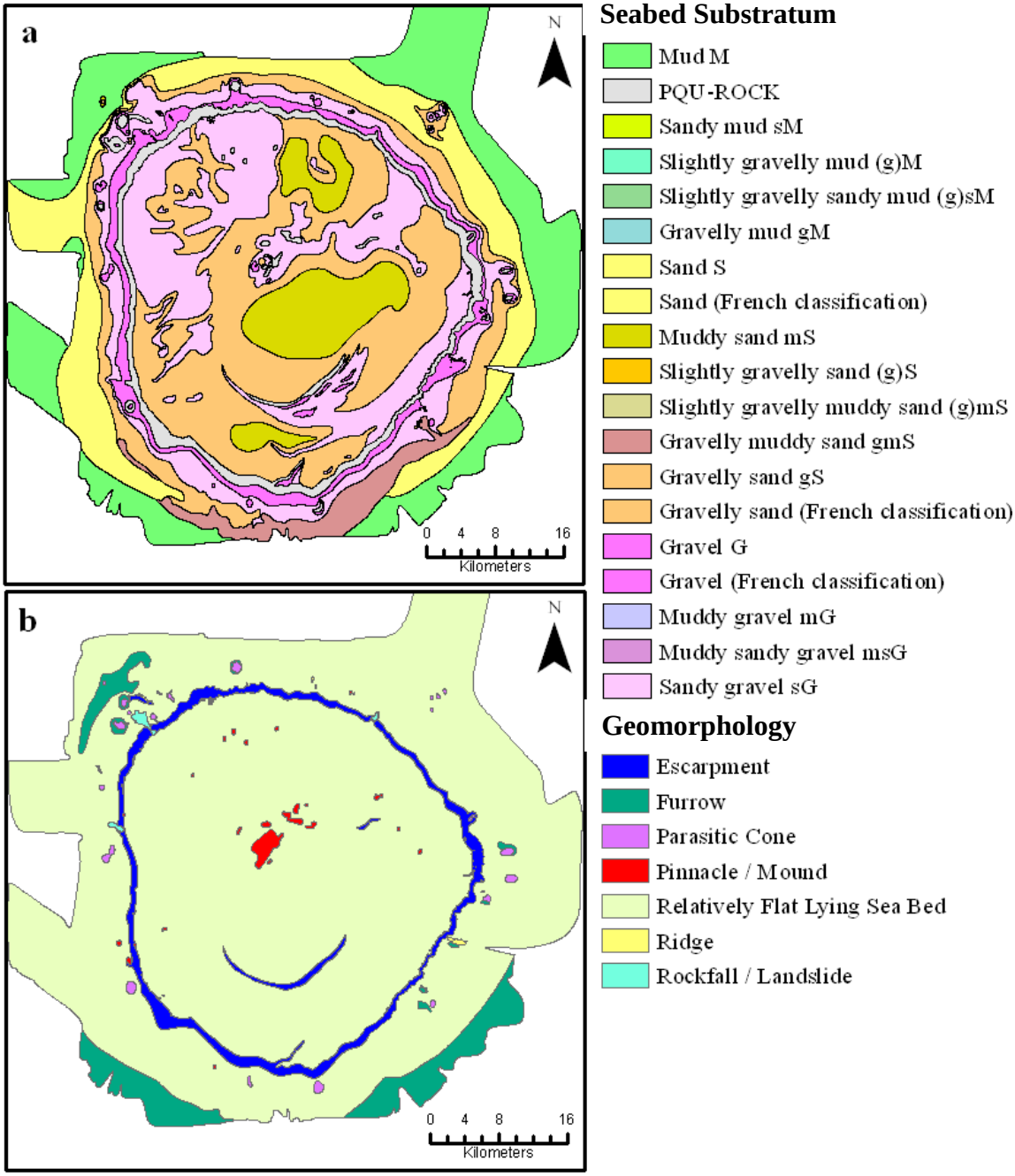

Fig. 5.2: Interpreted seabed substratum using the Folk scale (a) and geomorphology (b) layers for Anton Dohrn Seamount. For location of Anton Dohrn Seamount see Fig. 2.1 in Chapter 2.

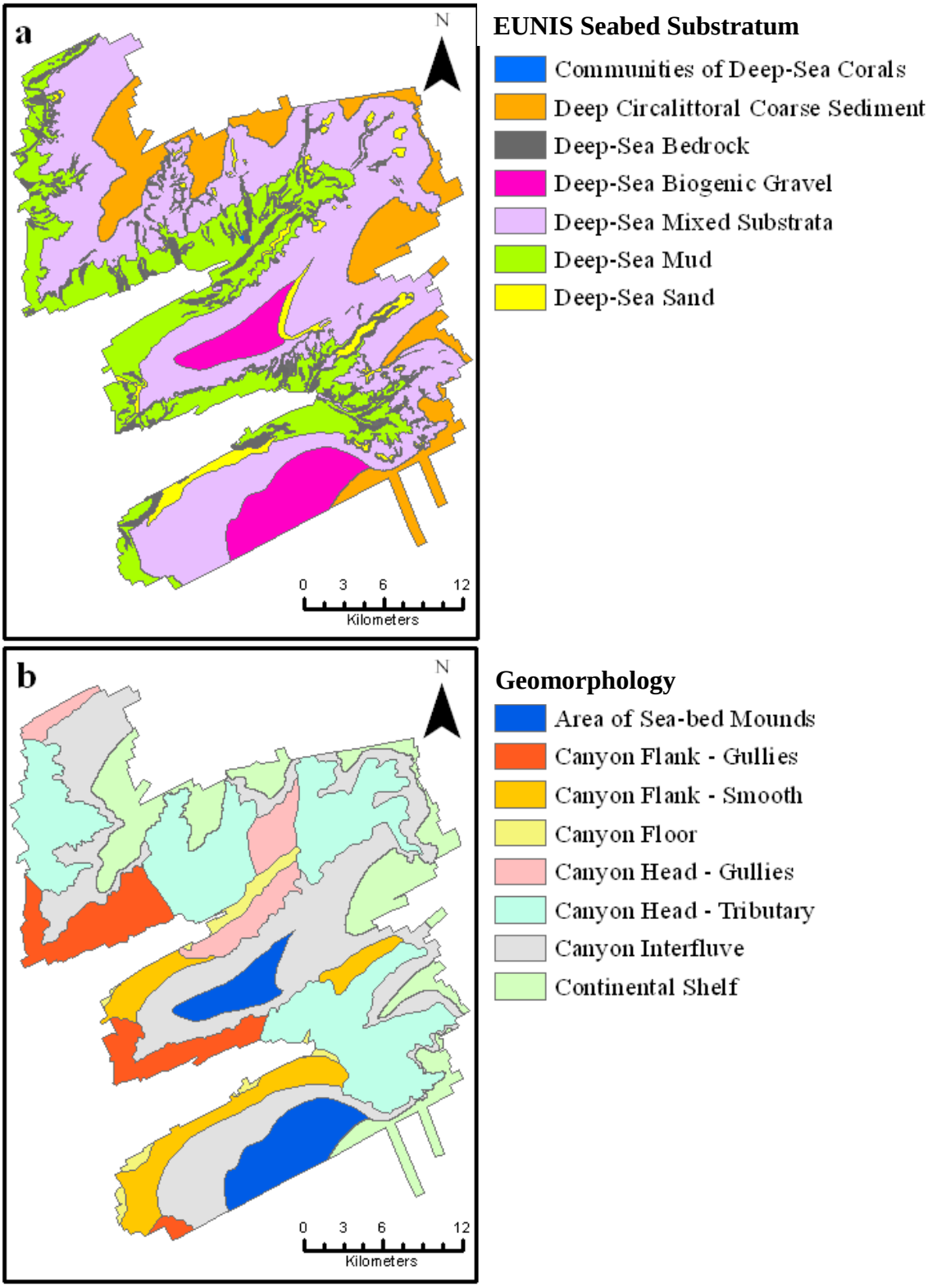

Fig. 5.3: Interpreted seabed substratum using the EUNIS classification (a) and geomorphology (b) layers for the submarine canyons of the SW Approaches. For location of the submarine canyons see Fig. 4.1.

5.2.1.ii. *Bathymetric Terrain analysis*

A suite of terrain parameters were derived from the created rasters using a standard 3 x 3 analysis window at the same cell size as the input raster data; slope layers were derived using the ESRI spatial analyst extension, aspect (4 cell algorithm) using the Digital Elevation Model v. 2 extension (Jenness 2010), and rugosity and standardised broad and fine scale BPI using the Benthic Terrain Modeler (BTM) extension (Wright *et al.* 2005).

Slope (in degrees) is a first order derivative and was calculated using Horn's method (uses an 8-cell algorithm, default setting in ArcGIS), which calculates the maximum rate of change between each cell and its neighbours; the lower the slope value, the flatter the terrain; the higher the slope value, the steeper the terrain. Rugosity is defined as the ratio of surface area to planar area. Values near one indicate flat, smooth areas whilst higher values indicate high-relief areas or areas with high variability. BPI is a second order derivative (derived from slope) which is a measure of where a cell is relative to the cells surrounding it. Positive BPI (high) cell values denote the cell is higher than the surrounding cells and thus represents positive features such as a ridge. While negative BPI (low) cell values denote features and regions that are lower than the surrounding area, e.g. valleys. BPI values near zero are either flat areas (where the slope is near zero) or areas of constant slope (where the slope of the point is significantly greater than zero).

5.2.1.iii. Biological data

The biotopes defined in Chapters 3 and 4 were used to map the change in biotopes along a video transect; these data together with the abiotic data (CTD and substratum) were converted into point shapefiles (data plus spatial reference) for use in ArcGIS 9.3.

Video data collected during the 2005 survey (see Sect. 2.2) were used as an additional data source to ground-truth the summit of Anton Dohrn Seamount, these videos were mapped using the mapping units defined by Howell *et al*. (2010b) and those from Chapter 3. The positioning data of the 2005 data was very poor, and as such was only used as an additional data source, thus no formal testing of relationships between biotopes and mapping parameters were undertaken.

5.2.2 *Mapping*

5.2.2.i *Establishing relationships between VME habitats and mapping parameters*

Regression tools can be used for habitat / species modelling to identify the variables that are responsible for the distribution of habitats / species (Guisan *et al*. 2000). Generalized additive models (GAMs) (Hastie & Tibshirani, 1986) are semi-parametric extensions of generalized linear models [(GLMs) Nelder & Wedderburn 1972]. GAMS identify relationships between the response and explanatory variables using a link function to establish a relationship between a smoothed term (explanatory variable) and the mean of the response variable (Guisan *et al*. 2000), and as such are advantageous over parametric methods (Yee & Mitchell 1991).

To restrict the size of the thesis, only VME biotopes were used in the modelling. Seven from Anton Dohrn Seamount and 4 from the SW Approaches (see chapters 3 and 4 for details). Video mapped data for each VME were converted to presence and absence data and made into point shapefiles in ArcGIS 9.3. To account for spatial auto-correlation, video mapped biotopes were rectified to one point per cell (to that of the resolution of the acoustic data). This was achieved by firstly converting the point shapefile to a raster (the same resolution as the bathymetric data) and then converting back to a point shapefile in ArcGIS. The Marine Geospatial Ecology Tools [MJET (v0.7)] in ArcGIS

were used to sample all raster layers to extract environmental and physical data for each biotope data point. Three categorical (factor) variables (substratum, meso and mega-scale geomorphology) and 7 physical variables (Slope, aspect, broad BPI, fine BPI, rugosity, depth and temperature) were extracted (see Table 5.1 and 5.2 for factor variables). Anton Dohrn Seamount included an additional categorical variable for side of seamount to account for potential differences at a megahabitat scale. Correlation between continuous variables was tested using a Pearson correlation test, and for those variables correlated ($p < 0.05$); one was removed prior to the modelling.

Explanatory models using a binomial distribution and logit link function were undertaken to test the strength of the relationship between variables and occurrence of biotopes. The relationship between the distribution of VMEs and continuous / factor variables were tested using the gam function in the MGCV package in the software R (R Development Core Team 2005 v2.14). Non-linear continuous variables require smoothing to allow the model to fit well, smooth terms were represented using a penalized regression spline, and appropriate smoothing parameters determined using Un-Biased Risk Estimator criterion (UBRE). Model selection was undertaken using the dredge function in the R package MuMin. The dredge function was chosen over stepwise regression, as this is being called into question as an appropriate model selection tool (Whittingham *et al*. 2006). The dredge function is computer intensive as it runs all possible combinations of the model and comes up with the best, thus selection of a subset of variables was needed to run the dredge. Akaike's Information Criterion (AIC) is a measure of the goodness of fit of a statistical model. The best model was determined by the lowest AICc score, but those models within 3 of the best model were also considered (Burnham & Anderson 2002). Each of the plausible models was fitted using a GAM and the model which performed the best was chosen to represent that

biotope. The performance of the model was determined using the R^2 [(adjusted coefficient) variability accounted for by the model] as a measure of goodness of fit, and the UBRE score. The residual plots were also checked to ensure that the model was not over fitting and thus converged. The residuals are the difference between the responses observed at each combination valves of the explanatory variables and the corresponding prediction of the response computed using the regression function.

Substratum	Mega Geo	Meso Geo
Sand	Canyon floor	Amphitheatre rim
Mud	Canyon head	Flute
Coral	Continental shelf	Incised channel
Deep Circalittoral Coarse Sediment	Flank	Mini-mound
Bedrock	Interfluve	Relatively flat seabed
Biogenic gravel		Tributary gullies
Mixed		

Table 5.1: Categorical (factor) variables of mega- and meso-scale geomorphology on the SW Approaches.

Substratum	Mega Geo	Meso Geo	Side of seamount
Bedrock	Flank	Cliff-top mounds	SE
Gravel	Summit	Escarpment	NW
Gravelly Muddy Sand		Flute	
Gravelly Sand		Furrow	
Sandy Gravel		Parasitic cone	
Sand		Radial ridge	
Slightly Gravelly Muddy sand		Relatively flat seabed	
		Rockfall	

Table 5.2: Categorical (factor) variables of mega- and meso-scale geomorphology on Anton Dohrn Seamount.

5.2.2.ii *Production of maps*

All data were projected in WGS84 UTM zone 29N coordinate system in ArcGIS 9.3. The UTM coordinate system is a grid-based system whereby the surface of the Earth is divided into sixty zones, the central meridian of each zone is separated from its neighbour by six degrees of longitude.

As production of a continuous biotope layer was needed, that may be used in software such as Marxan for network planning, the seabed substratum layer was taken as the 'base' or 'starting' polygon layer, as this provided a continuous layer to work from. Biotope mapped video tracks were overlaid on the base layer. The 'base' polygon layer was then modified appropriately (polygons split or modification of boundaries) using the polygon editing tool in ArcGIS to map changes in the biotope that corresponded to changes in the geomorphology or terrain parameters as identified as a significant relationship by the GAMs. Where possible, the association between geomorphology and terrain parameters were used to predict the occurrence of the biotope in areas lacking ground-truthing data. This process was undertaken for all biotopes classed as VMEs. For those biotopes not considered as VMEs, and thus not tested using GAMs, the base polygons were labelled with occurrences. This step-wise approach was applied for each biotope to modify the 'base' layer until a complete biotope map was produced. Polygons and boundaries could only be modified on the basis of the underlying acoustic data, if a change in biotope was visible along a video transect but no relationship was found from the GAMs then a boundary could not be delineated. In those instances, where more than one biotope occurred within a base polygon and could not be further divided based on the acoustic layers, polygons were allocated multiple biotopes.

To aid in the interpretation of the maps, and identify those areas which had been mapped using higher resolution acoustic data and ground-truthing data, a confidence layer was also produced for each megahabitat feature. This was particularly important for ADS as two varying resolution acoustic datasets were used to produce the full coverage map. Complete biotope and confidence layers were cleaned using the ArcGIS extension ET Geowizard v. 10 to eliminate any topology issues (overlapping polygons or gaps).

5.3 Results

5.3.1 *Bathymetric Terrain analysis*

Fig. 5.4, 5.5 and 5.6 illustrate the terrain parameters in relation to the bathymetry from the high resolution acoustic data acquired from the NW and SE side of Anton Dohrn Seamount and the SW Approaches respectively.

Those areas with high rugosity and slope corresponded to the upper part of the Seamount flanks and to positive geomorphological features (parasitic cones and radial ridges). Slope, rugosity and aspect layers followed the general topography of the survey area, while BPI refined the smaller features such as cliff-top mounds, the summit of the parasitic cones and crest of the radial ridges. The areas of high rugosity were predominantly located in the canyon heads, along incised channels and tributaries. Aspect highlighted the dramatic variation in broad scale topography within the canyons.

When two parameters were correlated < 0.05, one was removed prior to the GAMs analysis (see Appendix A5.1 for results of correlation test). For both ADS and the SW Approaches depth and temperature were highly correlated ($p = 0.97$ and $p = 0.95$ respectively), temperature was removed from further analysis. Four variables showed a degree of correlation, but $p < 0.05$ so they were not removed. Fine BPI and broad BPI (ADS = 0.945, SWA = 0.928) and rugosity and slope (ADS = 0.912, SWA 0.873). These parameters may show different infinities for delineating biotope boundaries, but due to their high correlation, they were placed in the same model.

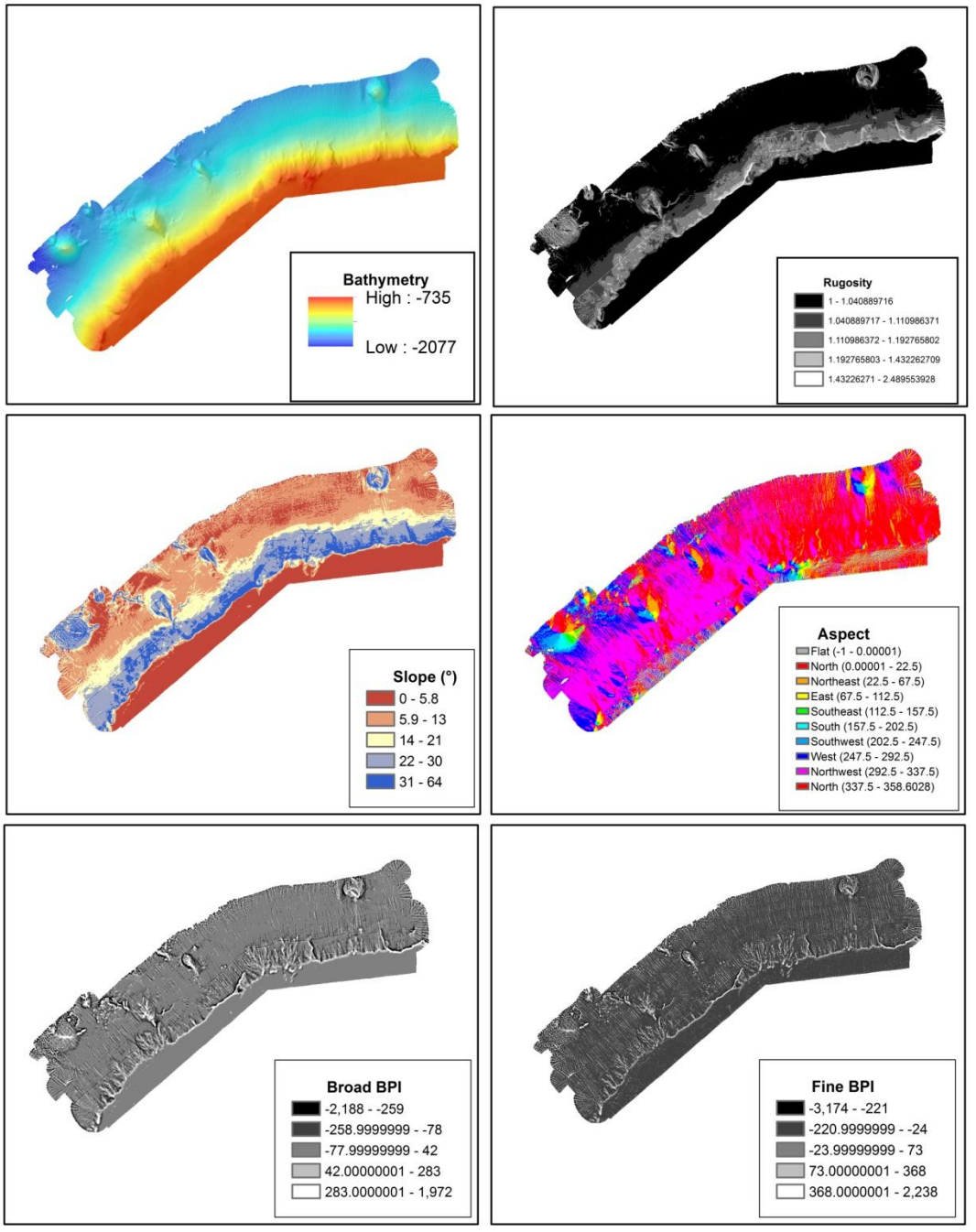

Fig. 5.4: Bathymetry and derived layers from the NW side of Anton Dohrn Seamount. Aspect is categorised as slope direction.

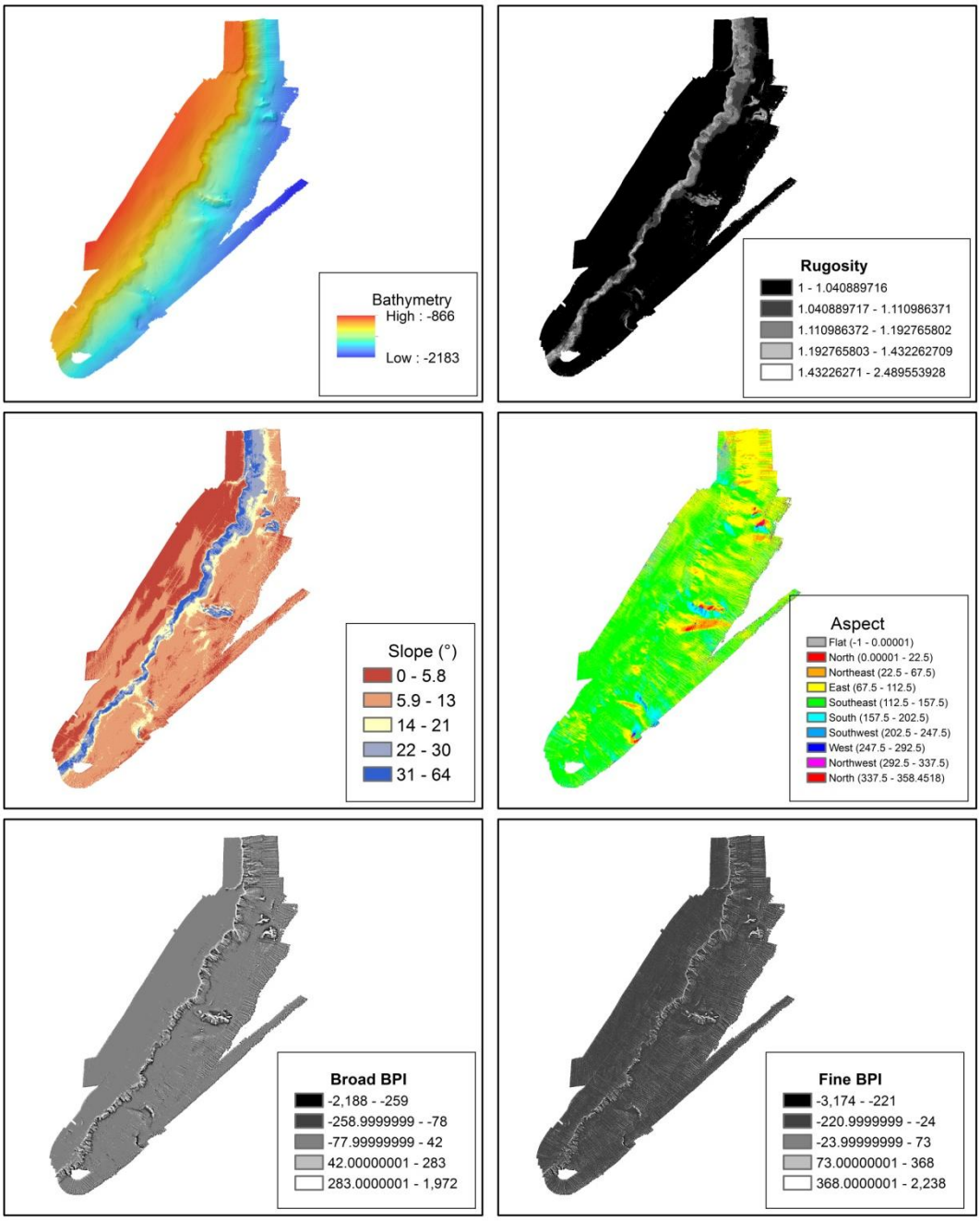

Fig. 5.5: Bathymetry and derived layers from the SE side of Anton Dohrn Seamount. Aspect is categorised as slope direction.

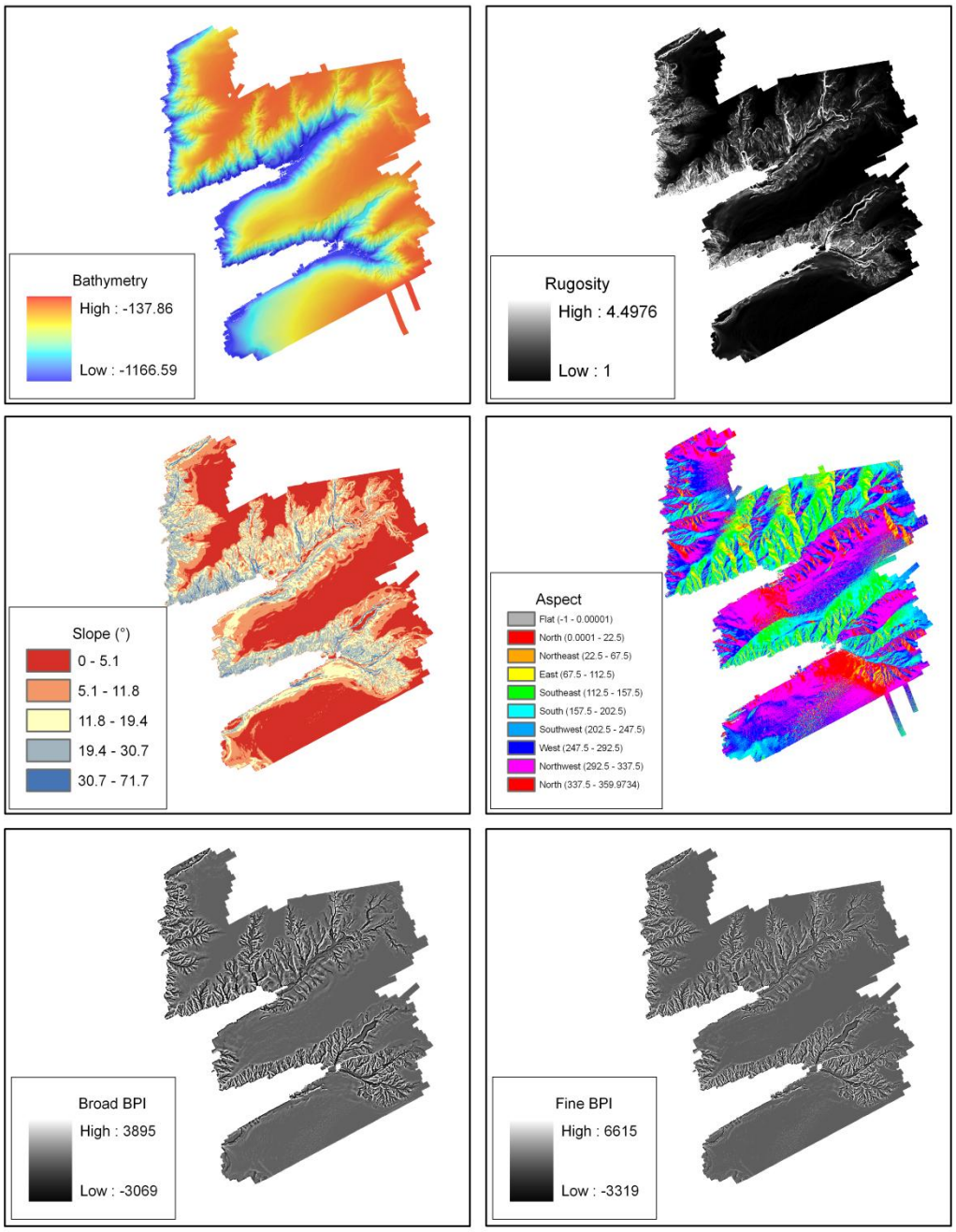

Fig. 5.6: Bathymetry and derived parameters from the SW Approaches. Bathymetry, rugosity and standardised BPI are displayed as ranges while slope is categorised. Aspect is categorised as slope direction.

5.3.2 *Mapping*

5.3.2.i *Establishing relationships between VME habitats and mapping parameters*

The final model used to test the relationship of each biotope and parameter, as determined from the model selection dredge function (see Appendix A5.2 for results of dredge model selection), identified those variables which were significant (see Appendix A5.3 for significance values). For Anton Dohrn Seamount, depth was the only parameter that was significant for explaining the occurrence of all the biotopes. Terrain parameters were useful surrogates, aspect was a significant surrogate ($p < 0.05$) for all of the coral biotopes, except the Lep.Ker coral garden. Slope was only useful for the two xenophyophore biotopes, which were associated with areas of low slope. Broad BPI was highly significant ($p < 0.05$) for both of the coral garden biotopes (Gor.Lop and Lep.Ker) and the predominantly dead coral framework with encrusting sponges biotope. Meso-scale geomorphology was only significant for two reef biotopes, *Lophelia pertusa* reef (on a radial ridge and cliff-top mounds) and Predominantly dead low-lying coral framework (on flute and radial ridge features), and at a larger scale, canyon flank only explained the occurrence of the xenophyophore biotope Syr.Cer. Side of the seamount was significant for 3 biotopes, Lop.Por, and the two xenophyophore biotopes (Syr.Cer and Syr.Oph). Broad substratum (interpreted polygon layer from the BGS) was significant for 3 biotopes, the coral garden on Bedrock (Lep.Ker) and the two xenophyophore biotopes (Syr.Cer and Syr.Oph).

For the SW Approaches, BPI was the only variable that significantly explained the relationship between VMEs and parameters. Broad scale BPI for the sea pen biotope Kop.Cer, *L. pertusa* reef (Lop.Mad) and the dead framework reef (Lop.Hal), while fine scale BPI was only significant for the rubble associated biotope Oph.Mun on the interfluves. Depth was a useful surrogate for all biotopes except the rubble Oph.Mun,

slope for *L. pertusa* reef (Lop.Mad) and dead framework (Lop.Hal). Aspect was only useful for the sea pen biotope Kop.Cer, and meso-scale geomorphology for the rubble biotope Oph.Mun which occurred associated with small cliff-top mounds.

Biotope	Model	Dev explained	R^2	UBRE	Slope	Aspect	Rugosity	Broad BPI	Fine BPI	Depth	Substratum	Side of seamount	MesG	MesG
Gor.Lop	31	65.5%	0.631	-0.79242		***		***		***				
Lep.Ker	254	69.6%	0.567	-0.83909				***		**	** (Bedrock)			
Lop.Por	128	65.8%	0.664	-0.64704		**		***		***		***		
Lop.Mad	125	89.1%	0.849	-0.93339		**			*	**			*** (RR) ***(CTM)	
Lop.Oph	127	49.2%	0.399	-0.62629		*				***			*** (FL) ***(RR)	
Syr.Oph	128	69.8%	0.757	-0.8139	**					***	*** (Sandy gravel) * (Gravel)	***		
Syr.Cer	504	92.8%	0.939	-90863	***			*		***	*** (Gravelly sand)	*		* (Flank)

Table 5.3: Results of fitted GAMs for VME biotopes on ADS. Significance values are indicated by '***' 0.001 '**' 0.01 '*' 0.05. For factor variables, the significant class is also given.

Biotope	Model	Dev explained	R^2	UBRE	Slope	Aspect	Rugosity	Broad BPI	Fine BPI	Depth	Fine substratum	Broad substratum	MesG	MesG
Kop.Cer	60	60.21%	0.617	-0.4911		**		***		***		*** (Mud) *** (Sand)		
Lop.Hal	120	82.7%	0.766	-0.9046	***			***		***				
Lop.Mad	117	65.6%	0.505	-0.8762	**			***		***				
Oph.Mun	30	89.9%	0.879	0.0028					**					*** (MM)

Table 5.3: Results of fitted GAMs for VME biotopes on the SW Approaches. Significance values are indicated by '***' 0.001 '**' 0.01 '*' 0.05. For factor variables, the significant class is also given.

5.3.2.ii Vulnerable Marine Ecosystems (VMEs)

Coral gardens

Two coral biotopes were identified from Anton Dohrn Seamount, 'Coral garden with bamboo corals and antipatharians on bedrock' and 'Gorgonian dominated coral garden'. Coral gardens were identified from ground-truthing data on two meso-scale geomorphological features on the NW and SE flank of Anton Dohrn Seamount (see Chapter 3). The Coral garden with bamboo corals and antipatharians on bedrock biotope occurred on a parasitic cone on the NW flank and a radial ridge on the SE flank; and the 'Gorgonian dominated coral garden' occurred only on the NW side of ADS on a radial ridge and parasitic cone.

On the parasitic cone and radial ridge on the NW side (Fig. 5.7) the 'Gorgonian dominated coral garden' biotope was associated with areas of high BPI [286.01-1,650 ($p < 0.001$)] on the south/southwest side [identified from the aspect layer ($p < 0.001$)] of the feature. Broad BPI, aspect and depth were useful surrogates for the presence of this biotope ($p < 0.001$) but meso-scale geomorphology was not ($p > 0.05$), suggesting that this biotope is a deep biotope associated with areas of high terrain complexity (BPI). The biotope was not mapped on the SE side, as that radial ridge was sampled and this biotope was not observed. The combination of aspect and broad BPI were used to infer the occurrence of this biotope across the seamount.

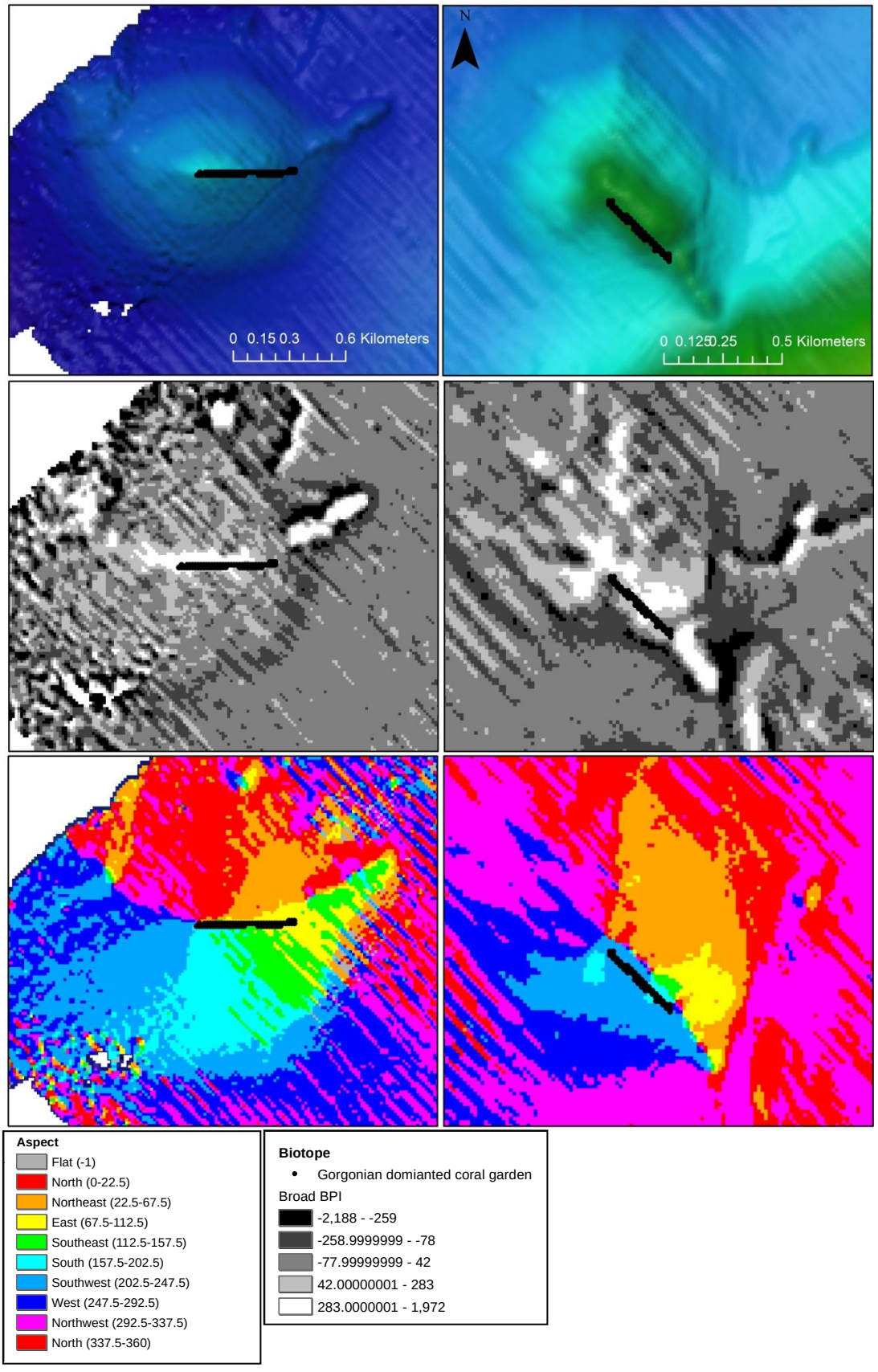

Fig 5.7: Distribution of the Gorgonian dominated coral garden biotope on distinct mesohabitats on the NW flank of ADS. (a) illustrates the biotope occurrence on a parasitic cone and (b) a radial ridge associated with an area of high broad BPI and aspect.

The second coral garden biotope 'Coral garden with bamboo corals and antipatharians on bedrock' was associated with bedrock substratum ($p < 0.01$) on areas of high broad BPI ($p < 0.001$) or proximal. Substratum, depth ($p < 0.01$) and broad BPI were useful surrogates for the distribution of this biotope, but meso-scale geomorphology or side of the seamount were not ($p > 0.05$). These results suggest that this is a deep biotope that occurs on areas of bedrock substratum on or near topographical high features, and these conditions do not vary significantly between the NW and SE side of the seamount. These surrogates were used to infer potential occurrences of this biotope on areas with no ground-truthing.

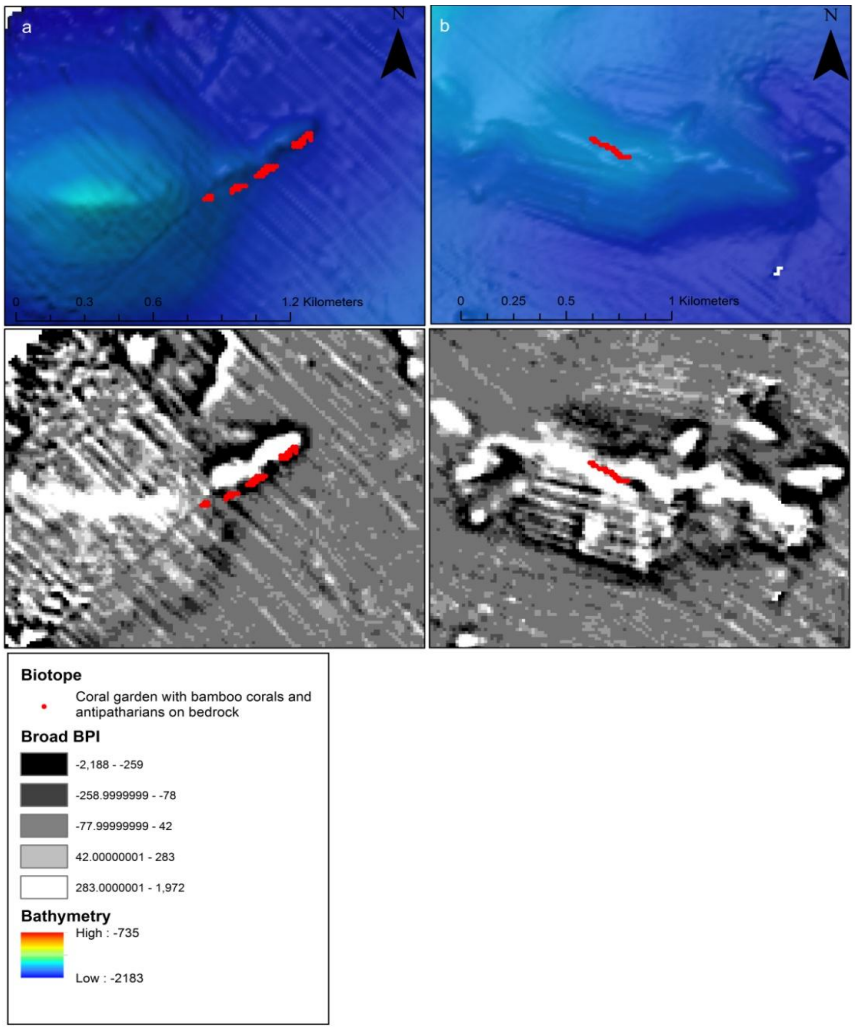

Fig. 5.8: Parasitic cone and radial ridge identified from high resolution multibeam on the NW (a) and SE (b) sides of Anton Dohrn Seamount. Mapped video transect of a 'Coral garden with bamboo corals and antipatharians on bedrock' overlaid on a BPI layer to illustrate the association.

Multibeam of the deep areas of Anton Dohrn Seamount were not covered by the high resolution multibeam (15m), and as the resolution of the full coverage acoustic data acquired during the 2005 survey was at a much coarser scale, due to data quality deteriorating with depth, these areas could not confidently be interpreted as hosting coral garden biotopes and thus were labelled with seabed substratum alone.

Coral gardens were not observed in the SW Canyon study area.

Cold-water coral reef

Cold-water coral reef assemblages occurred on ridge, mound (Fig. 5.9) and flute features (Fig. 5.11) on Anton Dohrn Seamount and flute features, canyon flank (Fig. 5.12) and mini-mounds (Fig 5.13) in the submarine canyons of the SW Approaches. Ground-truthing video data identified the occurrence of 3 cold-water coral assemblages from the seamount: *Lophelia pertusa* reef, predominantly dead, low-lying coral framework and predominantly dead, low-lying coral framework with encrusting sponges. Ground-truthing data from the cliff-top mound features (see Sect. 4.3.1 for more detail about the mound features) located on the NW side of Anton Dohrn Seamount also revealed the occurrence of two cold-water coral assemblages (Fig. 5.9). '*Lophelia pertusa* reef' occurred on the summit of the mounds, while 'predominantly dead, low-lying coral framework' occurred on the slopes and around the base of the mounds. *L. pertusa* reef was associated with areas of high fine BPI ($p < 0.05$) along the axis between the north and south side [as identified by aspect ($p < 0.01$)] of cliff-top mounds and also on a radial ridge ($p < 0.001$). Fine scale BPI was found to most accurately delineate the extent of the *L. pertusa* reef boundary ($p < 0.05$) and was used to map the distribution of these biotopes on the other cliff top-mound features that did not have any video ground-truthing data.

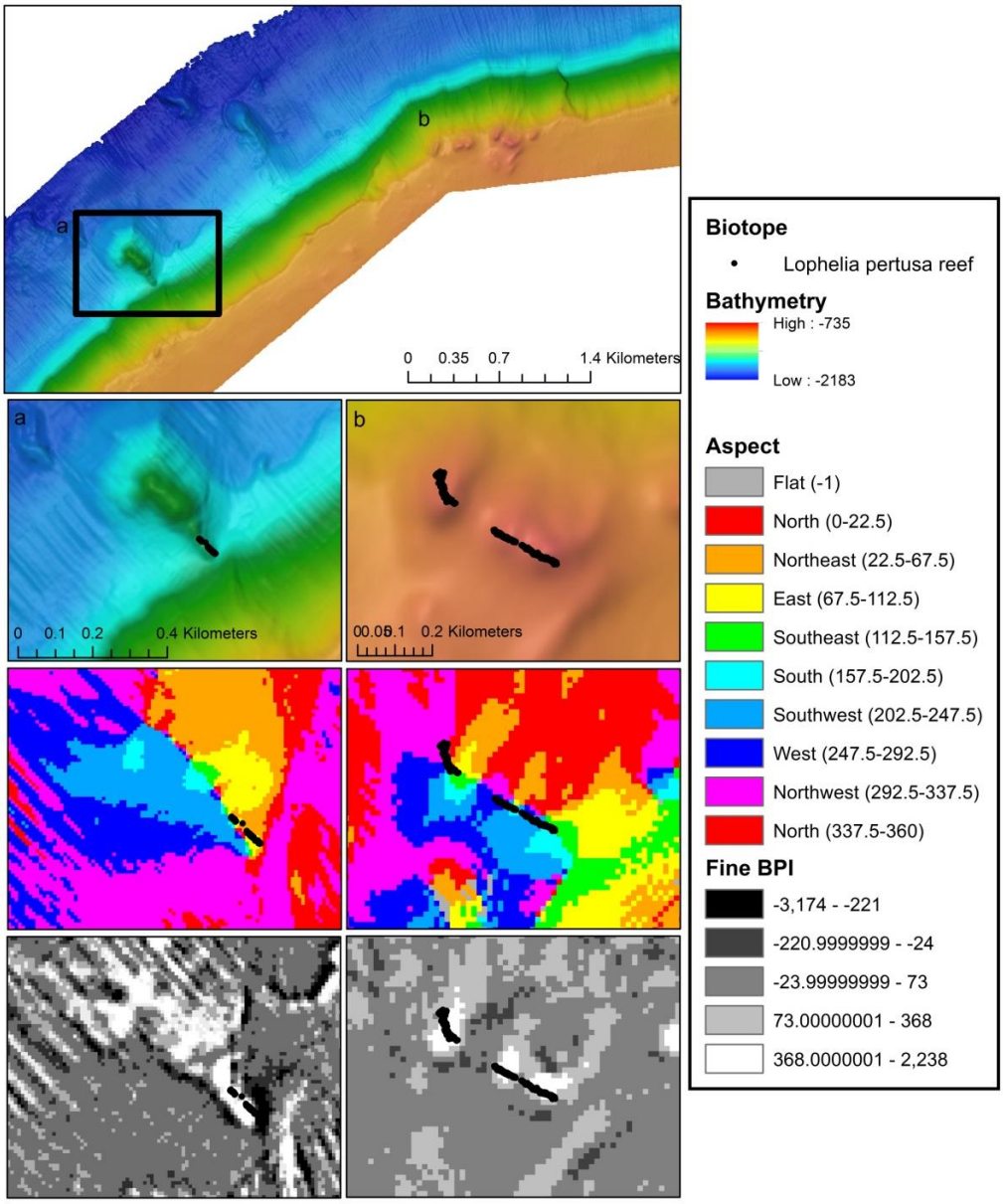

Fig. 5.9: Distribution of cold-water coral reef assemblages on a radial ridge (a) and cliff-top mounds (b) from the NW side of Anton Dohrn Seamount. Fig (a) and (b) illustrate the distribution of the *L. pertusa* reef in relation to aspect and BPI (fine) derived layers.

Fig 5.10 illustrates the use of aspect and BPI variables as a surrogate to map the distribution of *Lophelia pertusa* reef on a radial ridge on the NE flank of ADS lacking ground-truthing data.

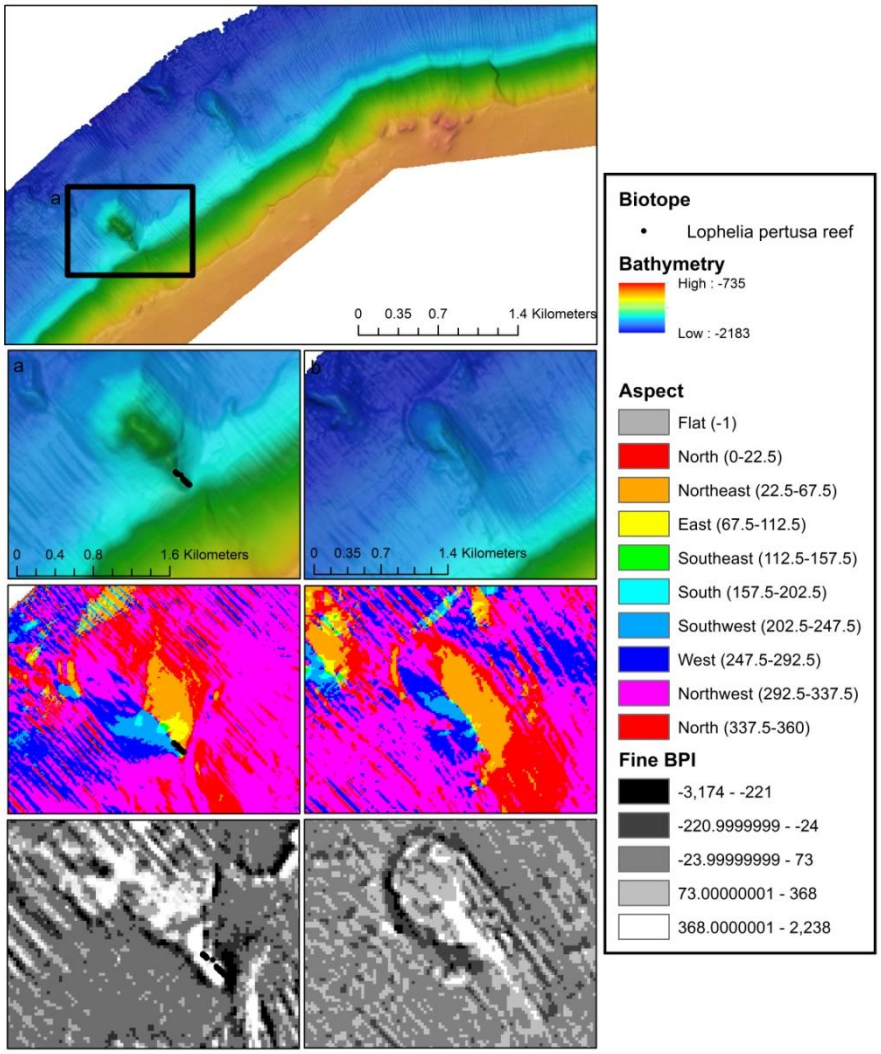

Fig 5.10: The prediction of *L. pertusa* reef on a radial ridge on the NE flank of ADS (b) using the surrogates identified as significant by the GAMs (a), the axis between north and south as indicated by the aspect layer ($p < 0.01$) of radial ridge ($p < 0.001$).

The results of the GAMs revealed Predominantly dead, low-lying coral framework to be associated with deep, meso-scale geomorphic features ($p < 0.001$), namely radial ridges and flute features with contrasting aspect ($p < 0.05$) [see Fig 5.11]. While the deeper dead framework biotope (Lop.Por) occured on a parasitic cone and rockfall on the NW flank and a radial ridge on the SE flank. Meos-scale geomorphology was not identified as a significant surroagte, but depth, broad BPI, side of the seamount ($p < 0.001$) and aspect ($p < 0.01$) were.

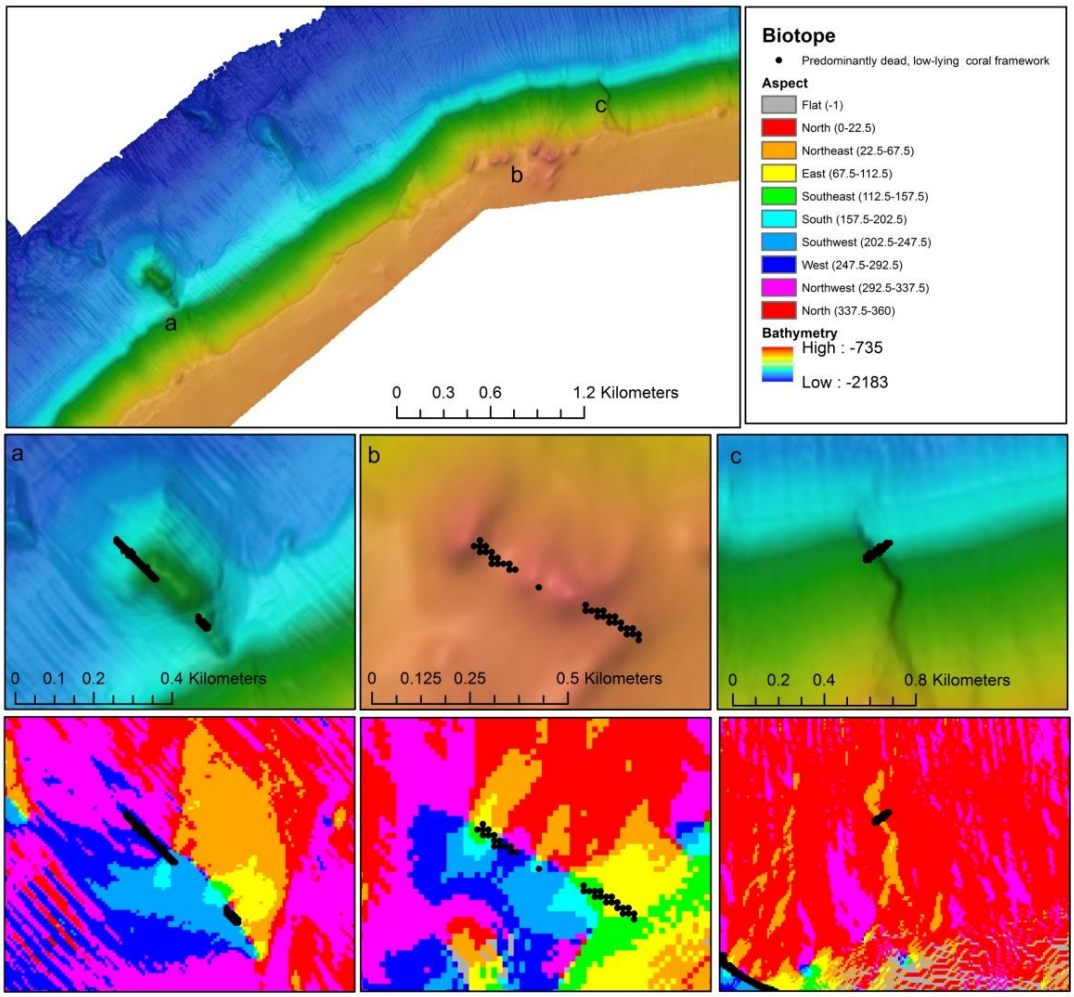

Fig 5.11: Occurrence of the biotope Lop.Oph (Predominantly dead, low-lying coral framework) on meso-scale geomorphic features on the NW flank of ADS as labelled on the inset map. (a) is a radial ridge, (b) cliff-top mounds and (c) a flute-like feature on the escarpment. The distribution of the biotope is overlaid on the bathymetry to illustrate the geomorphic feature, and aspect to show the association as identified from the GAMs.

Lophelia pertusa reef occurred on a flute feature located on the northern flank of Explorer canyon, associated with areas of high slope and broad BPI ($p < 0.01$). Despite the abrupt change in topography of the flute (Fig. 5.12a) this biotope could not be predicted across other flute features ($p > 0.05$). Despite the apparent association ($p < 0.05$) with BPI and slope, the video track crossed boundaries between high and low BPI, and thus the extent of this biotope was unclear.

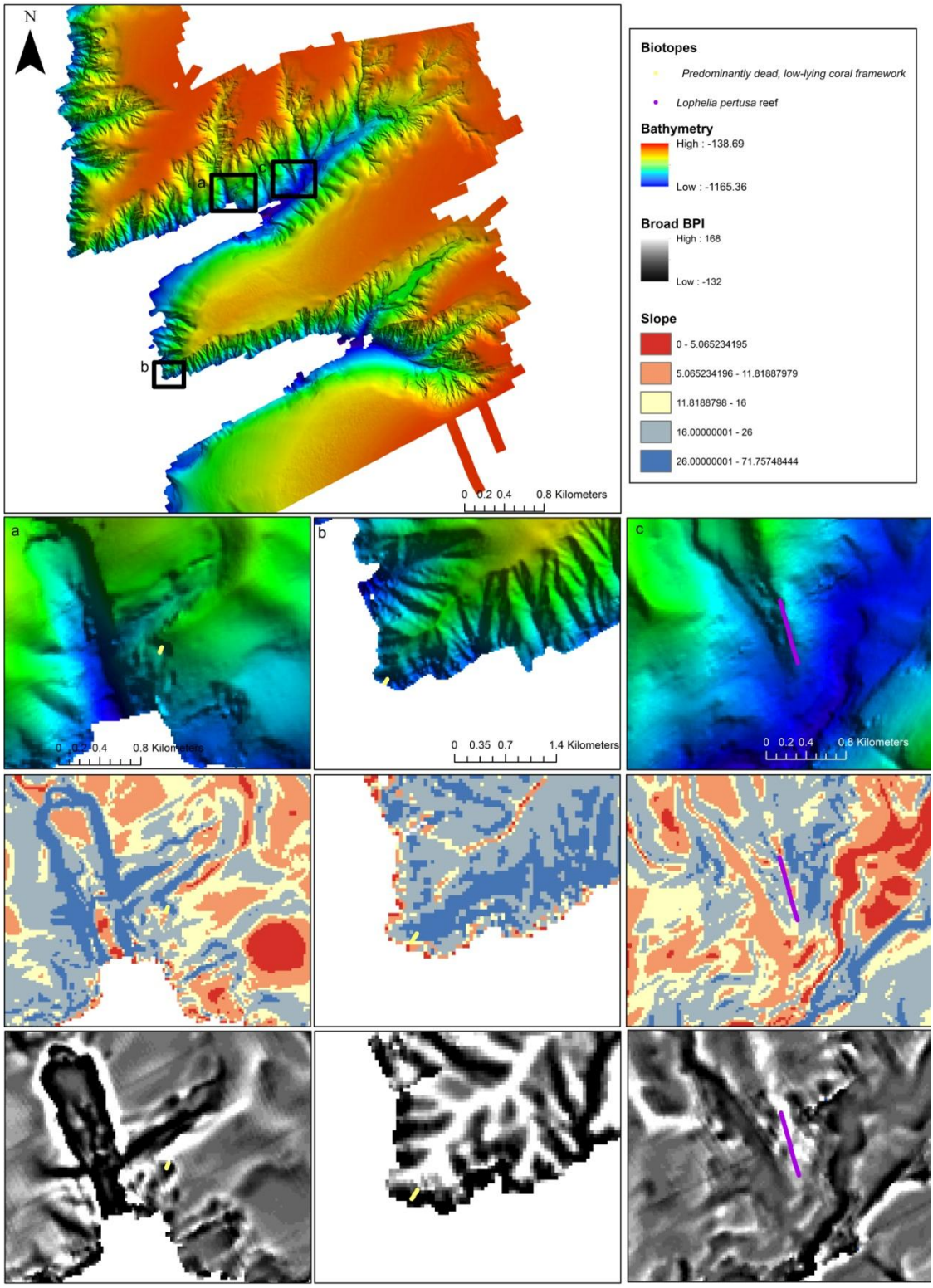

Fig. 5.12: Distribution of cold-water coral reef assemblages on a flute (a), canyon flank (b) and a flute feature at the end of the interfluve (c) in the SW Approaches; insert maps show close up views of the features. Inset (a) shows *Lophelia pertusa* reef associated with a flute, and predominantly dead, low-lying coral framework observed on the canyon flank (b) and (c) flute feature at the end of the interfluve. Each overlaid on slope and broad BPI layer.

Fig 5.12a shows the occurrence of 'predominantly dead, low-lying coral framework' on the northern flank of Explorer canyon associated with slope and broad BPI, delineation of boundary was unclear and this biotope could not be predicted across the canyons. The *Lophelia pertusa* habitats that occurred on the flute feature at the end of interfluve (Fig. 5.12b) could not be delineated further using significant terrain parameters of slope and broad BPI ($p < 0.001$) and thus the substratum polygon was used. This is most likely due to reaching the limits of the acoustic data due to depth, and thus inaccurate.

The 'Ophiuroids and *Munida sarsi* associated with coral rubble' biotope was identified by high fine BPI ($p < 0.01$) on mini-mounds ($p < 0.001$) located on the interfluves of the canyons (Fig. 5.13). For spatial reference, the *Munida sarsi* and *Leptometra celtica* on mixed substratum biotope which occurred between the mini-mounds (but not tested using a GAM) is also displayed on Fig. 5.13. Due to the small size of the mounds, each individual mound was not delineated, but the larger polygon on the interfluves labelled with the two biotopes.

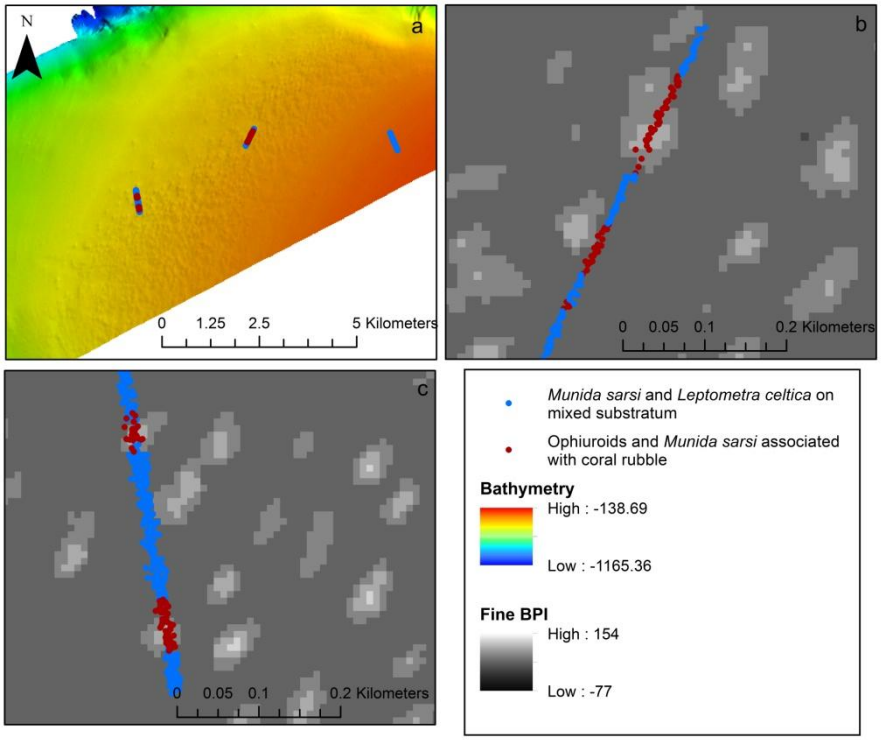

Fig. 5.13: *Munida sarsi* biotopes distributed on the mini-mound features. Image (a) is an overview of multibeam bathymetry data acquired over the mini-mounds. Images (b) and (c) show the change in biotope mapped video across the mini-mounds, the areas of high BPI correspond to the mound features.

Sea pen and burrowing megafauna communities

The *Kophobelemnon stelliferum* and cerianthid assemblage was the most common biotope observed from video footage throughout the submarine canyons on the flanks. This biotope was associated with areas of low BPI ($p < 0.001$) on sand and mud substratum ($p < 0.001$). The depth and substratum that this biotope occurred at were useful surrogates ($p < 0.001$) for mapping this biotope across the canyons and coincided with the larger sand and mud substratum polygons; although no further delineation of the substratum polygons was possible as the BPI within these polygons was the same.

Xenophyophore communities

Two xenophyophore assemblages were identified from Anton Dohrn Seamount. These were either found on ridges, or were found proximal to these same topographical features. The Syr.Cer biotope was associated with areas of low slope ($p < 0.001$) and broad BPI ($p < 0.05$) on gravelly sand ($p < 0.001$) on the flank ($p < 0.05$) of the seamount. The Syr.Oph biotope is a deep biotope ($p < 0.001$) associated with areas of low slope on sandy gravel and gravel substratum ($p< 0.05$) found on both sides of the seamount.

5.3.2.iii All other assemblages

Once the process of mapping VME biotopes using surrogates, geomorphology, and/or seabed substratum was complete, the remaining non VME biotopes were mapped across the features using the base layer and the presence of the biotope allocated to each polygon. However, on the Anton Dohrn Seamount, where two multibeam datasets were used that were of differing resolution (20m and 15m grid size), the disparity in resolution between the coarse scale acoustic data (20m) and video ground truthing on the summit of the Seamount, coupled with poor positioning of the video ground-truthing obtained over the summit area, did not allow for further subdivision of ‘base’ substratum polygons to a single biotope polygon, and thus mixed biotope polygons were assigned.

Biotope	NW geomorphology	SE geomorphology	Parameters
Ophiomusium lymani and cerianthid anemones on mixed substratum		Flank	Substratum
Xenophyophores and ophiuroids on mixed substratum	Flank	Radial ridge	Substratum* Slope**
Xenophyophores and caryophyllids on gravelly sand and mixed substratum	Flank	Summit edge	Substratum** Slope*** BPI* Flank *
Serpulids, encrusting sponges and *Psolus* on mixed substratum	Summit	Summit	Substratum
Psolus, caryophyllids and lamellate sponges on mixed, boulder and bedrock	Escarpment	Escarpment	Substratum
***Lophelia pertusa* and encrusting sponges on bedrock**	Landslide/rockfall Parasitic cone	Radial ridge	Substratum
Predominantly dead, low-lying coral framework with encrusting sponges	Parasitic cone Landslide/rockfall Radial ridge	Radial ridge	Aspect** BPI*** Depth**
Gorgonian dominated 'coral garden'	Parasitic cone Radial ridge		BPI *** Aspect*** Depth***
Predominantly dead, low-lying coral framework	Cliff-top mounds Radial ridge Flute	Cliff edge Radial ridge	Aspect* Depth*** Meso-geomorphology***
Live biogenic coral reef	Cliff-top mounds Radial ridge		Aspect** BPI* Meso-geomorphology***
Coral garden with bamboo corals and antipatharians on bedrock	Parasitic cone	Radial ridge	BPI*** Depth** Substratum **
Bathylasma hirsutum – Dallina septigera – Macandrevia cranium assemblage	Pinnacles (summit)		Substratum
Brachiopods on coarse sediment	Pinnacles (summit) and summit		Substratum
Lanice bed	Summit		Substratum
White and blue encrusting sponges, ophiuroids and majids on coarse sediment	Pinnacles (summit) and summit		Substratum

Table 5.4: Parameters used to delineate and map the spatial distribution of biotopes on Anton Dohrn Seamount. Those mapped from the 2009 video are separated into occurrence of biotopes on the NW and SE sides of the Seamount while those mapped from the 2005 video occurred on the summit. VME biotopes mapped assisted my GAM results are in bold, and the significance level denoted by *** 0.001, ** 0.01, * 0.05.

Biotope	Geomorphology	Parameter
cf. *Bathylasma* sp. assemblage on bedrock	Incised channel	Substratum
Amphiuridae ophiuroids and cerianthid anemones on bioturbated mud/sand	Flank Canyon head Continental shelf	Substratum
***Kophobelemnon stelliferum* and cerianthids assemblage on mud/muddy sand**	Flank Incised channel (canyon head)	Aspect** BPI*** Depth*** Substratum***
Annelids, hydroids and cerianthids on bedrock ledges	Canyon head Incised channel (canyon floor)	Substratum
L. pertusa and crinoids on bedrock	Tributary gullies (Canyon head) Incised channels Amphitheatre rim Flank	Substratum
Predominantly dead low-lying coral framework	Flank Canyon floor (end of ridge)	Rugosity and substratum* Substratum**
***Lophelia pertusa* reef**	Flute	Slope** BPI*** Depth***
Cerianthids on sediment draped bedrock	Amphitheatre rims Canyon head Flanks Incised channels	Substratum
Burrowing (*Amphiura* sp.) and surface dwelling ophiuroids on mud/sand	Flank Amphitheatre rims Tributary gullies	Substratum
Serpulids and brachiopods on mixed substratum	Flank	Substratum
Munida sarsi and *Leptometra celtica* on mixed substratum	Interfluves Canyon head	Substratum
Ophiuroids and *Munida sarsi* associated with coral rubble	Mini mounds Incised channels	BPI** Meso-geomorphology***

Table 5.5: Parameters used to delineate and map the spatial distribution of biotopes in the SW Canyons. VME biotopes mapped assisted my GAM results are in bold, and the significance level denoted by *** 0.001, ** 0.01, * 0.05.

Full coverage biotope maps were produced for Anton Dohrn Seamount and the SW Approaches using the relationships identified (GAMs) between VME biotope and the multibeam bathymetry, its derived layers, interpreted seabed substratum and geomorphology, to then predict (where possible) the spatial distribution of all biotopes across each feature. Where a predicted biotope could not be inferred from the data, due

to a lack of ground-truthing data for example, then the relevant polygons were labelled only with the seabed substratum.

Full coverage biotope maps of the Anton Dohrn Seamount were composed of single biotope polygons, multiple biotope polygons (with a maximum of 3 shared biotopes), and base level substratum polygons. These maps are intended for use in a GIS environment, where queries can be made regarding specific biotopes and displayed as appropriate. Thus, due to the size and complexity of the maps, and the difficulties of displaying so much information, for ease in interpretation, a number of maps are represented. For ADS, firstly the NW and SE sides where the higher resolution acoustic data were acquired are presented; Fig. 5.14 illustrates the primary biotopes found in each polygon across the areas and Fig. 5.15 the secondary biotopes found in each polygon. The complete biotope map for ADS is presented in Fig 5.16 and Fig 5.17, accompanied by a confidence map in Fig. 5.18.

Fig. 5.14: Areas mapped on the NW (top) and SE (bottom) side of Anton Dohrn Seamount using the high resolution multibeam echosounder data. For ease of interpretation, only primary biotopes are labelled as occurring in polygons. Grey polygons are those where biotopes could not be predicted, and thus polygons where labelled with substratum. See opposite page for figure legend.

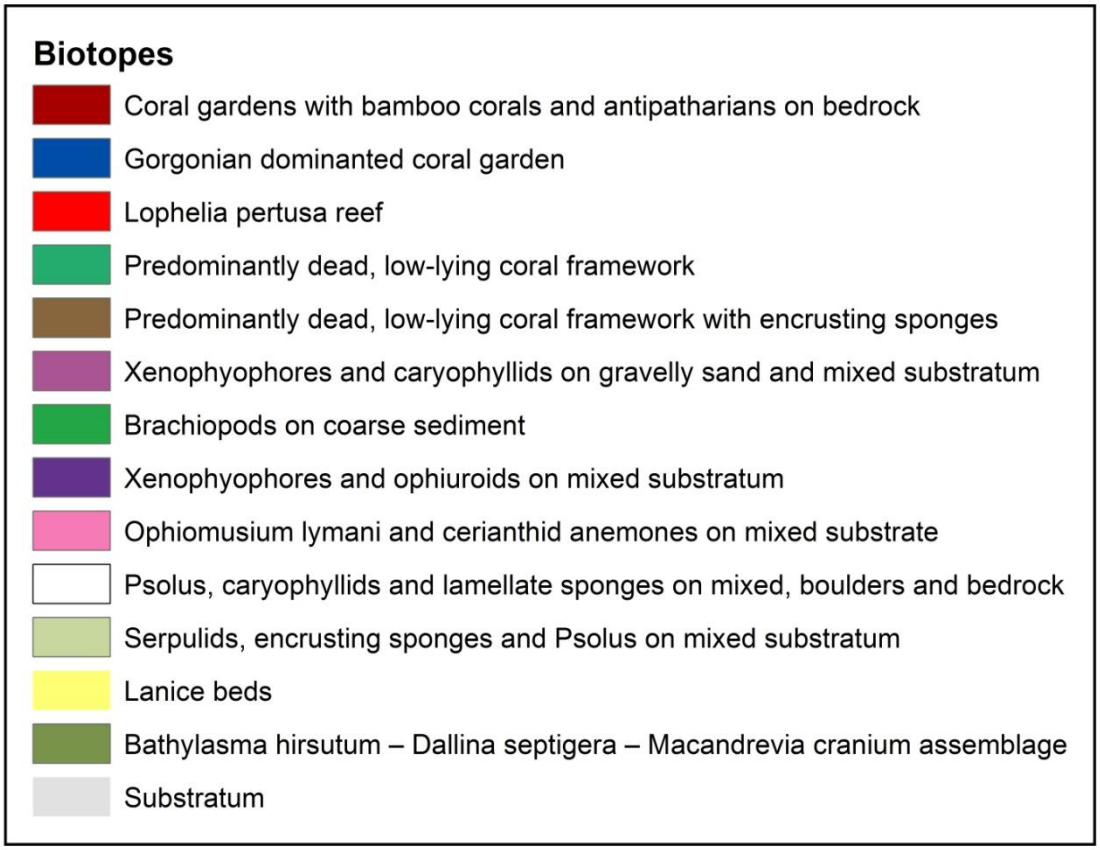

Fig. 5.14 shows the distribution of all biotopes on the NW and SE side of ADS. The summit of the seamount was mapped as 'Serpulids, encrusting sponges and *Psolus* on mixed substratum', on the steep escarpment *Psolus*, caryophyllids and lamellate sponges dominate. Small flute features on the NW escarpment are mapped with the *Lophelia* habitat 'Predominantly dead, low-lying coral framework'. These biotopes give way to a large expanse of the Xenophyophore and caryophyllid biotope at the base of the flank. Distinct geomorphological features on the flank are mapped, on the summit/crest of the radial ridge and parasitic cone features on the NW flank, Gorgonian dominated coral gardens are delineated. Off the summit / crest of these features, dead framework biotopes are mapped. The 'Coral garden with bamboo corals and antipatharians on bedrock' biotope is mapped from small crest features associated with the lower part of the parasitic cone and on the SE side of the seamount. *Lophelia pertusa* reef is mapped on a small part of the crest of the radial ridge and on the cliff-top mounds on the NW side of the seamount.

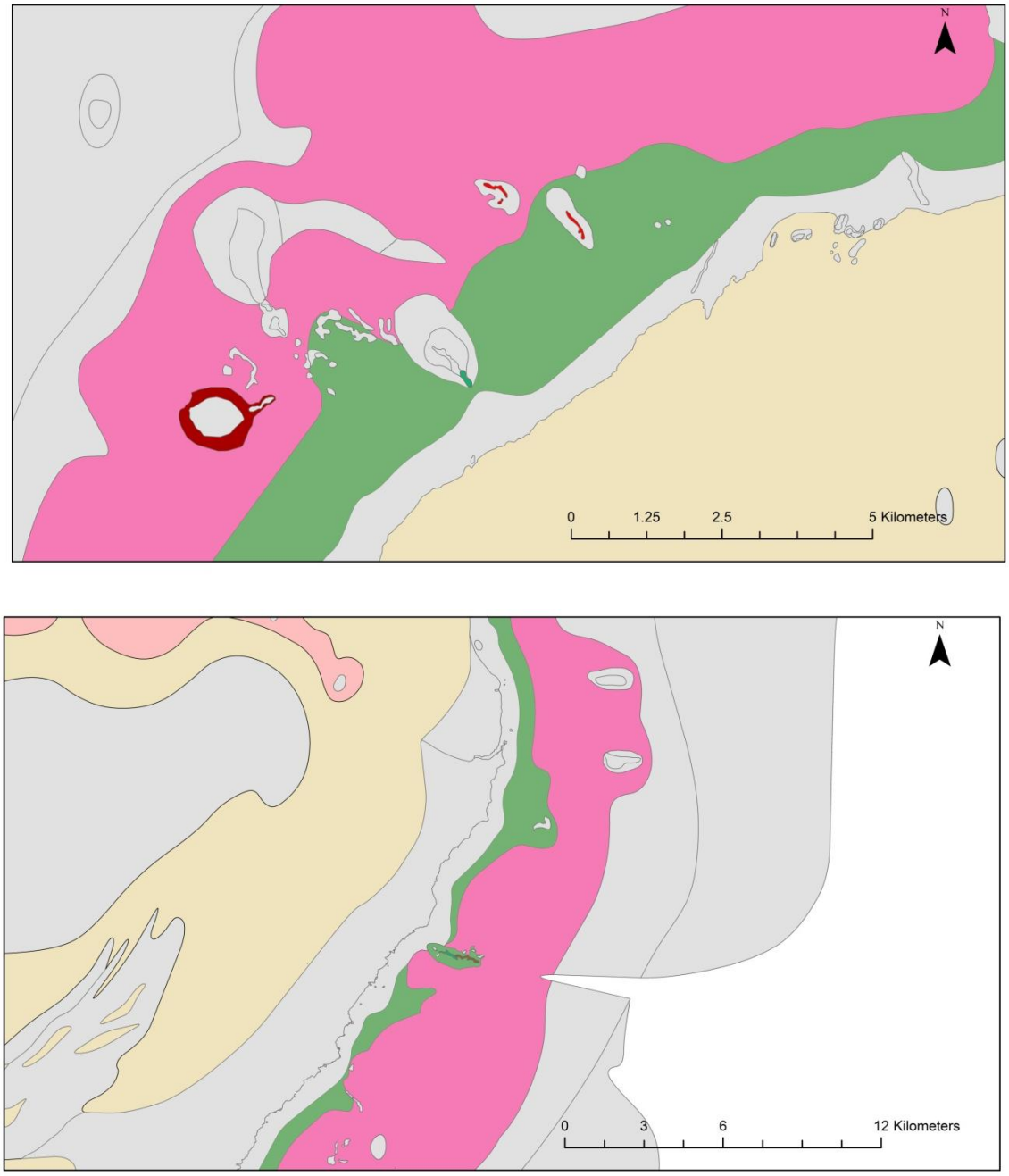

Fig. 5.15: Areas mapped on the NW and SE side of Anton Dohrn Seamount using the high resolution multibeam echosounder data. For ease of interpretation, only secondary biotopes in polygons are displayed. Those areas in grey are either polygons where biotopes could not be predicted and substratum labelled, or where when no secondary biotopes occurred. See opposite page for figure legend.

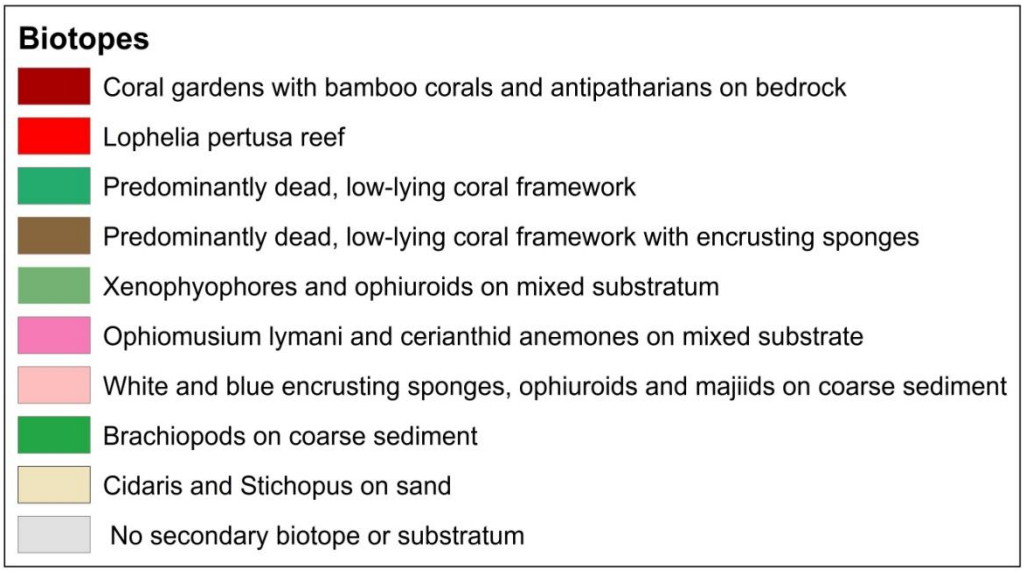

Fig 5.15 illustrates the secondary biotopes mapped from ADS. On the summit of the seamount, the large polygon mapped with Serpulids, encrusting sponges and *Psolus* is also co-mapped with the biotope *Cidaris* and *Stichopus*. No other biotope was observed on the escarpment. On the flank below the escarpment, Xenophyophores and ophiuroids share the same polygon as xenophyophores and caryophyllids (as illustrated in Fig 5.14). At the base of the flank, the large polygon with Xenophyophore and caryophyllids in the previous figure is also mapped with the deep biotope *Ophiomusim lymani*. Coral garden with bamboo corals and antipatharians on bedrock biotope is mapped off summit on the parasitic cone on the NW flank, with *Lophelia pertusa* reef on the crest of two un-sampled radial ridges (NW flank), while both dead coral framework biotopes are on the crest of the radial ridge on the SE flank.

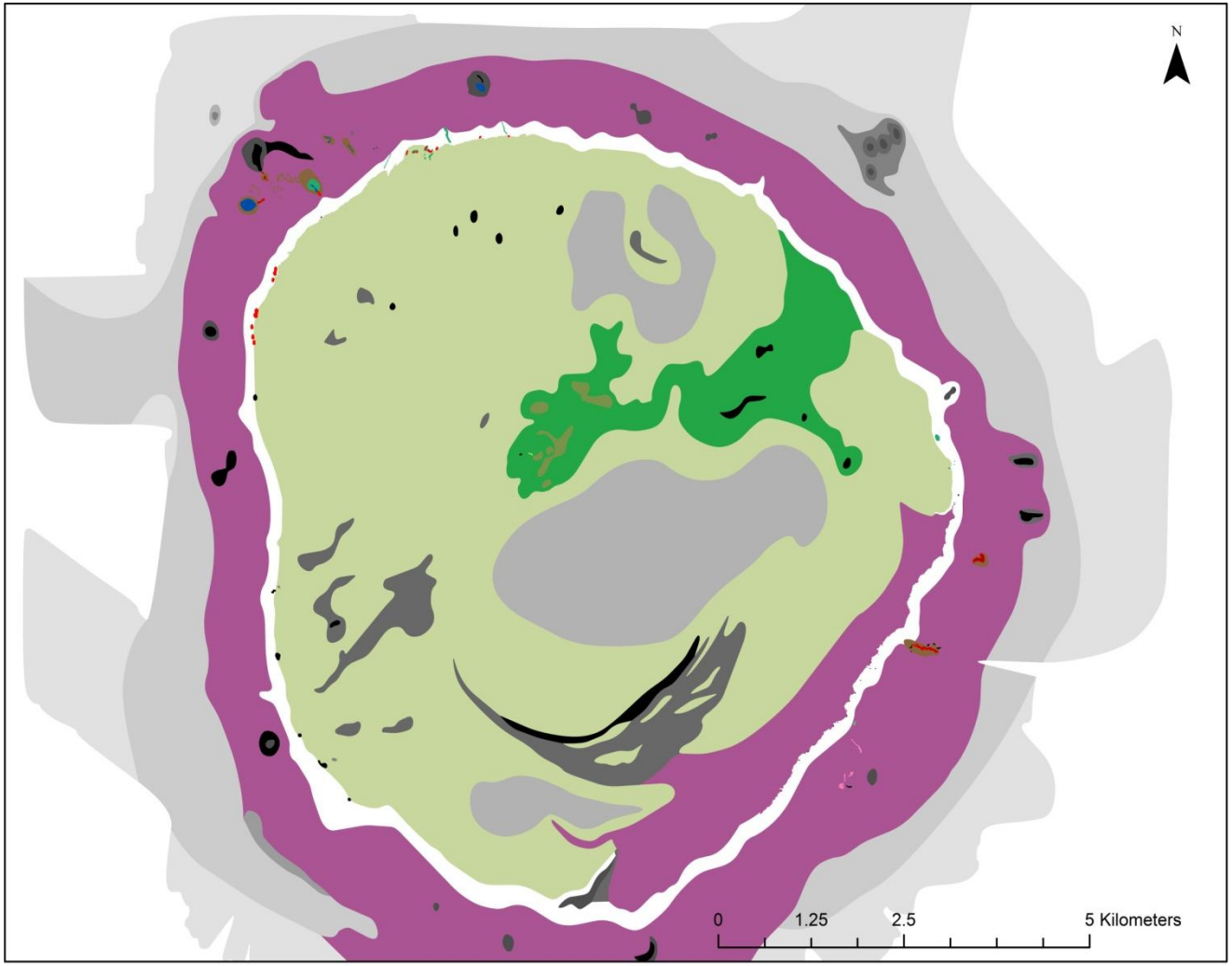

Fig. 5.16: Full coverage biotope map (primary biotopes) for Anton Dohrn Seamount, incorporating interpretations of both high and low resolution acoustic datasets (see figure legend opposite).

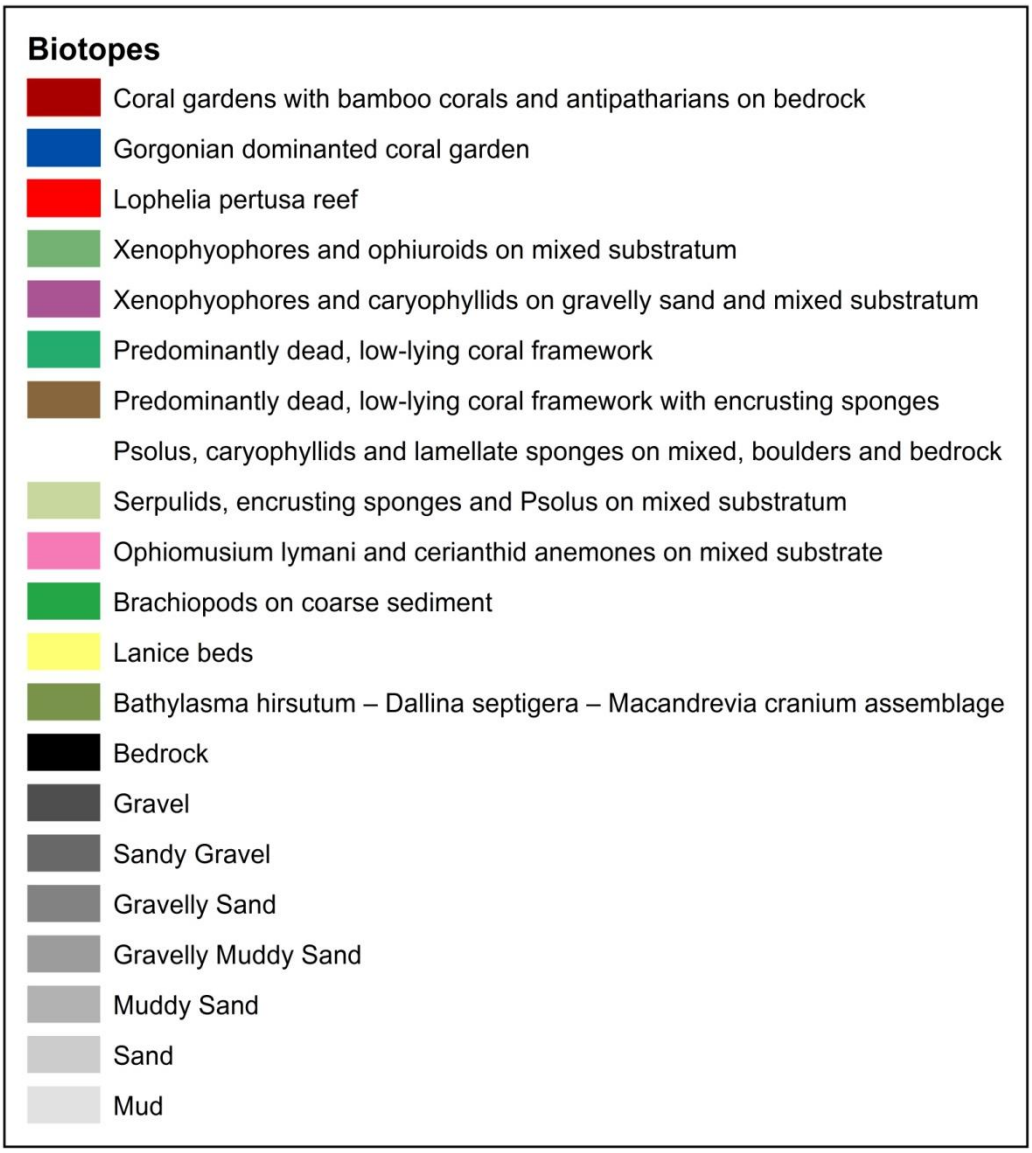

Due to constraints of displaying a complex map out of a GIS environment, the full biotope map is displayed with primary and secondary biotopes mapped in each polygon separately. Those polygons where either there was no ground-truthing or no support for predicting a biotope, substratum was kept as the label.

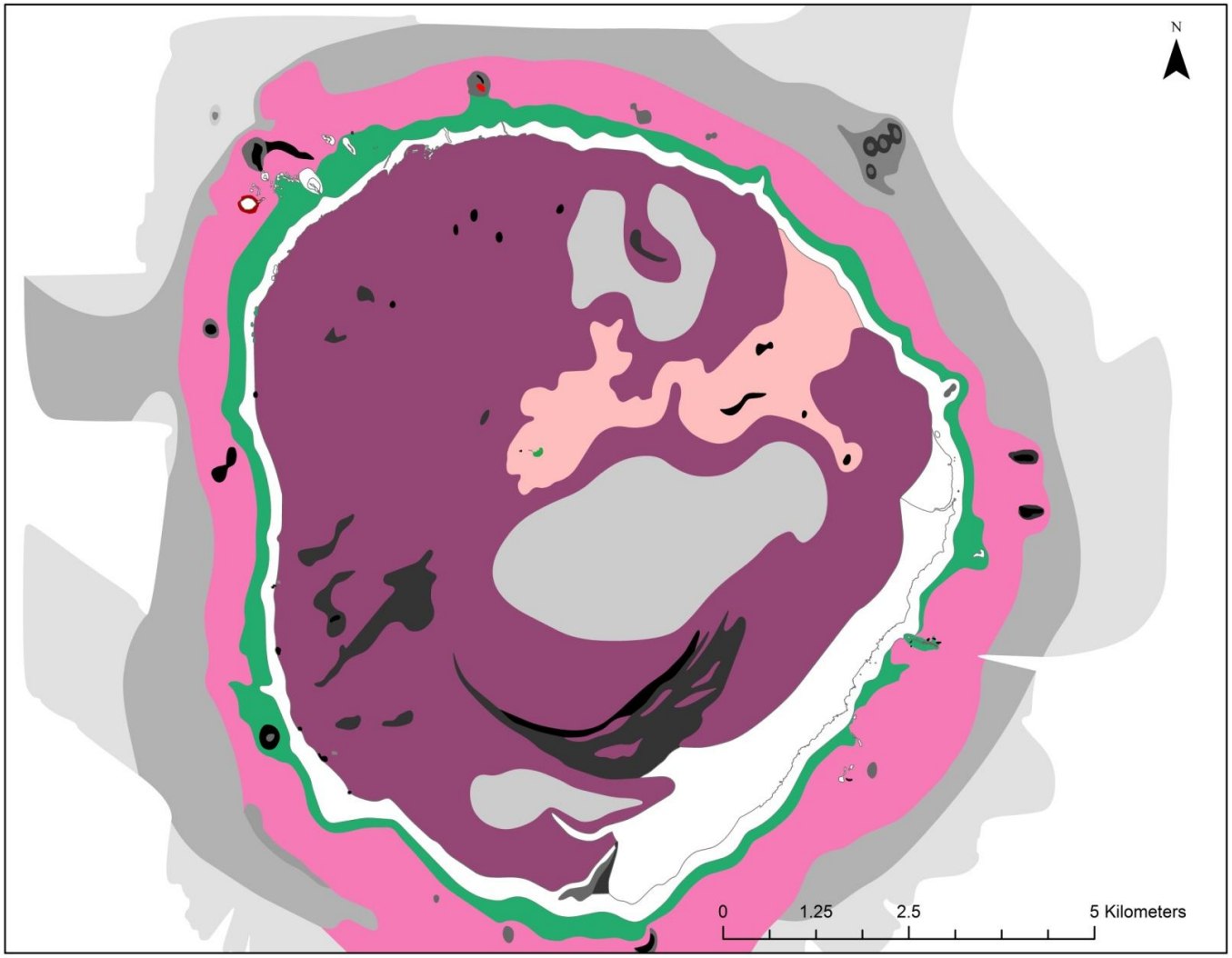

Fig. 5.17: Full coverage biotope map (secondary biotopes) for Anton Dohrn Seamount, mapped using 2 resolutions of acoustic data. Polygons are labelled with secondary biotopes that occurred in them. See figure legend opposite.

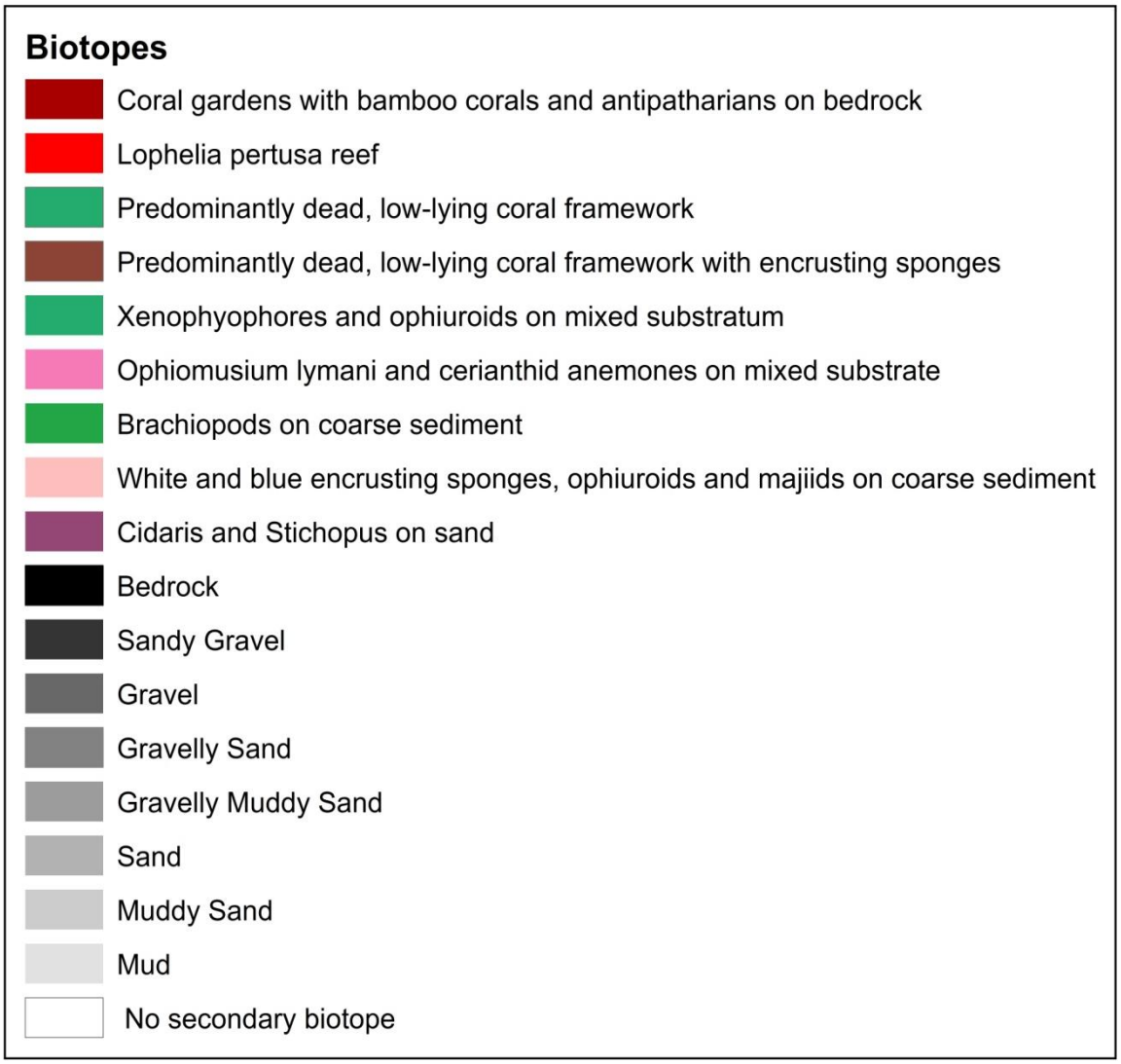

Fig 5.18 represents a continuous polygon layer for secondary biotopes mapped across ADS. Those polygons where no secondary biotope occurred are coloured white.

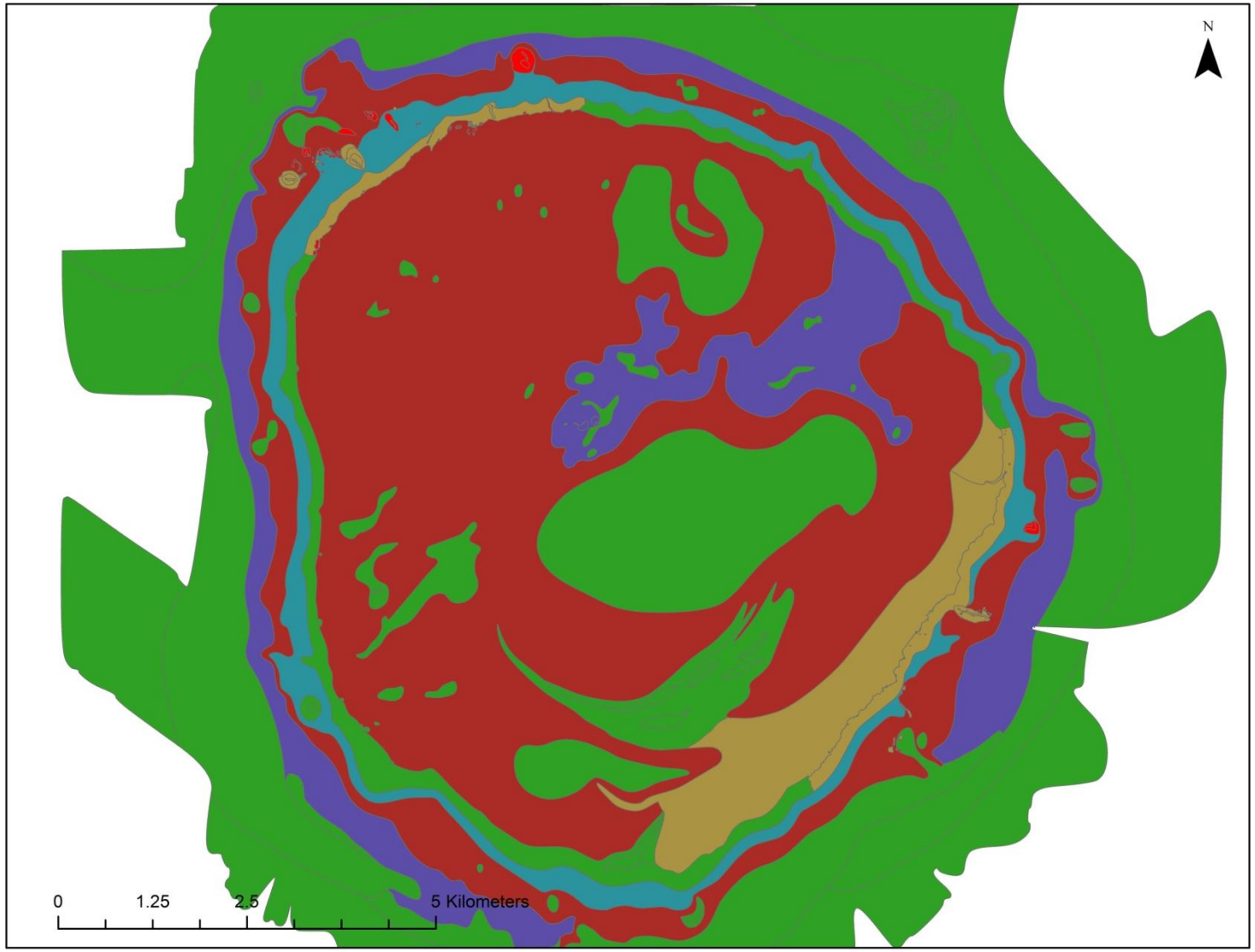

Fig 5.18: A confidence layer to accompany the full coverage biotope map of ADS. Colours represent the resolution of acoustic data and if ground-truthing was used in the interpretation. See figure legend on opposite page.

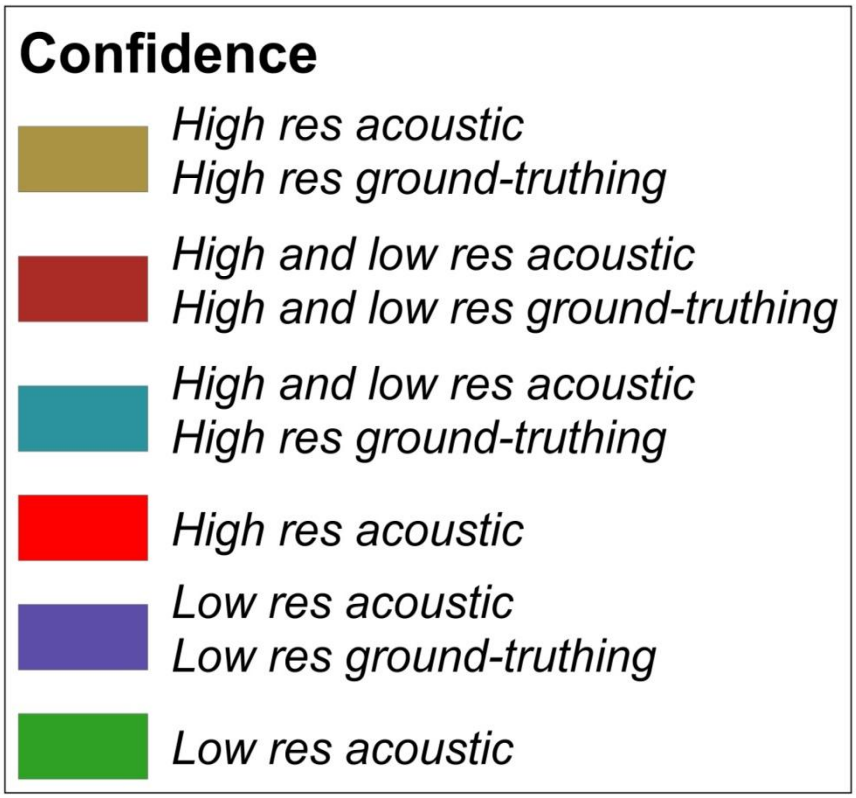

Figure 5.18 represents a confidence layer for the biotope map of ADS. It relates to the resolution of acoustic data and the use of ground-truth data. Those areas where high resolution acoustic data and ground-truthing data from the 2009 survey used in the interpretation of distribution of biotopes are clearly visible on the NW and SE side of the seamount. The summit of the seamount is covered by both high and low resolution acoustic data, and also has high and low resolution ground-truthing data (from both surveys). Green areas are where only low resolution acoustic data were acquired, with no ground-truthing data collected.

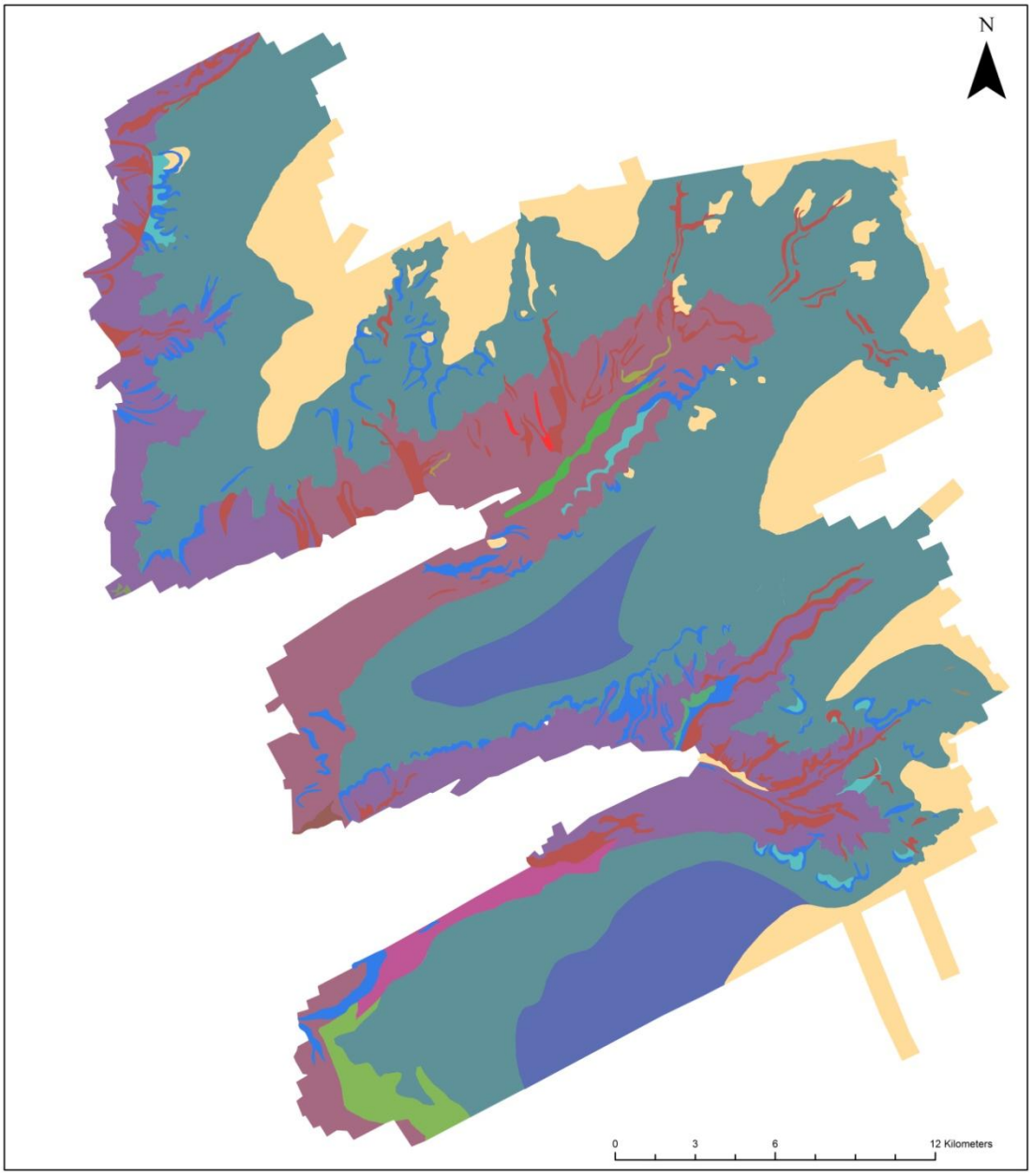

Fig. 5.19: Full coverage biotope map for the SW Canyons (see legend opposite). Polygons are labelled with all biotopes occurring in that polygon. See Fig. 5.20 for confidence layer.

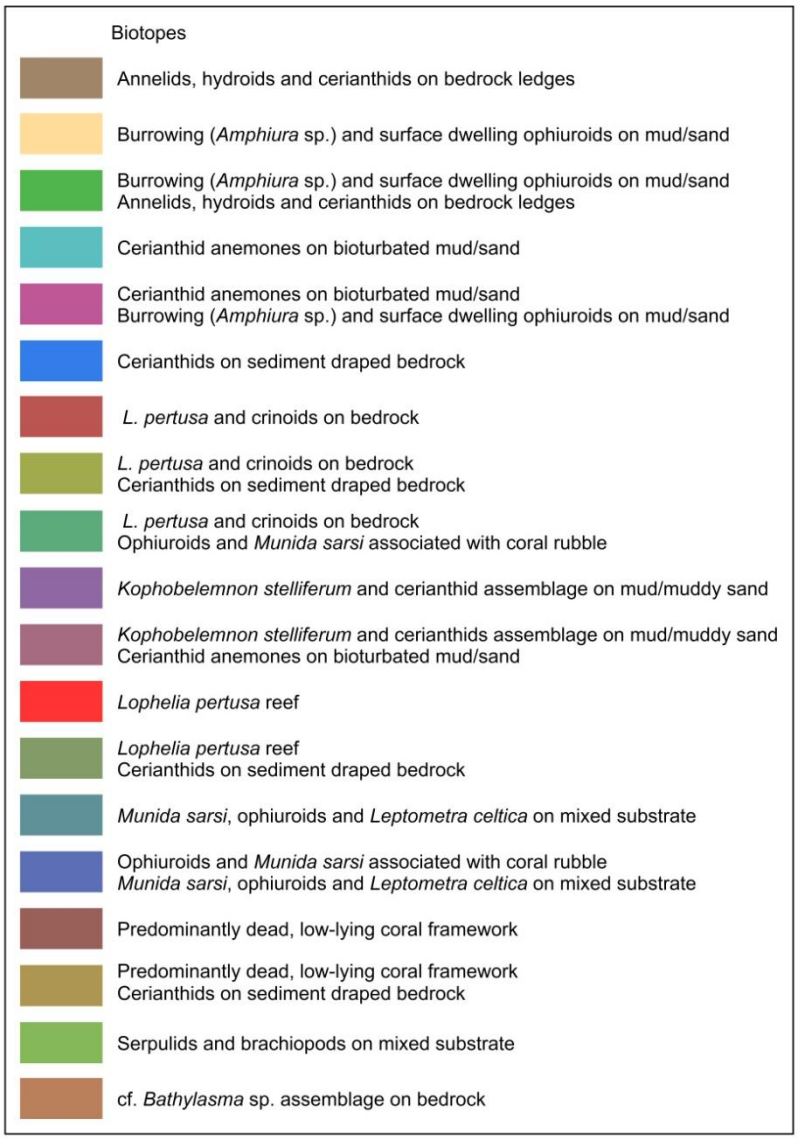

Simplistically, the upper part of the canyon system on the continental shelf is characterised by the soft sediment biotope 'burrowing (*Amphiura* sp.) and surface dwelling ophiuroids'. Moving further into the canyon system, the interfluve areas are inhabited by *'Munida sarsi*, ophiuroids and *Leptometra* celtica on mixed substratum'. The two areas of mini-mounds interrupt this relatively flat topography and the summit of the mounds host coral rubble associated fauna (Ophiuroids and *Munida sarsi* associated with coral rubble). The interfluves give way to steep flanks that are characterised by the sea pen biotope '*Kophobelemnon stelliferum* and cerianthids' and 'cerianthid anemones on bioturbated mud / sand'. *Lophelia pertusa* biotopes occur on distinct flute-like features.

Fig 5.20: Confidence layer for biotope map of the SW Approaches. Those areas which had ground-truthing to inform the occurrence of biotopes within polygons are denoted in purple. Those polygons that lacked ground-truthing are in green.

5.4 Discussion

The production of complete coverage maps of the distribution of benthic faunal assemblages is a necessary part of the process of designing, monitoring and implementing MPAs if software such as Marxan is to be used in the planning process. These maps allow assessment of the distribution and extent of biotopes, including VMEs; and assessments of the representativeness of MPA networks to be made. This study is the first to produce complete coverage biotope maps for two features identified as biodiversity hotspots, canyons and seamounts.

5.4.1 *Bathymetric Terrain analysis*

Multibeam bathymetry data and its derived layers proved significant in mapping and predicting the distribution of benthic assemblages across two megahabitat features, although to varying degrees. In all cases the interpreted substratum layer was used as a starting point for biotope mapping. Where polygons could not be further delineated using terrain parameters, and base polygons labelled with biotopes, it needs to be understood that these maps identify that the biotope occurs within the polygon, but may not occur throughout that area.

The multibeam bathymetry and terrain parameters highlighted differences in topographical complexity between the NW and SE sides of Anton Dohrn Seamount, suggesting the NW flank to have greater geomorphic diversity. On Anton Dohrn Seamount, depth was the only parameter that had a significant relationship for all biotopes ($p < 0.01$), suggesting that depth is a strong driver for the distribution of biotopes on ADS. Slope was only significant for the two xenophyophore biotopes, which occurred associated with areas of low slope angles. Coral (Lep.Ker, Gor.Lop, Lop.Mad and Lop.Por) biotopes were associated with topographical high areas as

identified by BPI and aspect parameters. Meso-scale geomorphology was only significant for the *L. pertusa* reef and predominantly dead, low-lying coral framework biotopes. Side of seamount was not significant overall, as it only explained the distribution of 3 biotopes ($p < 0.05$) on the NW and SE side of ADS, and that this was due to difference in terrain/parameters associated with a biotope either side of the seamount.

BPI was a good surrogate in identifying areas of high topographical relief on ADS and can be used to infer areas of fast currents. This means it lends itself well to delineating coral assemblages as a result of the dependence of those assemblages on relatively fast current speeds (Genin *et al.* 1986; Frederiksen *et al.* 1992; Thiem *et al.* 2006). In the canyons, with the exception of the mini-mounds (that actually lie outside the main canyon system), slope, BPI and depth were significant variables for coral reef communities. Aspect may act as a surrogate for geomorphology and hydrodynamics because it measures the orientation of the seabed, and was highly significant for coral biotopes on ADS.

Despite the use of terrain parameters, the ability to delineate boundaries to a single biotope reduces with increased acoustic footprint, which was illustrated in areas of increased water depth, and where lower resolution (2005) acoustic data was used.

5.4.2 *Mapping*

5.4.2.i Vulnerable Marine Ecosystems (VMEs)

Coral gardens

The gorgonian dominated coral garden associated with areas of high BPI and aspect found on parasitic cone and radial ridge features on the NW flank of ADS, were not

observed under the same conditions on the radial ridge sampled on the SE flank. Instead the coral gardens with bamboo coral and antipatharians biotope was observed. Corals are known to concentrate along ridges or rocky outcrops where currents are accelerated (Ramirez-Llodra *et al.* 2010) and this is a primary factor influencing the distribution of gorgonians (Barham and Davies 1968; Kinzie 1973). The high BPI values are indicative of a greater change in the depth between one area of seafloor and the areas local. It is possible that in areas where topography changes more rapidly, bottom current speeds may be increased, thus areas of high densities of corals would be more likely to occur in areas of high BPI. The results from ADS support this, with coral habitats occurring along the crest and summit of radial and parasitic cones. Interestingly, despite depth and BPI being significant variables explaining the distribution of both coral garden biotopes, aspect was not found to be significant for the later biotope. The occurrence of these biotopes was not explained by meso-scale geomorphology or side of the seamount ($p > 0.05$), but may simply be due to availability of substratum and hydrodynamic activity.

The parasitic cones on the NW flank have well development moats or furrows present where those on the SE flank do not. This suggests that there may be differences in current speeds on either side of the flank, with those on the NW side being faster (Long *et al.* 2010). Anecdotal evidence also supports this theory. A relatively thick layer of marine snow was clearly visible on video footage on the SE side of Anton Dohrn but absent from the NW side at similar depths and on similar substrata, which may also suggest that the currents are slower on the SE side allowing deposition of marine snow; although data on current regime would be needed to test this. This may account for the difference in distribution of coral garden biotopes.

These findings suggest that for the coral garden VMEs, while multibeam and its derived layers are useful surrogates in mapping the distribution of this biotope, they may not adequately represent the environmental variability of relevance to the distribution of this habitat. In this instance other environmental parameters such as broad scale current regime and / or water mass structure may play an important role in determining the distribution of the biotope.

Lophelia pertusa reef

The derived layers that proved significant in mapping the distribution of *L. pertusa* reef assemblages differed between the seamount and canyon megahabitat features. For raised features in both areas (mound and ridge features on Anton Dohrn Seamount and mini-mound features on the interfluves of the canyons) BPI was most significant for mapping and predicting the distribution of reef assemblages. However, for occurrences of reef habitat within the canyons, although associated with BPI and slope, the video track crossed boundaries between high and low BPI, and the boundary of this biotope was unclear, this is most likely due to the increased acoustic footprint with depth, or due to inaccurate positioning of video data.

As with the coral garden VME, it is likely that areas of high slope and BPI are areas of high current speeds and are thus favourable to coral growth and reef formation. Therefore for certain geomorphic features these derived layers may prove effective in predictive mapping. However, within the canyon habitat, additional environmental parameters may be required to adequately map the distribution of this VME. Canyons are very different systems to seamounts. They are often associated with increased sedimentation rates and sediment transport (Shepard 1951; Heezen *et al.* 1955) both of which adversely affect coral growth (Rogers 1990). Observations from video ground-

truthing within the canyon system suggested the *L. pertusa* reefs were highly sediment covered and despite repeat sampling of high slope 'flute' features there were only limited observations of reef structures within the canyon system. The apparent lack of large reef structures from otherwise seemingly suitable substratum and slope (current) areas suggests that sedimentation may indeed be an important factor influencing reef formation within the canyon system (see Chapter 4 for a more complete discussion of this point).

Sea pens and burrowing megafauna

Substratum and depth ($p < 0.001$) act as a good surrogate for this biotope in the canyons. While geomorphology was not important in explaining the distribution of this biotope, sea pens and burrowing megafauna require areas of fine sediment and organic enrichment, thus hydrodynamic regime is important, and information regarding this may be useful for mapping this assemblage, and may explain why delineation of the large substratum polygons was not possible using other terrain parameters such as BPI.

Xenophyophore communities

Two xenophyophore communities occurred on Anton Dohrn Seamount and were either on, or proximal to, topographical features. No xenophyophore assemblages were observed from the canyons, however this is likely to be a result of the shallower depth range investigated in the canyon system. Xenophyophores have been recorded at great depth in submarine canyons, occurring on the floor of the Nazaré canyon at a depth of 4300m (Tyler *et al.* 2009). Xenophyophore aggregations are often found in areas with enhanced organic carbon fluxes, such as beneath highly productive surface waters, on sloped topography, or near certain topographic features such as cauldera walls, basalt outcrops, or on the sides of sediment mounds and small ridges as well on larger features

such as canyons, seamounts and continental slopes (Tendal, 1972, 1979; Levin and Thomas, 1988; Levin and Gooday, 1992; Hughes and Gooday, 2004). Rogers (1994) suggested that this may be a result of topographically-enhanced currents or high concentrations of suspended matter associated with these regions, which provide an increased food supply for suspension feeding organisms such as xenophyophores.

Given that the xenophyophore aggregations observed were situated at the base of the seamount, it is likely that any topographically enhanced currents that may be important in determining the distribution of this biotope, would be produced by the presence of the seamount itself, and are therefore on a scale greater than that captured by the multibeam data used in this study.

Depth and side of the seamount explained the distribution of these biotopes; the GAM suggests that dependent on which side of the seamount the depth of these biotopes varies. Interestingly, on the NW flank of the seamount, the xenophyophore and ophiuroids biotopes occur bathymetrically above (1076-1388 m) the xenophyophore and caryophyllids biotope (1368-1770 m), while on the SE flank it is the reverse; xenophyophore and caryophyllids (1104-1154 m) and xenophyophore and ophiuroids (1100-1554 m). This suggested that in order to map xenophyophore assemblages across broad areas, other environmental layers, such as broad scale hydrographic data, should also be taken into consideration.

4.2.3 Summary

Multibeam and derived parameters combined with meso-scale geomorphology and substratum can act as reliable surrogates in mapping biotopes on two different megahabitat features, as illustrated through statistical testing. Multibeam was

particularly useful in mapping coral communities that are dependent upon elevated currents for food, and for which multibeam and its derivatives acts as a good surrogate. These findings suggest that multibeam habitat mapping techniques may be a method that can be adopted to map these communities in other areas.

However, multibeam and its derivatives were not significant surrogates for mapping all biotopes. It was particularly poor at enabling mapping of soft sediment communities, most likely because it failed to represent adequately those environmental factors that are important in determining the distribution of these assemblages, such as productivity, sedimentation and hydrodynamic regime. Even where the acoustic layers acted as surrogates for mapping specific habitats, additional environmental data appeared to be required in order to predicatively map across larger areas. This suggests that when mapping biotopes over large scale features a combination of acoustic layers and other environmental layers will result in more confident predictions of biotope distributions. Critically however, the additional environmental data used must be relevant to the assemblage that is the target of the mapping effort.

Related to this is the need to consider geomorphology at different scales, particularly in the absence of appropriate environmental data. Different terrain parameters were significant in mapping biotopes in the canyons and on the seamount; this was particularly the case for cold-water coral communities. When considering the multibeam data and its derived layers from both the canyon and seamount, the areas appear broadly similar in terms of the range of slope, rugosity, BPI etc. However, the mere fact that one is a canyon and other is a seamount, suggest immediately that the two areas are likely to be environmentally quite different. Therefore there is a need to nest

mapping efforts within a broader geomorphological context in order to develop the best maps possible.

As identified from the GAM analysis, spatial scale is important in terms of distribution of some biotopes on a seamount. Taken at a large scale and incorporating side of seamount as a factor, the GAM identified potential differences in environmental conditions either side of the seamount. Specifically, for the two xenophyophore assemblages, the distribution of this biotope was attributed to variation in depth on the NW and SE side of the seamount. The shift in zonation of these biotopes either side of the seamount suggests varying conditions that may be related to hydrodynamic condition or organic enrichment. In terms of the other biotopes where side of seamount was significant, predominantly dead, low-lying coral framework, depth did not account for the difference on the NW and SE side of the seamount, but was related to variation in BPI and aspect either side of the seamount. As the biotope was associated with areas of higher BPI and aspect on the SE side, this may suggest that currents may indeed be slower on the SE side; and thus for the biotope to benefit from the same environmental conditions as that of the NW flank, it occurs on higher topographical areas on the SE flank in order to achieve this.

It is still unclear how important geomorphology is as a surrogate for mapping the distribution of biotopes on a seamount and canyon. While meso-scale geomorphology was only significant for three coral biotopes, it is possible that the classification units used for geomorphology are not biologically meaningful and hence a significant relationship was not found overall. The fact that one is a cliff-top mound and the other a parasitic cone makes no difference to the biology, they are both mound features, but the scale of the features is different.

The production of full coverage maps, although labour intensive, allows the identification of potential relationships between assemblage distribution and the ecological parameters influencing that distribution. The maps also visually represent the distribution of biotopes varies across and between megahabitat features; which is particularly important for VMEs. Such maps will support future efforts to map biotope distributions using other methods such as predictive modelling. Importantly they provide ecological maps on which management efforts may be based. In spite of their practical use, these maps are complex and are not designed in their current format to be displayed outside of a GIS environment, they are best served as a tool that can be queried and data extracted from, such that VME can be displayed for example. The maps need to be interpreted in the context of the methods underlying them. To produce complete coverage map, base polygons had to be used to enable this, and this needs to be clear that while a polygon is labelled with the occurrence of a biotope within that polygon, an assumption of continuity within that polygon is made. Ideally ground-truthing of map would determine the accuracy of using full coverage polygon layers.

5.4.4 *Conclusions*

Depth is a strong driver for the distribution of biotopes on ADS and the SW Approaches; and it is widely accepted that most deep-sea species have predictable and restricted depth ranges (Howell, 2010). The combination of depth and terrain parameters can successfully be used to map the distribution of VME biotopes on a topographically elevated seamount megahabitat feature, but this method is more limited in submarine canyon systems. Additional data, at a scale appropriate to that of the biotopes in canyons, are necessary. Scale is an important variable that needs to be tested and considered when mapping the distribution of biotopes. While multibeam can in some instances be used with confidence, with statistical rigour, this work has

highlighted that this is not the case for all biotopes, and this needs to be considered when producing habitat maps.

The difference in the ability to map effectively across the two features is most likely a result of: the necessary use of low resolution acoustic data on the seamount; the difference in size of each feature, with Anton Dohrn Seamount being very much larger than the canyon system; and the difference in the extent of video ground-truthing carried out at the two features.

CHAPTER 6

FINAL DISCUSSION AND CONCLUSIONS

6.1 Introduction

The main tool that is currently available for nations to protect species and habitats in the deep sea / high sea is through the identification of vulnerable habitats and Marine Protected Areas (MPAs). In order to develop MPA networks that are representative it is necessary to use, and therefore produce, ecologically meaningful maps upon which to base network design. While maps can be produced using surrogates that represent the principle variation in the fauna at a very broad scale (Howell 2010), finer scale approaches are possible and desirable, particularly where there is a requirement to include, within the network design, a focus on particular habitats (biological assemblages) of conservation concern, such as vulnerable marine ecosystems (VMEs).

The use of acoustic survey offers a means to rapidly map large areas of seabed at a relatively low cost. Coupling acoustic survey with biological sampling, or 'ground-truthing', provides a means to map the distribution of biological assemblages over wide areas by inferring some relationship between the observed communities and the acoustic signal (Germano *et al.* 1989; Kostylev *et al.* 2001; Solan *et al.* 2003). These methods are increasingly being used in shallow water marine environments to map the distribution of defined biological assemblages and their associated environmental parameters or 'biotopes' (Kostylev *et al.* 2001; Roberts *et al.* 2005; Robinson *et al.* 2011). However, to date, there are few examples of this approach being applied in the deep sea. Where this approach has been applied in the deep sea, it has generally been over small areas focused on specific habitats (using ROV acquired acoustic data), such

as cold water coral reefs (Dolan *et al.* 2008; Anderson *et al.* 2011), seeps (Sager *et al.* 1999; Baco *et al.* 2010) or vents (Desbruyères *et al.* 2001; Kelley *et al.* 2001), using project-specific mapping units (or facies / biotopes).

In order to tackle the difficult task of designing representative networks of MPAs over regional and even global scales, it is necessary to produce maps that are comparable across broad areas. This requires the use of standard terms (e.g. defined biological assemblage mapping units or biotopes) set within a hierarchical classification system, which incorporates both broad scale, and finer scale units that collectively represent the principle variation in the biology. While a number of classification systems exist that are relevant to the deep sea (EUNIS, Greene *et al*. 2009; Valentine *et al*. 2003), none provide adequate descriptions of deep-sea biological assemblages for use as mapping units. In addition, the relationship between acoustic data and biological assemblages has never been explicitly assessed, despite the growing use of these methods in map production and MPA network design.

The work presented within this thesis supports deep-sea habitat mapping efforts by developing descriptions of deep-sea assemblages for use as mapping units (biotopes) and assessing the use of acoustic data in predicting the distribution of these biotopes across deep-sea features. In addition, the work collectively represents the first attempt to produce complete coverage biotope maps of megahabitat (kilometre to tens of kilometres scale) features, namely a seamount and submarine canyon. The biotopes defined in Chapters 3 (Anton Dohrn Seamount) and 4 (SW Canyons) have been submitted for inclusion into the pan-European habitat classification system EUNIS.

6.2 Megahabitat features

Anton Dohrn Seamount

The NW and SE sides of Anton Dohrn Seamount (ADS) are topographically complex and harbour diverse biological assemblages, some of which agree with current definitions of 'listed' habitats of conservation concern. A combination of multivariate analysis of still imagery and video ground-truthing defined 11 comprehensive descriptions of biotopes that function as mapping units in an applied context. Some of these biotopes have been described from other megahabitat features (continental shelf and banks), while other have not previously been described. Of the VMEs identified, *Lophelia pertusa* reef and predominantly dead, low-lying coral framework are the most accepted in terms of other descriptions from the literature. Despite no comprehensive description of xenophyophore assemblages, it would appear that the two biotopes described from ADS are not unique but similar to observations (Narayanaswamy *et al*. 2006) from other features in the region, although these have not been defined statistically. The coral garden biotopes provide much needed, comprehensive descriptions of these listed habitats that have not previously been described from UK waters.

The diversity indices aided in providing comprehensive descriptions of biotopes from a seamount feature, and also highlighted the advantage of measuring diversity using multivariate indices rather than one diversity index in isolation. Standardisation for sample size allowed the comparison of diversity between biotopes, and particularly with the diversity of assemblages from previous reports, for example between zones of *L. pertusa* reef. The 'dead coral framework' biotope was more diverse than the 'live summit zone' (*sensu* Mortensen *et al*. 1995), supporting previous findings (Jensen and Frederiksen 1992; Mortensen *et al.* 1995).

Overall assemblage composition varied between the NW and SE side of the seamount, and was not explained by location alone, but by an interaction between depth, substratum and side of the seamount. With limited numbers of transects on either side of the seamount, it may be that unbalanced sampling of depth and substratum was undertaken, and thus it is difficult to conclude whether the difference between overall assemblage composition either side of the seamount is a result of different hydrographic influences. However, the well-formed moats existing at the base of the parasitic cone features on the NE flank of ADS suggest faster currents, and the marine snow observed from video transects on the SE side also suggest varying current speeds either side of the seamount, and this may account for the differences in assemblage composition described.

SW Approaches

The SW Approaches (SWA) is an area of complex terrain, and intensive ground-truthing revealed the canyons to be dominated by soft sediment assemblages. A combination of multivariate analysis of still imagery and video ground-truthing identified 12 benthic assemblages (biotopes) at an appropriate scale to act as mapping units. Of these biotopes, five adhered to current definitions of habitats of conservation concern, four of which were classed as VMEs. Some of the biotopes relate to descriptions of communities from other megahabitat features (continental shelf and seamounts), although it appears that they may be modified versions, and may be due to the inferred high rates of sedimentation in the canyons. Other biotopes described appear to be unique to canyons, particularly the sea pen biotope *Kophobelemnon stelliferum* and cerianthids.

Only one *Lophelia pertusa* reef was observed in the canyons on a flute feature in Explorer canyon, and had the highest diversity of the defined biotopes. The soft sediment biotopes had the lowest diversity, and the sea pen biotope *Kophobelemnon stelliferum* and cerianthid ranged between the soft sediment and reef biotopes. This may reflect the occurrence of sea pens which have been reported as increasing local diversity by increasing habitat heterogeneity (Buhl-Mortensen *et al.* 2010).

The work does not support previous findings that canyons have high habitat heterogeneity, as limited hard strata were sampled from the SW Approaches. This may be a consequence of depth, as the canyons were not sampled deeper than 1100 m.

Seamount v canyon

Twenty three biotopes have been described from two megahabitat features, 12 from the SWA, and 11 from ADS. Taken against current definitions of assemblages of conservation concern, five biotopes from the SWA satisfied the definition of 'listed' habitats and of these, four were classed as VMEs; while nine from ADS were classed as 'listed' habitats and of these, seven were classed as VMEs. Two biotopes could be considered common between the seamount and canyons: *Lophelia pertusa* reef, and predominantly dead, low-lying coral framework. There were found at comparable depths on each megahabitat feature [*L. pertusa* reef (ADS 747-1337 m, SWA 795-940 m) and predominantly dead, low-lying coral framework (ADS 758-1445 m, SWA 697-927 m)]. The canyons were not sampled deeper than 1100 m so it is not known if the *L. pertusa* biotope occurs deeper. Overall, the two biotopes from ADS were more diverse than those from the SWA. *L.pertusa* reef on ADS had a much higher diversity than the reef from the SWA. In terms of mean species richness, reef on ADS had a species richness of 14.7 compared to 8.9 of that of the canyons reef. Simpson's Reciprocal

Index was also higher for the reef biotope from ADS (ADS 3.7, SWA 1.9) and the expected species richness (Sobs) extrapolated from the rarefaction curves was over double (ADS 38, SWA 17.7). The difference in diversity between the predominantly dead, low-lying coral framework biotopes from the two megahabitat features was more pronounced. The mean species richness of the biotope on ADS was almost three times that of the canyons biotope (ADS 14.7, SWA 5), and the expected species richness (Sobs) over three times greater (ADS 48, SWA 14). Surprisingly, the dead framework biotope from the SWA had a greater Simpson Reciprocal Index than that from ADS (ADS 1.49, SWA 1.6), although only marginally. While this suggests that the biogenic reef biotopes found on ADS are more diverse than those from the SWA, the biogenic reef biotopes from the SWA are inferred to be subject to higher levels of sedimentation, this would account for the lower epibenthic diversity of these biotopes in the canyons. The biogenic reef biotopes from the canyons have large areas of sediment infill and this is illustrated by being characterised by sediment-dwelling species such as cerianthid and halcampoid anemones. This may account for the differences in diversity of reef biotopes between the canyons and seamount, and we may infer that the reefs in the canyons harbour a higher infaunal diversity.

These results suggest that *L.pertusa* reef from a canyon is different to that from a seamount, and as such should be treated independently.

6.3 Vulnerable Marine Ecosystems

A bottom-up approach was undertaken to map two megahabitat features. A necessary prelude to this process was to define or classify the biological communities into functional mapping units or biotopes.

The need to define biological assemblage units is particularly important given the requirement under the United Nations General Assembly resolution (UNGA 2006) to protect VMEs[4], and the requirement under OSPAR to protect 'listed' habitats. Existing definitions of VMEs are poor, and by no means comprehensive. To adequately protect vulnerable habitats, there is a need for clarity in the working definitions used. Habitats such as *Lophelia pertusa* reefs have been widely documented (Wilson 1979; Mortensen *et al.* 1995; De Mol *et al.* 2002; Roberts *et al.* 2003) and the definition of these habitats is more widely recognised. This is not the case with all cold-water habitats; and this is particularly true for the OSPAR habitat 'coral gardens'. The OSPAR definition[5] is very broad and incorporates both hard and soft substratum assemblages; this may lead to misinterpretation, and thus misrepresentation of this habitat within a network of MPAs. Soft-bottom coral gardens can be dominated by solitary scleractinians (caryophyllids), sea pens or certain types of bamboo corals (e.g. *Acanella* sp.), whilst hard-bottom coral gardens are often found to be dominated by gorgonians, stylasterids, and/or black corals (ICES 2007).

Under the OSPAR definition, the 'gorgonian dominated coral gardens', 'coral gardens with bamboo corals and antipatharians' and '*Kophobelemnon stelliferum* and cerianthid' biotopes, identified in Chapters 3 and 4 respectively, could all be considered coral gardens.

[4]VMES are defined as 'any deep-sea ecosystem (ecotopes: finest scale units used for mapping ecosystems) which has very high vulnerability to one or more kinds of fishing activity' (FAO 2008).

[5] Coral gardens are defined as 'a habitat which has a relatively dense aggregation of individuals or colonies of one or more coral species which can occur on a wide range of soft and hard substrates' (OSPAR 2010b).

The coral gardens described from ADS fulfil a number of the criteria given by the Food and Agriculture Organization of the United Nations (FAO 2009) for classifying an assemblage as a VME. As they were only observed on parasitic cone and radial ridge features on the NW and SE flank of ADS, and have not been recorded elsewhere in UK waters, this suggests that this assemblage may only occur in discrete areas which fulfil the 'uniqueness or rarity of an ecosystem' criterion. The high abundance of orange roughy (*Hoplostethus atlanticus*) observed associated with the coral gardens from the radial ridge on the NW Flank of the seamount, suggests that this habitat may also play a functional role for fish species. Orange roughy are listed under Annex V of OSPAR as 'threatened and/or declining species' and the association of this species fulfils the 'functional significance of the habitat' criterion. Gorgonian corals, which characterise the coral garden biotopes, are known to provide structural complexity, which in turn provides habitat for other associated species; they are also slow growing which makes them less resilient following anthropogenic disturbance (Buhl-Mortensen *et al.* 2010).

The '*Kophobelemnon stelliferum* and cerianthid' biotope described from the submarine canyons of the SWA may also satisfy the criteria for being classed as a VME; however it is a fundamentally different assemblage to that described from ADS. This assemblage is 'unique or rare' in the sense that it may be unique to canyons, and sea pens are known to be vulnerable to fishing activities (Troffe *et al.* 2006) and provide structural complexity for associated species (Buhl-Mortensen *et al.* 2010); it does not appear to provide a functional habitat for fish, although this has not been specifically addressed by this thesis.

In the context of conserving representative habitats and VMEs, both these assemblages are of conservation concern. However they are faunally, environmentally and

functionally dissimilar and these differences need to be recognised rather than considering them both under the same banner as OPSAR defined ‘coral gardens’.

With easily recognised, defined biological assemblage units, the identification of assemblages that could be considered VMEs becomes much simpler and more comprehensive, i.e. not restricted to those communities that have received the most research attention. Efforts to map the distribution of VMEs are more easily combined across studies and / or regions. In addition, the classification of all benthic assemblages into named ‘habitats’ allows a more effective assessment of the representativeness of a network, and consideration of anthropogenic impacts on habitats other than those that are highly ‘charismatic’, such as cold water coral assemblages.

6.4 Habitat classification

Seamounts and canyons are broad scale, or megahabitat scale, geomorphological feature classes, and have both been identified as biodiversity hotspots (Clark *et al.* 2006; Samadi *et al.* 2006; De Leo *et al.* 2010) and are listed as potentially harbouring VMEs (FAO 2008). The results from Chapter 5 suggest that some biological assemblages could be linked to particular geomorphological features, but this occurred at varying scales, and the relationship is still unclear. To allow representation of assemblages in a network of MPAs, the inclusion of meso-scale geomorphology nested within megahabitats, would address this issue. In the current EUNIS habitat classification, canyons and seamounts are still at the megahabitat scale and do not have biological assemblages nested within these scales, therefore failing to adequately represent the range of mesohabitats. The findings from this study suggest that mapping at a mesohabitat scale may give a better representation of the biology, although further research is required. As seen from the canyons and seamount, the geomorphic diversity

can vary between megahabitat features, thus when deciding which features should be included in MPAs, meso-scale geomorphic diversity should be taken into account.

Howell (2010) puts forward a biologically meaningful benthic classification system which may aid in the implementation of MPAs. The hierarchical system is based on four surrogates known to represent changes in faunal composition at progressively finer scales: biogeography, depth, substratum and biological assemblages. Geomorphology, although noted to be important, was omitted, as the link between biological communities and geomorphology is ambiguous. The work from Chapter 5 illustrates that using a bottom-up approach allows the incorporation of finer scale data, such as biotopes, nested within increasing scales of geomorphology. The relationship between some benthic assemblages and meso-scale geomorphology suggested in Chapters 5 illustrates the potential use of meso-scale geomorphology as a surrogate for some benthic assemblages. Mapping to the level of meso-scale geomorphology is faster and more cost effective than mapping to the biotope level. Thus clarifying the relationship between the biological and geomorphological will significantly enhance progress in mapping of the deep-sea bed.

6.5 Mapping at a megahabitat scale

The use of acoustic survey in mapping deep-sea areas, has in many cases involved the use of geomorphology as a classifier. That is, deep-sea areas have been subdivided (mapped) using geomorphological classes such as seamount, canyons, bank and continental slope (Greene *et al.* 1999; Williams *et al.* 2009) at broad scales; and classes such as mound, moat, channel and scour at finer scales (Greene *et al.* 1999; Nichol *et al. in press*). However, the use of these variables in the production of maps for the purpose of MPA network design assumes these terms are biologically meaningful. To date, the

link between biology and geomorphology has been assumed, although there is some evidence to support (Howell 2010) and reject (Howell *et al.* 2010a) this assumption for some features at broad scales. At fine scales the relationship is even less clear.

Mapping using a landscape or megahabitat approach has been widely used (Harris 2007; Heap and Harris 2008; Buhl-Mortensen *et al.* 2009) as large scale geomorphological features are readily identifiable from broad scale acoustic data, for example GEBCO bathymetry can be used to identify megahabitats globally. It has been suggested that mega- and meso-scale geomorphology may potentially be sufficient units to use for MPA selection (Harris 2007).

The mapping of ADS and the SWA canyons revealed that these megahabitat features support different biological assemblages, with only two assemblages in common. This is not surprising given the difference in the depth range sampled at each and the very different physical environmental conditions existing at these features. Fundamentally, seamounts protrude from the seabed and canyons are incised into it. Seamounts are raised topographical features which act as obstacles and create a complex hydrodynamic regime, and while canyons are also areas of complex hydrodynamic activity they have high organic material and sediment inputs. The use of the terms "Seamount" and "Canyon" in mapping at a landscape level seems appropriate, based on the findings of this thesis. However, bank features are more morphologically similar to seamounts than canyons and have been suggested to have comparable benthic assemblages (Howell *et al.* 2010a). Further work is needed to assess which geomorphological classes are biologically meaningful at the megahabitat scale.

6.6 Mapping at a mesohabitat scale

Mapping benthic assemblages on meso-scale geomorphological features requires higher quality data and is more labour intensive, but has previously been achieved for features such as carbonate mounds (De Mol *et al.* 2002; Kenyon *et al.* 2003; Wienberg *et al.* 2008). The advantage of mapping at this scale is that as you begin to understand the ecology of meso-scale features, it may be possible to 'scale it up' to mega-scale features. However, while the findings from Chapters 3 and 4 suggest that some biological assemblages can be related to specific meso-scale geomorphological features, the findings from Chapter 5 suggest this relationship is complex and that meso-scale geomorphology alone would be unlikely to reflect faunal variation adequately.

Multibeam and its derived layers are routinely used to map the distribution of biotopes in shallow water, but to enable mapping of meso-scale geomorphological features in the deep sea, high resolution acoustic data is needed, and once acquired, may not be sufficient, without other parameters, to map all meso-scale features. The results of Chapter 5 suggest that the distribution of biological assemblages do relate, at least to some degree, to multibeam bathymetry (water depth) and its interpreted and derived layers, such that these layers can collectively be used to map VME biotope distribution. Multibeam and derived layers were significant surrogates for mapping the distribution of some VME biotopes, particularly those for which local hydrography was thought to be important in determining the distribution of key species, since it is likely that the layers collectively act as a surrogate for bottom current speed and direction. However, for others, for example soft sediment biotopes, multibeam and its derivatives could not be used to adequately represent the distribution of biotopes. Whilst this suggests that multibeam bathymetry is a useful tool for mapping the distribution of biotopes, the ability to map communities is also dependent on scale, and the combination of

environmental factors influencing the distribution of the biology. In respect to mapping deep-sea habitats, these findings suggest that we can be confident with using some meso-scale features as surrogates, such as in the case of mounds and pinnacles, but still need information that is not captured by the multibeam, such as oceanic currents, sedimentation and productivity to map with greater confidence. The relationship between biotopes and the mapping parameters can prove useful for future survey work, for example, the relationship between depth and aspect for coral garden biotopes could help focus survey efforts if this was a target habitat. Having *a prior* knowledge of potential locations of biotopes of conservation interest can greatly increase the efficiency of expensive deep-sea survey work.

Another option for mapping is to use predictive modelling; this has been achieved for single species mapping and has recently been applied to habitat mapping (Dolan *et al.* 2008; Guinan *et al.* 2009; Howell *et al.* 2011). Robinson *et al*. (2011) produced a series of biotope maps using a multi-parameter rule-based approach as part of the UK's Irish Sea Habitat Mapping project (HABMAP). The accuracy of predicted habitats is dependent on data quality and quantity and the use of biotope level data complicated the rule-based model due to associations with overlapping ecological niches. Although this study highlighted the potential of modelling in biotope mapping, it was undertaken in shallower water (<=100m) and thus the problems associated with data resolution would be significantly increased when used for deep-water areas. The main obstacle to the widespread use of predictive modelling in the deep sea is the development of full coverage datasets adequate for predicting benthos at an appropriate scale (Holmes *et al.* 2008). Many of the environmental data layers that may be available, such as hydrographic data sets, are at a coarse scale and thus are less likely to be relevant at the

biotope level. These data are also often derived from models themselves leading to increased error in mapping predictions.

6.7 Designing MPAs

The full coverage maps produced provide an overview of the distribution of biotopes on two megahabitat features, which can greatly influence future survey work by identifying areas of interest for specific biotopes or VMEs. They also give an indication of variability of benthic assemblages across larger scales and differences between megahabitats. As only one seamount and two canyons were surveyed, the relationships found between biotopes and environmental, geophysical and geological parameters requires testing on other megahabitats, to determine if these relationships can be used as surrogates on other deep-sea features. The work has revealed that there are few biotopes in common between the megahabitat features, and, as such, relationships between biotopes and parameters cannot be applied across the features. Canyons and seamounts need to be treated separately, as it would appear that the scale of multibeam and its derivatives used did not adequately capture environmental conditions in the canyons.

The data from ADS suggest complex hydrodynamic conditions are not always captured at the scale of the acoustic data, and this raises the need for caution when making generalisations about seamounts. The assumption cannot be made that the biology will be the same on different sides of the seamount, and this needs to be taken into consideration when implementing networks of MPAs.

The limitations of the full coverage maps are that only relationships between VMEs and mapping parameters have been statistically tested. Despite a confidence layer being provided for each of the maps, to illustrate the data used to map the distribution of

biotopes, caution should be taken. As the methods underlying the mapping of the VMEs have been undertaken statistically (both though the definition of biotopes and testing the relationship of mapping parameters), these maps should be used in the context of VME distribution.

The development of habitat maps across broad areas of the deep sea will inevitably result in the need to bring together datasets of varying resolution, acquired over decadal time scales, using a variety of equipment types. Producing practical, useful maps from these disparate datasets is a challenge, but one that must be tackled as part of an ecosystem approach to management of the deep sea.

Mapping the Anton Dohrn Seamount (Chapter 5) involved bringing together two acoustic datasets of very different resolution, a low resolution dataset that covered the entire seamount, and a nested high resolution dataset from areas on the NW and SE sides. The broad scale acoustic data was adequate for interpretation of substratum and geomorphology across the seamount, but it did not allow for accurate delineation of biotope boundaries; this suggests that broad-scale acoustic data may be a useful tool in MPA design over large areas, but of limited use in focusing on VMEs. The high resolution data allowed for the delineation of single biotope distributions in many cases (for example cliff-top mounds); while the higher acoustic footprint associated with the lower resolution acoustic data prevented this.

The approach of combining low resolution broad coverage acoustic data with targeted areas of higher resolution data may allow for full coverage maps to be produced for use in MPA design. However, the variation in resolutions would need to be incorporated in the process of designing MPAs, which can be achieved by producing confidence layers associated with created habitat maps. The confidence layers identify those areas that

were mapped, using low or high resolution data, and would therefore allow informed use of developed habitat maps. The disparity between varying resolution of acoustic data, and the affect it has on the ability to map benthic assemblages across megahabitat features, reinforces the requirement for confidence layers for maps. These layers should reflect the variation in not only the resolution of the acoustic data, but also the biology. To enable delineation of biotopes on deep-sea meso-scale geomorphological features, higher resolution (greater number of acoustic pings) datasets are needed and can be acquired using Remotely Operated Vehicles (ROVs) (multibeam integrated), Automated Underwater Vehicles (AUVs) and sidescan sonar.

6.8 Final conclusions and limitations

To adequately manage the deep sea we need to put into place MPAs that represent the diversity of habitats; and for this we need maps. This study has contributed to international efforts to address this problem by providing biological assemblage (biotope) definitions, for use as functional mapping units, from two distinctly different deep-sea megahabitats: a seamount and canyon, which are of conservation concern. It has also demonstrated that seamount and canyon communities are almost entirely dissimilar, which supports the use of these megahabitat features as units in broad-scale mapping efforts. Fine-scale geomorphology (meso-scale), despite being a significant surrogate for some biotopes, does not adequately represent differences in biological communities across megahabitat features, and the use of multibeam and its derived layers alone are of variable use in mapping the distribution of benthic biotopes. Listed habitats do show some relationship to seabed topography and geomorphology, and has been shown statistically to be significant, but this relationship still needs clarification in terms as a surrogate for mapping. This work has shown that it is possible to produce complete coverage maps for megahabitat features, which may be used in software like

Marxan. But the final product is comprised of mixed biotope polygons, and the confidence varies across the feature, this is particularly true for soft sediment areas.

As this is the first attempt made to map complete megahabitat features, the associations between meso-scale features and biotopes suggested here needs to be tested on other seamounts and canyons, as well as from different megahabitat features in the same region. With the limited time, and budgets, available to nations to design MPA networks it is not feasible to produce full coverage biotope maps for their entire offshore areas. However, where fine-scale acoustic data are already available, biotope maps may be produced to aid in establishing relationships between biological assemblages and larger scale features that are easily mapped. With the task of designing MPA networks, the need to take a broad-scale approach is clear. However, if this is coupled with the development of finer-scale maps of targeted areas, our ability to achieve a representative network is increased. The ability to map a megahabitat feature is largely dependent on the resolution of the underlying acoustic data and also the amount of ground-truthing data. This was a limitation with mapping Anton Dohrn Seamount in comparison to the SW Approaches, as the Seamount is much larger and had significantly less ground-truthing, and did not have complete coverage, high resolution multibeam. These factors need to be taken into account when producing broad-scale habitat maps.

6.8 Further work

While the UK's deep-sea has been well sampled, little was known about Anton Dohrn Seamount and the canyons of the SW Approaches. This work has extended our knowledge of the ecology of two megahabitat features. Despite this, mapping of these features have identified many complex issues that need addressing. With time

limitations, it is not feasible to map the deep sea using the techniques employed here, we need to take an approach where ecological knowledge, such as that gained from this work, can be incorporated into a modelling approach. A modelling approach would allow statistical methods to be employed across larger areas. Before this approach can be undertaken, consideration of data layers is necessary, as shown in chapter 5; multibeam and its derivatives alone do not explain the distribution of all assemblages. Full multi-scale analysis of geophysical data is required, to determine the scale at which the explanatory variables best explain the distribution of biotopes; and also to determine the scale of the variables that may be used for mapping soft-sediment biotopes, particularly in submarine canyons. This needs to be investigated on other megahabitat features to determine if there are any commonalities between seamounts and canyons, and whether a common approach can be taken. Such a project would need to address what resolution of acoustic data, combined with what level of ground-truthing, is needed to produce maps that are accurate enough at an appropriate mapping scale for protecting habitats. The accuracy of the maps would also need to be assessed, and to do this they would need to be resampled. This is a substantial amount of work that warrants further investigation, and would be another PhD in itself.

REFERENCES

The Mining Code. International Seabed Authority. Regulations on Prospecting and Exploration for Polymetallic Nodules in the Area.

92/43/EEC Council Directive 92/43/EEC of 21 May 1992 on the conservation of natural habitats and of wild fauna and flora. OJ L206, 22.07.92. p.7.

1972, E. 1972 Act of Accession of Denmark, Ireland, Norway and the UK to the EC. OJ L73, 27.3.72. p.1.

Ali, T. A. (2009). Building of robust multi-scale representations of LiDAR-based digital terrain model based on scale-space theory. Optics and Lasers in Engineering **48**(3): 316-319.

Allaby, A. and Allaby, M. (1990). Concise dictionary of Earth Sciences. Oxford University Press.

Allen, S. E., Vindeirinho, C., Thomson, R. E., Foreman, M. G. G. and Mackas, D. L. (2001). Physical and biological processes over a submarine canyon during an upwelling event. Canadian Journal of Fisheries and Aquatic Sciences **58**: 671-684.

Anderson, M. J., Gorley, R. N and Clarke, K. R. (2008). PERMANOVA+ for PRIMER; Guide to Software and Statistical Methods. PRIMER-E Plymouth, UK.

Anderson, T. J., Nichol, S. L., Syms, C., Przeslawski, R. and Harris, P. T. (2011). Deep-sea bio-physical variables as surroagtes for biological assemblages, an example from the Lord Howe Rise. Deep-sea Research II **in press**.

Baco, A. R., Rowden, A. A., Levin, L. A., Smith, C. R. and Bowden, D. A. (2010). Initial characterization of cold seep faunal communities on the New Zealand Hikurangi margin. Marine Geology **272**(1-4): 251-259.

Ball, I.R., H.P. Possingham, and M. Watts. 2009. Marxan and relatives: Software for spatial conservation prioritisation. Chapter 14: Pages 185-195 in Spatial conservation prioritisation: Quantitative methods and computational tools. Eds Moilanen, A., K.A. Wilson, and H.P. Possingham. Oxford University Press, Oxford, UK.

Barham, E. G. and Davies, I. E. (1968). Gorgonians and water motion studies in Gulf of California. Underwater Naturalist **5**: 24-28.

Belderson, R. H. and Kenyon, N. H. (1976). Long-range sonar views of submarine canyons. Marine Geology **22**: 69-74.

Bett, B. J. (2001). UK Atlantic Margin Environmental Survey: Introduction and overview of bathyal benthic ecology. Continental Shelf Research **21**(8-10): 917-956.

Boldreel, L. O. and Anderson, M. S. (1993). Late Paleocene to Miocene compression in the Faeroe-Rockall area. In: Parker, J.R. (Ed.), Petroleum Geology of Northwest Europe: Proceedings of the Fourth Conference. The Geological Society, London: 1025-1034.

Brodeur, R. D. (2001). Habitat-specific distribution of Pacific ocean perch (*Sebastes alutus*) in Pribilof Canyon, Bering Sea. Continental Shelf Research **21**(3): 207-224.

Bruntse, G. and Tendal, O. S. (2001). Marine biological investigations and assemblages of benthic invertebrates from Faroe Islands. Kaldbak Marine Biological Laboratory, Faroe Islands,: 1-80.

Bryan, T. L. and Metaxas, A. (2007). Predicting suitable habitat for deep-water gorgonian corals on the Atlantic and Pacific Continental Margins of North America. Marine Ecology Progress Series **330**: 113-126.

Buckland, S. T., Magurran, A. E., Green, R. E. and Fewster, R. M. (2005). Monitoring change in biodiversity through composite indices. Philosophical Transactions of the Royal Society B **360**: 243-254.

Buhl-Mortensen, L. and Mortensen, P. B. (2004). Symbiosis in deep-water corals. Symbiosis **37**: 33-61.

Buhl-Mortensen, P., Dolan, M. and Buhl-Mortensen, L. (2009). Prediction of benthic biotopes on a Norwegian offshore bank using a combination of multivariate analysis and GIS classification. ICES Journal of Marine Science **66**: 2026-2032.

Buhl-Mortensen, L., Vanreusel, A., Gooday, A. J., Levin, L. A., Priede, I. G., Buhl-Mortensen, P., Gheerardyn, H., King, N. J. and Raes, M. (2010). Biological structures as a source of habitat heterogeneity and biodiversity on the deep ocean margins. Marine Ecology **31**: 21-50.

Buhl-Mortensen, P., Buhl-Mortensen, L., Dolan, M., Dannheim, J. and Kröger, K. (2009). Megafaunal diversity associated with marine landscapes of northern Norway: a preliminary assessment. Norwegian Journal of Geology **89**: 163-171.

Burnham, K. P and Anderson, D. R. (2002). Model selection and multimodal inference. A practical information-theoretic approach. 2nd ed , New York Springer-Verlag

Cairns, S. D. (1992). Worldwide distribution of the Stylasteridae (Cnidaria: Hydrozoa). Scientia Marina **56**: 125-130.

Carpine, C. and Grasshoff, M. (1975). Les gorgonaires de la Médieterranée. Bulletin de l'Institute Océanographique **71**(1430).

Cartes, J. E., Company, J. B. and Maynou, F. (1994). Deep-water decapod crustacean communities in the Northwestern Mediterranean: influence of submarine canyons and season. Marine Biology **120**: 221-229.

Cartes, J. E. and Sardá, F. (1993). Zonation of deep-sea decapod fauna in the Catalan Sea (Western Mediterranean). Marine Ecology Progress Series **94**: 27-34.

CBD (2004). Secretariat of the Convention on Biological Diversity. Technical advice on the establishment and management of a national system of marine and coastal protected areas, SCBD. CBD Technical Series no. 13.

CBD (2010) Convention on Biological Diversity, COP Decision X/2, Strategic Plan for Biodiversity 2011-2020.

Clark, M. R., Tittensor, D., Rogers, A. D., Brewin, P., Schlacher, T. A., Rowden, A. A., Stocks, K. and Consalvey, M. (2006). Seamounts, deep sea corals and fisheries: vulnerability of deep sea corals to fishing on seamount beyond areas of national jurisdiction. UNEPWCMC, Cambridge, UK.

Clark, M. R., Rowden, A. A., Williams, A., Consalvey, M., Stocka, K. I., Rogers, A. D., O'Hara, T. D., White, M., Shank, T. M. and Hall-Spencer, J. M. (2010). The ecology of seamounts: structure, function, and human impacts. Annual Review of Marine Science **2**: 253-278.

Clarke, K. R. (1993). Non-parametric multivariate analyses of changes in community structure. Australian Journal of Ecology **18**: 117-143.

Clarke, K. R. and Gorley, R. N. (2006). PRIMER v6: User Manual/Tutorial. PRIMER-E, Plymouth.

Clarke, K. R., Somerfield, P. J. and Gorley, R. N. (2008). Testing the null hypotheses in exploratory community analyses: similarity profiles and biota-environment linkage. Journal of Experimental Marine Biology and Ecology **366**: 56-69.

Clarke, K. R. and Warwick, R. M. (2001). Changes in Marine Communities: An Approach to Statistical Analysis and Interpretation. 2nd edition. PRIMER-E, Plymouth, UK: 172.

Cogan, C. B. and Noji, T. T. (2007). Marine classification, mapping, and biodiversity analysis, in Todd, B. J. , and Greene, H. G., eds. Mapping the seafloor for habitat characterization: Geological Association of Canada, Special Paper 47, p.129-139.

Colwell, R. K. 2009. EstimateS: Statistical estimation of species richness and shared species from samples. Version 8.2. User's Guide and application published at: http://purl.oclc.org/estimates.

Colwell, R. K., Chao, A., Gotelli, N. J., Lin, S-Y., Xuan Moao, C., Chazdon, R. L. and Longino, J. T. (2012). Models and estimators linking individual-based and sample-based rarefaction, extrapolation and comparison of assemblages. Journal of Plant Ecology **5**(1) 3-21.

Connor, D. W. and Hiscock, K. (1996). Data collection methods (with Appendices 5 - 10). In: *Marine Nature Conservation Review: rationale and methods*, ed. by K. Hiscock, 51-65, 126-158. Peterborough, Joint Nature Conservation Committee. (Coasts and seas of the United Kingdom. MNCR series.)

Cunningham, M. J., Hodgson, S., Masson, D. G. and Parson, L. M. (2005). An evaluation of along and down-slope sediment transport processes between Goban Spur and Brenot Spur on the Celtic Margin of the Bay of Biscay. Sedimentary Geology **179**: 99-116.

Dahl, F. (1908). Grundsaetze und grundbegriffe der biocoenotischen forshung. Zoologische Anzeiger **33**: 349-353.

De Leo, F. C., Smith, C. R., Rowden, A. A., Bowden, D. A. and Clark, M. R. (2010). Submarine canyons: hotspots of benthic biomass and productivity in the deep sea. Proceedings of the Royal Society B: Biological Sciences **in press**.

De Mol, B., Van Rensbergen, P., Pillen, S., Van Herreweghe, K., Van Rooij, D., McDonnell, A., Huvenne, V., Ivanov, V., Swennen, R. and Henriet, J. P. (2002). Large deep-water coral banks in the Porcupine Basin, southwest of Ireland. Marine Geology **188**: 193-231.

De Mol, B., Van Rensbergen, P., Pillen, S., Van Herreweghe, K., Van Rooij, D., McDonnell, A., Huvenne, V. A. I., Ivanov, M., Swennen, R. and Henriet, J. P. (2002). Large deep-water coral banks in the Porcupine Basin, southwest of Ireland. Marine Geology **188**: 193-231.

De Mol, L., Van Rooij, D., Pirlet, H., Greinert, J., Frank, N., Quemmerais, F. and Henriet, J.-P. (2010). Cold-water coral habitats in the Penmarch and Guilvinec Canyons (Bay of Biscay): Deep-water versus shallow-water settings. Marine Geology **In Press**.

De Santo, E. M. and Jones, P. J. S. (2007). Offshore marine conservation policies in the North East Atlantic: Emerging tensions and opportunities. Marine Policy **31**(3): 336-347.

Desbruyères, D., Biscoito, M., Caprais, J. C., Colaço, A., Comtet, T., Crassous, P., Fouquet, Y., Khripounoff, A., Le Bris, N., Olu, K., Riso, R., Sarradin, P. M., Segonzac, M. and Vangriesheim, A. (2001). Variations in deep-sea hydrothermal vent

communities on the Mid-Atlantic Ridge near the Azores plateau. Deep Sea Research Part I: Oceanographic Research Papers **48**(5): 1325-1346.

Diaz, R. J., Solan, M. and Valente, R. M. (2004). A review of approaches for classifying benthic habitats and evaluating habitat quality. Journal of Environmental Management **73**(3): 165-181.

Dinmore, T. A., Duplisea, D. E., Rackam, B. D., Maxwell, D. L. and Jennings, S. (2003). Impact of a largescale area closure on patterns of fishing disturbance and the consequences for benthic communities. ICES Journal of Marine Science **60**(2): 371-380.

Dolan, M. F. J., Grehan, A. J., Guinan, J. C. and Brown, C. (2008). Modelling the local distribution of cold-water corals in relation to bathymetric variables: Adding spatial context to deep-sea video data. Deep-sea Research I **55**: 1564-1579.

Douvere, F. and C. N. Ehler (2007). International Workshop on Marine Spatial Planning, UNESCO, Paris, 8-10 November 2006: A summary. Marine Policy **31**(4): 582-583.

Duineveld, G. C. A., Lavaleye, M. S. S., Berghuis, E. M., deWilde, P., vanderWeele, J., Kok, A., Batten, S. D. and deLeeuw, J. W. (1997). Patterns of benthic fauna and benthic respiration on the Celtic continental margin in relation to the distribution of phytodetritus. Internationale Revue Der Gesamten Hydrobiologie **82**(3): 395-424.

Duineveld, G., Lavaleye, M., Berghuis, E. and Wilde, P. (2001). Activity and composition of the benthic fauna in the Whittard Canyon and the adjacent continental slope (NE Atlantic). Oceanologica Acta **24**(1): 69-83.

Dullo, W.-C., Flögel, S. and Rüggeberg, A. (2008). Cold-water coral growth in relation to the hydrography of the Celtic and Nordic European continental margin. Marine Ecology Progress Series **371**: 165-176.

Durán Muñoz, P., Sacau, M., Sayago-Gill, M., Patrocinio, T., Fernández-Salas, L. M., Murillo, F. J., Dıàz del Rıo, V., Serrano, A. and Parra, A. (2007). ECOVUL /ARPA (Estudio de los eCOsistemas VULnerablesy los ARtes de PescA): a Spanish interdisciplinary research project focused on the study of the Hatton Bank deep-sea fisheries (ICES XIIb and VIb1) and their relationship with vulnerable ecosystems/habitats, integrating fisheries biology, geomorphology, benthic ecology and sedimentology. ICES CM 2007/A: 01: p17.

Durán Muñoz, P., Sayago-Gill, M., Cristobo, J., Parra, S., Serrano, A., Díaz del Rio, V., Patrocinio, T., Sacau, M., Murillo, F. J., Palomino, D. and Fernández-Salas, L. M. (2009). Seabed mapping for selecting cold-water coral protection areas on Hatton Bank, Northeast Atlantic. ICES Journal of Marine Science **66**: 2013-2025.

Džeroski, S. and Drumm, D. (2003). Using regression trees to identify the habitat preference of the sea cucumber (Holothuria leucospilota) on Rarotonga, Cook Islands. Ecological Modelling **170**: 219-226.

Eastwood, O. D., Souissi, S., Rogers, S. I., Coggan, R. A. and Brown, C. J. (2006). Mapping seabed assemblages using comparative top-down and bottom-up classification approaches. Canadian Journal of Fisheries and Aquatic Sciences **63**(7): 1536-1578.

EC (2008). EC. L19. Official Journal of the European Union; 2008. Council Regulation (EC) No 40/2008 of 16 January 2008 fixing for 2008 the fishing opportunities and associated conditions for certain fish stocks and groups of fish stocks, applicable in Community waters and, for Community vessels, in waters where catch limitations are required; p. 159. 23 January 2008.

Emery, K. O. and Hülsemann, J. (1963). Submarine canyons of southern California. Part 1, Topography, water and sediment.

Enachescu, M. E. (2004). Conspicuous deepwater submarine mounds in the northeastern Orphan Basin and on the Orphan Knoll, offshore Newfoundland. Lead Edge **23**: 1290-1294.

Ellett, D. J., Edwards, A. and Bowers, R. (1986). The hydrography of the Rockall Channel - an overview. Proceedings of the Royal Society of Edinburgh **88**(B): 61-81.

Etter, R. J. and Grassle, J. F. (1992) Patterns of species diversity in the deep-sea as a function of sediment particle size diversity. Nature **360**: 576-578.

Evans, C. D. R. (1990). United Kingdom offshore regional report: the geology of the western English Channel and its western approaches. London: HMSO for the British Geological Survey.

Evans, C. D. R. and Hughes, M. J. (1984). The Neogene succession of the South Western Approaches, Great Britain. Journal of the Geological Society of London **141**: 315-326.

FAO (2008). Report of the FAO Workshop on Vulnerable Ecosystems and Destructive Fishing on Deep-sea Fisheries. Rome, 26-29 June 2007. FAO Fisheries Report. No. 829.

FAO (2009). International Guidelines for the Management of Deep-sea Fisheries in the High Seas. Rome.

Flach, E. and Heip, C. (1996). Vertical distribution of macrozoobenthos within the sediment on the continental slope of the Goban Spur area (NE Atlantic). Marine Ecology Progress Series **141**(1-3): 55-66.

Flach, E. and Thomsen, L. (1998). Do physical and chemical factors structure the macrobenthic community at a continental slope in the NE Atlantic? Hydrobiologia **376**: 265-285.

Folk, R. L. (1954). The distinction between grain size and mineral composition in sedimentary rock nomenclature. Journal of Geology **62**(4): 344-359.

Frederiksen, R., Jensen, A. and Westerberg, H. (1992). The distribution of the scleractinian coral *Lophelia pertusa* around the Faroe Islands and the relation to internal mixing. Sarsia **77**: 157-171.

Freiwald, A., Fosså, J. H., Grehan, A., Koslow, T. and Roberts, J. M. (2004). Cold-water coral reefs, out of sight - no longer out of mind. United Nations Environmental Programme - World Conservation Monitoring Centre Report Biodiversity Series **22**: 84pp.

Freiwald, A., Wilson, J. B. and Henrich, R. (1999). Grounding Pleistocene icebergs shape recent deep-water coral reefs. Sediment Geology **125**: 1-8.

Gage, J. D. (1986). The benthic fauna of the Rockall Trough: regional distribution and bathymetric zonation. Proceedings of the Royal Society of Edinburgh **88B**: 159-174.

Gage, J. D., Lamont, P. A. and Tyler, P. A. (1995). Deep-sea macrobenthic communities at contrasting sites off Portugal, preliminary results .1. Introduction and diversity comparisons. Internationale Revue Der Gesamten Hydrobiologie **80**(2): 235-250.

Gardner, W. D. (1989). Baltimore Canyon as a modern conduit of sediment to the deep sea. Deep-Sea Research **36**: 323-358.

Genin, A., Dayton, P. K., Lonsdale, P. F. and Speiss, F. N. (1986). Corals on seamount peaks provide evidence of current acceleration over deep-sea topography. Nature **322**: 59-61.

Germano, J. D., Rhoads, D. C., Boyrt, L. F., Menzie, C. A. T. and Ryther, J. A. J. (1989). REMOTSR imaging and sidescan sonar: efficient tools for mapping sea floor topography, sediment type, bedforms, and biology. In: Hood, D.W., Schoener, A., Park,

P.K. (Eds.),. Oceanic Processes in Marine Pollution. Scientific Monitoring Strategies for Ocean Waste Disposal, vol. 4. R.E. Krieger Publishing, Malabar, FL: 39-48.

Glover, A. G. and Smith, C. R. (2003). The deep-sea floor ecosystem: current status and prospects of anthropogenic change by the year 2025. Environmental Conservation **30**(3): 219-241.

Gotelli, N. J and Colwell, R. K. (2010) Estimating species richness. In Biological Diversity. Frontiers in Measurement and Assessment. Edited by Anne E. Magurran and Brian J. McGill.

Gotelli, N. J. and Colwell, R. K. (2001). Quantifying biodiversity: procedures and pitfalls in the measurement and comparison of species richness. Ecology Letters **4**: 379-391.

Graham, C.C. (1990). Foula. Sheet 60°N-04°W. Sea-bed Sediments. 1:250 000 map series. British Geological Survey.

Grasshoff, M. (1972). The Gorgonia of the eastern North Atlantic and Mediterranean. I. Family Ellisellidae (Cnidaria: Anthozoa). Results of the Atlantic Seamount Cruises 1967 with RV Meteor. . Meteor Forsch. Ergebnisse **10**: 73-87.

Grasshoff, M. (1973). Die Gorgonaria des östlichen Nordatlantik und des Mittelmeeres II. Die Gattung Acanthogorgia (Cnidaria: Anthozoa) Auswertung der Atlantischen Kuppenfahrten 1967 von FS Meteor. Meteor Forsch.Ergebnisse **13**: 1-10.

Grasshoff, M. (1977). Die Gorgonarien des östlichen Nordatlantik und des Mittelmeeres. III Die Familie Paramuriceidae (Cnidaria, Anthozoa). Meteor Forsch. Ergebnisse **27**: 5-76.

Grasshoff, M. (1981a). Gorgonaria und Pennatularia (Cnidaria: Anthozoa) vom Mittelatlantischen Rucken SW der Azoren. Steenstrupia **7**: 213-230.

Grasshoff, M. (1981b). Die Gorgonaria, Pennatularia und Antipatharia des tiefwassers der Biskaya (Cnidaria, Anthozoa). II Taxonomischer Teil. Bulletin de la Musee d'Histoire Naturelle de Paris **3**: 941-978.

Grasshoff, M. (1981c). Die Gorgonaria, Pennatularia und Antipatharia des tiefwassers der Biskaya (Cnidaria, Anthozoa). I Allgemeiner Teil. Bulletin de la Musee d'Histoire Naturelle de Paris **3**: 731-766.

Grasshoff, M. (1985). Die Gorgonaria und Antipatharia der Großen Meteor-Bank und der Josephine- Bank. (Cnidaria: Anthozoa). Senckenb. Marit. **17**: 65-87.

Greene, C. H., Weibe, P. H., Burczynski, J. and Youngbluth, M. J. (1988). Acoustical detection of high-density demersal krill layers in the submarine canyons off Georges Bank. Science **241**: 359-361.

Greene, H. G., Yoklavich, M. M., Starr, R. M., O'Connell, V. M., Wakefield, W. W., Sullivan, D. E., McRea Jr, J. E. and Cailliet, G. M. (1999). A classification scheme for deep seafloor habitats. Oceanologica Acta **22**(6): 663-678.

Guinan, J., Brown, C., Dolan, M. F. J. and Grehan, A. J. (2009). Ecological niche modelling of the distribution of cold-water coral habitat using underwater remote sensing data. Ecological Informatics **4**(2): 83-92.

Guisan, A., Edwards, T. C., Trevor, E. Jr. And Hastie, T. (2002). Generalized linear and generalized additive models in studies of species distribution: setting the scene. Ecological Modelling **157**: 89-100.

Haedrich, R. L., Rowe, G. T. and Polloni, P. T. (1975). Zonation and faunal composition of epibenthic populations on the continental slope south of New England. Journal of Marine Research **33**: 191-212.

Halfar, J. and Fujita, R. M. (2007). Dangers of deep-sea mining. Science **316**: 987.

Hansen, B. and Østerhus, S. (2000). North Atlantic-Nordic Seas exchanges. Progress in Oceanography **45**(2): 109-208.

Harris, P. T. (2007). Applications of geophysical information to the design of a representative system of marine protected areas in Southeastern Australia, in Todd, B. J. and Greene, H. G., eds. Mapping the seafloor for habitat characterization: Geological Association of Canada, Special Paper 47, 463-482.

Harris, P. T. and Whiteway, T. (2009). High sea marine protected areas: Benthic environmental conservation priorities from a GIS analysis of global ocean biophysical data. Ocean and Coastal Management **52**: 22-38.

Harrold, C., Light, K. and Lisin, S. (1998). Organic enrichment of submarine-canyon and continental-shelf benthic communities by macroalgal drift imported from nearshore kelp forests. Limnology and Oceanography **43**(4): 669-678.

Hastie, T. J. and Tibshirani, R. J. (1986). Generalized Additive Models. Statistical Science **1**: 297-318.

Hayek. L. C. and Buzas. (1997). Surveying natural populations. Columbia University Press. New York.

Headrich, R. L., Rowe, G. T. and Polloni, P. T. (1975). Zonation and faunal composition of epibenthic populations on the continental slope of New England. Journal of Marine Research **33**: 191-212.

He, T., Spence, G. D., Riedel, M., Hyndman, R. D. And Chapman, N. R. (2007). Fluid flow and origin of a carbonate mound offshore Vancouver Island: Seismic and heat flow constraints. Marine Geology **239**: 83-98.

Heap, A. D. and Harris, P. T. (2008). Geomorphology of the Australian margin and adjacent. Australian Journal of Earth Sciences **55**: 555-585.

Hecker, B., Logan, D. T., Gandarillas, F. E. and Gibson, P. R. (1988). Canyon and slope processes study, III. Biological processes, Lamont-Doherty Geological Observatory, Columbia Universiy, New York. **III:** 1-134.

Heezen, B. C., Ewing, M. and Menzies, R. J. (1955). The influence of Submarine Turbidity Currents on Abyssal Productivity. Oikos **6**(170-182).

Heifetz, J., Wing, B. L., Stone, R. P., Malecha, P. W. and Courtney, D. L. (2005). Corals of the Aleutian Islands. Fisheries Oceanography **14**: 131-138.

Hellmann, J. J. and Fowler, G. W. (1999). Bias, precision, and accuracy of four measures of species richness. Ecological Applications **9**(3): 824-834.

Henry, L. A. and Roberts, J. M. (2007). Biodiversity and ecological composition of macrobenthos on cold-water coral mounds and adjacent off-mound habitat in the bathyal Porcupine Seabight, NE Atlantic. Deep-Sea Research II **54**(4): 654-672.

Hewitt, J. E., Thrush, S. F., Legendre, P., Funnell, G. A., Ellis, J. and Morrison, M. (2004). Mapping of marine soft-sediment communities: integration sampling for ecological interpretation. Ecological Applications **14**(4): 1203-1216.

Hickey, B. M. (1995). Coastal submarine canyons. In: Muller, P. and D. Henderson (eds), Proceedings of the University of Hawaii 'Aha Huliko'a Workshop on Flow Topography Interactions, Honolulu, Hawaii, SOEST Special Publication**:** 265p.

Hiscock, K. (ed.) (1996). Marine Nature Conservation Review: rationale and methods. Peterborough: Joint Nature Conservation Committee. [Coasts and seas of the United Kingdom. MNCR series.].

Hixon, M. A., Tissot, B. N. and Pearcy, W. G. (1991). Fish assemblages of rocky banks of the Pacific Northwest [Heceta, Coquille, and Daisy Banks]. USDI Minerals Management Service, OCS Study MMS 91-0052, Camarillo, CA.

Holmes, K. W., Van Niel, K. P., Radford, B., Kendrick, G. A. and Grove, S. L. (2008). Modelling distribution of marine benthos from hydroacoustics and underwater video. Continental Shelf Research **28**: 1800-1810.

Houston, K. A. and Haedrich, R. L. (1984). Abundance and biomass of macrobenthos in the vicinity of Carson Submarine Canyon, northwest Atlantic Ocean. Marine Biology **82**: 301-305.

Howell, K. L. (2010). A benthic classification system to aid in the implementation of marine protected area networks in the deep/high seas of the NE Atlantic. Biological Conservation **143**: 1041-1056.

Howell, K.L. and Davies, J.S. (2010) Deep-sea species image catalogue. Marine Biology and Ecology Research Centre, Marine Institute at the University of Plymouth. On-line version http://www.marlin.ac.uk/deep-sea-species-image-catalogue/

Howell, K. L., Davies, J. S., Hughes, D. J. and Narayanaswamy, B. E. (2007). Strategic Environmental Assessment/Special Area for Conservation Photographic Analysis Report. Department of Trade and Industry, Strategic Environmental Assessment Report, UK: 163p.

Howell, K. L., Mowles, S. L. and Foggo, A. (2010a). Mounting evidence: near-slope seamounts are faunally indistinct from an adjacent bank. Marine Ecology **31**(Suppl. 1): 1-11.

Howell, K. L., Davies, J. S. and Narayanaswamy, B. E. (2010b). Identifying deep-sea megafaunal epibenthic assemblages for use in habitat mapping and marine protected area network design. Journal of the Marine Biological Association of the United Kingdom **90**(1): 33-68.

Howell, K. L., Holt, R., Pulido Endrino, I. and Stewart, H. (2011). When the species is also a habitat: Comparing the predictively modelled distribution of Lophelia pertusa and the reef habitat it forms. Biological Conservation **144**(11): 2656-2665.

Huang, Z., Brooke, B. P. and Harris, P. T. (2011). A new approach to mapping marine benthic habitats using physical environmental data. Continental Shelf Research **31** (2, Suppl. 1): S4-S16.

Hubbs, C. L. (1959). Initial discoveries of fish fauna on seamounts and offshore banks in the Eastern Pacific. Pacific Science **13**: 311-316.

Hughes, J. A. and Gooday, A. J. (2002). The distribution of the xenophyophore *Syringammina fragilissima* in the northeast Atlantic and its influence on the diversity of bathyal foraminiferal assemblages. Newsletter of Micropalaeontology **66**: 15-16.

Hughes, J. A. and Gooday, A. J. (2004). Associations between living benthic foraminifera and dead tests of Syringammina fragilissima (Xenophyophorea) in the Darwin Mounds region (NE Atlantic). Deep-sea Research Part I **51**: 1741-1758.

ICES (2007). Report of the Working Group on Deep-Water Ecology (WGDEC), 10-14 March 2008. ICES Journal of Marine Science: 1-122.

Inman, D. L., Nordstrom, C. E. and Flick, R. E. (1976). Currents in submarine canyons: an air-sea land interaction. Annual Review of Fluid Mechanics, **8**: 275-310.

Jenness, J. (2010). DEM Surface Tools v. 2.1.254. Jenness Enterprises.

Jensen, A. and Frederiksen, R. (1992). The fauna associated with the bank-forming deepwater coral *Lophelia pertusa* (Scleractinaria) on the Faroe shelf. Sarsia **77**: 53-69.

Johnson, C., Sherwin, T., Smythe-Wright, D., Shimmield, T. and Turrell, W. (2010). Wyville Thomson Ridge Overflow Water: Spatial and temporal distribution in the Rockall Trough. Deep-sea Research I **57**: 1153-1162.

Jones, J. B. (1992). Environmental impact of trawling on the seabed: a review. New Zealand Journal of Marine and Freshwater Research, **26**: 59-67.

Jones, E. J. W., Ramsay, A. T. S., Preston, N. J. and Smith, A. C. S. (1974). Cretaceous guyot in the Rockall Trough. Nature **251**: 129-131.

Jones, E. J. W., Siddall, R., Thirlwall, M. F., Chroston, P. N. and Lloyd, A. J. (1994). Anton Dohrn Seamount and the evolution of the Rockall Trough. Oceanologica Acta **17**: 237-247.

Kelley, D. S., Delaney, J. R. and Yoerger, D. R. (2001). Geology and venting characteristics of the Mothra hydrothermal field, Endeavour segment, Juan de Fuca Ridge Geology **29**: 959-962.

Kenyon, N. H., Akhmetzhanov, A. M., Wheeler, A. J., van Weering, T. C. E., de Haas, H. and Ivanov, M. K. (2003). Giant carbonate mud mounds in the southern Rockall Trough. Marine Geology **195**: 5-30.

Kinzie, R. A. (1973). The zonation of West Indian gorgonians. Bulletin of Marine Science **23**: 93-155.

Kopf, A. J. (2002) Significance of mud volcanism. Review of Geophysics **40** (2): 1005.

Kostylev, V. E., Todd, B. J., Fader, G. B. J., Courtney, R. C., Cameron, G. D. M. and Rickrill, R. A. (2001). Benthic habitat mapping on the Scotian Shelf based on multibeam bathymetry, surficial geology and sea floor photographs. Marine Ecology Progress Series **219**: 121-137.

Kottke, B., Schwenk, T., Breitzke, M., Wiedicke, M., Kudrass, H. R. and Spiess, V. (2003). Acoustic facies and depositional processes in the upper submarine canyon Swatch of No Ground (Bay of Bengal). Deep-Sea Research Part II - Topical Research papers **50**: 979-1001.

Lande, R., DeVries, P. J. And Walla, T. R. (2000). When species accumulation curves intersect: implications for ranking diversity using small samples. Oikos **89**(3): 601-605.

Laubier, I. and Monniot, C. (1985). Les peuplements du golfe de Gascogne, Campagnes BIOGAS. Brest: Ifremer: 630.

Lavaleye, M. S. S., Duineveld, G. C. A., Berghuis, E. M., Kok, A. and Witbaard, R. (2002). A comparison between the megafauna communities on the N.W. Iberian and Celtic continental margins - effects of coastal upwelling? Progress in Oceanography **52**: 459-476.

Le Danois, E. (1948). Les profondeurs de la mer, trente ans de recherches sur la faune sous-marine au large des côtes de France. Payot, Paris: 303.

Lekkerkerk, H., J., van der Velden, R., Roders, J., Haycock, T., de Vries, R., Jansen, P. and Beemster, C. (2006). Handbook of Offshore Surveying. Book Two. (London: Clarkson Research Services Limited) ISBN 1-902157-74-5.

Levin, L. A. (1991). Interactions between metazoans and large, agglutinated protozoans: implications for the community structure of the deep-sea benthos. American Zoologist **31**: 886-900.

Levin, L. A. (1994). Paleoecology and ecology of xenophyophores. Palaios **9**: 32-41.

Levin, L. A., DeMaster, D. J., McCann, L. D. and Thomas, C. L. (1986). Effects of giant protozoans (class: Xenophyophorea) on deep-seamount benthos. Marine Ecology Progress Series **29**: 99-104.

Levin, L. A. and Thomas, C. L. (1988). The ecology of xenophyophores (Protista) on eastern Pacific seamounts. Deep-Sea Research **35**: 2003-2027.

Long, D., Howell, K. L., Davies, J. and Stewart, H. (2010). JNCC Offshore Natura survey of Anton Dohrn Seamount and East Rockall Bank Areas of Search. JNCC Report Series 437.

Lonsdale, P. and Hollister, C. D. (1979). Near-bottom traverse of Rockall Trough - Hydrographic and geologic inferences. Oceanologica Acta **2**(1): 91-105.

López-González, P. J. and Williams, G. C. (2009). A new deep-sea pennatulacean (Anthozoa: Octocorallia: Chunellidae) from the Porcupine Abyssal Plain (NE Atlantic). Helgol Marine Research.

Ludwig, John A. and James F. Reynolds. 1988. Statistical ecology: a primer of methods and computing. Wiley Press, New York, New York. 337 pp.

Lundblad, E. D., Wright, J., Miller, J., Larkin, E. A., Rinehart, R. W., Naar, D. F., Donahue, B. T., Anderson, S. M. and Battista, T. (2006). A Benthic Terrain Classification Scheme for American Samoa. Marine Geodesy **29**(2): 89-111.

MacIsaac, K., Bourbonnais, C., JKenchington, E., Gorden, D. J. and Gass, S. (2001). Observations on the occurrence and habitat preference of corals in Atlantic Canada. In: Willison JHM, Hall J, Gass SE, Kenchington ELR, Butler M, Doherty P (eds). Proceedings of the First International Symposium on Deep-Sea Corals, 30 July–3 August 2000. Ecology Action Center and the Nova Scotia Museum, Halifax: 58-75.

Margaled, R. (1958). Information theory in ecology. General Systems **3**: 36-71.

Masson, D. G., Bett, B. J., Billett, D. S. M., Jacobs, C. L., Wheeler, A. J. and Wynn, R. B. (2003). The origin of deep-water, coral-topped mounds in the northern Rockall Trough, Northeast Atlantic. Marine Geology **194**(3-4): 159-180.

Maurer, D., Robertson, G. and Gerlinger, T. (1994). Comparison of Community Structure of Soft-Bottom Macrobenthos of the Newport Submarine Canyon, California and the Adjoining Shelf. Internationale Revue der gesamten Hydrobiologie und Hydrographie **79**(4): 591-603.

McClain, C. R. (2007). Seamounts: identity crisis or split personality? Journal of Biogeography **34**(12): 2001-2008.

McRea, J. J. E., Greene, H. G., O'Connell, V. M. and Wakefield, W. W. (1999). Mapping marine habitats with high resolution sidescan sonar. Oceanologica Acta **22**: 679-686.

Meredith, M. P., Watkins, J. L., Murphy, E. J., Cunningham, N. J., Wood, A. G., Korb, R., Whitehouse, M. J. And Thorpe, S. E. (2003). An anticyclonic circulation above the Northwest Georgia Rise, Southern Ocean. Geophysical Research Letters **30** (20): 2061.

Miensis, F., de Stigter, H. C., White, M., Duineveld, G., de Haas, H. and Van Weering, T. C. E. (2007). Hydrodynamic controls on cold-water coral growth and carbonate-mound development at the SW and SE Rockall Trough Margin, NE Atlantic Ocean. Deep-sea Research I **54**: 1655-1674.

Mohn, C. and Beckmann, A. (2002). Numerical studies on flow amplification at an isolated shelfbreak bank, with application to Porcupine Bank. Continental Shelf Research **22**(9): 1325-1338.

Monaco, A., Biscaye, P. E., Soyer, J., Pocklington, R. and Heussner, S. (1990). Particle fluxes and ecosystem responses on a continental margin: the 1985-1988 Mediterranean ECOMARGE experiment. Continental Shelf Research **10**: 809-839.

Moore, J. A., Auster, P. J., Calini, D., Heinonen, K., Barber, K. and Hecker, B. (2008). False Boarfish *Neocyttus helgae* in the Western North Atlantic. Bulletin of the Peabody Museum of Natural History **49**(1): 31-41.

Morato, T., Varkey, D. A., Damaso, C., Machete, M., Santos, M., Prieto, R., Santos, R. S. and Pitcher, T. J. (2008). Evidence of a seamount effect on aggregating visitors. Marine Ecology-Progress Series **357**: 23-32.

Mortensen, P. B., Hovland, M., Brattegard, T. and Farestveit, R. (1995). Deep water bioherms of the scleractinian coral *Lophelia pertusa* (L.) at 64^{o} N on the Norwegian shelf: structure and associated megafauna. Sarsia **80**: 145-158.

Mortensen, P. B. and Buhl-Mortensen, L. (2005). Deep-water corals and their habitats in the Gully, a submarine canyon off Atlantic Canada. Cold-water Corals and Ecosystems. A. R. In: Freiwald, J.M. (Eds.), Springer-Verlag, Berlin.**:** 227-257.

Mortensen, P. B., Buhl-Mortensen, L., Gebruk, A. V. and Krylova, E. M. (2008). Occurrence of deep-water corals on the Mid-Atlantic Ridge based on MAR-ECO data. Deep-Sea Research Part II - Topical Research papers **55**: 142-152.

Narayanaswamy, B. E., Howell, K. L., Hughes, D. J., Davies, J. S., Roberts, J. M. and Black, K. D. (2006). Strategic Environmental Assessment Area 7 - Photographic Analysis. Department of Trade and Industry, Strategic Environmental Assessment Report, UK: 178p.

NEAFC (2007). North East Atlantic Fisheries Commission (NEAFC; 2007. Recommendation IX: 2007). Recommendation by the North East Atlantic Fisheries Commission at its annual meeting in November 2006 to adopt conservation and management measures by closing certain areas in the Regulatory Area in order to project deep-water corals.

NEAFC (2008). North East Atlantic Fisheries Commission (NEAFC; 2008. Recommendation IX: 2008). Recommendation by the North East Atlantic Fisheries Commission in accordance with article 5 of the convention on future multilateral

cooperation in Northeast Atlantic fisheries at its annual meeting in November 2007 to adopt conservation and management measures by closing certain areas in the regulatory area in order to protect deep-water corals.

NEAFC (2009). Response of the North East Atlantic Fisheries Commission, NEAFC, to the Secretary - General of the UN on actions taken pursuant to paragraphs 83-84 of resolution 61/105, 5pp.

Nelder, J. & Wedderburn, R. W. M. (1972). Deneralized Linear Models. The Journal of the Royal Statistical Society, Series A **135**: 370-384.

Nichol, S. L., Heap, A. D. and Daniell, J. (*in press*). High resolution geomorphic map of a submerged marginal plateau, northern Lord Howe Rise, east Australian margin. Deep Sea Research Part II: Topical Studies in Oceanography.

O'Hara, T. D. (2007). Seamounts: centres of endemism or species richness for ophiuroids? Global Ecology and Biogeography **16**: 720-732.

O'Hara, T. D., Rowden, A. A. and Williams, A. (2008). Cold-water coral habitats on seamounts: do they have a specialist fauna? Diversity and Distribution **14**: 925-934.

Okey, T. O. (1997). Sediment flushing observations, earthquake slumping, and benthic community changes in Monterey Canyon head. Continental Shelf Research **17**(8): 877-897.

Okey, T. O. (2003). Macrobenthic colonist guilds and renegades in Monterey Canyon (USA) drift algae: partitioning multidimensions. Ecological monographs **73**(3): 415-440.

OSPAR, MASH. (07/4). OSPAR Convention for the protection of the marine environment of the North-East Atlantic. Meeting of the Working Group on Marine Protected Areas Species and Habitats (MASH). Brest (France): 5-8 NOVEMBER 2007.

OSPAR (2010a). Background document to carbonate mounds. Biodiversity Series.

OSPAR (2010b). Background Document for Coral Gardens. Biodiversity Series**:** 38p.

OSPAR (Agreement 2008-6). OSPAR Agreement 2008-6 that replaced an earlier version of the list contained in OSPAR Agreement 2004-6 (see also the Summary Record of the 2008 meeting of the OSPAR Commission contained in OSPAR 08/24/1, Para. 7.12).

Parin, N. V., Mironov, A. N., Nesis, K. N., Blaxter, J. H. S., Southward A. J.A., Gebruk V., Southward E. C. and Tyler, P. A. (1997). Biology of the Nazca and Sala y Gòmez Submarine Ridges, an Outpost of the Indo-West Pacific Fauna in the Eastern Pacific Ocean: Composition and Distribution of the Fauna, its Communities and History. Advances in Marine Biology, Academic Press. **Volume 32:** 145-242.

Pfannkuche, O., Bannert, B., Beck, T., Beuck, L., Dullo, W. C., Flögel, S., Freiwald, A., Gass, S., Gektidis, M., Heger, A., Jamieson, A., Kavanagh, F., King, N., Kuhanec, B., Linke, P., Martin, B., Neulinger, S., Noe, S., Queisser, W., Rüggeberg, A., Ruseler, S.,

Schiemer, I., Schmidt, S., Schönfeld, J., Taviani, M., Türk, M., Vertino, A. and Wigham, B. (2004). Geo-Biological Investigations on Azooxanthellate Cold-Water Coral Reefs on the Carbonate Mounds along the Celtic Continental Slope. L. A. t. M. Meteror Cruise No. 61, 2004, Lisbon – Cork.

Pilskaln, C. H., Churchill, J. H. and Mayer, L. M. (1998). Resuspension of sediment by bottom trawling in the Gulf of Maine and potential geochemical consequences. Conservation Biology, **12** (6) 1223-1229.

Post, A. L. (2008). The application of physical surrogates to predict the distribution of marine benthic organisms. Ocean and Coastal Management **51**: 161-179.

Ramirez-Llodra, E., Ballesteros, M., Company, J. B., Dantart, L. and Sardá, F. (2008). Spatio-temporal variations in the diversity, biomass and abundance of bathyal invertebrates in the Catalan Sea (Western Mediterranean). Marine Biology **153**: 297-309.

Ramirez-Llodra, E., Brandt, A., Danovaro, R., De Mol, B., Escobar, E., German, C. R., Levin, L. A., Martinez Arbizu, P., Menot, L., Buhl-Mortensen, P., Narayanaswamy, B. E., Smith, C. R., Tittensor, D. P., Tyler, P. A., Vanreusel, A. and Vecchione, M. (2010). Deep, diverse and definitely different: unique attributes of the world's largest ecosystem. Biogeosciences **7**: 2851-2899.

Regulation (EEC), N. Regulation (EEC) No 2141/70 of the Council of 20 October 1970 laying down a common structural policy for the fishing industry. OJ L236, 27.10.70, p. 1

Rice, A. L., Tyler, P. A. and Paterson, G. J. L. (1992). The pennatulid *Kophobelemnon stelliferum* (Cnidaria: Octocorallia) in the Porcupine Seabight (North-East Atlantic Ocean). Journal of the Marine Biological Association of the United Kingdom **72**: 417-434.

Richardson, P. L. (1980). Mesoscale flow and thermohaline structure around Fieberling seamount. Journal of Geophysical Research **96**: 16653-16672.

Richardson, E. A., M. J. Kaiser, J. G. Hiddink, M. Galanidi and E. J. Donald (2006). Developing Scenarios for a Network of Marine Protected Areas. Report for Defra.

Richer de Forges, B., Koslow, J. A. and Poore, G. C. B. (2000). Diversity and endemism of the benthic seamount fauna in the south-west Pacific. Nature **405**: 944-947.

Roberts, J. M., Brown, C. J., Long, C. R. and Bates, C. R. (2005). Acoustic mapping using a multibeam echosounder reveals cold-water coral reefs and surrounding habitats. Coral reefs **24**: 654-669.

Roberts, J. M., Long, D., Wilson, J. B., Mortensen, P. B. and Gage, J. D. (2003). The cold-water coral *Lophelia pertusa* (Scleractinia) and enigmatic seabed mounds along the north-east Atlantic margin: are they related? Marine Pollution Bulletin **46**(1): 7-20.

Roberts, J. M., Wheeler, A. J. and Freiwald, A. (2006). Reefs of the deep: The biology and geology of cold-water coral ecosystems. Science **312**(5773): 543-547.

Roberts, J. M., Wheeler, A. L., Freiwald, A. and Cairns, A. (2009). Cold-water corals. The biology and Geology of Deep-Sea Coral Habitats. New York.

Robinson, K. A., Ramsay, K., Lindenbaum, C., Frost, N., Moore, J., Wright, A. P. and Petrey, D. (2011). Predicting the distribution of seabed biotopes in the southern Irish Sea. Continental Shelf Research **31** (2): S120-131.

Rogers, A. D. (1994). The Biology of Seamounts. Advances in Marine Biology **30**: 305-340.

Rogers, A. D. (1999). The biology of Lophelia pertusa (Linnaeus 1758) and other deep-water reef forming corals and impacts from human activity. International Review of Hydrobiology **844**: 315-406.

Rogers, C. S. (1990). Responses of coral reefs and reef organisms to sedimentation. Marine Ecology Progress Series **62**: 185-202.

Rooper, C. N. and Zimmermann, M. (2007). A bottom-up methodology for integrating underwater video and acoustic mapping for seafloor substrate classification. Continental Shelf Research **27**: 947-957.

Rowden, A. A., Sclacher, T. A., Williams, A., Clark, M. R., Stewart, R., Althaus, F., Bowden, D. A., Consalvey, M., Robinson, W. and Dowdney, J. (2010). A test of the seamount oasis hypothesis: seamounts support higher epibenthic megafaunal biomass than adjacent slopes. Marine Ecology **31**(Suppl. 1): 1-12.

Rowe, G. T. (1971). Observations on bottom currents and epibenthic populations in Hatteras Submarine Canyon. Deep Sea Research and Oceanographic Abstracts **18**(6): 569-576.

Rowe, G. T., Polloni, P. T. and Haedrich, R. L. (1982). The deep-sea macrobenthos on the continental-margin of the Northwest Atlantic Ocean. Deep-Sea Research Part A - Oceanographic Research Papers **29**(2): 257-278.

Sager, W. W., Lee, C. S., MacDonald, I. R. and Schroeder, W. W. (1999). High-frequency near-bottom acoustic reflection signatures of hydrocarbon seeps on the Northern Gulf of Mexico continental slope. Geo-Marine Letters **18**(4): 267-276.

Samadi, S., Bottan, L., Macpherson, E., Richer De Forges, B. and Boisselier, M. C. (2006). Seamount endemism questioned by the geographical distribution and population genetic structure of marine invertebrates. Marine Biology **149**: 1463-1475.

Sardà, F., Cartes, J. E. and Company, J. B. (1994). Spatio-temporal variation in megabenthos abundance in three different habitats of the Catalan deep-sea (Western Mediterranean). Marine Biology **120**: 211-219.

Schlacher, T. A., Schlacher-Hoenlinger, M. A., Williams, A., Althaus, F., Hooper, J. N. A. and Kloser, R. (2007). Richness and distribution of sponge megabenthos in continental margin canyons off southeastern Australia. Marine Ecology Progress Series **340**: 73-88.

Schlacher, T. A., Williams, A., Althaus, F. and Schlacher-Hoenlinger, M. A. (2010). High-resoution seabed imagery as a tool for biodiversity conservation planning on continental margins. Marine Ecology **31**: 200-221.

Shank, T. M. (2010). Seamounts. Deep-ocean laboratories of faunal connectivity, evolution, and endemism. Oceanography **23**: 108-122.

Shannon, C. E., and W. Weiner. 1963. The Mathematical Theory of Communication. University of Illinois Press, Urbana, Illinois, USA.

Shepard, F. P. (1951). Mass movement in submarine canyon heads. Transactions American Geophysical Union **32**: 405-419.

Shepard, F. P. and Marshall, N. F. (1973). Currents along floors of submarine canyons. American Association of Petroleum Geologists Bulletin **57**(2): 244-264.

Shmueli, G. (2010). The explain or predict? Statistical Science **25**(3): 289-310.

Shumchenia, E. J. and King, J. W. (2010). Comparison of methods for integrating biological and physical data for marine habitat mapping and classification. Continental Shelf Research **30**: 1717-1729.

Siebenaller, J. and Somero, G. N. (1978). Pressure-adaptive differences in lactate dehydrogenases of congeneric fishes living at different depths. Science **21**: 255-257.

Simpson, E. H. (1949). Measurement of Diversity. Nature **163**: 668.

Smith, C. R., De Leo, F. C., Bernardino, A. F., Sweetman, A. K. and Arbizu, P. M. (2008). Abyssal food limitation, ecosystem structure and climate change. Trends in Ecology & Evolution **23**: 518-528.

Smith, C. D. and Pontius, J. S. (2006). Jackknife estimator of species richness with S-PLUS. Journal of Statistical Software **15**(3): 1-12.

Solan, M., Germano, J. D., Rhoads, D. C., Smith, C., Michaud, E., Parry, D., Wenzho¨fer, F., Kennedy, B., Henriques, C., Battle, E., Carey, D., Iocco, L., Valente, R., Watson, J. and Rosenberg, R. (2003). Towards a greater understanding of pattern, scale and process in marine benthic systems: a picture is worth a thousand worms. Journal of Experimental Marine Biology and Ecology **285-286**: 313-338.

SSTI (2000). R. v. Secretary of State for Trade and Industry (SSTI), ex parte Greenpeace (No. 2) [2000] 2 CMLR 94.

Stafford-Smith, M. G. (1993). Sediment-rejection efficiency of 22 species of Australian scleractinian corals. Marine Biology **115**: 229-243.

Stevens, T. and Connolly, R. M. (2004). Testing the utility of abiotic surrogates for marine habitat mapping at scales relevant to management. Biological Conservation **119**: 351-362.

Stewart, H.A. 2011. The sea-bed geology of selected areas of the UK deep-sea. British Geological Survey Open Report. OR/11/050.

Stewart, H. A. and Davies, J. S. (2007). SW Approaches MESH Survey, R/V Celtic Explorer Cruise CE0705, BGS Project 07/06, Operations Report. British Geological Survey Commercial Report **CR/07/123.**

Stewart, H., Davies, J. S., Long, D., Strömberg, H. and Hitchen, K. (2009). JNCC Offshore Natura Survey. Anton Dohrn Seamount and East Rockall Bank Areas of Search. 2009/03-JNCC Cruise Report. Report Number CR/09/113.

Stoddart, D. R. (1969). Ecology and morphology of recent coral reefs. Biological reviews **44**: 433-498.

Stoker, M. S. (2002). British Geological Survey 1:500,000 Solid Geology map series. Central Rockall Basin. Sheet 56-58N, 08-15W.

Szuman, M., Berndt, C., Jacobs, C. and Best, A. (2006). Seabed characterization through a range of high-resolution acoustic systems - a case study offshore Oman. Marine Geophysical Researches **27**(3): 167-180.

Tendal, O. S. (1972). A monograph of the Xenophyophoria (Rhizopodea, Protozoa). Galathea Report **12**: 7-99.

Tews, J., Brose, U., Grimm, V., Tielbörger, K., Wichmann, M. C., Schwager, M. and Jeltsch, F. (2004). Animal species diversity driven by habitat heterogeneity/diversity: the importance of keystone structures. Journal of Biogeography **31**: 79-92.

Thiem, O., Ravagnan, E., Fosså, J. H. and Berntsen, J. (2006). Food supply mechanisms for cold-water corals along a continental shelf edge. Journal of Marine Systems **60**: 207-219.

Thursh, S. F., Hewitt, J. E., Funnell, G. A., Cummings, V. J., Ellis, J. Schultz, D., Talley, D. And Norkko, A. (2001). Fishing disturbance and marine biodiversity: the role of habitat structure in simple soft-sediment systems. Marine Ecology Progress Series **223**: 277-286.

Todd, B. J., Fader, G. B. J., Courtney, R. C. and Oickrill, R. A. (1999). Quaternary geology and surficial sediment processes, Browns Bank, Scotian Shelf, based on multibeam bathymetry. Marine Geology **162**: 167-216.

Troffe, P. M., Levings, C. D., Piercey, G. E. and Keong, V. (2006). Fishing gear effects and ecology of the sea whip (*Halipteris willemoesi* (Cnidaria: Octocorallia: Pennatulacea)) in British Columbia, Canada: preliminary observations. Aquatic Conservation: Marine and Freshwater Ecosystems **15**: 523-533.

Turner, J. And Klaus, R. (2005). Coral reefs of the Mascarenes, Western Indian Ocean. Philosophical Transactions of the Royal Society A **363**: 229–250.

Tyler, P. A., Amaro, T. and Arzola, R. (2009). Europe's Grand Canyon Nazare Submarine Canyon Oceanography **22**(1): 46-57.

UKBAP UK Biodiversity Action Plan for Mud habitats in deep water. http://www.ukbap.org.uk/UKPlans.aspx?ID=41.

Underwood, A. J**.** and M. G. Chapman (2005). Design and analysis in benthic surveys. *Methods for the study of marine benthos*. A. Eleftheriou and A. D. McIntyre. Oxford, Blackwell Science: 1-42.

UNGA (2006). Resolution 61/105 Sustainable fisheries, including through the 1995 Agreement for the Implementation of the Provisions of the United Nations Convention on the Law of the Sea of 10 December 1982 relating to the Conservation and Management of Straddling Fish Stocks and Highly Migratory Fish Stocks, and related instruments. UNGA A/RES/61/105.

van Aken, H. M. (2000). The hydrography of the mid-latitude northeast Atlantic Ocean I: The deep water masses. Deep-Sea Research Part I - Oceanographic Research Papers **47**(5): 757-788.

Van Weering, Tj. C. E., Dullo, C. And Henriet, J. P. (2003) An introduction to geosphere – biosphere coupling; cold seep related carbonate and mound formation and ecology. Marine Geology **198**: 1-3.

Veale, L. O., Hill, A. S., Hawkins, S. J. and Brand, A. R. (2000). Effects of long-term physical disturbance by commercial scallop fishing on sub-tidal epifaunal assemblages and habitats. Marine Biology **137**: 325-337.

Vetter, E. W. (1994). Hotspots of benthic production. Nature **372**: 47.

Vetter, E. W. and Dayton, P. K. (1998). Macrofaunal communities within and adjacent to a detritus-rich submarine canyon system. Deep-Sea Research II **45**.

Vetter, E. W. and Dayton, P. K. (1999). Organic enrichment by macrophyte detritus, and abundance patterns of megafaunal populations in submarine canyons. Marine Ecology Progress Series **186**: 137-148.

Vetter, E. W., Smith, C. R. and De Leo, F. C. (2010). Hawaiian hotspots: enhanced megafaunal abundance and diversity in submarine canyons on the oceanic islands of Hawaii. Marine Ecology **31**: 183-199.

Wentworth, C. K. (1922). A scale of grade and class terms for clastic sediment. Journal of Geology **30**: 377-392.

Wheeler, A. J., Beyer, A., Freiwald, A., de Haas, H., Huvenne, V. A. I., Kozachenko, M., Olu-Le Roy, K. and Opderbecke, J. (2007). Morphology and environment of cold-water coral carbonate mounds on the NW European margin. International Journal of Earth Sciences **96**(1): 37-56.

Whittingham, M. J., Stephens, P. A., Bradbury, R. B. and Freckleton, R. P. (2006). Why do we still use stepwise modelling in ecology and behaviour? *Journal of Animal Ecology* **75**: 1182-1189.

Wienberg, C., Beuck, L., Heidkamp, S., Hebbeln, D., Freiwald, A., Pfannkuche, O. and Monteys, X. (2008). Franken Mound: facies and biocoenoses on a newly-discovered "carbonate mound" on the western Rockall Bank, NE Atlantic. Facies **54**: 1-24.

Williams, V. L., Witkowski, E. T. F. and Balkwill, K. (2005). Application of diversity indices to appraise plant availability in the traditional medicinal markets of Johannesburg, South Africa. Biodiversity and Conservation **14**: 2971-3001.

Williams, A., Althaus, F., Barker, B., Kloser, R. J. and Keith, G. (2007). Using data from the Zeehan candidate MPA to provide an inventory of benthic habitats and biodiversity, and evaluate prospective indicators for monitoring and performance assessment. Final Report to the Department of Environment and Water Resources: 187pp.

Williams, A., Bax, N. J., Kloser, R. J., Althaus, F., Barker, B. and Keith, G. (2009). Australia's deep-water reserve network: implications of false homogeneity for classifying abiotic surrogates of biodiversity. ICES Journal of Marine Science **66**: 214-224.

Wilson, J. B. (1979). Patch development of the deep-water coral *Lophelia pertusa* (L.) on Rockall Bank. Journal of the Marine Biological Association of the United Kingdom **59**: 165-177.

Wilson, W.H., 1991. Competition and predation in marine soft sediment communities. Annual Review of Ecology and Systematics **21**: 221–241.

Wilson, M. F. J., O'Connell, B., Brown, C., Guinan, J. C. and Grehan, A. J. (2007). Multiscale terrain analysis of multibeam bathymetry data for habitat mapping on the Continental Slope. Marine Geodesy **30**(1): 3-35.

Wright, D. J., Lundblad, E. R., Larkin, E. M., Rinehart, R. W., Murphy, J., Cary-Kothera, L. and Draganov, K. (2005). ArcGIS Benthic Terrain Modeler. Corvallis, Oregon, Oregon State University, Davey Jones Locker Seafloor Mapping/Marine GIS Laboratory and NOAA Coastal Services Center.

Yee, T. W and Mitchell, N. D. (1991) Generalized additive models in plant ecology. Journal of Vegetation Science **2**: 587-602.

Yoklavich, M. M., Greene, H. G., Cailliet, G. M. and Sullivan, D. E. (2000). Habitat associations of deep-water rockfishes in a submarine canyon: an example of a natural refuge. Fisheries Bulletin **98**: 625-641.

Zibrowius, H. (1980). Les Scléractiniaires de la Méditerranée et de l'Atlantique nord-orienta. Mémoires de l'Institut Océanographique, Monaco **11**: 1-284.

A3.1 SIMPER results from multivariate cluster analysis of quantitative data from Anton Dohrn Seamount

Characterising species for each assemblage as identified by the SIMPER routine are indicated in bold.

Group a
Less than 2 samples in group

Group b
Less than 2 samples in group

Group c
Less than 2 samples in group

Group d
Less than 2 samples in group

Group e
Less than 2 samples in group

Group f
Average similarity: 21.68

Species	Av.Abund	Av.Sim	Sim/SD	Contrib%	Cum.%
Ophiomusium lymani	**0.06**	**11.56**	**0.94**	**53.33**	**53.33**
Unknown sp. 29	**0.04**	**4.33**	**0.43**	**19.99**	**73.32**
Crinoidea sp. 7	**0.03**	**3.15**	**0.41**	**14.52**	**87.84**
Halcampoididae sp. 3	0.01	0.72	0.22	3.34	91.18
Caryophyllia sp. 3	0.01	0.46	0.23	2.13	93.31
Ophiuroidea sp. 2	0.01	0.32	0.16	1.50	94.80
Pandalus borealis	0.01	0.22	0.16	1.01	95.82

Holothuroidea sp. 4	0.01	0.14	0.09	0.63	96.44
Syringammina fragillissima	0.01	0.12	0.09	0.55	97.00
Porifera encrusting sp. 40	0.00	0.12	0.16	0.53	97.53
Porifera boring sp. 1	0.01	0.11	0.09	0.53	98.06
Ophiuroidea sp. 8	0.01	0.10	0.09	0.47	98.52
Actiniaria sp. 16	0.00	0.10	0.09	0.45	98.97
Ophiuroidea sp. 1	0.01	0.09	0.09	0.41	99.39
Caryophyllia sp. 2	0.00	0.07	0.09	0.34	99.73
Porifera encrusting sp. 28	0.00	0.06	0.09	0.27	100.00

Group g
Average similarity: 19.54

Species	Av.Abund	Av.Sim	Sim/SD	Contrib%	Cum.%
Lophelia pertusa	**0.03**	**7.27**	**0.46**	**37.21**	**37.21**
***Caryophyllia* sp. 2**	**0.03**	**3.56**	**0.58**	**18.21**	**55.41**
***Keratoisis* sp. 2**	**0.02**	**2.45**	**0.42**	**12.52**	**67.93**
Porifera encrusting sp. 28	**0.04**	**2.20**	**0.33**	**11.28**	**79.21**
***Lepidisis* sp.**	**0.02**	**1.27**	**0.34**	**6.51**	**85.72**
Actiniaria sp.	0.01	0.77	0.23	3.94	89.66
Porifera encrusting sp. 6	0.01	0.48	0.24	2.44	92.10
Bathypathes patula	0.01	0.47	0.23	2.41	94.51
Leiopathes sp. 1	0.01	0.38	0.13	1.96	96.48
Porifera massive lobose sp. 18	0.01	0.32	0.13	1.63	98.10
Anthomastus grandiflora	0.01	0.21	0.13	1.08	99.18
Psolus squamatus	0.01	0.16	0.13	0.82	100.00

Group h
Less than 2 samples in group

Group i
Average similarity: 20.38

Species	Av.Abund	Av.Sim	Sim/SD	Contrib%	Cum.%

Porifera encrusting sp. 1	**0.08**	**4.13**	**1.99**	**20.25**	**20.25**
Ophiuroidea sp. 2	**0.12**	**3.93**	**0.58**	**19.26**	**39.51**
Porifera encrusting sp. 26	**0.06**	**3.61**	**3.00**	**17.71**	**57.22**
Halcampoididae sp. 1	**0.08**	**2.78**	**0.58**	**13.62**	**70.84**
Porifera massive globose sp. 12	**0.08**	**2.53**	**0.58**	**12.42**	**83.26**
Porifera encrusting sp. 40	**0.03**	**1.53**	**5.34**	**7.50**	**90.76**
Porifera encrusting sp. 28	0.04	0.77	0.58	3.80	94.56
Porifera encrusting sp. 3	0.02	0.72	0.58	3.54	98.10
Porifera encrusting sp. 10	0.02	0.39	0.58	1.90	100.00

Group j

Average similarity: 24.27

Species	Av.Abund	Av.Sim	Sim/SD	Contrib%	Cum.%
Ophiuroidea sp. 8	**0.08**	**5.80**	**0.74**	**23.90**	**23.90**
Caryophyllia sp. 2	**0.05**	**3.87**	**0.70**	**15.94**	**39.83**
Cnidaria sp. 1	**0.07**	**3.79**	**0.44**	**15.61**	**55.44**
Ophiuroidea sp. 2	**0.04**	**2.92**	**0.55**	**12.04**	**67.49**
Syringammina fragillissima	**0.04**	**2.49**	**0.56**	**10.24**	**77.73**
Ophiactis balli	**0.03**	**1.21**	**0.26**	**5.01**	**82.73**
Ophiactis abyssicola	0.03	0.93	0.30	3.81	86.55
Porifera encrusting sp. 22	0.02	0.57	0.24	2.35	88.89
Pandalus borealis	0.01	0.52	0.27	2.13	91.03
Porifera encrusting sp. 1	0.01	0.29	0.25	1.18	92.20
Cerianthidae sp. 1	0.01	0.27	0.21	1.11	93.31
Porifera encrusting sp. 28	0.01	0.22	0.19	0.90	94.21
Ophiomusium lymani	0.01	0.18	0.14	0.74	94.96
Ascidiacea sp. 2	0.01	0.16	0.14	0.65	95.61
Actiniaria sp. 20	0.01	0.15	0.14	0.63	96.24
Echinus acutus	0.01	0.15	0.14	0.60	96.84
Pennatula phosphorea	0.01	0.13	0.11	0.52	97.36
Crinoidea sp. 1	0.01	0.09	0.11	0.38	97.74
Porifera encrusting sp. 6	0.00	0.07	0.17	0.30	98.04
Psolus squamatus	0.01	0.06	0.11	0.27	98.31
Porifera encrusting sp. 10	0.00	0.06	0.16	0.26	98.57
Porifera encrusting sp. 25	0.00	0.05	0.13	0.20	98.77

Lophelia pertusa (dead structure)	0.01	0.04	0.08	0.18	98.95
Stichopathes cf. gravieri	0.01	0.04	0.08	0.18	99.13
Ophiuroidea sp. 1	0.00	0.03	0.08	0.13	99.26
Porifera massive lobose sp. 12	0.00	0.02	0.08	0.09	99.36
Holothuroidea sp. 4	0.00	0.02	0.04	0.08	99.44
Paguridae spp.	0.00	0.02	0.04	0.07	99.50
Porifera massive globose sp. 11	0.00	0.01	0.04	0.06	99.56
Pentametrocrinus atlanticus	0.00	0.01	0.04	0.06	99.62
Serpulidae sp. 1	0.00	0.01	0.04	0.05	99.67
Actiniaria sp. 9	0.00	0.01	0.04	0.05	99.72
Actiniaria sp.	0.00	0.01	0.04	0.04	99.76
Crinoidea sp. 8	0.00	0.01	0.04	0.04	99.80
Porifera massive lobose sp. 16	0.00	0.01	0.04	0.04	99.85
Echinus spp.	0.00	0.01	0.04	0.04	99.89
Benthogone sp.	0.00	0.01	0.04	0.04	99.93
Holothuroidea sp. 3	0.00	0.01	0.04	0.04	99.97
Porifera encrusting sp. 20	0.00	0.01	0.04	0.03	100.00

Group k

Average similarity: 22.70

Species	Av.Abund	Av.Sim	Sim/SD	Contrib%	Cum.%
Porifera encrusting sp. 22	**0.06**	**8.79**	**1.39**	**38.74**	**38.74**
Porifera encrusting sp. 1	**0.02**	**2.70**	**0.68**	**11.88**	**50.62**
***Lophelia pertusa* (dead structure)**	**0.04**	**2.25**	**0.50**	**9.91**	**60.54**
Porifera lamellate sp. 7	**0.03**	**1.79**	**0.50**	**7.88**	**68.42**
Crinoidea sp. 8	**0.02**	**1.27**	**0.51**	**5.60**	**74.02**
Porifera encrusting sp. 10	0.01	1.11	0.67	4.90	78.92
Stichopathes cf. *gravieri*	0.01	0.66	0.34	2.90	81.82
Henricia sanguinolenta	0.01	0.60	0.34	2.63	84.45
Porifera encrusting sp. 41	0.01	0.46	0.19	2.02	86.47
Ophiactis abyssicola	0.02	0.44	0.19	1.94	88.41
Caryophyllia sp. 2	0.01	0.40	0.19	1.78	90.19
Porifera encrusting sp. 3	0.00	0.22	0.33	0.98	91.17
Porifera encrusting sp. 2	0.01	0.22	0.19	0.97	92.14
Ceramaster/*Peltaster*/*Plinthaster*	0.01	0.22	0.19	0.95	93.10
Cidaris cidaris	0.01	0.22	0.19	0.95	94.05

Lophelia pertusa	0.01	0.21	0.19	0.91	94.96
Madrepora oculata	0.01	0.19	0.19	0.83	95.78
Porifera massive lobose sp. 12	0.01	0.19	0.19	0.82	96.60
Psolus squamatus	0.01	0.18	0.19	0.78	97.38
Porifera massive lobose sp. 23	0.01	0.16	0.19	0.71	98.09
Stichopathes sp.	0.01	0.15	0.19	0.66	98.75
Porifera encrusting sp. 15	0.01	0.15	0.19	0.64	99.39
Porifera encrusting sp. 6	0.00	0.14	0.34	0.61	100.00

Group l
Average similarity: 39.89

Species	Av.Abund	Av.Sim	Sim/SD	Contrib%	Cum.%
***Lophelia pertusa* (dead structure)**	**0.12**	**27.39**	**3.37**	**68.67**	**68.67**
Lophelia pertusa	**0.04**	**5.35**	**0.82**	**13.40**	**82.07**
Gorgonacea	**0.03**	**2.42**	**0.40**	**6.07**	**88.14**
Anthomastus grandiflora	0.02	1.17	0.39	2.93	91.07
Porifera encrusting sp. 41	0.02	0.56	0.22	1.40	92.46
Gorgonacea sp. 15	0.01	0.48	0.22	1.22	93.68
Psolus squamatus	0.02	0.47	0.22	1.18	94.86
Porifera encrusting sp. 10	0.01	0.41	0.39	1.04	95.89
Porifera encrusting sp. 42	0.01	0.37	0.22	0.93	96.83
Keratoisis sp. 1	0.01	0.35	0.22	0.89	97.71
Caryophyllia sp. 2	0.01	0.34	0.22	0.86	98.57
Porifera encrusting sp. 6	0.01	0.30	0.22	0.75	99.32
Gorgonacea sp. 6	0.01	0.27	0.22	0.68	100.00

Group m
Less than 2 samples in group

Group n
Average similarity: 44.00

Species	Av.Abund	Av.Sim	Sim/SD	Contrib%	Cum.%

***Lophelia pertusa* (dead structure)**	**0.20**	**16.25**	**#######**	**36.93**	**36.93**
Protanthea simple	**0.16**	**9.16**	**#######**	**20.81**	**57.74**
Madrepora oculata	**0.10**	**8.21**	**#######**	**18.67**	**76.40**
Cerianthidae sp. 1	**0.10**	**3.46**	**#######**	**7.87**	**84.27**
Ophiuroidea sp. 2	**0.06**	**3.46**	**#######**	**7.87**	**92.13**
Serpulidae sp. 1	**0.07**	**3.46**	**#######**	**7.87**	**100.00**

Group o
Less than 2 samples in group

Group p
Less than 2 samples in group

Group q
Average similarity: 61.70

Species	Av.Abund	Av.Sim	Sim/SD	Contrib%	Cum.%
***Lophelia pertusa* (dead structure)**	**0.52**	**29.75**	**5.10**	**48.21**	**48.21**
Lophelia pertusa	**0.13**	**5.89**	**2.23**	**9.54**	**57.75**
Decapoda sp. 5	**0.09**	**5.78**	**7.19**	**9.37**	**67.13**
Madrepora oculata	**0.08**	**5.21**	**4.30**	**8.45**	**75.57**
Cidaris cidaris	**0.07**	**3.68**	**2.92**	**5.97**	**81.54**
Actiniaria sp.	**0.06**	**3.16**	**1.62**	**5.13**	**86.67**
Gorgonacea sp. 14	0.05	2.26	1.09	3.66	90.34
Munida sarsi	0.05	1.96	1.07	3.17	93.51
Leiopathes sp. 1	0.04	1.40	0.75	2.27	95.78
Actiniaria sp. 9	0.03	0.75	0.57	1.21	96.99
Gastropoda sp. 1	0.02	0.35	0.44	0.56	97.55
Porifera encrusting sp. 15	0.01	0.25	0.43	0.41	97.97
Corallimorphidae sp. 2	0.03	0.25	0.27	0.41	98.37
Caryophyllia sp. 2	0.01	0.24	0.30	0.39	98.76
Margarites sp. 1	0.01	0.18	0.30	0.29	99.05
Protanthea simple	0.03	0.16	0.17	0.25	99.30
Halcampoididae sp. 3	0.01	0.11	0.17	0.17	99.48

Stichastrella rosea	0.01	0.08	0.17	0.13	99.60
Ophiactis balli	0.01	0.07	0.17	0.12	99.72
Ascidiacea sp. 2	0.01	0.06	0.17	0.10	99.82
Henricia sanguinolenta	0.01	0.06	0.17	0.10	99.92
Hydrozoa (bushy)	0.01	0.05	0.17	0.08	100.00

Group r

Average similarity: 35.38

Species	Av.Abund	Av.Sim	Sim/SD	Contrib%	Cum.%
Ophiactis abyssicola	**0.34**	**11.45**	**4.40**	**32.36**	**32.36**
***Lophelia pertusa* (dead structure)**	**0.19**	**8.30**	**3.37**	**23.45**	**55.81**
Ophiuroidea sp. 6	**0.14**	**3.96**	**0.90**	**11.20**	**67.01**
Psolus squamatus	**0.07**	**2.34**	**0.85**	**6.62**	**73.63**
Porifera encrusting sp. 42	0.04	1.69	0.89	4.76	78.39
Majidae sp. 1	0.16	1.67	0.41	4.71	83.10
Porifera encrusting sp. 10	0.03	1.56	4.10	4.42	87.52
Ascidiacea sp. 5	0.06	1.50	0.84	4.25	91.77
Halcampoididae sp. 1	0.03	0.78	0.41	2.19	93.96
Zoanthidea sp. 2	0.07	0.66	0.41	1.86	95.83
Porifera massive lobose sp. 20	0.04	0.45	0.41	1.26	97.09
Crinoidea sp. 1	0.05	0.43	0.41	1.21	98.30
Ascidiacea sp. 2	0.05	0.30	0.41	0.85	99.15
Stylaster sp. 1	0.05	0.30	0.41	0.85	100.00

Group s

Average similarity: 40.27

Species	Av.Abund	Av.Sim	Sim/SD	Contrib%	Cum.%
***Lophelia pertusa* (dead structure)**	**0.15**	**16.32**	**3.76**	**40.53**	**40.53**
Porifera encrusting sp. 28	**0.06**	**5.30**	**2.53**	**13.17**	**53.70**
Ophiuroidea sp. 8	**0.06**	**4.30**	**1.06**	**10.68**	**64.38**
Ophiactis balli	**0.07**	**3.95**	**0.74**	**9.81**	**74.19**
Porifera encrusting sp. 6	**0.04**	**2.16**	**1.12**	**5.37**	**79.56**
Porifera encrusting sp. 1	0.03	2.00	0.71	4.97	84.53
Stichopathes cf. gravieri	0.04	1.06	0.47	2.64	87.17
Caryophyllia sp. 2	0.02	0.74	0.47	1.84	89.01

Pandalus borealis	0.03	0.74	0.47	1.84	90.85
Porifera encrusting sp. 40	0.02	0.69	0.43	1.72	92.57
Porifera encrusting sp. 25	0.01	0.50	0.48	1.25	93.82
Porifera encrusting sp. 10	0.01	0.39	0.47	0.97	94.79
Syringammina fragillissima	0.02	0.32	0.26	0.80	95.59
Lophelia pertusa	0.08	0.31	0.26	0.76	96.36
Ophiactis abyssicola	0.02	0.29	0.26	0.71	97.06
Crinoidea sp. 8	0.01	0.28	0.26	0.71	97.77
Porifera encrusting sp. 22	0.01	0.22	0.26	0.54	98.31
Actiniaria sp. 9	0.01	0.20	0.26	0.50	98.81
Ascidiacea sp. 2	0.02	0.20	0.26	0.50	99.31
cf. *Sibopathes*/*Parantipathes*	0.01	0.20	0.26	0.50	99.81
Porifera encrusting sp. 33	0.01	0.08	0.26	0.19	100.00

Group t

Average similarity: 52.75

Species	Av.Abund	Av.Sim	Sim/SD	Contrib%	Cum.%
Ophiactis balli	**0.19**	**11.39**	**6.68**	**21.60**	**21.60**
Ophiactis abyssicola	**0.19**	**9.59**	**3.18**	**18.18**	**39.78**
Ophiuroidea sp. 8	**0.13**	**7.09**	**1.87**	**13.43**	**53.21**
Ophiuroidea sp. 2	**0.16**	**6.62**	**8.53**	**12.55**	**65.76**
Syringammina fragillissima	**0.11**	**6.15**	**8.37**	**11.65**	**77.41**
Cnidaria sp. 1	**0.09**	**4.35**	**8.37**	**8.24**	**85.65**
Psolus squamatus	0.05	2.20	0.58	4.17	89.82
Lophelia pertusa (dead structure)	0.04	1.20	0.58	2.27	92.09
Porifera encrusting sp. 6	0.02	0.96	1.81	1.82	93.91
Caryophyllia sp. 2	0.07	0.88	0.58	1.68	95.59
Pandalus borealis	0.04	0.88	0.58	1.68	97.26
Porifera encrusting sp. 22	0.04	0.68	0.58	1.29	98.55
Porifera encrusting sp. 25	0.02	0.52	0.58	0.99	99.54
Porifera encrusting sp. 10	0.01	0.24	0.58	0.46	100.00

Group u

Average similarity: 51.84

Species	Av.Abund	Av.Sim	Sim/SD	Contrib%	Cum.%
Ophiactis abyssicola	**0.53**	**18.41**	**3.39**	**35.52**	**35.52**
***Lophelia pertusa* (dead structure)**	**0.26**	**8.21**	**3.82**	**15.84**	**51.35**
Ophiuroidea sp. 2	**0.25**	**7.95**	**4.35**	**15.34**	**66.69**
Ophiuroidea sp. 8	**0.16**	**3.16**	**0.95**	**6.10**	**72.80**
Porifera encrusting sp. 28	0.07	2.17	1.46	4.19	76.99
Crinoidea sp. 8	0.10	1.76	0.98	3.39	80.38
Porifera encrusting sp. 39	0.07	1.41	1.40	2.71	83.10
Caryophyllia sp. 2	0.06	1.34	1.09	2.59	85.68
Ascidiacea sp. 1	0.07	1.16	0.62	2.23	87.92
Porifera encrusting sp. 22	0.04	0.80	0.59	1.55	89.46
Porifera massive lobose sp. 18	0.05	0.79	0.57	1.52	90.99
Psolus squamatus	0.04	0.72	0.62	1.38	92.37
Porifera encrusting sp. 1	0.05	0.70	0.55	1.35	93.72
Porifera encrusting sp. 6	0.03	0.60	2.46	1.16	94.88
Porifera encrusting sp. 42	0.03	0.47	0.61	0.91	95.79
Lophelia pertusa	0.04	0.46	0.32	0.88	96.67
Porifera massive lobose sp. 12	0.03	0.40	0.60	0.77	97.44
Porifera encrusting sp. 25	0.03	0.36	0.61	0.70	98.13
Porifera encrusting sp. 10	0.03	0.34	0.50	0.66	98.80
Keratoisis sp. 1	0.02	0.25	0.32	0.49	99.28
Syringammina fragillissima	0.02	0.18	0.32	0.34	99.63
Halcampoididae sp. 1	0.02	0.16	0.32	0.31	99.93
Porifera encrusting sp. 3	0.01	0.03	0.32	0.07	100.00

Group v
Average similarity: 51.77

Species	Av.Abund	Av.Sim	Sim/SD	Contrib%	Cum.%
***Lophelia pertusa* (dead structure)**	**0.23**	**12.91**	**2.44**	**24.94**	**24.94**
Ophiuroidea sp. 2	**0.20**	**9.95**	**1.89**	**19.23**	**44.16**
Ophiuroidea sp. 8	**0.15**	**7.02**	**2.12**	**13.56**	**57.72**
Lophelia pertusa	**0.08**	**3.10**	**1.04**	**5.99**	**63.71**
Crinoidea sp. 1	**0.06**	**2.70**	**1.62**	**5.21**	**68.92**

Caryophyllia sp. 2	**0.06**	**2.70**	**1.24**	**5.21**	**74.12**
Psolus squamatus	0.05	2.35	1.80	4.54	78.66
Ophiactis balli	0.07	2.13	0.63	4.12	82.78
Porifera encrusting sp. 39	0.04	1.58	1.28	3.05	85.82
Porifera encrusting sp. 6	0.03	1.52	2.47	2.93	88.75
Porifera encrusting sp. 10	0.03	0.82	0.68	1.58	90.33
Porifera encrusting sp. 28	0.03	0.74	0.65	1.44	91.77
Ophiactis abyssicola	0.03	0.52	0.42	1.01	92.77
Porifera encrusting sp. 22	0.02	0.48	0.41	0.92	93.70
Ascidiacea sp. 2	0.02	0.45	0.44	0.86	94.56
Porifera encrusting sp. 1	0.02	0.43	0.50	0.83	95.39
Porifera encrusting sp. 42	0.02	0.32	0.31	0.62	96.01
Echinus acutus	0.01	0.29	0.37	0.56	96.57
Stichopathes cf. gravieri	0.01	0.21	0.30	0.41	96.98
Crinoidea sp. 8	0.01	0.15	0.24	0.30	97.28
Actiniaria sp.	0.01	0.15	0.24	0.28	97.56
Koehlermetra porrecta	0.01	0.14	0.25	0.27	97.83
Crinoidea sp. 9	0.01	0.14	0.25	0.27	98.10
Pandalus borealis	0.01	0.14	0.25	0.26	98.36
Keratoisis sp. 1	0.01	0.10	0.19	0.20	98.56
Porifera massive lobose sp. 18	0.01	0.10	0.19	0.19	98.75
Brisingella coronata / *Brisinga endecacnemos*	0.01	0.09	0.19	0.17	98.92
Ceramaster/*Peltaster*/*Plinthaster*	0.01	0.08	0.19	0.15	99.07
Porifera massive lobose sp. 12	0.01	0.07	0.19	0.14	99.20
Pentametrocrinus atlanticus	0.01	0.05	0.13	0.10	99.30
Actiniaria sp. 6	0.01	0.04	0.13	0.08	99.38
Ascidiacea sp. 1	0.01	0.04	0.13	0.08	99.46
Ascidiacea sp. 4	0.01	0.04	0.13	0.07	99.53
Antipatharia sp. 3	0.01	0.03	0.13	0.06	99.60
Porifera encrusting sp. 2	0.01	0.03	0.08	0.06	99.65
Reteporella sp. 2	0.01	0.03	0.08	0.05	99.71
cf. *Sibopathes*/*Parantipathes*	0.01	0.02	0.08	0.04	99.75
Porifera encrusting sp. 25	0.00	0.02	0.13	0.04	99.79
Decapoda sp. 5	0.00	0.02	0.08	0.03	99.82
Ophiuroidea sp. 1	0.00	0.02	0.08	0.03	99.85
Actiniaria sp. 13	0.00	0.01	0.08	0.03	99.88
Porifera massive globose sp. 4	0.00	0.01	0.08	0.03	99.91

Cerianthidae sp. 1	0.00	0.01	0.08	0.02	99.93
Echinus spp.	0.00	0.01	0.08	0.02	99.96
Anthomastus grandiflora	0.00	0.01	0.08	0.02	99.98
Porifera encrusting sp. 3	0.00	0.01	0.13	0.02	100.00

Group w
Average similarity: 50.48

Species	Av.Abund	Av.Sim	Sim/SD	Contrib%	Cum.%
***Lophelia pertusa* (dead structure)**	**0.27**	**12.49**	**2.59**	**24.74**	**24.74**
Ophiuroidea sp. 2	**0.18**	**9.50**	**2.61**	**18.82**	**43.55**
Ophiactis balli	**0.17**	**6.19**	**1.08**	**12.26**	**55.81**
Ophiactis abyssicola	**0.13**	**4.79**	**1.18**	**9.49**	**65.29**
Ophiuroidea sp. 8	**0.12**	**4.49**	**1.16**	**8.90**	**74.19**
Porifera encrusting sp. 39	**0.07**	**2.45**	**1.26**	**5.86**	**80.05**
Porifera encrusting sp. 42	0.04	1.80	1.07	3.57	83.62
Porifera encrusting sp. 6	0.04	1.45	1.30	1.87	85.50
Caryophyllia sp. 2	0.04	1.09	0.68	2.16	87.65
Crinoidea sp. 8	0.05	0.92	0.57	1.83	89.48
Porifera encrusting sp. 28	0.04	0.78	0.54	1.54	91.02
Pandalus borealis	0.02	0.64	0.52	1.27	92.29
Lophelia pertusa	0.03	0.39	0.34	0.78	93.07
Syringammina fragillissima	0.02	0.38	0.35	0.76	93.83
Ascidiacea sp. 1	0.02	0.34	0.34	0.68	94.50
Psolus squamatus	0.03	0.33	0.30	0.66	95.16
Porifera massive lobose sp. 18	0.02	0.30	0.39	0.59	95.76
Porifera encrusting sp. 1	0.01	0.28	0.40	0.56	96.31
Porifera encrusting sp. 10	0.01	0.27	0.51	0.54	96.85
Ascidiacea sp. 2	0.02	0.27	0.30	0.54	97.39
Echinus acutus	0.01	0.19	0.26	0.38	97.77
Porifera encrusting sp. 22	0.01	0.17	0.22	0.33	98.10
Serpulidae sp. 1	0.02	0.16	0.21	0.32	98.42
Porifera encrusting sp. 25	0.01	0.16	0.45	0.32	98.74
Crinoidea sp. 9	0.01	0.14	0.22	0.27	99.01
Ophiuroidea sp. 1	0.01	0.09	0.18	0.17	99.18

Echinus spp.	0.01	0.09	0.18	0.17	99.35
Decapoda sp. 5	0.01	0.07	0.18	0.13	99.48
Pentametrocrinus atlanticus	0.01	0.05	0.14	0.10	99.58
Crinoidea sp. 1	0.01	0.04	0.14	0.09	99.67
Anthomastus grandiflora	0.01	0.02	0.10	0.05	99.72
Actiniaria sp.	0.01	0.02	0.10	0.05	99.76
Halcampoididae sp. 1	0.01	0.02	0.10	0.04	99.81
Porifera encrusting sp. 2	0.01	0.02	0.10	0.04	99.85
Cerianthidae sp. 1	0.01	0.02	0.10	0.04	99.89
Porifera encrusting sp. 3	0.00	0.02	0.14	0.03	99.92
Porifera massive lobose sp. 12	0.00	0.02	0.14	0.03	99.95
Ophiomusium lymani	0.00	0.01	0.06	0.02	99.97
Porifera massive globose sp. 4	0.00	0.01	0.06	0.01	99.99
Koehlermetra porrecta	0.01	0.01	0.06	0.01	100.00

Group x

Average similarity: 46.36

Species	Av.Abund	Av.Sim	Sim/SD	Contrib%	Cum.%
***Lophelia pertusa* (dead structure)**	**0.17**	**12.37**	**3.66**	**26.67**	**26.67**
Ophiactis balli	**0.17**	**11.03**	**3.24**	**23.80**	**50.47**
Ascidiacea sp. 2	**0.10**	**7.15**	**4.96**	**15.42**	**65.89**
Ophiactis abyssicola	**0.11**	**6.13**	**1.12**	**13.21**	**79.11**
Actiniaria sp. 13	0.05	1.48	0.58	3.19	82.30
Porifera encrusting sp. 42	0.03	1.29	0.60	2.78	85.08
Serpulidae sp. 1	0.03	0.78	0.39	1.67	86.75
Syringammina fragillissima	0.03	0.76	0.38	1.64	88.39
Psolus squamatus	0.03	0.75	0.40	1.62	90.01
Ophiuroidea sp. 2	0.03	0.66	0.40	1.41	91.43
Majidae sp. 1	0.04	0.62	0.36	1.35	92.77
Porifera encrusting sp. 6	0.01	0.52	0.91	1.12	93.90
Porifera massive lobose sp. 20	0.02	0.52	0.40	1.11	95.01
Lophelia pertusa	0.03	0.47	0.38	1.01	96.02
Porifera encrusting sp. 1	0.02	0.39	0.38	0.83	96.86
Ascidiacea sp. 5	0.03	0.28	0.22	0.60	97.46
Cerianthidae sp. 1	0.02	0.22	0.22	0.48	97.94

Hydrozoa (bushy)	0.02	0.16	0.22	0.36	98.30
Actiniaria sp. 20	0.01	0.15	0.22	0.33	98.63
Porifera encrusting sp. 10	0.01	0.14	0.40	0.30	98.93
Cidaris cidaris	0.01	0.13	0.22	0.28	99.21
Ophiuroidea sp. 7	0.02	0.13	0.22	0.28	99.50
Ophiuroidea sp. 6	0.03	0.12	0.22	0.26	99.76
Porifera encrusting sp. 28	0.01	0.11	0.22	0.24	100.00

Group y
Average similarity: 45.00

Species	Av.Abund	Av.Sim	Sim/SD	Contrib%	Cum.%
Ophiactis abyssicola	**0.21**	**12.99**	#######	**28.86**	**28.86**
***Lophelia pertusa* (dead structure)**	**0.18**	**9.25**	#######	**20.54**	**49.40**
Ophiactis balli	**0.18**	**5.81**	#######	**12.91**	**62.31**
Ascidiacea sp. 2	**0.04**	**2.60**	#######	**5.77**	**68.08**
Crinoidea sp. 1	**0.09**	**2.60**	#######	**5.77**	**73.86**
Galatheidae sp. 1	**0.04**	**2.60**	#######	**5.77**	**79.63**
Pandalus borealis	**0.04**	**2.60**	#######	**5.77**	**85.40**
***Stichopathes* sp.**	**0.06**	**2.60**	#######	**5.77**	**91.17**
Porifera encrusting sp. 28	0.05	2.51	#######	5.59	96.76
Porifera encrusting sp. 6	0.02	0.89	#######	1.98	98.74
Porifera encrusting sp. 25	0.01	0.57	#######	1.26	100.00

Group z
Average similarity: 53.60

Species	Av.Abund	Av.Sim	Sim/SD	Contrib%	Cum.%
Ophiactis balli	**0.23**	**13.88**	**3.61**	**25.89**	**25.89**
***Lophelia pertusa* (dead structure)**	**0.22**	**13.28**	**3.11**	**24.78**	**50.67**
Lophelia pertusa	**0.09**	**5.46**	**3.20**	**10.18**	**60.85**
Ophiuroidea sp. 2	**0.15**	**5.35**	**1.22**	**9.98**	**70.83**
Gorgonacea sp. 6	**0.04**	**2.60**	**1.98**	**5.85**	**76.68**
Porifera encrusting sp. 42	0.03	1.83	0.89	2.42	79.10
Crinoidea sp. 8	0.04	1.68	0.92	3.13	82.23

Keratoisis sp. 1	0.03	1.54	0.94	2.87	85.10
Porifera encrusting sp. 6	0.02	1.10	1.36	2.05	87.15
Porifera encrusting sp. 39	0.02	0.98	1.33	1.83	88.98
Anthomastus grandiflora	0.02	0.92	0.61	1.72	90.70
Ascidiacea sp. 2	0.03	0.82	0.61	1.53	92.24
Caryophyllia sp. 2	0.02	0.71	0.63	1.33	93.56
Ophiactis abyssicola	0.04	0.71	0.45	1.33	94.89
Decapoda sp. 5	0.02	0.30	0.39	0.57	95.46
Porifera massive lobose sp. 18	0.04	0.22	0.18	0.42	95.88
Brisingella coronata / *Brisinga endecacnemos*	0.01	0.21	0.32	0.39	96.27
Echinus spp.	0.01	0.21	0.33	0.38	96.65
Porifera encrusting sp. 10	0.01	0.20	0.60	0.36	97.01
Ophiuroidea sp. 8	0.01	0.13	0.20	0.24	97.26
Hydrozoa (bushy)	0.01	0.12	0.20	0.22	97.47
Actiniaria sp. 6	0.01	0.11	0.19	0.20	97.68
Porifera encrusting sp. 1	0.01	0.10	0.26	0.19	97.86
Porifera encrusting sp. 28	0.01	0.10	0.20	0.19	98.05
Pycnogonida sp. 2	0.01	0.10	0.20	0.19	98.24
Porifera massive lobose sp. 8	0.01	0.10	0.19	0.18	98.42
Gorgonacea sp. 15	0.01	0.09	0.20	0.18	98.60
Keratoisis sp. 2	0.01	0.09	0.20	0.17	98.77
Porifera encrusting sp. 25	0.00	0.09	0.46	0.16	98.93
Henricia sanguinolenta	0.01	0.08	0.20	0.15	99.08
Psolus squamatus	0.01	0.08	0.20	0.14	99.23
Porifera encrusting sp. 22	0.01	0.08	0.20	0.14	99.37
Koehlermetra porrecta	0.01	0.08	0.20	0.14	99.51
Porifera massive lobose sp. 12	0.01	0.06	0.19	0.10	99.61
Bathypathes patula	0.01	0.04	0.14	0.07	99.68
Ophiuroidea sp. 9	0.01	0.03	0.08	0.06	99.74
Gorgonacea sp. 12	0.00	0.02	0.08	0.03	99.77
Ceramaster/*Peltaster*/*Plinthaster*	0.00	0.02	0.08	0.03	99.80
Stichopathes sp.	0.00	0.02	0.08	0.03	99.83
Ophiuroidea sp. 7	0.00	0.01	0.08	0.03	99.86
Lepidisis sp.	0.00	0.01	0.08	0.03	99.89
Crinoidea sp. 1	0.01	0.01	0.08	0.03	99.91
Actiniaria sp. 13	0.00	0.01	0.08	0.02	99.94
Ascidiacea sp. 1	0.01	0.01	0.08	0.02	99.96

Isididae sp. 1	0.00	0.01	0.08	0.02	99.98
Anthothela grandiflora	0.00	0.01	0.08	0.02	100.00

Group aa
Average similarity: 53.71

Species	Av.Abund	Av.Sim	Sim/SD	Contrib%	Cum.%
Ophiactis balli	**0.43**	**23.90**	**4.09**	**44.49**	**44.49**
***Lophelia pertusa* (dead structure)**	**0.39**	**16.76**	**2.74**	**31.20**	**75.69**
Ophiactis abyssicola	**0.15**	**3.45**	**0.80**	**6.42**	**82.11**
Lophelia pertusa	0.08	2.63	0.93	4.90	87.02
Porifera encrusting sp. 42	0.05	1.96	1.05	3.65	90.66
Ascidiacea sp. 2	0.06	1.70	1.06	3.17	93.83
Porifera massive lobose sp. 12	0.02	0.39	0.44	0.73	94.56
Decapoda sp. 5	0.02	0.31	0.38	0.57	95.13
Caryophyllia sp. 2	0.02	0.27	0.31	0.51	95.64
Keratoisis sp. 1	0.02	0.25	0.32	0.47	96.11
Crinoidea sp. 8	0.02	0.24	0.33	0.46	96.56
Psolus squamatus	0.02	0.22	0.25	0.42	96.98
Porifera encrusting sp. 10	0.01	0.21	0.61	0.38	97.37
Porifera encrusting sp. 15	0.01	0.16	0.32	0.29	97.66
Stichopathes cf. *gravieri*	0.01	0.14	0.22	0.26	97.91
Ophiuroidea sp. 2	0.01	0.13	0.22	0.24	98.15
Porifera encrusting sp. 22	0.01	0.11	0.21	0.20	98.36
Porifera encrusting sp. 6	0.00	0.11	0.43	0.20	98.56
Syringammina fragillissima	0.02	0.11	0.16	0.20	98.75
Cidaris cidaris	0.01	0.08	0.16	0.15	98.90
Porifera encrusting sp. 1	0.01	0.08	0.20	0.15	99.05
Gorgonacea sp. 6	0.01	0.07	0.17	0.13	99.19
Crinoidea sp. 1	0.01	0.06	0.17	0.11	99.30
Porifera massive lobose sp. 18	0.01	0.06	0.22	0.11	99.41
Porifera massive lobose sp. 2	0.01	0.04	0.16	0.08	99.48
Porifera lamellate sp. 7	0.01	0.04	0.12	0.07	99.55
Echinus spp.	0.01	0.03	0.12	0.06	99.62
Actiniaria sp.	0.01	0.03	0.12	0.06	99.68
Porifera encrusting sp. 39	0.00	0.02	0.17	0.05	99.72

Anthothela grandiflora	0.00	0.02	0.16	0.05	99.77
Stichopathes sp.	0.01	0.01	0.07	0.03	99.79
Porifera massive globose sp. 4	0.01	0.01	0.07	0.02	99.82
Gorgonacea sp. 14	0.00	0.01	0.07	0.02	99.84
Munida sarsi	0.00	0.01	0.07	0.02	99.86
Serpulidae sp. 1	0.00	0.01	0.07	0.02	99.88
Margarites sp. 1	0.01	0.01	0.07	0.02	99.90
Ophiuroidea sp. 7	0.00	0.01	0.07	0.02	99.92
Corallimorphidae sp. 2	0.00	0.01	0.07	0.02	99.93
Henricia sanguinolenta	0.01	0.01	0.07	0.02	99.95
Porifera encrusting sp. 28	0.00	0.01	0.07	0.02	99.97
Hydrozoa (bushy)	0.00	0.01	0.07	0.02	99.99
Halcampoididae sp. 1	0.01	0.01	0.07	0.01	100.00

Group ab

Average similarity: 28.91

Species	Av.Abund	Av.Sim	Sim/SD	Contrib%	Cum.%
Porifera encrusting sp. 1	**0.05**	**3.55**	**1.11**	**12.27**	**12.27**
Serpulidae sp. 1	**0.07**	**3.28**	**0.77**	**11.35**	**23.63**
Psolus squamatus	**0.07**	**3.27**	**0.78**	**11.31**	**34.93**
Porifera massive globose sp. 12	**0.07**	**2.99**	**0.56**	**10.34**	**45.28**
Porifera encrusting sp. 28	**0.05**	**2.63**	**1.13**	**9.10**	**54.38**
Ophiuroidea sp. 6	**0.06**	**2.39**	**0.48**	**8.28**	**62.65**
Majidae sp. 1	**0.06**	**2.28**	**0.58**	**7.89**	**70.55**
Ophiactis abyssicola	**0.06**	**1.77**	**0.56**	**6.12**	**76.67**
Syringammina fragillissima	0.04	0.93	0.33	3.21	79.88
Serpulidae sp. 2	0.04	0.76	0.27	2.62	82.50
Porifera massive lobose sp. 20	0.03	0.73	0.49	2.51	85.01
Porifera encrusting sp. 22	0.02	0.63	0.31	2.18	87.19
Ophiuroidea sp. 2	0.03	0.51	0.27	1.75	88.94
Ophiactis balli	0.02	0.38	0.27	1.32	90.26
Porifera encrusting sp. 3	0.01	0.36	0.40	1.26	91.52
Gastropoda sp. 1	0.02	0.29	0.21	1.01	92.53
Porifera encrusting sp. 6	0.01	0.27	0.39	0.94	93.47
Porifera encrusting sp. 25	0.01	0.27	0.39	0.93	94.40
Porifera encrusting sp. 31	0.01	0.26	0.27	0.89	95.29

Reteporella sp. 2	0.02	0.24	0.21	0.83	96.12
Lanice sp. 1	0.02	0.19	0.14	0.65	96.77
Lophelia pertusa (dead structure)	0.02	0.19	0.20	0.64	97.41
Porifera massive globose sp. 4	0.02	0.14	0.19	0.50	97.91
Porifera encrusting sp. 10	0.01	0.10	0.21	0.34	98.25
Colus sp. 2	0.01	0.08	0.09	0.29	98.54
Porifera massive lobose sp. 19	0.01	0.07	0.14	0.25	98.79
Holothuroidea sp. 4	0.01	0.06	0.09	0.21	99.00
Porifera massive globose sp. 7	0.01	0.05	0.09	0.19	99.19
Ophiuroidea sp. 8	0.01	0.05	0.09	0.18	99.38
Porifera massive lobose sp. 12	0.01	0.03	0.14	0.12	99.50
Porifera encrusting sp. 40	0.01	0.03	0.09	0.10	99.59
Ascidiacea sp. 2	0.01	0.03	0.09	0.09	99.68
Porifera encrusting sp. 4	0.01	0.02	0.09	0.08	99.76
Cidaris cidaris	0.01	0.02	0.09	0.07	99.82
Porifera encrusting sp. 20	0.00	0.02	0.09	0.06	99.89
Lophelia pertusa	0.00	0.02	0.09	0.06	99.95
Porifera encrusting sp. 9	0.00	0.01	0.09	0.05	100.00

Group ac
Less than 2 samples in group

Group ad
Average similarity: 34.06

Species	Av.Abund	Av.Sim	Sim/SD	Contrib%	Cum.%
Psolus squamatus	**0.25**	**16.81**	**1.58**	**49.35**	**49.35**
Ophiactis balli	**0.10**	**3.23**	**0.65**	**9.49**	**58.83**
Porifera encrusting sp. 22	**0.06**	**2.77**	**0.99**	**8.12**	**66.95**
Porifera encrusting sp. 28	**0.04**	**1.93**	**0.86**	**5.67**	**72.62**
Porifera encrusting sp. 1	0.03	1.17	0.69	3.43	76.05
Lophelia pertusa (dead structure)	0.04	1.08	0.46	3.17	79.22
Caryophyllia sp. 2	0.03	1.06	0.52	3.10	82.32
Porifera encrusting sp. 41	0.03	0.87	0.41	2.56	84.88

Porifera encrusting sp. 10	0.01	0.68	0.73	2.00	86.89
Ascidiacea sp. 2	0.02	0.48	0.34	1.40	88.29
Ophiuroidea sp. 2	0.03	0.43	0.32	1.25	89.54
Cidaris cidaris	0.02	0.36	0.33	1.06	90.60
Ophiactis abyssicola	0.03	0.36	0.23	1.06	91.66
Syringammina fragillissima	0.01	0.24	0.24	0.71	92.37
Porifera encrusting sp. 4	0.01	0.23	0.29	0.67	93.03
Serpulidae sp. 1	0.01	0.21	0.17	0.63	93.66
Porifera massive lobose sp. 12	0.01	0.20	0.31	0.60	94.26
Porifera lamellate sp. 7	0.01	0.20	0.22	0.60	94.86
Actiniaria sp. 20	0.01	0.18	0.20	0.52	95.38
Munida sarsi	0.01	0.14	0.20	0.40	95.78
Porifera encrusting sp. 25	0.01	0.13	0.23	0.37	96.15
Porifera encrusting sp. 3	0.01	0.11	0.26	0.33	96.48
Cerianthidae sp. 1	0.01	0.10	0.16	0.28	96.76
Porifera encrusting sp. 6	0.01	0.09	0.26	0.26	97.03
Ceramaster/*Peltaster*/*Plinthaster*	0.01	0.08	0.14	0.24	97.27
Porifera encrusting sp. 40	0.00	0.08	0.19	0.24	97.51
Crinoidea sp. 1	0.01	0.07	0.14	0.22	97.73
Lophelia pertusa	0.01	0.07	0.14	0.21	97.94
Actiniaria sp.	0.01	0.05	0.12	0.16	98.10
Galatheidae sp. 1	0.00	0.05	0.11	0.15	98.25
Serpulidae sp. 2	0.01	0.05	0.10	0.13	98.39
Halcampoididae sp. 1	0.01	0.05	0.10	0.13	98.52
Henricia sanguinolenta	0.01	0.04	0.10	0.12	98.64
Pentametrocrinus atlanticus	0.01	0.04	0.11	0.12	98.76
Porifera encrusting sp. 15	0.01	0.03	0.10	0.10	98.86
Stichopathes cf. *gravieri*	0.00	0.03	0.09	0.09	98.95
Stichopathes sp.	0.01	0.03	0.09	0.09	99.04
Porifera massive lobose sp. 20	0.00	0.03	0.09	0.07	99.12
Actiniaria sp. 9	0.00	0.02	0.09	0.07	99.19
Porifera encrusting sp. 2	0.00	0.02	0.07	0.07	99.26
Holothuroidea sp. 3	0.00	0.02	0.07	0.06	99.32
Ascidiacea sp. 1	0.00	0.02	0.07	0.06	99.38
Porifera massive lobose sp. 19	0.01	0.02	0.06	0.06	99.43
Porifera encrusting sp. 16	0.00	0.02	0.06	0.05	99.49
*Stylaste*r sp. 1	0.00	0.02	0.07	0.05	99.53

Halcampoididae sp. 3	0.01	0.02	0.06	0.05	99.58
Majidae sp. 1	0.01	0.01	0.06	0.04	99.63
Porifera branching-erect sp. 2	0.01	0.01	0.07	0.04	99.67
Porifera massive globose sp. 4	0.01	0.01	0.06	0.04	99.71
Margarites sp. 1	0.01	0.01	0.07	0.04	99.75
Porifera encrusting sp. 20	0.00	0.01	0.08	0.03	99.78
Ascidiacea sp. 5	0.00	0.01	0.05	0.02	99.81
Porifera encrusting sp. 8	0.00	0.01	0.09	0.02	99.83
Brachiopoda sp. 1	0.00	0.01	0.05	0.02	99.85
Hydrozoa (bushy)	0.00	0.01	0.05	0.02	99.87
Ophiuroidea sp. 6	0.01	0.00	0.03	0.01	99.88
Porifera encrusting sp. 31	0.00	0.00	0.03	0.01	99.89
Porifera massive globose sp. 12	0.00	0.00	0.03	0.01	99.90
Pandalus borealis	0.00	0.00	0.03	0.01	99.91
Zoanthidea sp. 2	0.00	0.00	0.03	0.01	99.92
Porifera lamellate sp. 8	0.00	0.00	0.03	0.01	99.93
Leiopathes sp. 1	0.00	0.00	0.03	0.01	99.94
cf. *Sibopathes*/*Parantipathes*	0.00	0.00	0.03	0.01	99.94
Porifera encrusting sp. 26	0.00	0.00	0.03	0.01	99.95
Bathypathes patula	0.00	0.00	0.03	0.01	99.96
Porifera massive lobose sp. 13	0.00	0.00	0.03	0.01	99.96
Crinoidea sp. 5	0.00	0.00	0.03	0.01	99.97
Decapoda sp. 5	0.00	0.00	0.03	0.01	99.98
Porifera massive lobose sp. 17	0.00	0.00	0.03	0.01	99.98
Porifera massive lobose sp. 18	0.00	0.00	0.03	0.01	99.99
Madrepora oculata	0.00	0.00	0.03	0.01	99.99
Ophiuroidea sp. 1	0.00	0.00	0.03	0.00	100.00

Group ae
Average similarity: 15.21

Species	Av.Abund	Av.Sim	Sim/SD	Contrib%	Cum.%
Porifera encrusting sp. 1	**0.03**	**6.14**	**0.86**	**43.19**	**43.19**
Syringammina fragillissima	**0.04**	**3.61**	**0.37**	**25.41**	**68.60**
Serpulidae sp. 1	**0.03**	**1.58**	**0.22**	**11.09**	**79.69**

Ophiuroidea sp. 1	**0.02**	**1.16**	**0.22**	**8.19**	**87.88**
Actiniaria sp. 9	0.01	0.38	0.11	2.68	90.56
Porifera branching-erect sp. 2	0.02	0.29	0.11	2.03	92.58
Porifera encrusting sp. 28	0.01	0.28	0.18	1.94	94.52
Lanice sp. 1	0.01	0.13	0.08	0.95	95.47
Porifera encrusting sp. 3	0.00	0.11	0.13	0.75	96.22
Cerianthidae sp. 1	0.00	0.10	0.08	0.70	96.92
Amphiuridae sp. 1	0.01	0.10	0.05	0.68	97.60
Caryophyllia sp. 1	0.01	0.06	0.05	0.39	97.99
Porifera encrusting sp. 31	0.00	0.05	0.05	0.38	98.38
Actiniaria sp. 4	0.00	0.04	0.05	0.28	98.65
Anomiidae sp. 1	0.01	0.04	0.05	0.25	98.91
Ophiuroidea sp. 8	0.00	0.03	0.05	0.23	99.13
Psolus squamatus	0.00	0.03	0.05	0.21	99.34
Serpulidae sp. 2	0.01	0.03	0.05	0.21	99.55
Porifera encrusting sp. 25	0.00	0.03	0.07	0.18	99.74
Halcampoididae sp. 3	0.01	0.02	0.05	0.17	99.90
Porifera massive globose sp. 12	0.00	0.01	0.05	0.10	100.00

A3.2 Data for Species richness (mean) and the Simpson Index from Anton Dohrn Seamount

Species richness (mean)

Biotope	Mean	Std. Deviation	N
aa	14.7143	4.84915	21
ab	13.6471	6.08216	17
ad	14.5192	4.62936	52
ae	4.1333	2.63574	30
f	4.8125	2.45544	16
g	4.9091	2.21154	11
j	8.4375	3.18198	32
q	14.7778	3.80058	9
v	18.6842	3.54421	19
w	17.1200	4.14648	25
z	19.4444	5.58593	18
Total	12.3480	6.58852	250

Table 3.9: Mean species richness and standard deviation of biotope from Anton Dohrn Seamount.

			95% Confidence Interval	
Biotope	Mean	Std. Error	Lower Bound	Upper Bound
aa	14.714	.903	12.935	16.494
ab	13.647	1.004	11.669	15.625
ad	14.519	.574	13.389	15.650
ae	4.133	.756	2.645	5.622
f	4.813	1.035	2.774	6.851
g	4.909	1.248	2.451	7.368
j	8.438	.732	6.996	9.879
q	14.778	1.380	12.060	17.496
v	18.684	.950	16.814	20.555
w	17.120	.828	15.489	18.751
z	19.444	.976	17.523	21.366

Table 3.10: Mean species richness and 95% confidence intervals for biotopes from Anton Dohrn Seamount

Simpson's reciprocal Index

Biotope	Mean	Std. Deviation	N
aa	1.4949	.21547	21
ab	4.1591	1.71136	17
ad	2.7461	.96159	52
ae	1.8940	.94105	30
f	3.0060	2.08673	16
g	2.0494	1.04042	11
j	2.9285	.92923	32
q	3.7437	1.09662	9
v	3.0034	.99138	19
w	2.8686	.99103	25
z	2.3006	.53295	18
Total	2.6798	1.24892	250

Table 3.11: Simpson's reciprocal Index **a**nd standard deviation of biotope from Anton Dohrn Seamount.

			95% Confidence Interval	
Biotope	Mean	Std. Error	Lower Bound	Upper Bound
aa	1.495	.236	1.030	1.960
ab	4.159	.262	3.643	4.676
ad	2.746	.150	2.451	3.041
ae	1.894	.197	1.505	2.283
f	3.006	.270	2.474	3.538
g	2.049	.326	1.407	2.691
j	2.929	.191	2.552	3.305
q	3.744	.360	3.034	4.453
v	3.003	.248	2.515	3.492
w	2.869	.216	2.443	3.294
z	2.301	.255	1.799	2.803

Table 3.12: Simpson's reciprocal Index and 95% confidence intervals for biotopes from Anton Dohrn Seamount

A3.3 Rarefaction curves of biotopes identified from Anton Dohrn Seamount

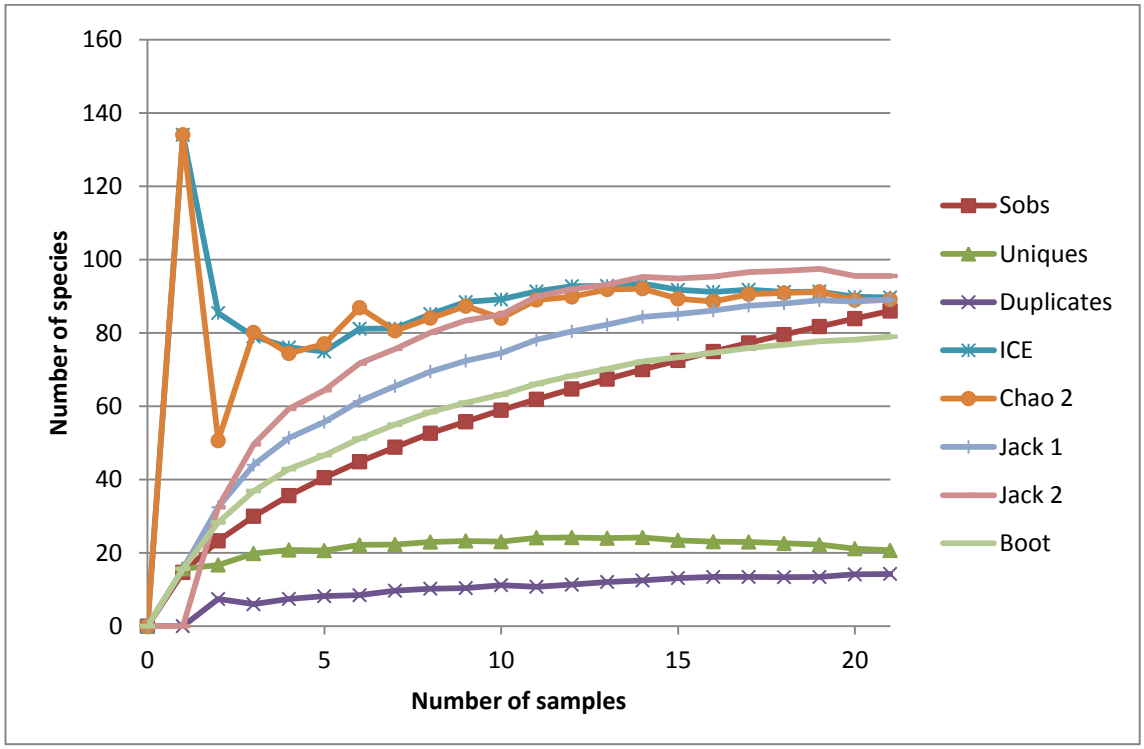

Fig. 3.12: Rarefaction curve for biotope aa. Expected species richness (Sobs) and estimated species richness plotted. Unique and duplicate species plotted at the bottom of the graph.

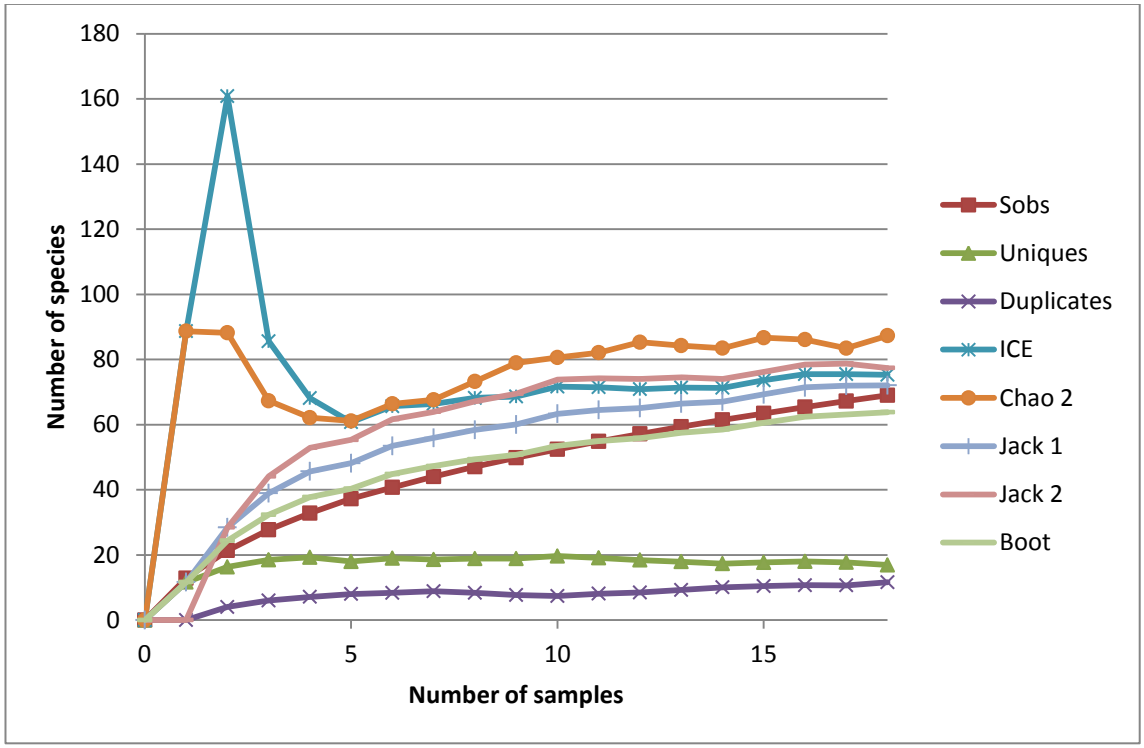

Fig. 3.13: Rarefaction curve for biotope ab. Expected species richness (Sobs) and estimated species richness plotted. Unique and duplicate species plotted at the bottom of the graph.

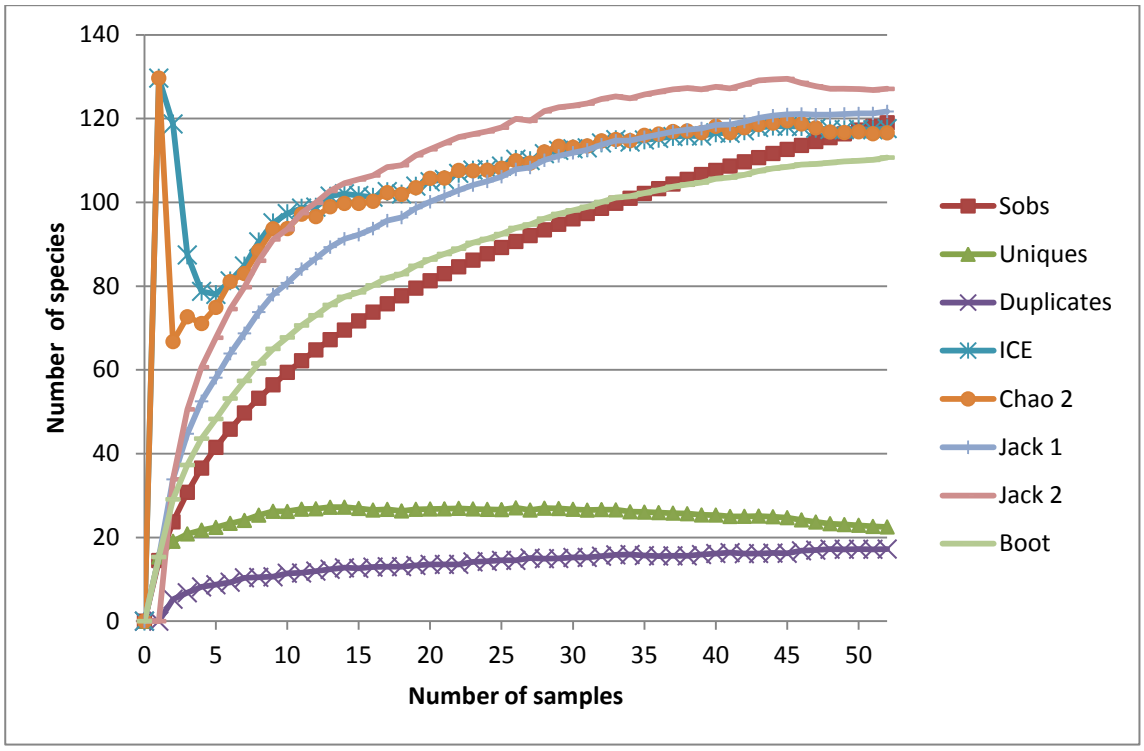

Fig. 3.14: Rarefaction curve for biotope ad. Expected species richness (Sobs) and estimated species richness plotted. Unique and duplicate species plotted at the bottom of the graph.

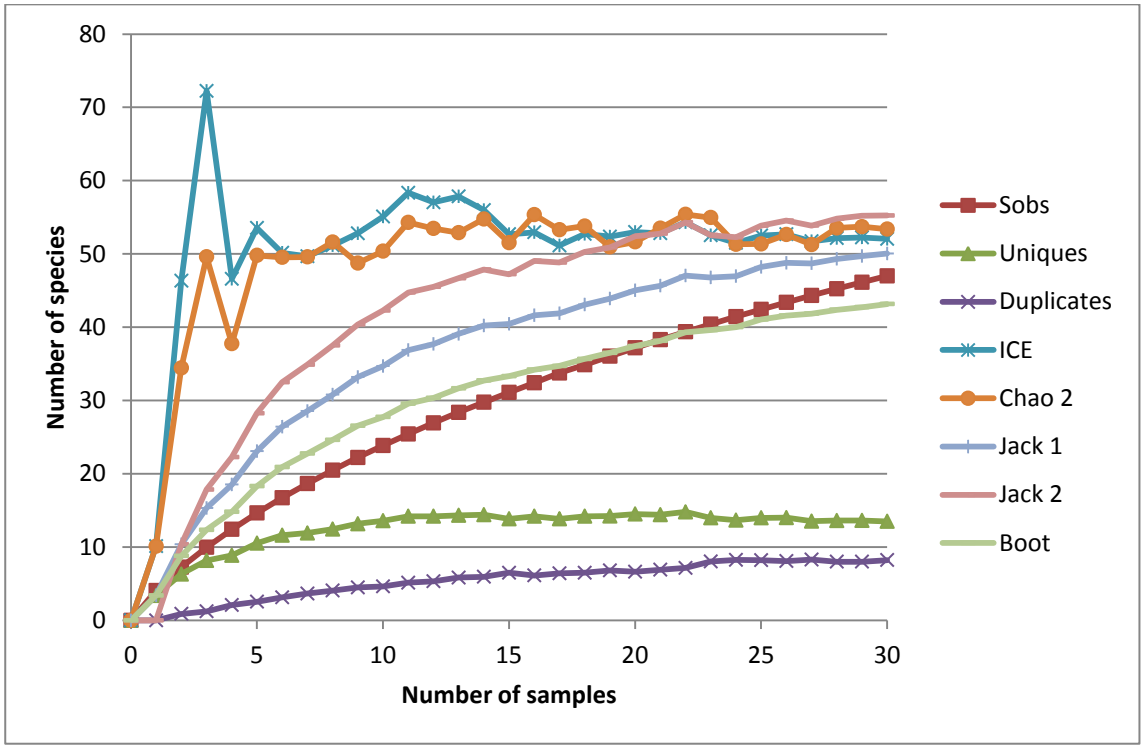

Fig. 3.15: Rarefaction curve for biotope ae. Expected species richness (Sobs) and estimated species richness plotted. Unique and duplicate species plotted at the bottom of the graph.

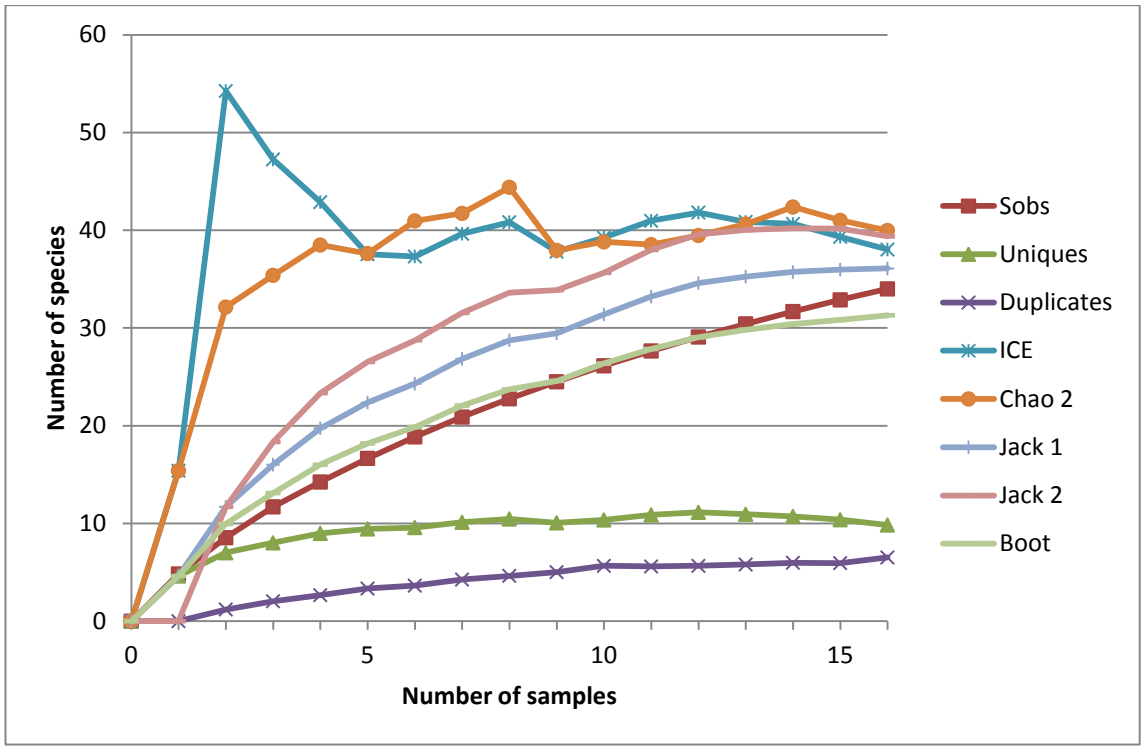

Fig. 3.16: Rarefaction curve for biotope f. Expected species richness (Sobs) and estimated species richness plotted. Unique and duplicate species plotted at the bottom of the graph.

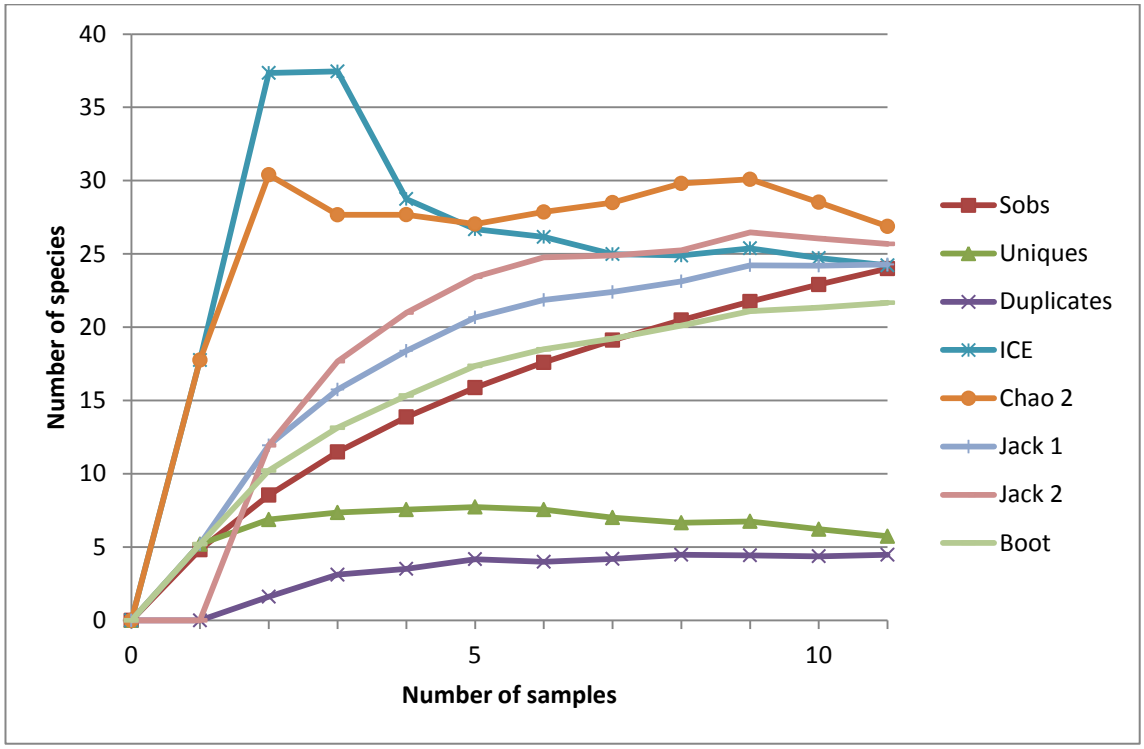

Fig. 3.17: Rarefaction curve for biotope g. Expected species richness (Sobs) and estimated species richness plotted. Unique and duplicate species plotted at the bottom of the graph.

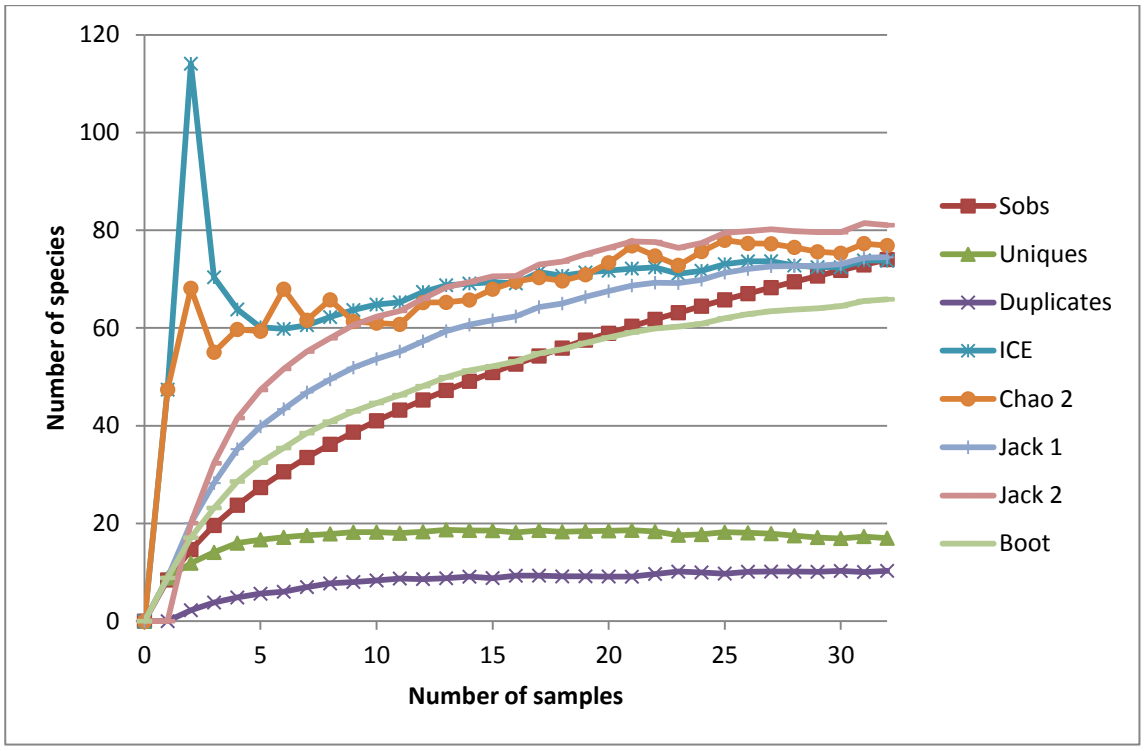

Fig. 3.18: Rarefaction curve for biotope j. Expected species richness (Sobs) and estimated species richness plotted. Unique and duplicate species plotted at the bottom of the graph.

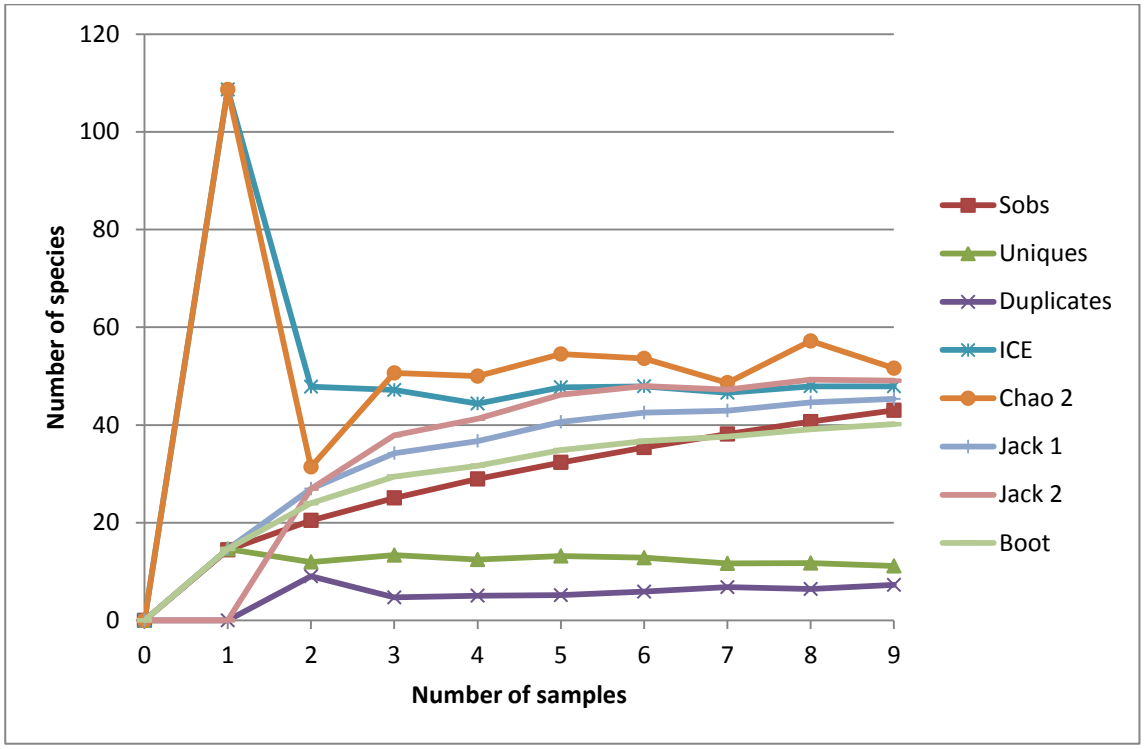

Fig. 3.19: Rarefaction curve for biotope q. Expected species richness (Sobs) and estimated species richness plotted. Unique and duplicate species plotted at the bottom of the graph.

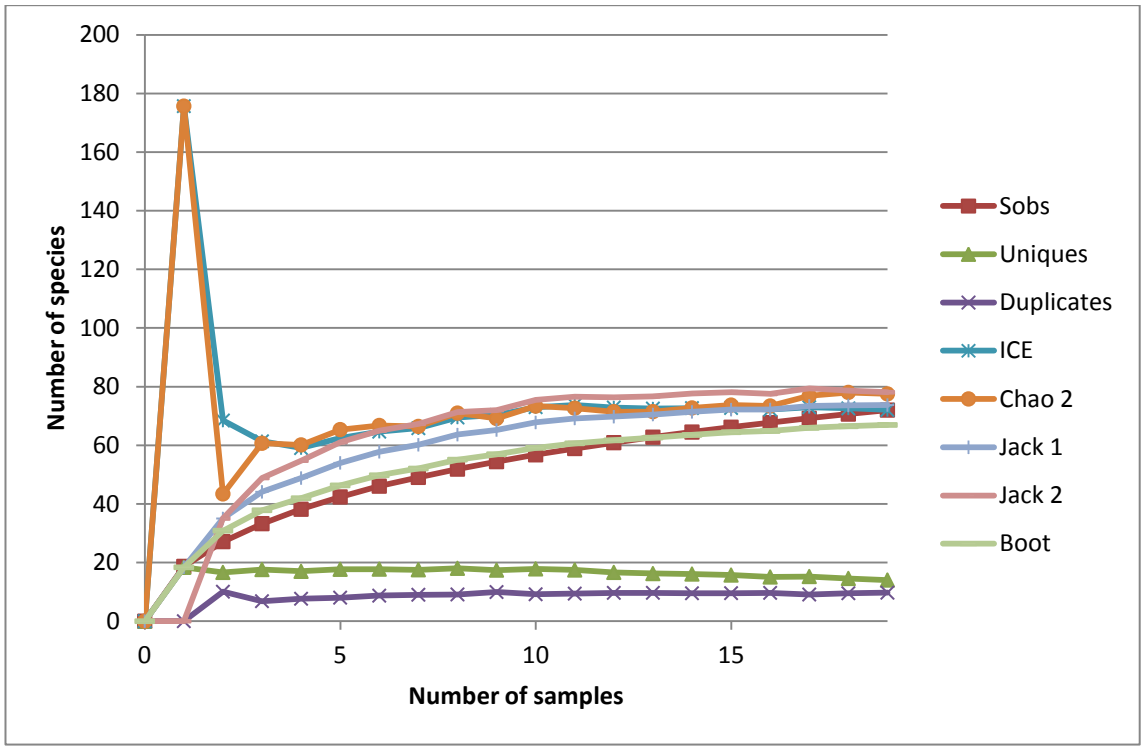

Fig. 3.20: Rarefaction curve for biotope v. Expected species richness (Sobs) and estimated species richness plotted. Unique and duplicate species plotted at the bottom of the graph.

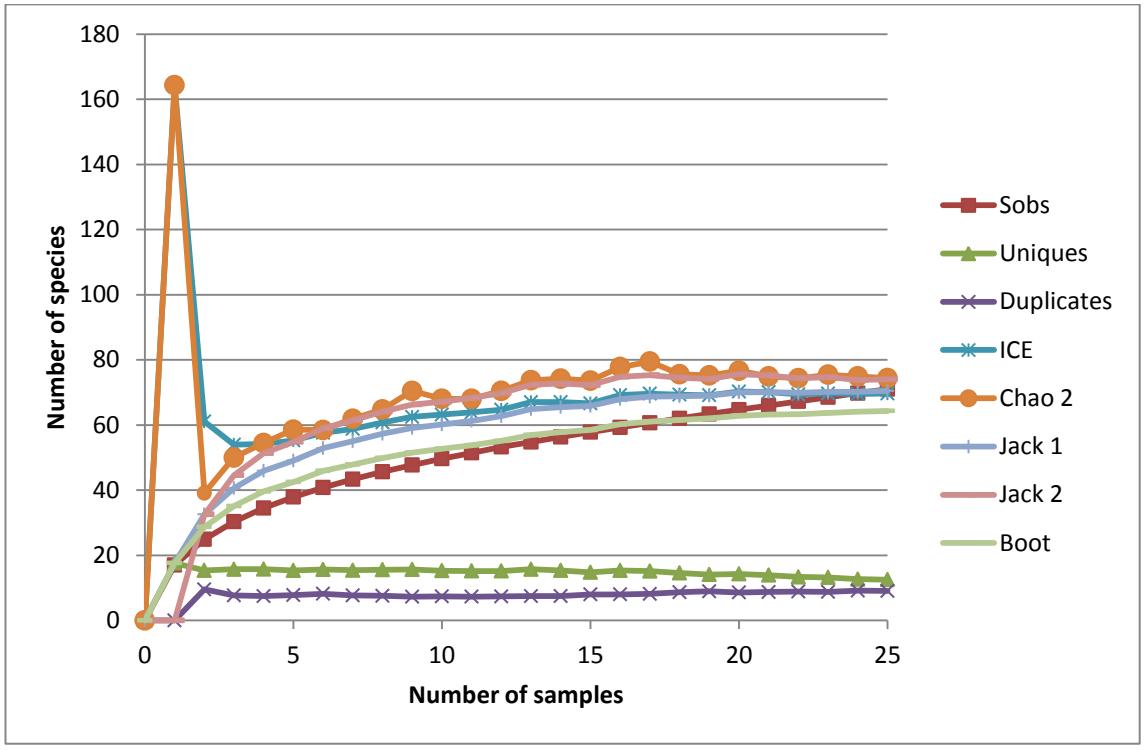

Fig. 3.21: Rarefaction curve for biotope w. Expected species richness (Sobs) and estimated species richness plotted. Unique and duplicate species plotted at the bottom of the graph.

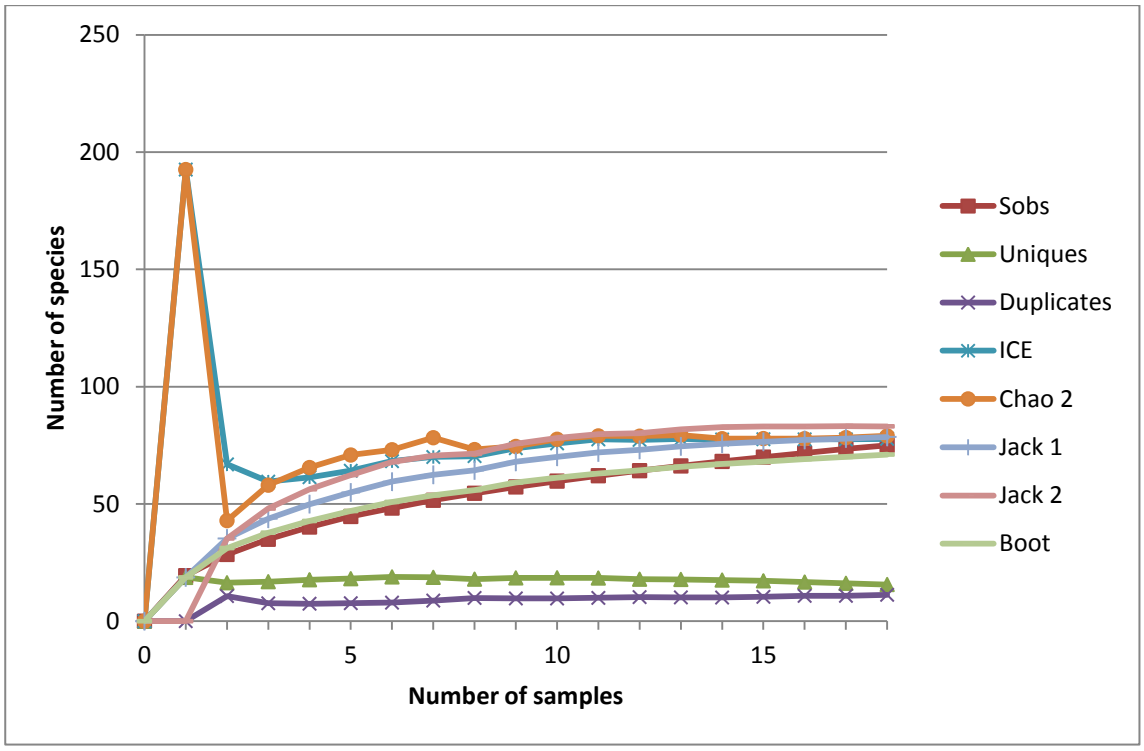

Fig. 3.22: Rarefaction curve for biotope z. Expected species richness (Sobs) and estimated species richness plotted. Unique and duplicate species plotted at the bottom of the graph, and almost cross.

A3.4 Figures of estimated species richness results per biotope

Box and whisker plots (Fig. 3.23- 3.32) showing the variability in species richness calculated by Sobs (interpolated from rarefaction curves) and species richness estimators. Individual figures for each biotope r-aq, estimated number of species on y axis and species richness indices on x. The box represents the standard deviation, with mean represented by the line in the centre of the box, for Sobs and Chao 2 whiskers represent 95% confidence intervals. Note the lower 95% confidence interval for Chao 2 is not represented.

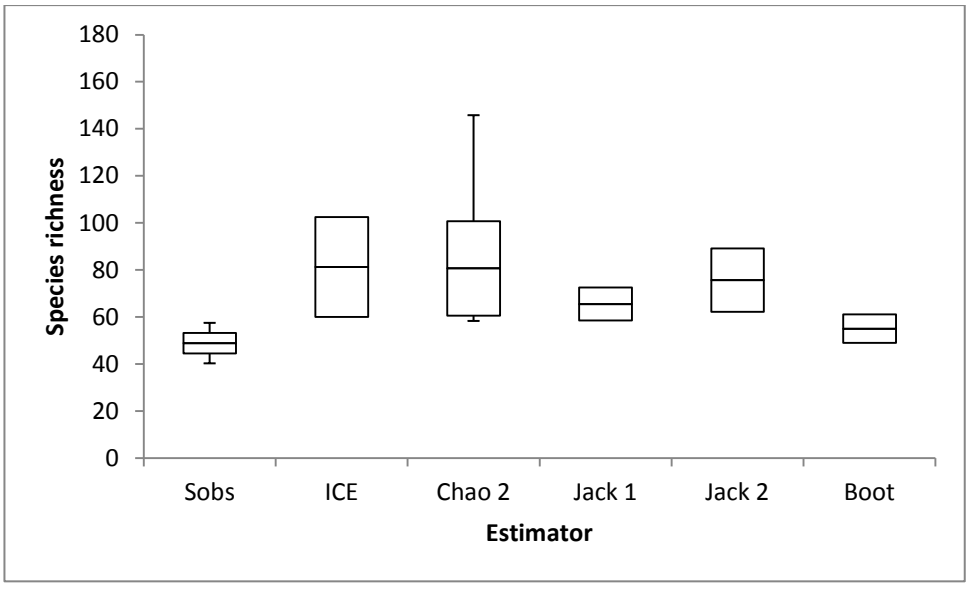

Fig 3.23: Expected and estimated species richness of biotope aa from rarefaction curves and estimators. ICE and Chao2 estimate the highest species richness, although they also have the highest SD.

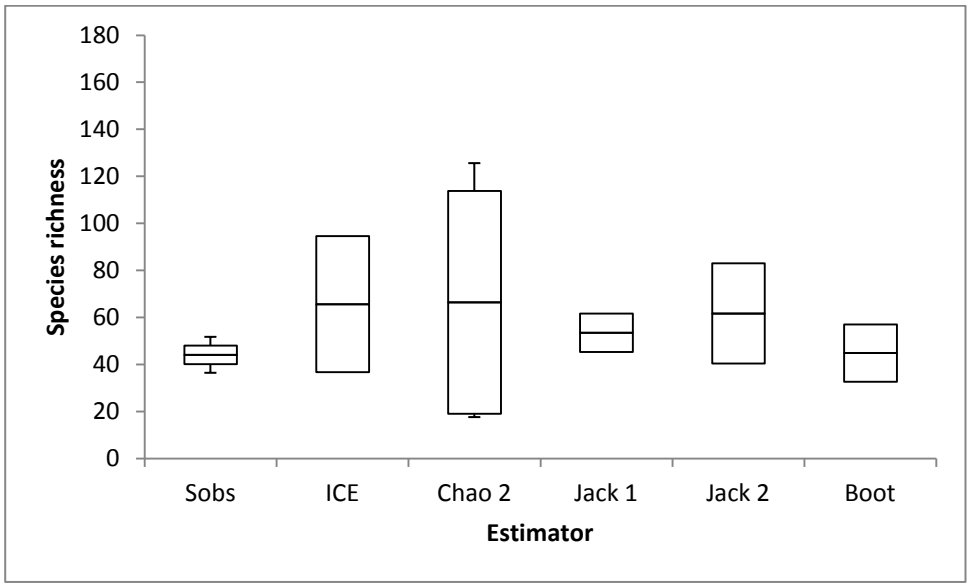

Fig 3.24: Expected and estimated species richness of biotope ab from rarefaction curves and estimators. ICE, Chao2 and Jack 2 estimate the highest species richness, although they also have the highest SD.

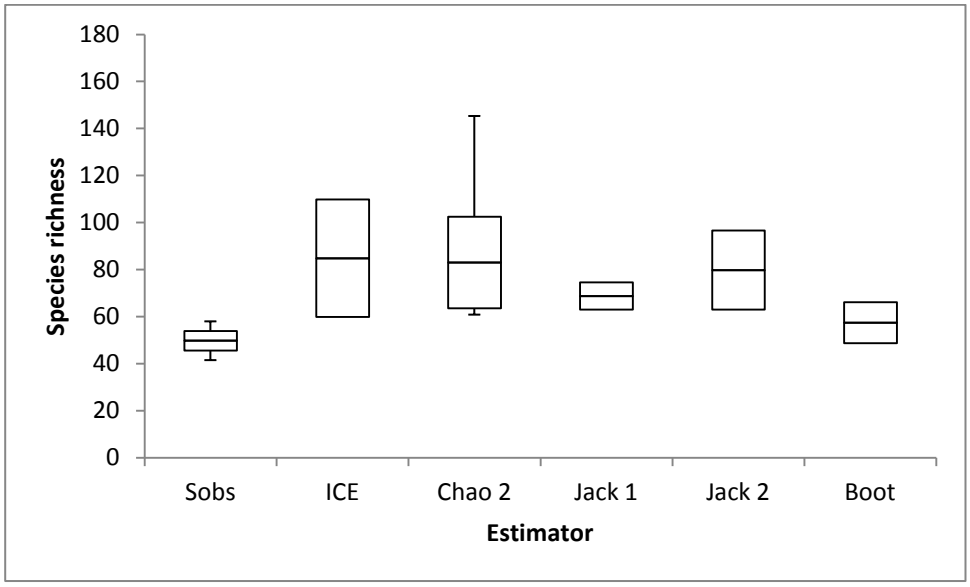

Fig 3.24: Expected and estimated species richness of biotope ad from rarefaction curves and estimators. ICE, Chao2 and Jack2 estimate the highest species richness, although they also have the highest SD.

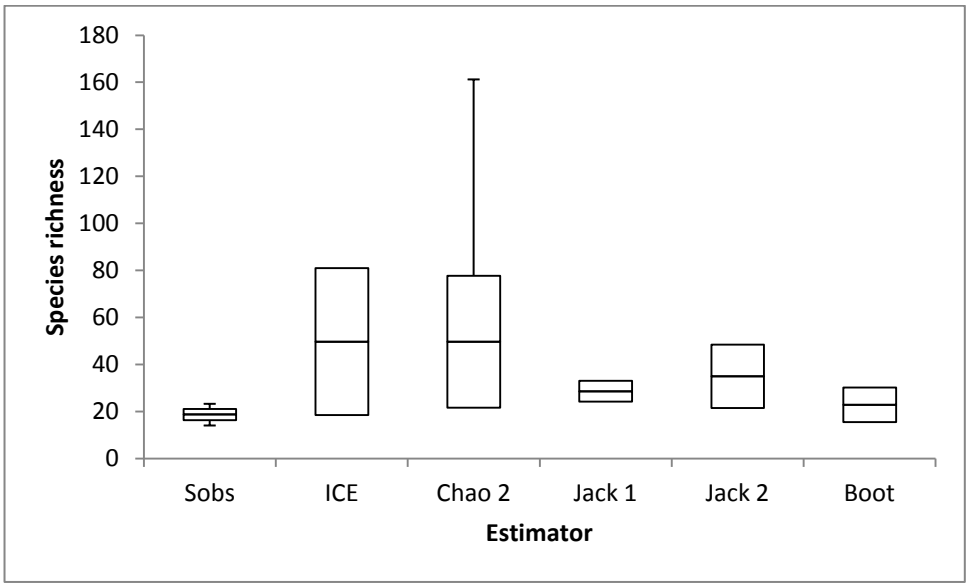

Fig 3.25: Expected and estimated species richness of biotope ae from rarefaction curves and estimators. ICE and Chao2 estimate the highest species richness, although they also have the highest SD.

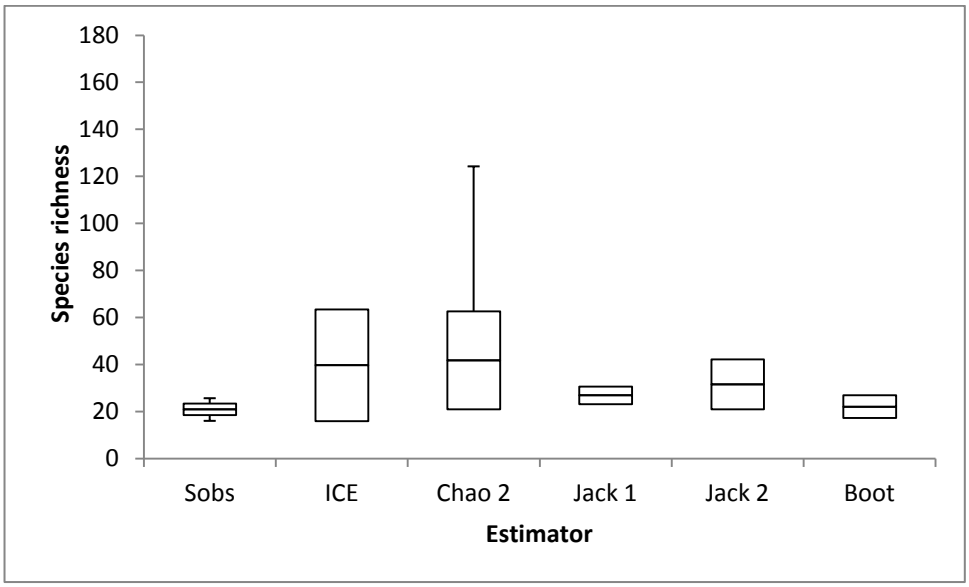

Fig 3.26: Expected and estimated species richness of biotope f from rarefaction curves and estimators. ICE and Chao2 estimate the highest species richness, although they also have the highest SD.

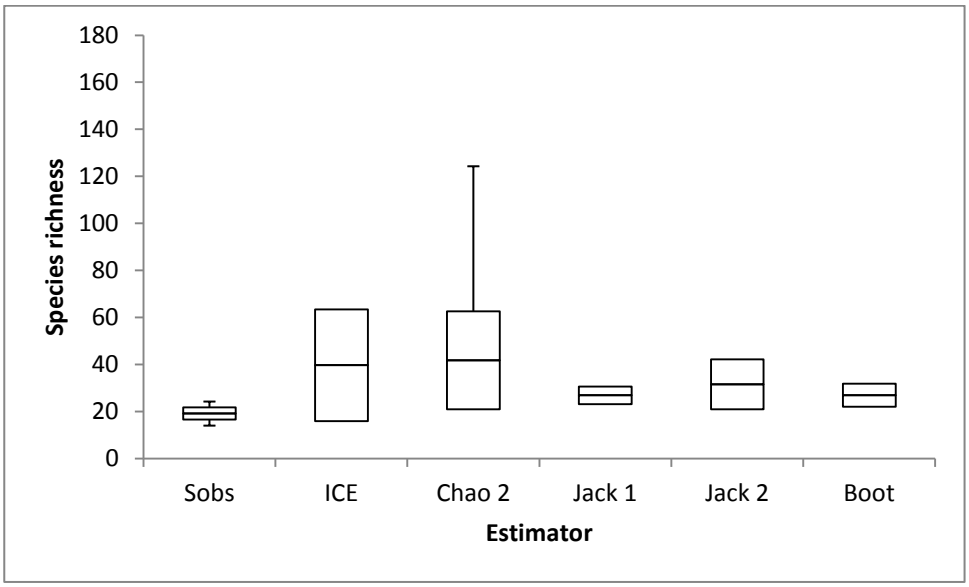

Fig 3.27: Expected and estimated species richness of biotope g from rarefaction curves and estimators. ICE and Chao2 estimate the highest species richness, although they also have the highest SD.

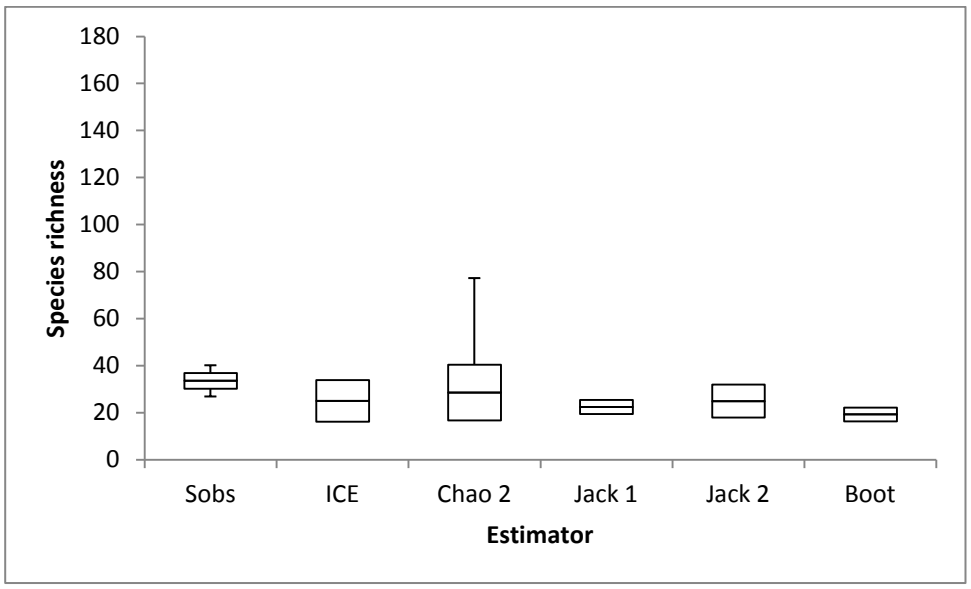

Fig 3.28: Expected and estimated species richness of biotope j from rarefaction curves and estimators. Sobs estimate the highest species richness.

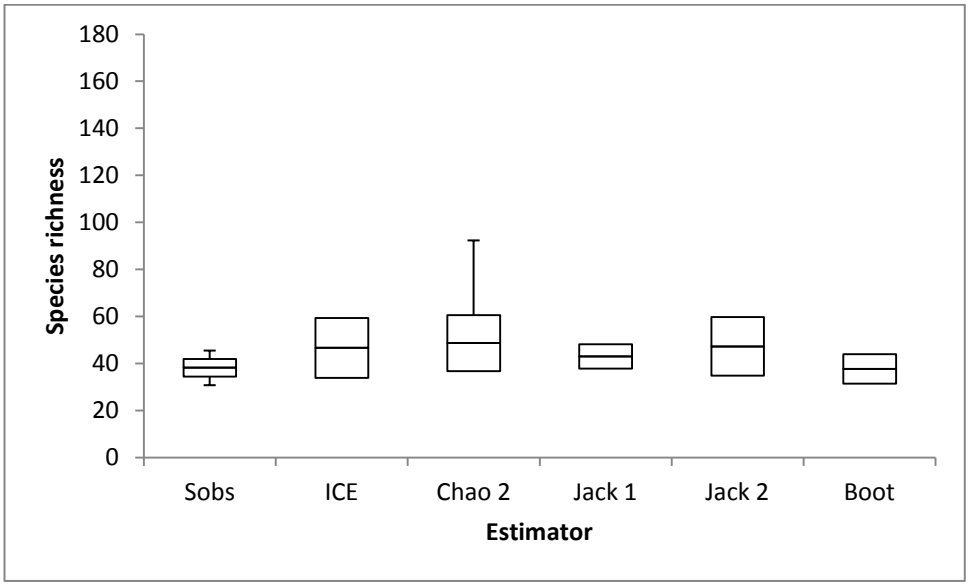

Fig 3.29: Expected and estimated species richness of biotope q from rarefaction curves and estimators. All estimators estimate higher species richness than the rarefaction curve (Sobs), but only marginally.

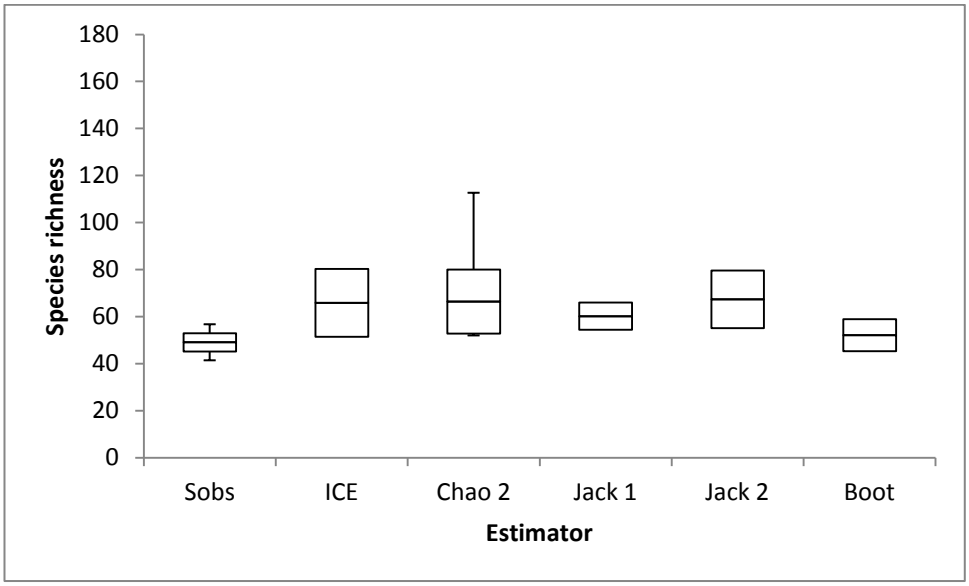

Fig 3.30: Expected and estimated species richness of biotope v from rarefaction curves and estimators. Estimator are similar to terms of species richness, Bootstrap having the lowest.

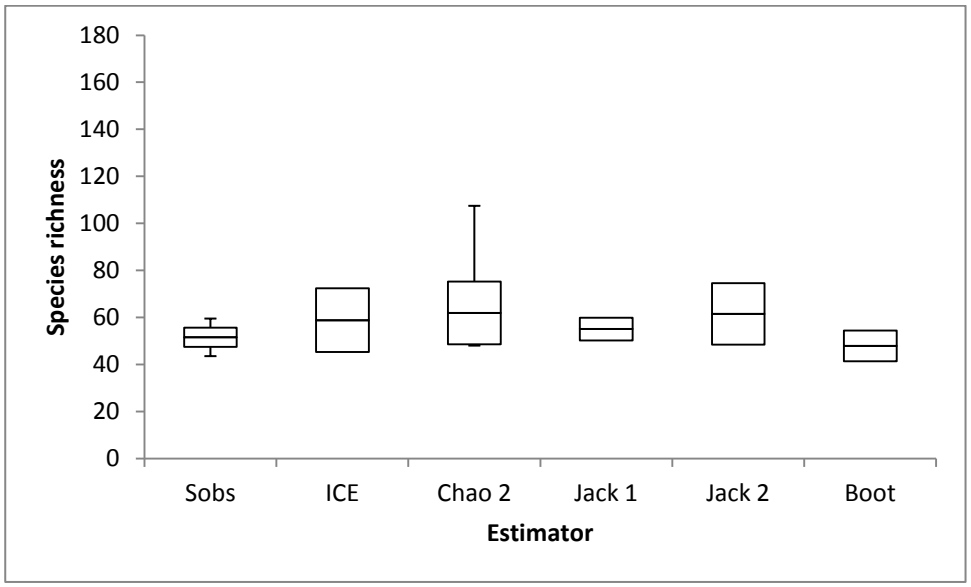

Fig 3.31: Expected and estimated species richness of biotope w from rarefaction curves and estimators. There is little variation between estimator species richness.

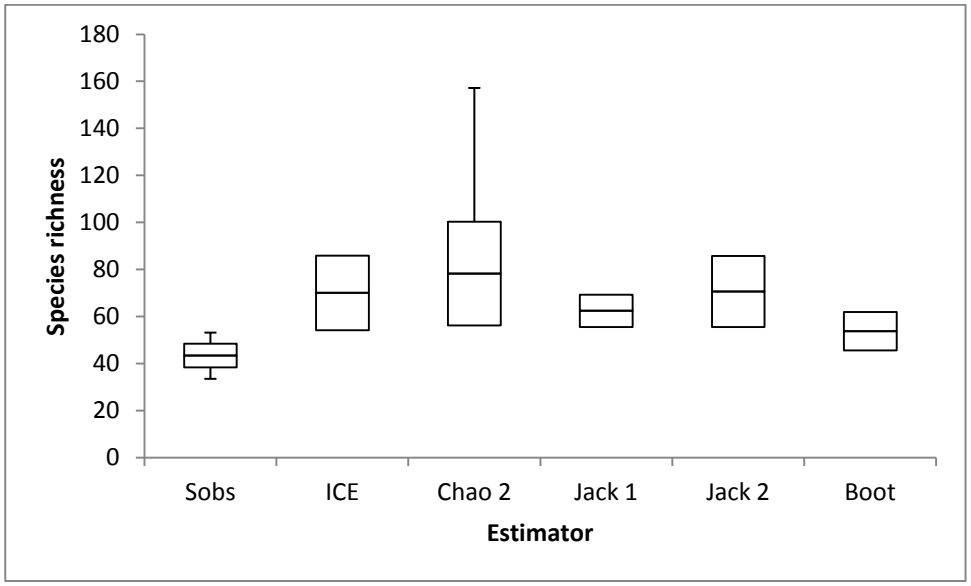

Fig 3.32: Expected and estimated species richness of biotope z from rarefaction curves and estimators. ICE, Chao2 and Jack 2 estimate the highest species richness, although they also have the highest SD.

A3.5 Biotope descriptions for Anton Dohrn Seamount

Cold water coral reef

Lophelia pertusa reef

Biotope Lop.Mad (cluster q) had a SIMPER similarity of 61.70% and was identified as biogenic reef characterised by the reef building corals *Lophelia pertusa* (live and dead) and *Madrepora oculata*, the pencil urchin *Cidaris cidaris*, anemones, and Decapoda sp.5,. Video footage also revealed the squat lobster *Munida sarsi*, gorgonians (Gorgonacea sp.18), and the antipatharian *Leiopathes* sp. to be conspicuous fauna. This assemblage was observed on cliff top mounds and a radial ridge on the NW side of Anton Dohrn Seamount over a depth of 747-1337 m and 5.5-9.1°C.

Predominantly dead, low-lying coral framework with encrusting sponges

Biotope Lop.Por (Cluster w) had a SIMPER similarity of 50.48% and was characterised by dead low-lying *L. pertusa* framework, a number of ophiuroid species (Ophiuroidea sp.2, Ophiuroidea sp.8, *Ophiactis abyssicola* and *Ophiactis balli*) and green (Porifera encrusting sp.39) encrusting sponges. This assemblage was observed from both survey areas over a depth of 1267-1756 m and a temperature of 3.8-5.9°C (1267-1756 m, 3.8-5.9°C on the NW side; 1497-1573 m, 4.8-4.9°C on the SE) on areas of lower relief such as at the base of the radial ridge, parasitic cone and flute features and on the landslide/rockfall feature at the base of the seamount. Video observations revealed the soft coral *Anthomastus*, the glass sponge *Aphrocallistes* and caryophyllids to be abundant.

Predominantly dead, low-lying coral framework

Biotope Lop.Oph (cluster aa) had a SIMPER similarity of 53.71% was characterised by dead *Lophelia pertusa* coral framework, and the ophiuroids *Ophiactis balli* and *Ophiactis abyssicola*. Non-sample images and video footage revealed the large anemone *Phelliactus* sp., ascidians and the corkscrew antipatharian *Stichopathes* sp. to also be characteristic of this assemblage. This assemblage was observed on both sides of Anton Dohrn Seamount at a depth of 758-1677 m and a temperature of 4.8-9°C associated with geomorphic features (cliff-top mounds, radial ridge and the cliff edge) in close proximity to live biogenic reef.

Xenophyophore communities

Xenophyophores and ophiuroids on mixed substratum

Biotope Syr.Pso (cluster j) had a SIMPER similarity of 15.21% and was characterised by the xenophyophore *Syringammina fragilissima*, an unidentified ophiuroid species (Ophiuroidea sp. 1), Porifera encrusting sp.1 and serpulids (Serpulidae sp. 1), and occurred on mixed substratum dominated by pebbles. This biotope was observed deep on the SE and NW flanks, on the edge of the seamount summit on the SE side and the radial ridge on the SE side over a depth of 1076-1554 m and a temperature of 4.5-7.9°C.

Xenophyophores and caryophyllids on gravelly sand and mixed substratum

While the biotope Syr.Car (cluster ae) was also characterised by xenophyophores (*Syringammina fragilissima*) it is easily distinguished from the xenophyophore and ophiuroid biotope by the presence of various anthozoan species. It had a SIMPER similarity of 24.27% and was also characterised by a solitary coral species [Cnidaria sp. 1), unidentified ophiuroids (Ophiuroidea sp.8, Ophiuroidea sp.2) and *Ophiactis* balli.

SIMPER did not rank the sea pens (*Pennatula phosphorea* and *Halipteris* sp.) as a species contributing highly towards the similarity, but upon inspection of the video footage it was apparent that they were the abundant characterising species of this assemblage. This assemblage was associated with gravelly sand and mixed substratum dominated by pebbles and was only observed on the deep NW flank over a depth range of 1714-1770 m and a temperature of 3.8-3.9°C.

Coral Gardens

Gorgonian dominated 'coral garden'

Biotope Gor.Lop (cluster z) had a SIMPER similarity of 53.6% and was characterised by dead *L. pertusa* framework, small growths of *L. pertusa* with an associated bamboo coral (*Keratoisis* sp.), ophiuroids (*Ophiactis balli* and Ophiuroidea sp. 2) and Gorgonacea sp. 6. Other conspicuous fauna identified from the video footage included the antipatharian *Antipathes* sp., *Leiopathes* sp., *Stichopathes* sp. and the glass sponge *Aphrocallistes* sp., lamellate and cup sponges. The coral gardens provide a suitable habitat for a diverse range of fish including the false boarfish *Neocyttus helgae*, *Lepidion eques*, and *Hoplostethus atlanticus*. This assemblage was associated with bedrock and mixed substratum on the radial ridge and parasitic cone on the NW side of Anton Dohrn Seamount. The assemblage was sampled over a depth of 1311-1634 m and a temperature of 4.0-5.5°C.

Coral garden with bamboo corals and antipatharians on bedrock

Biotope Lep.Ker (cluster g) had a SIMPER similarity of 19.54% and was characterised by the large bamboo coral *Lepidisis* sp. and *Keratoisis* sp. 2, the scleractinian coral *Lophelia pertusa*, solitary cup corals (*Caryophyllia* sp. 2) and an encrusting sponge

species (Porifera encrusting sp. 28). It was observed from both sides of the seamount on distinct meso-scale geomorphological features; a parasitic cone on the NW flank (1646-1753) and a radial ridge on the SE flank (1543-1567).

Other reef habitat under EU habitats directive

Lophelia pertusa and encrusting sponges on bedrock

Biotope Lop.Car (cluster v) had a SIMPER similarity of 51.77% and was characterised by small growths of *L. pertusa*, a number of ophiuroid species (Ophiuroidea sp. 2, Ophiuroidea sp. 8), crinoids (Crinoidea sp. 1), and cup corals (*Caryophyllia* sp. 2). The assemblage was associated with hard substratum (bedrock) and observed on the NW and SE flanks associated with distinct geomorphic features including mounds (parasitic cone) ridges (radial ridge) and raised areas of seabed at the base of the landslide/rockfall feature over a depth and temperature range of 1497-1742 m. Interestingly, this biotope was observed shallower (1497-1572 m) on the SE side than the NW (1704-1742 m).

Psolus, caryophyllids and lamellate sponges on mixed, boulder and bedrock substratum

Biotope Por.Pso (cluster ad) had a SIMPER similarity of 34.06% occurred on the steep escarpment which was comprised of bedrock outcrop with a boulder and cobble scree below. Characterising species as identified by SIMPER were the sessile holothurian*Psolus squamatus*, the ophiuroids *Ophiactis balli*, and encrusting sponges (Porifera encrusting sp. 22, Porifera encrusting sp. 28). Video observations also revealed this biotope to be characterised by large conspicuous antipatharian coral *Leiopathes* sp. and lamellate sponges. This assemblage was observed from both survey areas over a depth and temperature range of 854-1345 m and 5.1-9°C respectively.

Other habitats

Ophiomusium lymani and cerianthid anemones on mixed substratum

Biotope Oph.Unk (cluster e) had a SIMPER similarity of 28.64% and was characterised by the large ophiuroid *Ophiomusium lymani* and an unidentified species (unknown sp.29). Non-sample images and video revealed cerianthids to be a characterising species of this assemblage, as well as solitary corals (probably *Flabellum* sp.), stalked crinoids, holothurians and large anemones (Actinaria sp.16). This assemblage was associated with mixed substratum and bedrock with sand veneer at the base of the SE flank at a depth of 1791-1889 m and temperature 3.69-3.83°C.

Serpulids, encrusting sponges and *Psolus* on mixed substratum

Biotope Ser.Pso (cluster ab) had a SIMPER similarity of 28.91% and was characterised by a number of sessile fauna including serpulid worms (Serpulidae sp. 1), encrusting sponges (Porifera encrusting sp. 1, Porifera encrusting sp. 28), the holothurian *Psolus squamatus*, globose sponges (Porifera massive globose sp. 12), ophiuroids (*Ophiactis abyssicol*, Ophiuroidea sp. 6) and Majidae sp. 1. This assemblage was associated with mixed substratum and was observed from the summit of the seamount (NW and SE areas) at a depth of 814-1037 m and a temperature of 8-9.1°C.

A3.6 Biotope descriptions for non-listed habitats defined from Anton Dohrn Seamount

Ophiomusium lymani assemblage

The long armed ophiuroid *Ophiomusium lymani* is known to occur in deep water and has been previously described by a number of authors (including Gage 1986; Hughes and Gage, 2004) as occurring in association with the bamboo coral *Acanella arbuscula* in the lower bathyal depths (1920-2500 m) in the Rockall Trough. Narayanaswamy *et al*. (2006) describe an *Ophiomusium* assemblage at 1420 m on the NW flank of ADS associated with echinoids (probably *Echinus affinis*), solitary corals and the soft coral *Anthomastus grandiflorus*, and an *Ophiomusium* and *Echinus affinis* assemblage at 2025-2180 m on the Hebrides continental slope, associated with solitary polyps (possibly *Flabellum* sp.). A deep *O. lymani* assemblage was observed from the moat of Rosemary Bank associated with unidentified annelid species, echinoids (*Echinus* sp.), *Psolus squamatus* and brachiopods on mixed cobble and pebble substrate (J. Davies *pers. obs*.). This newly described biotope differs from previously described assemblages and was characterised by cerianthids, stalked crinoids, solitary corals (probably *Flabellum* sp.), large anemones and holothurians.

Serpulids, encrusting sponges and *Psolus* on mixed substratum

A similar assemblage has been described from Rockall Bank by Wienberg *et al*. (2008). They describe a dropstone associated community characterised by serpulid worms, bryozoans and *Psolus* sp. Howell *et al*. (2010) also describe a similar assemblage associated with mixed substrate (pebbles-boulders) and bedrock characterised by saddle oysters, *Psolus squamatus*, white encrusting sponges, serpulid worms and *Munida* sp.

A4.1 SIMPER results for the SW Approaches

Full lists of species present in each assemblage described in Sect. 4.3.2. Characterising species, as identified by the SIMPER routine, are indicated in bold. #### denotes where the number is infinitive or cannot calculated, as in the case of Sim/SD, where the SD is zero and cannot be divided.

Group a
All the similarities are zero

Group b
Less than 2 samples in group

Group c
Average similarity: 42.26

Species	Av.Abund	Av.Sim	Sim/SD	Contrib%	Cum.%
Sabellidae sp. 1	**0.46**	**42.26**	**#######**	**100.00**	**100.00**

Group d
Less than 2 samples in group

Group e
Less than 2 samples in group

Group f
Average similarity: 100.00

Species	Av.Abund	Av.Sim	Sim/SD	Contrib%	Cum.%
***Benthogone* sp.**	**0.16**	**100.00**	**#######**	**100.00**	**100.00**

Group g
Less than 2 samples in group

Group h
Less than 2 samples in group

Group i
Less than 2 samples in group

Group j
Less than 2 samples in group

Group k
Average similarity: 25.93

Species	Av.Abund	Av.Sim	Sim/SD	Contrib%	Cum.%
***Protoptilum* sp.**	**0.22**	**16.67**	**0.58**	**64.27**	**64.27**
***Pseudarchaster* sp.**	**0.17**	**9.27**	**0.58**	**35.73**	**100.00**

Group l
Average similarity: 68.45

Species	Av.Abund	Av.Sim	Sim/SD	Contrib%	Cum.%
Edwardsiidae sp. 1	**0.27**	**68.45**	**4.76**	**100.00**	**100.00**

Group m
Average similarity: 44.15

Species	Av.Abund	Av.Sim	Sim/SD	Contrib%	Cum.%
Halcampoididae sp. 3	**0.32**	**24.63**	**0.58**	**55.78**	**55.78**
Unknown sp. 13	**0.22**	**19.53**	**0.58**	**44.22**	**100.00**

Group n
Average similarity: 49.42

Species	Av.Abund	Av.Sim	Sim/SD	Contrib%	Cum.%
Unknown sp. 15	**0.19**	**49.42**	**#######**	**100.00**	**100.00**

Group o
Average similarity: 50.48

Species	Av.Abund	Av.Sim	Sim/SD	Contrib%	Cum.%
Sagartiidae sp. 3	**0.29**	**48.48**	**1.78**	**96.05**	**96.05**
Kophobelemnon stelliferum	0.06	1.70	0.22	3.38	99.42
Calveriosoma fenestratum	0.02	0.29	0.09	0.58	100.00

Group p
Average similarity: 18.04

Species	Av.Abund	Av.Sim	Sim/SD	Contrib%	Cum.%
Actiniaria sp. 14	**0.05**	**10.48**	**0.39**	**58.07**	**58.07**
Cerianthidae sp. 3	**0.10**	**6.14**	**0.44**	**34.04**	**92.11**
Crinoidea sp. 1	0.07	1.42	0.26	7.89	100.00

Group q
Average similarity: 10.73

Species	Av.Abund	Av.Sim	Sim/SD	Contrib%	Cum.%
***Caryophyllia* sp. 2**	**0.11**	**4.00**	**0.32**	**37.27**	**37.27**
Porifera encrusting sp. 1	**0.09**	**3.60**	**0.31**	**33.50**	**70.77**
Hydrozoa (flat branched)	**0.15**	**2.15**	**0.24**	**19.99**	**90.75**
Bathynectes sp.	0.04	0.40	0.13	3.71	94.47
Bolocera tuediae	0.05	0.30	0.13	2.77	97.23
Cerithioidea sp.	0.05	0.30	0.13	2.77	100.00

Group r
Average similarity: 25.07

Species	Av.Abund	Av.Sim	Sim/SD	Contrib%	Cum.%
cf. *Bathylasma* sp.	**0.42**	**16.33**	**0.58**	**65.13**	**65.13**
Hydrozoa (bushy)	**0.14**	**8.74**	**0.57**	**34.87**	**100.00**

Group s
Average similarity: 14.78

Species	Av.Abund	Av.Sim	Sim/SD	Contrib%	Cum.%
Terebellidae sp. 1	**0.26**	**14.94**	**0.79**	**60.27**	**60.27**
Actiniaria sp. 17	**0.15**	**8.96**	**0.39**	**36.16**	**96.43**
Serpulidae sp. 1	0.04	0.47	0.17	1.91	98.34
Bonellia viridis	0.06	0.41	0.17	1.66	100.00

Group t
Average similarity: 38.99

Species	Av.Abund	Av.Sim	Sim/SD	Contrib%	Cum.%
Amphipoda sp. 1	**0.25**	**38.99**	*******	**100.00**	**100.00**

Group u
Average similarity: 20.08

Species	Av.Abund	Av.Sim	Sim/SD	Contrib%	Cum.%
***Colus* sp. 2**	**0.35**	**20.08**	**1.28**	**100.00**	**100.00**

Group v
Average similarity: 49.37

Species	Av.Abund	Av.Sim	Sim/SD	Contrib%	Cum.%
Pachycerianthus multiplicatus	**0.38**	**42.08**	**3.23**	**85.22**	**85.22**
Cerianthidae sp. 1	**0.11**	**7.30**	**0.58**	**14.78**	**100.00**

Group w
Less than 2 samples in group

Group x
Average similarity: 54.39

Species	Av.Abund	Av.Sim	Sim/SD	Contrib%	Cum.%
Cerianthidae sp. 1	**0.31**	**54.10**	**2.63**	**99.47**	**99.47**
Sagartiidae sp. 3	0.01	0.06	0.05	0.10	99.57
Echinus spp.	0.01	0.05	0.05	0.10	99.67
Munida sarsi	0.01	0.05	0.05	0.09	99.76
Cerianthidae sp. 3	0.01	0.03	0.03	0.05	99.81
Unknown sp. 26	0.01	0.02	0.03	0.04	99.85
Ophiothrix fragilis	0.01	0.02	0.03	0.04	99.89
Pseudarchaster sp.	0.01	0.02	0.03	0.03	99.92
Caryophyllia sp. 2	0.01	0.02	0.03	0.03	99.95
Kophobelemnon stelliferum	0.00	0.02	0.03	0.03	99.98
Halcampoididae sp. 1	0.01	0.01	0.03	0.02	100.00

Group y
Average similarity: 49.80

Species	Av.Abund	Av.Sim	Sim/SD	Contrib%	Cum.%
Kophobelemnon stelliferum	**0.34**	**42.07**	**2.54**	**84.46**	**84.46**
Cerianthidae sp. 1	**0.14**	**7.03**	**0.55**	**14.12**	**98.59**
Ophiuroidea sp.1	0.04	0.41	0.11	0.82	99.41
Halcampoididae sp.3	0.02	0.13	0.06	0.27	99.68
Pentametrocrinus atlanticus	0.02	0.06	0.06	0.13	99.81

Crinoidea sp. 2	0.03	0.04	0.04	0.08	99.89
Ophiactis balli	0.01	0.04	0.04	0.07	99.96
Acanella sp.	0.01	0.02	0.04	0.04	100.00

Group z
Average similarity: 41.11

Species	Av.Abund	Av.Sim	Sim/SD	Contrib%	Cum.%
Ophiactis balli	**0.71**	**38.06**	**2.29**	**92.59**	**92.59**
Cerianthidae sp. 1	0.07	1.82	0.27	4.42	97.01
Munida sarsi	0.08	0.60	0.20	1.46	98.47
Serpulidae sp. 1	0.05	0.20	0.11	0.49	98.96
Actinauge richardi	0.02	0.13	0.06	0.32	99.28
Halcampoididae sp. 1	0.05	0.12	0.11	0.29	99.57
Zoanthidea sp. 1	0.03	0.06	0.06	0.16	99.72
Unknown sp. 26	0.02	0.06	0.06	0.15	99.87
Echinus spp.	0.01	0.03	0.06	0.07	99.94
Hydrozoa (bushy)	0.02	0.02	0.06	0.06	100.00

Group aa
Less than 2 samples in group

Group ab
Average similarity: 31.57

Species	Av.Abund	Av.Sim	Sim/SD	Contrib%	Cum.%
Sabellidae sp. 2	**0.76**	**31.57**	**9.59**	**100.00**	**100.00**

Group ac
Average similarity: 47.47

Species	Av.Abund	Av.Sim	Sim/SD	Contrib%	Cum.%
Unknown sp. 26	**1.03**	**36.24**	**2.41**	**76.36**	**76.36**
Cerianthidae sp. 1	**0.26**	**6.79**	**0.93**	**14.31**	**90.67**
Ophiactis balli	0.32	2.32	0.36	4.88	95.55
Lophelia pertusa (dead structure)	0.10	0.74	0.20	1.57	97.11
Halcampoididae sp. 1	0.09	0.58	0.23	1.21	98.33
Amphiuridae sp. 1	0.05	0.26	0.14	0.55	98.88
Ophiuroidea sp. 1	0.06	0.19	0.13	0.41	99.29
Munida sarsi	0.03	0.12	0.11	0.26	99.55
Lophelia pertusa	0.04	0.07	0.09	0.15	99.69
Terebellidae sp. 1	0.01	0.04	0.08	0.09	99.78
Psolus squamatus	0.02	0.03	0.08	0.06	99.84
Echinus spp.	0.02	0.02	0.07	0.05	99.89
Sagartiidae sp. 3	0.01	0.01	0.03	0.02	99.91
Brachiopoda sp. 1	0.01	0.01	0.03	0.02	99.92
Bathynectes sp.	0.01	0.01	0.03	0.01	99.94
Ascidiacea sp. 2	0.01	0.01	0.03	0.01	99.95
Bolocera tuediae	0.01	0.01	0.03	0.01	99.96
Crinoidea sp. 1	0.00	0.01	0.03	0.01	99.97
Galatheidae sp. 1	0.01	0.01	0.03	0.01	99.98
Pandalus borealis	0.02	0.00	0.03	0.01	99.99
Actiniaria sp. 9	0.01	0.00	0.03	0.01	100.00

Group ad
Average similarity: 59.02

Species	Av.Abund	Av.Sim	Sim/SD	Contrib%	Cum.%
***Lophelia pertusa* (dead structure)**	**0.41**	**58.36**	**3.76**	**98.89**	**98.89**
Munida sarsi	0.04	0.66	0.26	1.11	100.00

Group ae
Less than 2 samples in group

Group af
Less than 2 samples in group

Group ag
Less than 2 samples in group

Group ah
Average similarity: 66.25

Species	Av.Abund	Av.Sim	Sim/SD	Contrib%	Cum.%
***Lophelia pertusa* (dead structure)**	**0.78**	**21.36**	**5.39**	**32.24**	**32.24**
Lophelia pertusa	**0.55**	**14.17**	**3.49**	**21.39**	**53.63**
Madrepora oculata	**0.46**	**11.60**	**2.99**	**17.51**	**71.14**
Unknown sp. 26	**0.46**	**5.49**	**0.70**	**8.28**	**79.42**
Actiniaria sp. 13	**0.28**	**4.06**	**0.99**	**6.12**	**85.54**
Pandalus borealis	0.15	2.79	1.20	4.21	89.75
Cerianthidae sp. 1	0.14	2.51	1.09	3.79	93.54
Halcampoididae sp. 1	0.18	2.16	0.70	3.25	96.79
Cidaris cidaris	0.10	1.47	0.68	2.22	99.01
Bathynectes sp.	0.04	0.32	0.33	0.49	99.50
Hydrozoa (bushy)	0.05	0.21	0.21	0.31	99.81
Koehlermetra porrecta	0.04	0.04	0.07	0.06	99.87
Hydrozoa (flat branched)	0.02	0.03	0.08	0.05	99.92
Porania pulvillus	0.01	0.03	0.08	0.04	99.96
Gastropoda sp. 1	0.01	0.01	0.05	0.01	99.97
Munida sarsi	0.01	0.01	0.05	0.01	99.98
Brisingella coronata / *Brisinga endecacnemos*	0.03	0.01	0.05	0.01	99.99
Henricia sanguinolenta	0.01	0.01	0.05	0.01	100.00

Group ai
Average similarity: 61.28

Species	Av.Abund	Av.Sim	Sim/SD	Contrib%	Cum.%
Unknown sp. 26	**2.70**	**34.64**	**3.31**	**56.53**	**56.53**
***Lophelia pertusa* (dead structure)**	**0.81**	**11.70**	**8.18**	**19.09**	**75.61**
Madrepora oculata	**0.45**	**6.09**	**3.62**	**9.93**	**85.55**
Lophelia pertusa	0.42	2.49	0.58	4.07	89.61
Actiniaria sp. 13	0.46	2.40	0.58	3.92	93.53
Edwardsiidae sp. 1	0.28	1.98	0.58	3.23	96.77
Halcampoididae sp. 1	0.32	1.98	0.58	3.23	100.00

Group aj
Average similarity: 54.00

Species	Av.Abund	Av.Sim	Sim/SD	Contrib%	Cum.%
***Lophelia pertusa* (dead structure)**	**0.55**	**30.59**	**3.35**	**56.65**	**56.65**
Halcampoididae sp. 1	**0.20**	**8.73**	**1.27**	**16.16**	**72.80**

Lophelia pertusa	**0.21**	**6.92**	**0.76**	**12.82**	**85.63**
Cerianthidae sp. 1	**0.24**	**6.16**	**0.77**	**11.40**	**97.03**
Madrepora oculata	0.17	1.60	0.26	2.97	100.00

Group ak
Average similarity: 66.33

Species	Av.Abund	Av.Sim	Sim/SD	Contrib%	Cum.%
Halcampoididae sp. 5	**0.30**	**66.33**	**4.38**	**100.00**	**100.00**

Group al
Average similarity: 53.22

Species	Av.Abund	Av.Sim	Sim/SD	Contrib%	Cum.%
Amphiuridae sp. 1	**0.62**	**40.91**	**2.56**	**57.53**	**57.53**
Cerianthidae sp. 1	**0.46**	**20.85**	**1.18**	**41.59**	**99.12**
Munida sarsi	0.05	0.34	0.13	0.64	99.76
Ophiuroidea sp. 5	0.02	0.05	0.05	0.08	99.84
Terebellidae sp. 1	0.01	0.03	0.03	0.05	99.89
Kophobelemnon stelliferum	0.01	0.02	0.02	0.03	99.93
Brachiopoda sp. 1	0.01	0.01	0.02	0.02	99.95
Pachycerianthus multiplicatus	0.01	0.01	0.02	0.02	99.97
Edwardsiidae sp. 1	0.01	0.01	0.03	0.02	99.99
Caryophyllia sp. 3	0.01	0.00	0.02	0.01	100.00

Group am
Average similarity: 47.39

Species	Av.Abund	Av.Sim	Sim/SD	Contrib%	Cum.%
Ophiuroidea sp. 1	**1.12**	**46.57**	**2.13**	**98.27**	**98.27**
Amphiuridae sp. 1	0.07	0.48	0.14	1.01	99.28
Munida sarsi	0.02	0.07	0.05	0.15	99.43
Ophiactis balli	0.03	0.07	0.06	0.14	99.56
Cerianthidae sp. 1	0.02	0.05	0.06	0.10	99.67
Caryophyllia sp. 1	0.03	0.03	0.04	0.07	99.74
Serpulidae sp. 1	0.02	0.03	0.04	0.06	99.80
Porifera encrusting sp. 1	0.01	0.01	0.02	0.02	99.82
Ophiuroidea sp. 5	0.02	0.01	0.03	0.02	99.84
Kophobelemnon stelliferum	0.01	0.01	0.03	0.02	99.86
Actinauge richardi	0.01	0.01	0.02	0.02	99.88
Caryophyllia smithii	0.01	0.01	0.02	0.02	99.90
Leptometra celtica	0.01	0.01	0.02	0.01	99.91
Crinoidea sp. 5	0.01	0.01	0.02	0.01	99.92
Polychaeta sp. 7	0.00	0.00	0.01	0.01	99.93
Actiniaria sp. 17	0.01	0.00	0.01	0.01	99.94
Terebellidae sp. 1	0.01	0.00	0.01	0.01	99.94
Majidae sp. 1	0.00	0.00	0.01	0.01	99.95
Ophiothrix fragilis	0.01	0.00	0.01	0.01	99.96
Sagartiidae sp. 3	0.00	0.00	0.01	0.01	99.96
Cerianthidae sp. 3	0.01	0.00	0.01	0.01	99.97
Ophiactis abyssicola	0.01	0.00	0.01	0.01	99.97
Polychaeta sp. 5	0.01	0.00	0.01	0.00	99.98
Astropecten irregularis	0.00	0.00	0.01	0.00	99.98
Virgularia mirabilis	0.00	0.00	0.01	0.00	99.98
Paguridae spp.	0.00	0.00	0.01	0.00	99.99
Unknown sp. 15	0.00	0.00	0.01	0.00	99.99
Brachiopoda sp. 1	0.00	0.00	0.01	0.00	99.99
Caryophyllia sp. 2	0.00	0.00	0.01	0.00	99.99
Pandalus borealis	0.00	0.00	0.01	0.00	99.99
Polychaeta sp. 1	0.01	0.00	0.01	0.00	99.99

Pentametrocrinus atlanticus	0.00	0.00	0.01	0.00	99.99
Unknown sp. 13	0.00	0.00	0.01	0.00	99.99
Tubularia sp. 2	0.00	0.00	0.01	0.00	100.00

Group an
Average similarity: 49.67

Species	Av.Abund	Av.Sim	Sim/SD	Contrib%	Cum.%
Crinoidea sp. 5	**0.39**	**45.53**	**2.16**	**91.66**	**91.66**
Stichopathes* cf. *gravieri	**0.12**	**4.14**	**0.44**	**8.34**	**100.00**

Group ao
Average similarity: 27.51

Species	Av.Abund	Av.Sim	Sim/SD	Contrib%	Cum.%
Serpulidae sp. 1	**0.39**	**20.63**	**0.99**	**74.99**	**74.99**
Brachiopoda sp. 1	**0.11**	**4.52**	**0.26**	**16.42**	**91.40**
Munida sarsi	**0.12**	**1.57**	**0.23**	**5.69**	**97.10**
Caryophyllia smithii	0.05	0.63	0.14	2.28	99.38
Ophiuroidea sp. 1	0.03	0.10	0.06	0.36	99.73
Actinauge richardi	0.01	0.07	0.06	0.27	100.00

Group ap
Average similarity: 41.38

Species	Av.Abund	Av.Sim	Sim/SD	Contrib%	Cum.%
Ophiuroidea sp. 5	**1.13**	**37.87**	**2.36**	**61.53**	**61.53**
Munida sarsi	**0.75**	**12.22**	**1.33**	**35.36**	**96.89**
Leptometra celtica	0.06	0.35	0.17	0.86	97.74
Amphiuridae sp. 1	0.07	0.25	0.12	0.62	98.36
Hydrozoa (bushy)	0.05	0.25	0.12	0.61	98.97
Serpulidae sp. 2	0.05	0.14	0.07	0.34	99.31
Paguridae spp.	0.04	0.10	0.13	0.25	99.55
Brachiopoda sp. 1	0.03	0.07	0.07	0.16	99.72
Echinus spp.	0.03	0.06	0.07	0.15	99.87
Cerianthidae sp. 1	0.03	0.05	0.07	0.13	100.00

Group aq
Average similarity: 33.11

Species	Av.Abund	Av.Sim	Sim/SD	Contrib%	Cum.%
Munida sarsi	**0.31**	**28.05**	**1.21**	**84.74**	**84.74**
Leptometra celtica	**0.16**	**3.18**	**0.30**	**9.60**	**94.33**
Crinoidea sp. 5	0.07	0.89	0.18	2.70	97.03
Cerianthidae sp. 1	0.03	0.42	0.14	1.25	98.29
Caryophyllia smithii	0.03	0.20	0.08	0.61	98.90
Ophiuroidea sp. 1	0.03	0.13	0.08	0.38	99.28
Ophiactis balli	0.03	0.11	0.07	0.33	99.61
Caryophyllia sp. 2	0.02	0.05	0.04	0.15	99.76
Echinus spp.	0.01	0.03	0.03	0.08	99.84
Porifera encrusting sp. 31	0.01	0.02	0.03	0.07	99.90
Porifera encrusting sp. 3	0.01	0.01	0.03	0.04	99.94
Actinauge richardi	0.01	0.01	0.03	0.03	99.98
Ophiuroidea sp. 5	0.01	0.01	0.03	0.02	100.00

A4.2 Raw data for figures 4.7 (a) and (b)

Mean species richness

biotope	Mean	Std. Error	95% Confidence Interval	
			Lower Bound	Upper Bound
ac	4.413	.211	3.998	4.828
ah	8.967	.262	8.453	9.481
aj	5.000	.585	3.851	6.149
al	2.056	.170	1.722	2.390
am	2.040	.086	1.871	2.209
ao	2.292	.293	1.717	2.866
ap	3.050	.321	2.421	3.679
aq	2.529	.201	2.135	2.924
r	2.714	.542	1.650	3.778
x	1.898	.205	1.496	2.300
y	2.308	.230	1.857	2.758

Simpson Index

Biotope	Mean	Std. Error	95% Confidence Interval	
			Lower Bound	Upper Bound
ac	1.702	.097	1.512	1.892
ah	1.987	.120	1.752	2.223
aj	1.637	.268	1.111	2.163
al	1.511	.077	1.359	1.663
am	1.389	.039	1.311	1.466
ao	1.759	.134	1.497	2.022
ap	1.600	.147	1.312	1.888
aq	1.644	.092	1.464	1.824
r	1.488	.248	1.001	1.975
x	1.561	.094	1.377	1.745
y	1.850	.105	1.643	2.056

A4.3 Rarefaction curves for biotopes identified from cluster analysis.

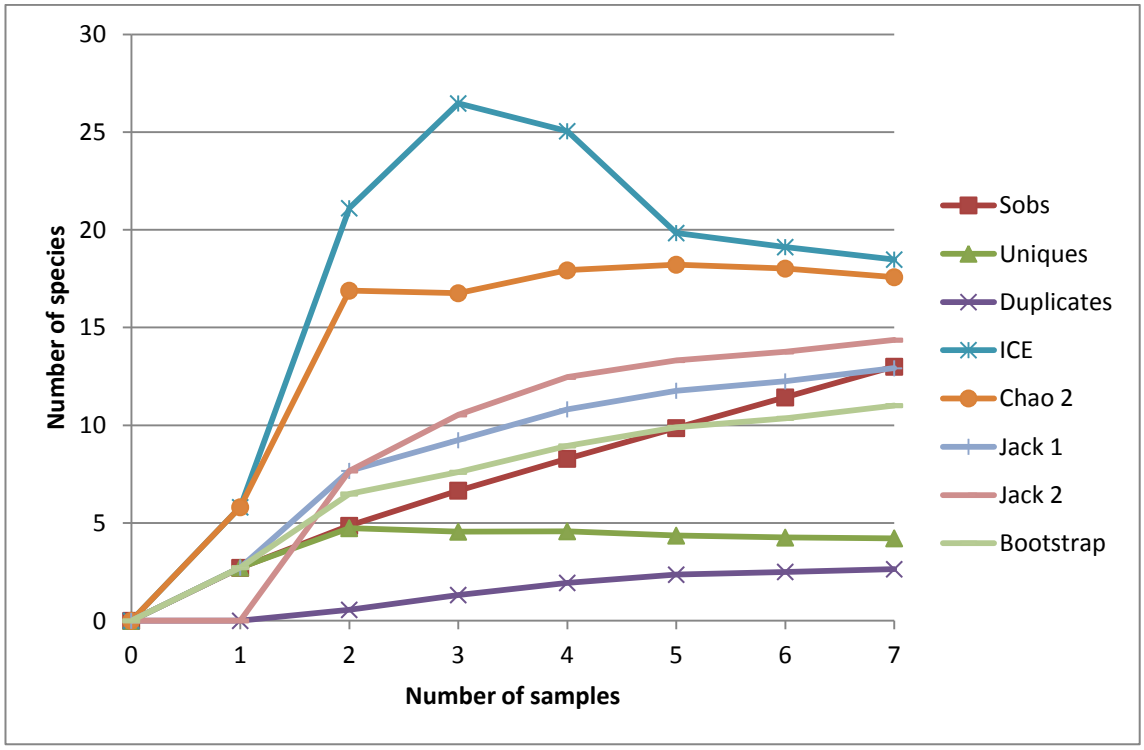

Fig. 4.9: Rarefaction curve and species richness estimators for biotope r. The Sobs curve showing no sign of reaching asymptote, and no convergence of estimator curves.

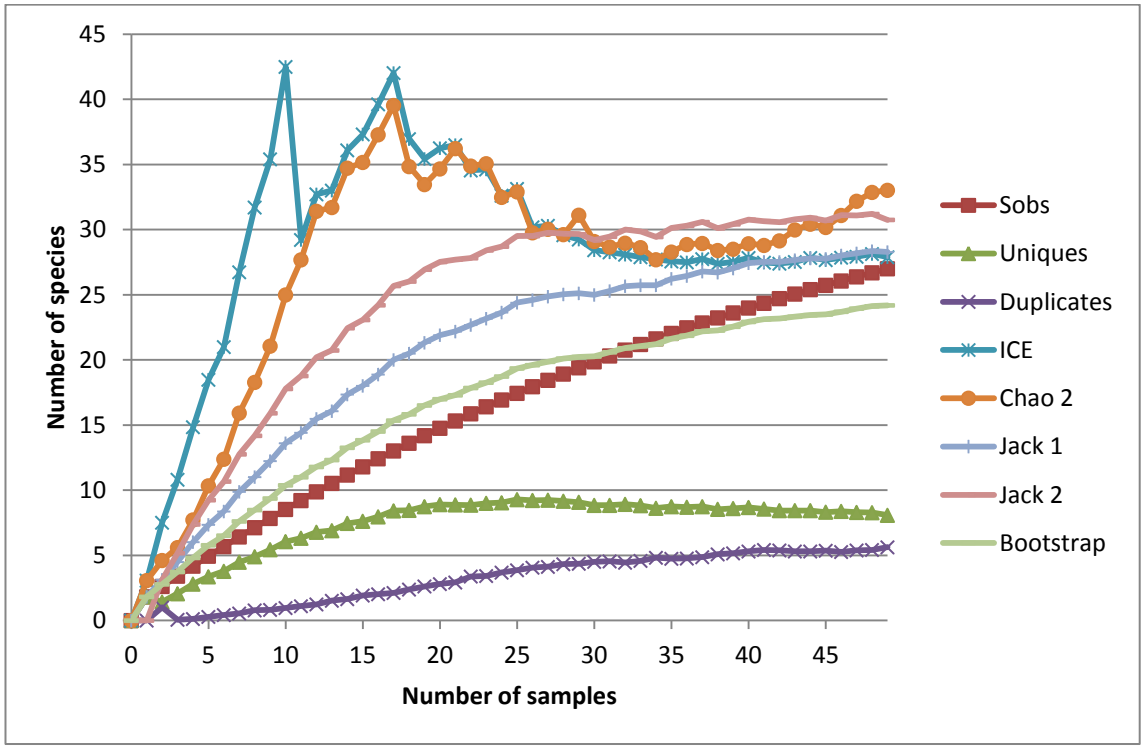

Fig. 4.10: Rarefaction curve and species richness estimators for biotope x. The Sobs and estimator curves have not reached asymptote. Unique and Duplicate species curves appear to be close to crossing.

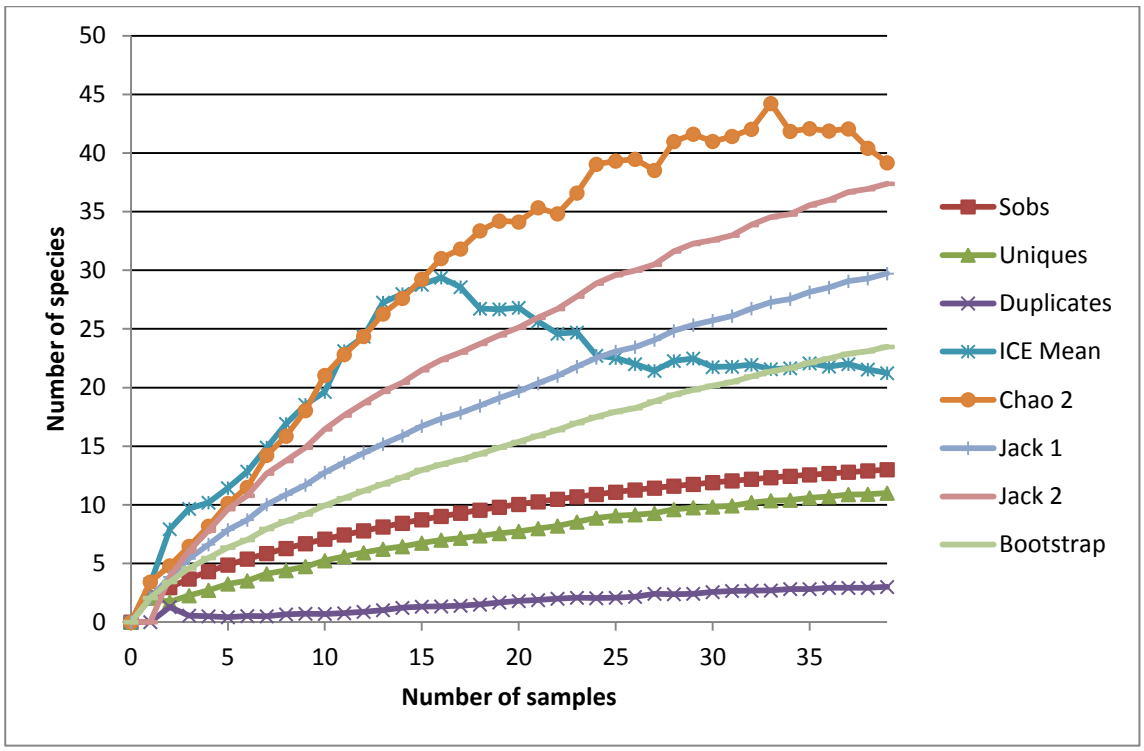

Fig. 4.11 Rarefaction curve and species richness estimators for biotope y. Estimator curves are much steeper than the expected species richness (Sobs), with Chao2 being the steepest curve, suggesting this biotopes has not been adequately sampled.

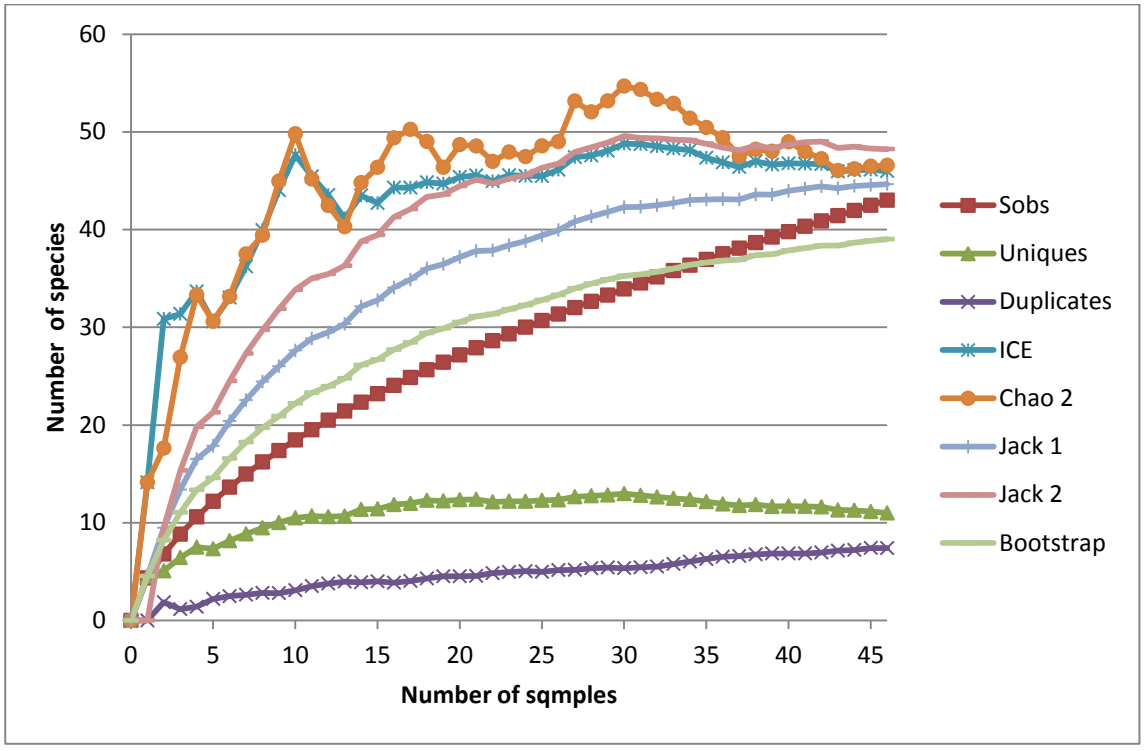

Fig. 4.12: Rarefaction curve and species richness estimators for biotope ac. Steep curves for the estimators begin to level off after *approx*. 35 samples, which is illustrated by the near crossing of the Unique and Duplicate species curves.

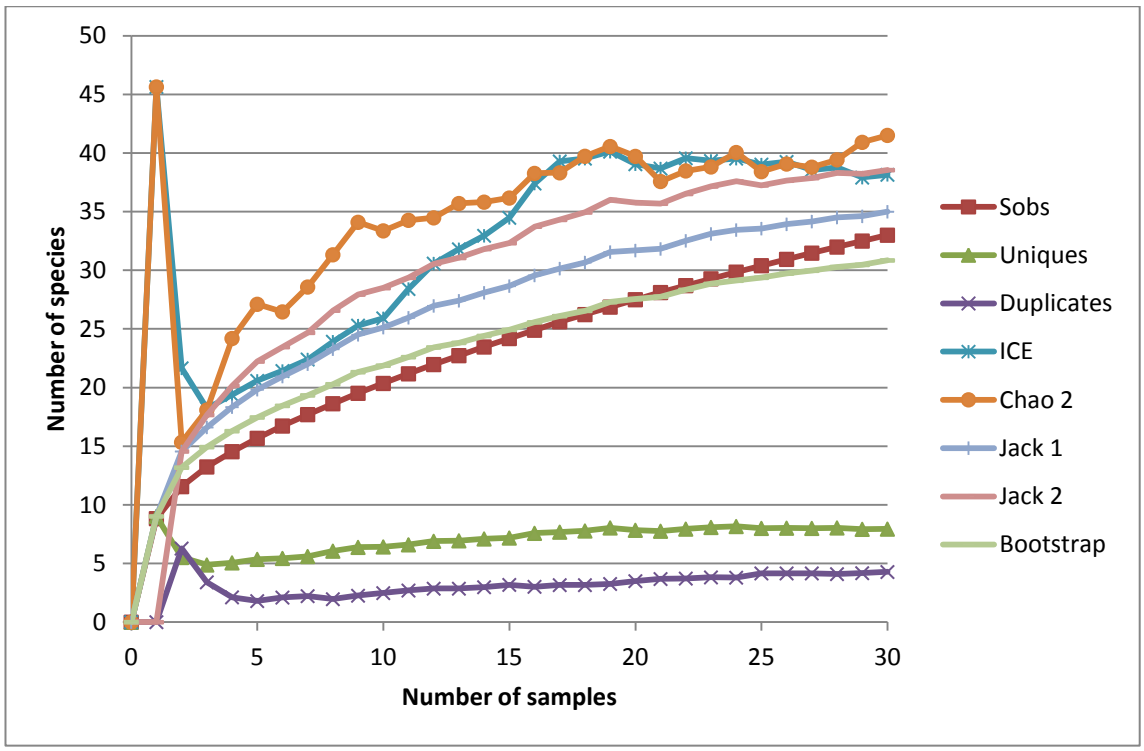

Fig. 4.13: Rarefaction curve and species richness estimators for biotope ah. The Bootstrap estimator follows nearly the same trajectory as the expected species richness (Sobs), while the other estimator curves are higher than Sobs.

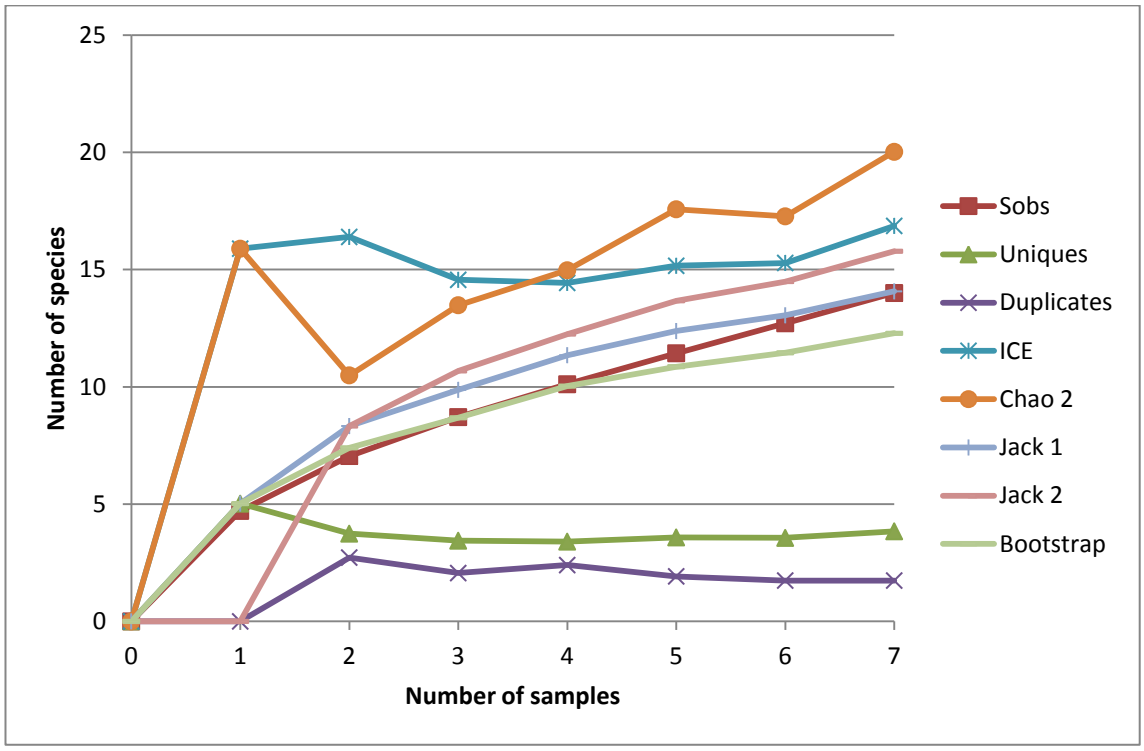

Fig. 4.14: Rarefaction curve and species richness estimators for biotope aj.

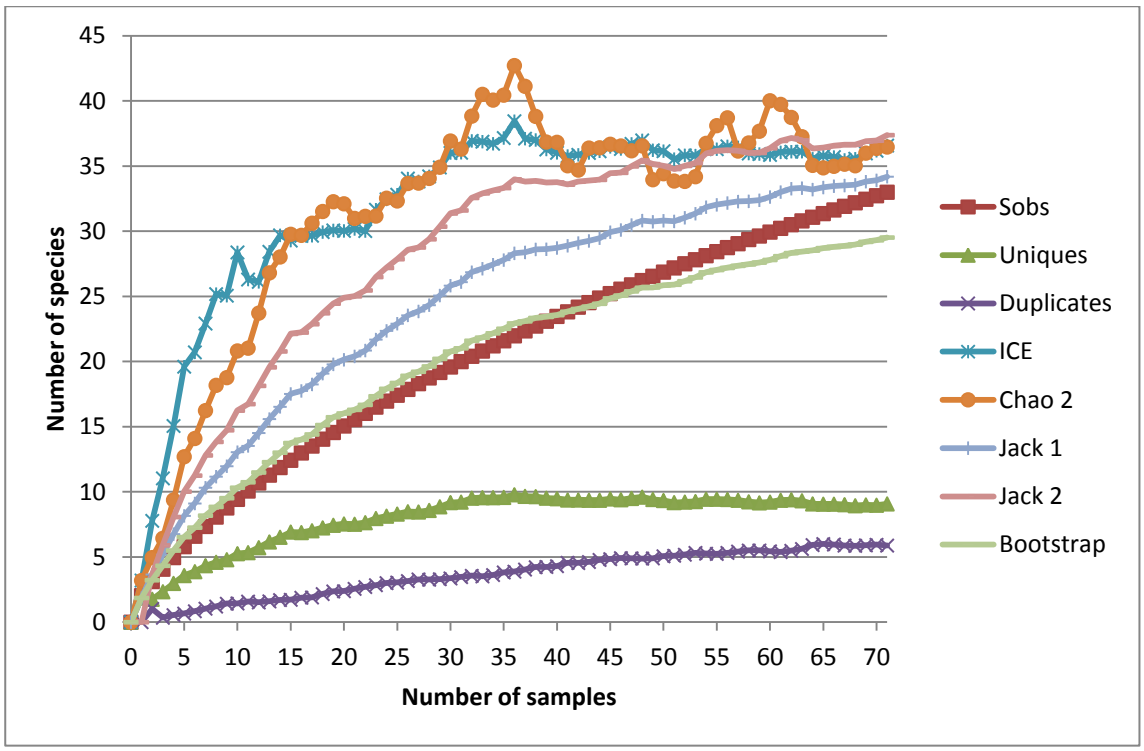

Fig. 4.15: Rarefaction curve and species richness estimators for biotope al.

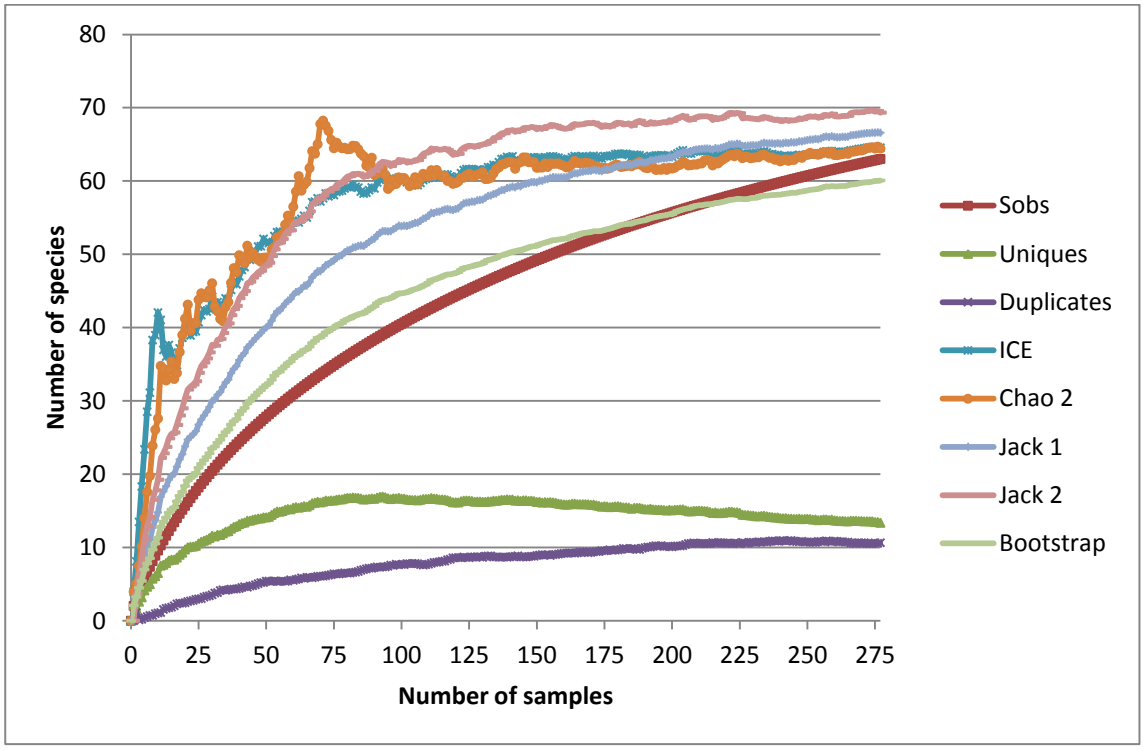

Fig. 4.16: Rarefaction curve and species richness estimators for biotope am.

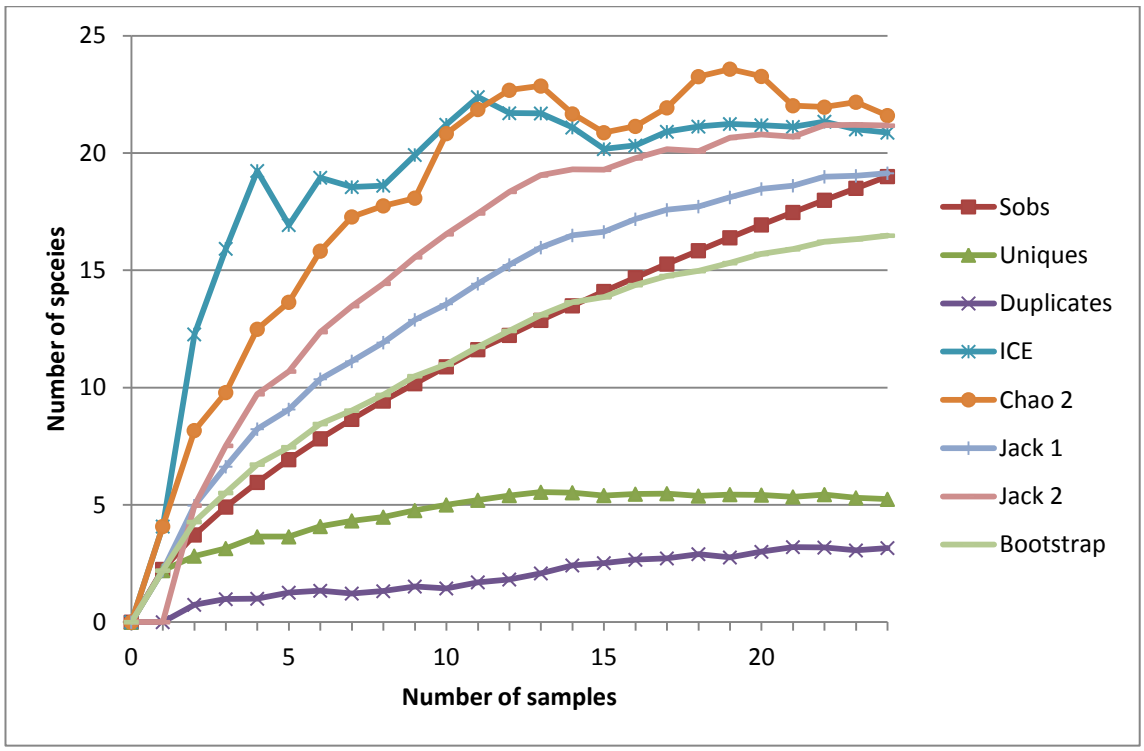

Fig. 4.17: Rarefaction curve and species richness estimators for biotope ao.

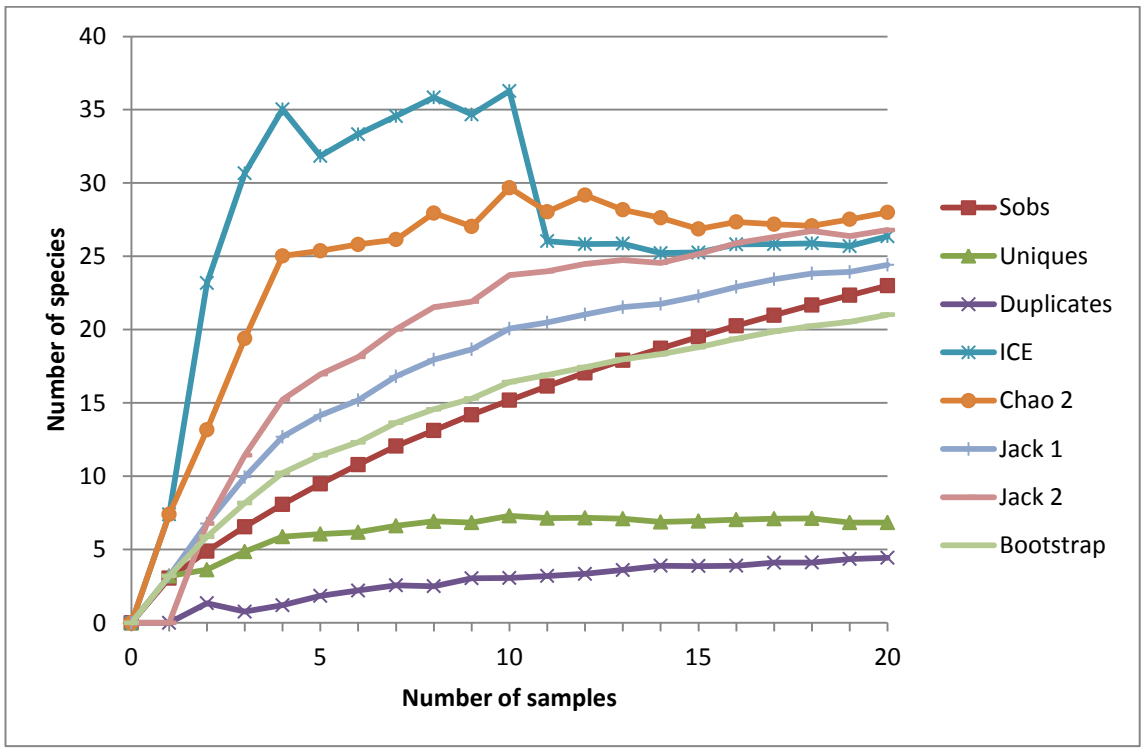

Fig. 4.18: Rarefaction curve and species richness estimators for biotope ap. Non crossover of unique and duplicate curves.

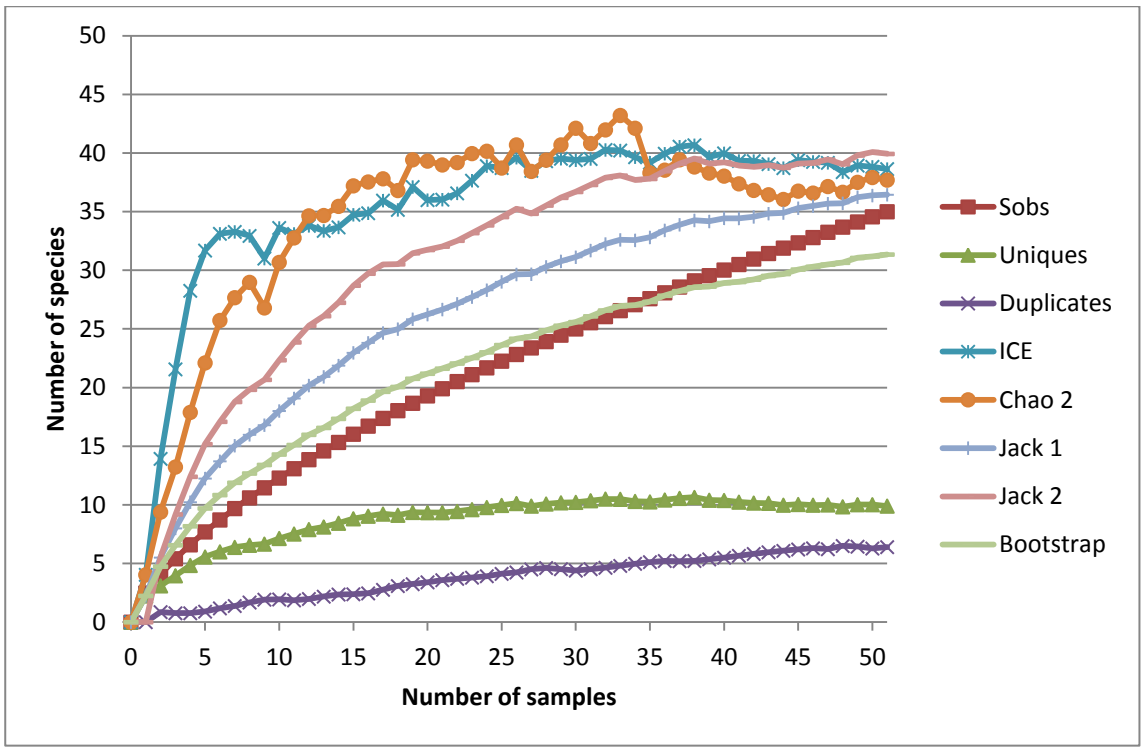

Fig. 4.19: Rarefaction curve and species richness estimators for biotope aq. The curves for the estimators begin to asymptote after *approx*. 40 samples, while the Sobs curve does not.

A4.4 Figures of estimated species richness results per biotope

Variability in species richness calculated by Sobs (interpolated from rarefaction curves) and species richness estimators for standardised numbers of samples (7). Individual graphs are per biotope r-aq, with estimated number of species on the y axis. Boxes represent standard deviation (SD), with the mean represented by the line in the centre of the box; for Sobs and Chao 2 whiskers represent 95% confidence intervals. Note that the lower 95% confidence interval for Chao 2 is not represented, as the SD was higher. The abbreviations denote Sobs (expected species richness), ICE (Incidence-based estimator), Jack 1 (Jackknife 1), Jack 2 (Jackknife 2) and Boot (Bootstrap). In general the Jack 1, Boot and Sobs had the lowest SD, with ICE, Chao 2 and Jack 2 having the highest.

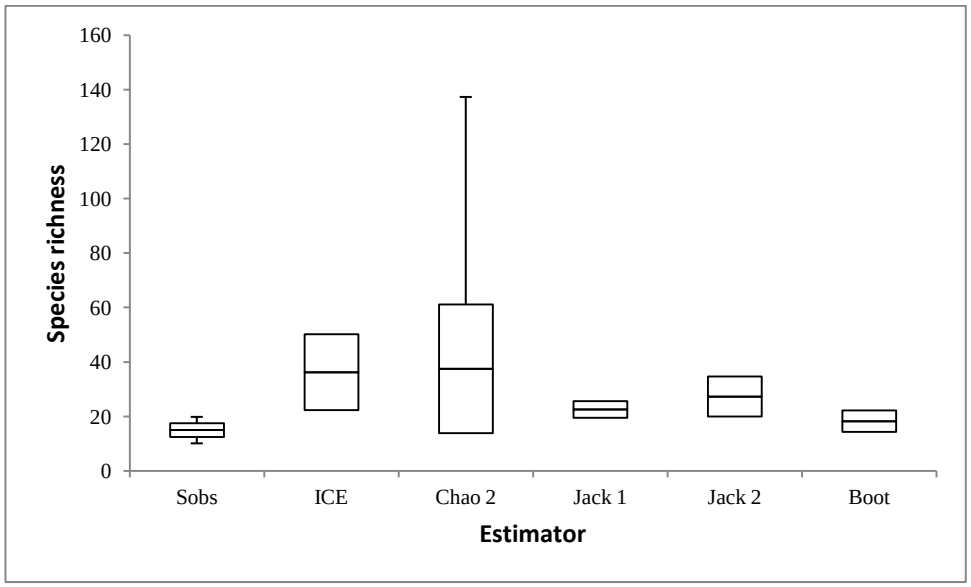

Fig. 4.20: Expected and estimated species richness of biotope ac from rarefaction curves and estimators. ICE and Chao2 estimate the highest species richness, although they also have the highest SD.

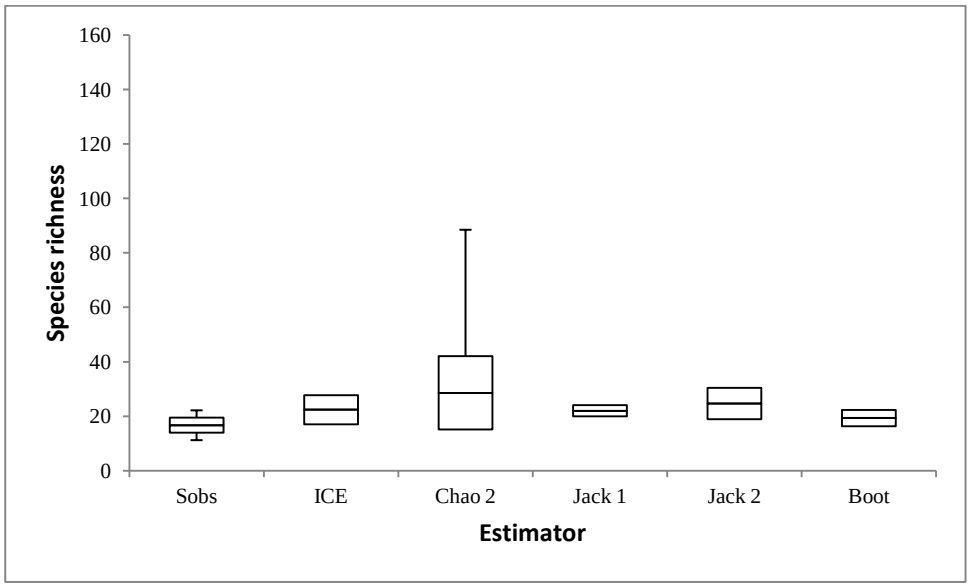

Fig. 4.21: Expected and estimated species richness of biotope ah from rarefaction curves and estimators. Chao2 and Jack 2 estimate the highest species richness, although they also have the highest SD.

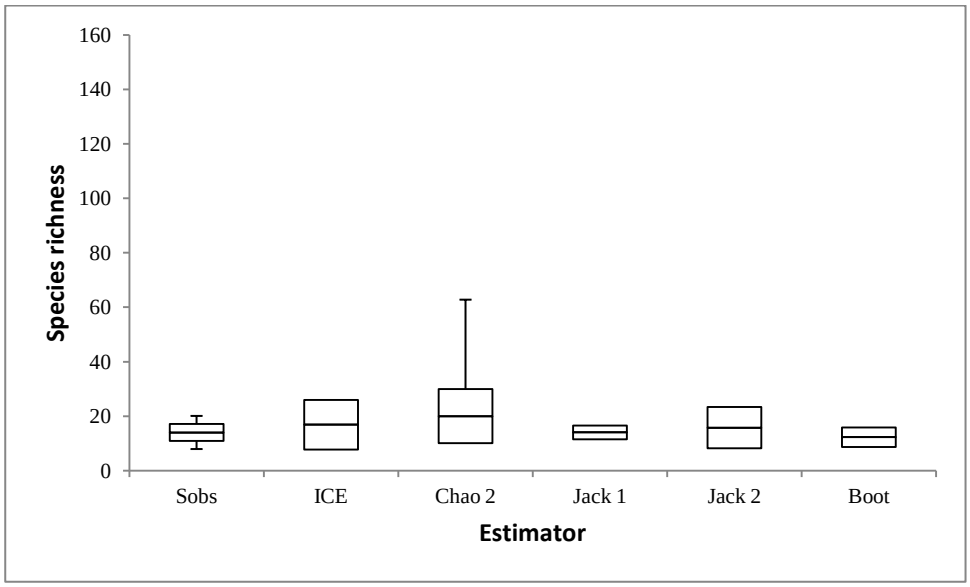

Fig. 4.22: Expected and estimated species richness of biotope aj from rarefaction curves and estimators. All estimators and Sobs results are similar, although Chao2 and Jack 2 have the highest SD.

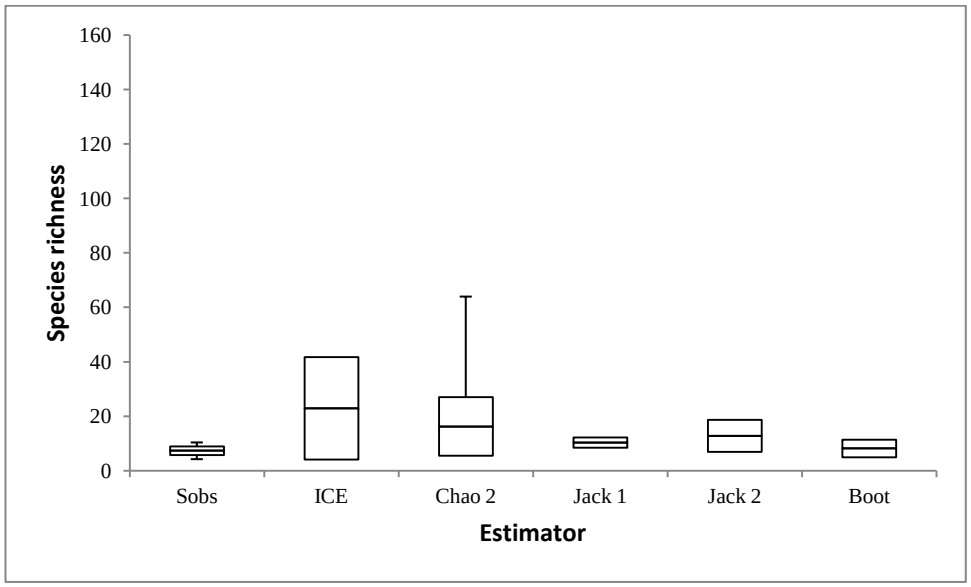

Fig. 4.23: Expected and estimated species richness of biotope al from rarefaction curves and estimators. ICE estimate the highest species richness, but with a large SD.

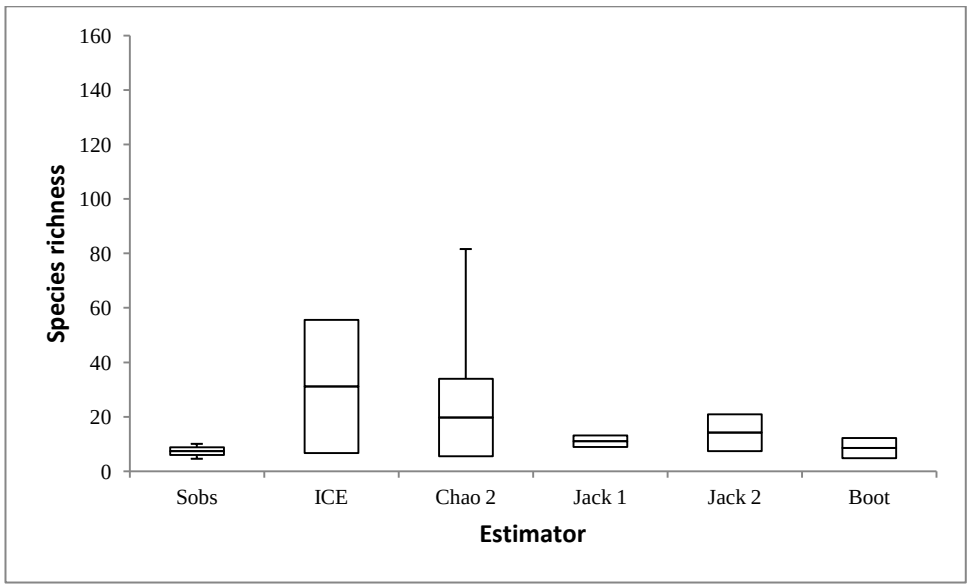

Fig 4.24: Expected and estimated species richness of biotope am from rarefaction curves and estimators. ICE estimates significantly higher species richness than Sobs, but with a large SD.

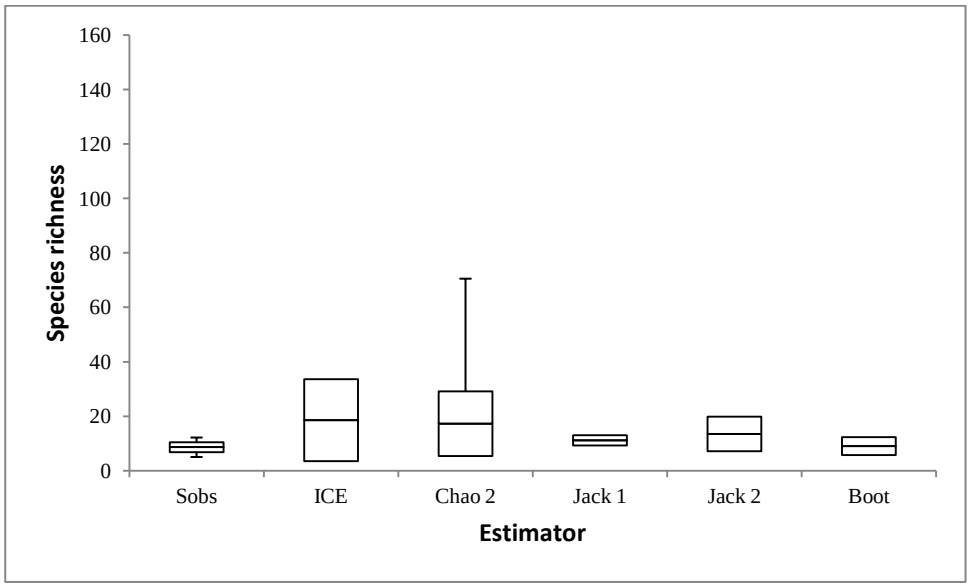

Fig. 4.25: Expected and estimated species richness of biotope ao from rarefaction curves and estimators. ICE, Chao 2 and Jack 2 estimate higher species richness than Sobs, but with a large SD.

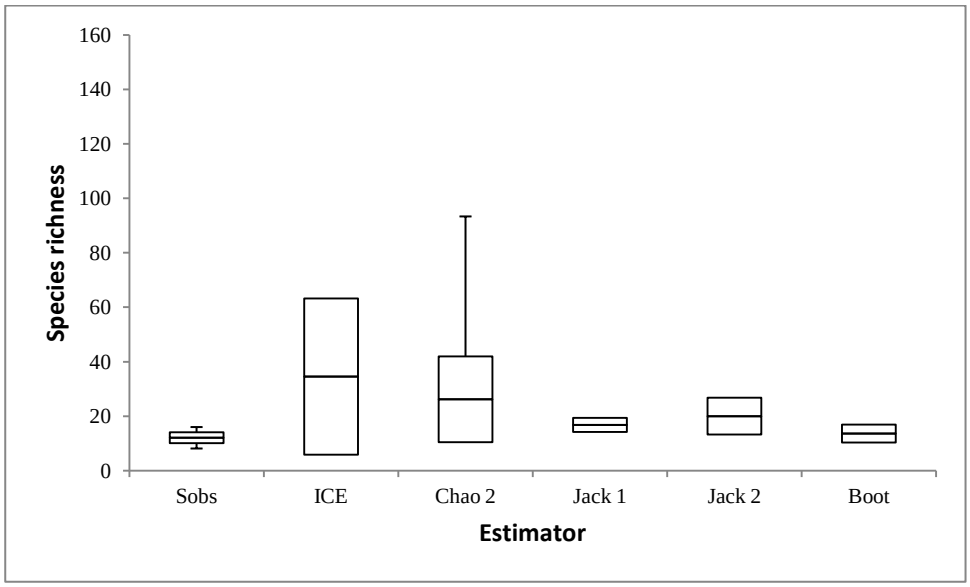

Fig. 4.26: Expected and estimated species richness of biotope ap from rarefaction curves and estimators. ICE and Chao 2 estimate higher species richness than Sobs, but with a large SD.

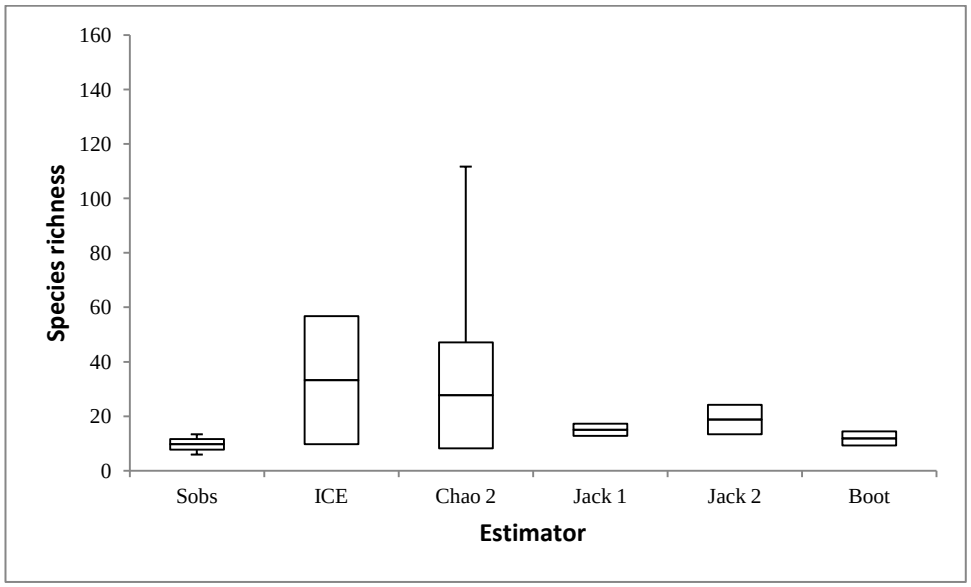

Fig. 4.27: Expected and estimated species richness of biotope aq from rarefaction curves and estimators. ICE and Chao 2 estimate higher species richness than Sobs, but with a large SD.

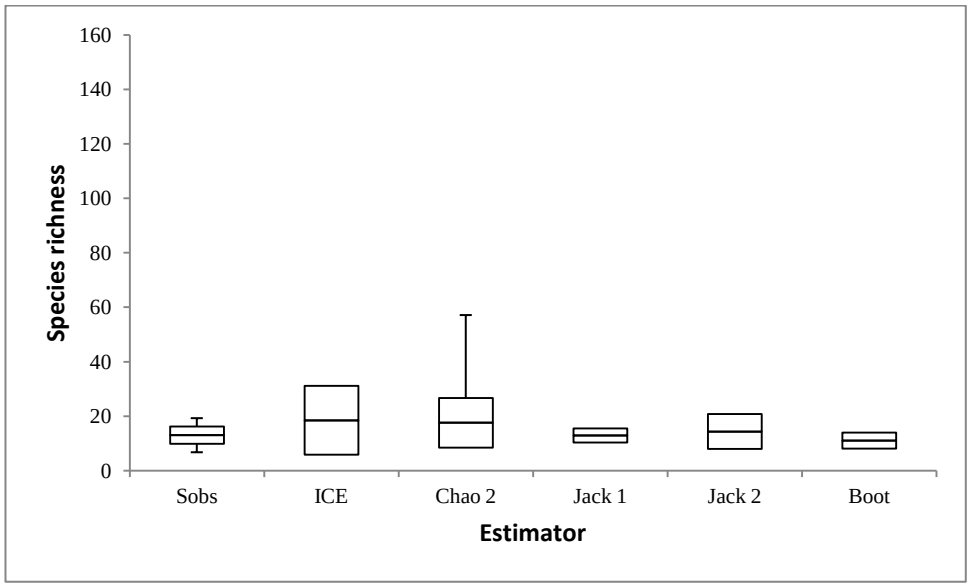

Fig. 4.28: Expected and estimated species richness of biotope r from rarefaction curves and estimators. All estimators estimate similar species richness to the expected richness, but ICE, Chao2 and Jack 2 with higher SD.

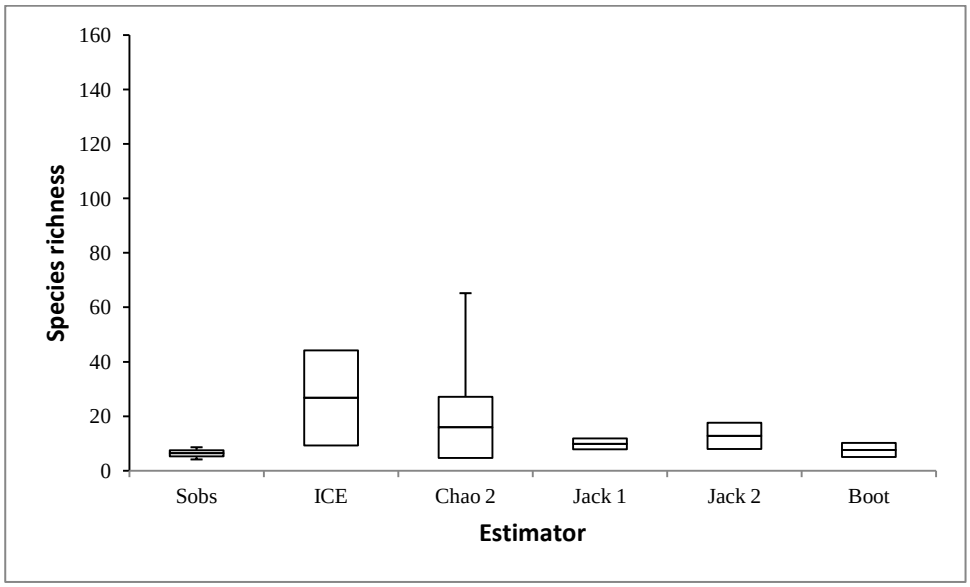

Fig. 4.29: Expected and estimated species richness of biotope x from rarefaction curves and estimators.

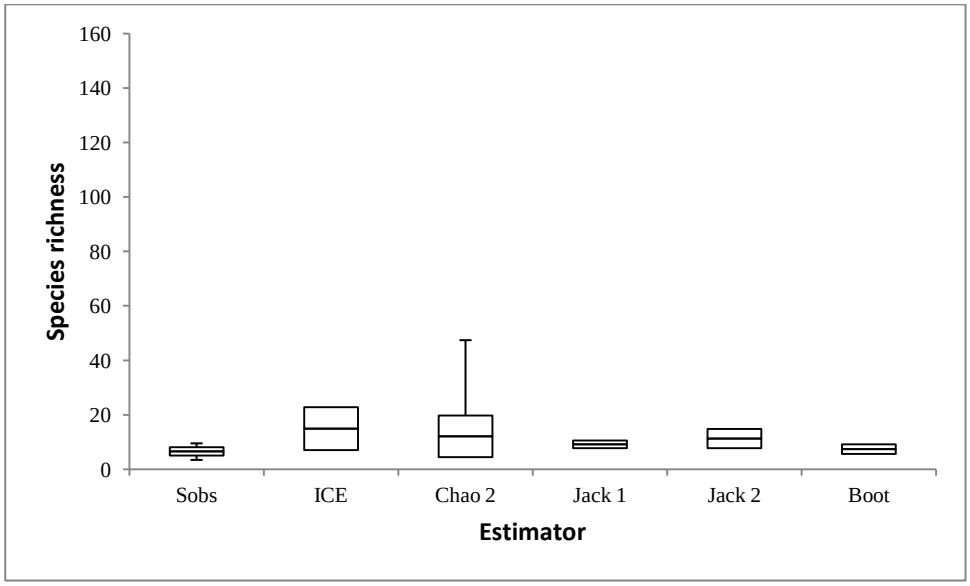

Fig. 4.30: Expected and estimated species richness of biotope y from rarefaction curves and estimators.

A4.5 Biotope descriptions for the SW Approaches

Biogenic reef

Lophelia pertusa reef

The biotope Lop.Mad, identified as cluster ah, had a similarity of 66.25% and was characterised by dead *Lophelia pertusa* framework, live *L. pertusa* and *Madrepora oculata*, small anemones (Actiniaria sp.13) and an unidentified species (Unknown sp.26; probably an annelid species) associated with *Lophelia*; halcampoid anemones (Halcampoididae sp.1) inhabited the inter-dispersed sediment patches in the reef. This biotope was observed on the crest of a prominent ridge (flute) on the northern flank of Explorer canyon over a depth and temperature range of 795-940 m and 9.41-9.92°C, respectively.

Predominantly dead low-lying coral framework

The biotope Lop.Hal, identified as cluster aj, had a similarity of 54% and was characterised by dead sediment clogged *L. pertusa* framework and halcampoid anemones (Halcampoididae sp.1), live *L. pertusa* and cerianthid species (Cerianthidae sp. 1). Inspection of image and video data revealed small live growths of *M. oculata* with associated ascidians, crinoids and the bamboo coral *Acanella* sp. to also be abundant species. Cerianthid anemones (Cerianthidae sp.1) dominated the soft sediment habitats between the coral framework. This assemblage was observed from both Dangaard and Explorer canyon on flute features (at the end of interfluves) and flank features over a depth range of 697-927 m and a temperature of 8.97-9.77°C.

Ophiuroids and *Munida sarsi* associated with coral rubble

The biotope Oph.Mun, identified as cluster ap, had a similarity of 41.38% and was observed from both the Explorer and Dangaard canyon over a depth range of 303-1017 m and a temperature of 7.98-11.5°C associated with the mini-mound features and incised channels. The coral rubble was dominated by the squat lobster *Munida sarsi*, and Ophiuroidea sp.5.

Sea pen and burrowing megafauna communities

Kophobelemnon stelliferum and cerianthids on mud/sand

The biotope Kop.Cer, identified as cluster y, had a similarity of 49.80% and was characterised by the pennatulid *Kophobelemnon stelliferum* and cerianthid anemone. Although not identified by SIMPER, mapping of the video highlighted the dominance of the large anemone Sagartiidae sp. 3 (cf. *Bolocera* sp.). This assemblage was observed associated with mud and muddy sand substratum primarily on the flanks of the three submarine canyons (one observation was made on an incised channel) over a depth and temperature of 463-1059 m and 8.87-10.85°C. Other conspicuous fauna identified from the video as characterising this assemblage were the pennatulid species *Halipteris* sp., the asteroid *Pseudarchaster* sp., the crinoid *Pentametrocrinus atlanticus*, the holothurian *Benthogone* sp. and cerianthid anemones.

Others

cf. Bathy*lasma* sp. and hydroid assemblage on bedrock

The biotope Bat.Hyd, identified as Cluster r, had a similarity of 25.07% and was characterised by the barnacle cf. *Bathylasma* sp. which dominated the bedrock and Hydrozoa (bushy). It was observed from a single tow on an incised channel in Explorer canyon at a depth of 902-912 m (temperature 8.99-9°C).

Amphiuridae ophiuroids and cerianthid anemones on bioturbated mud/sand

The biotope Amp.Cer, identified as cluster al, had a similarity of 53.22%. It was characterised by cerianthid anemones and was observed on the flank, canyon head and continental shelf features associated with mud and sand substratum in all three canyons over a water depth and temperature of 184-943 m and 9.59-11.69°C respectively.

Annelids, hydroids and cerianthids on bedrock ledges

The biotope Unk.Cer, identified as cluster ac, had a similarity of 47.47% and was characterised by an annelid species (Unknown sp.26) and cerianthid anemones. Observation of the video highlighted ophiuroid species as commonly associated with this assemblage, although not identified by SIMPER. This assemblage was associated with bedrock ledge features over a water depth 238-1070 m and a temperature of 8.36-11.51°C from the canyon head and incised channels in Explorer and Dangaard canyons.

Cerianthids on sediment draped bedrock

The biotope Cer, identified as cluster x, had a similarity of 54.39% and was characterised by cerianthid anemones. This assemblage was associated with amphitheatre rims, canyon flank, canyon head and incised channel features on bedrock with sand veneer in all three canyons over a depth of 360-1064 m (temperature 8.98-11.3°C).

Burrowing (*Amphiura* sp.) and surface dwelling ophiuroids on mud/sand

The biotope Oph, identified from video as cluster am, had a similarity of 47.39% and was characterised by the surface dwelling ophiuroid Ophiuroidea sp.1 and the burrowing ophiuroid *Amphiura* sp. (identified from video). The assemblage was observed in all three canyons from amphitheatre rims, canyon flank and tributary

gullies, and was associated with soft sediment (mud/sand) over a depth of 184-1094 m and temperature of 7.67-11.69°C.

Serpulids and brachiopods on mixed substratum

The biotope Ser.Bra, identified as cluster ao, had a similarity of 27.51% and was characterised by Serpulidae sp. 1, brachiopods (Brachiopoda sp.1) and the squat lobster *Munida sarsi*. It occurred on mixed substratum of cobbles and pebble size between 691-764 m (temperature 10.1-10.5°C) from the flank of Dangaard canyon.

Munida sarsi and *Leptometra celtica* on mixed substratum

The biotope Mun.Lep, identified as cluster aq, had a similarity of 31.11% and was characterised by the squat lobster *Munida sarsi* and the crinoid *Leptometra celtica*. It was associated with mixed substratum and biogenic gravel (shell hash) at a depth and temperature of 183-792 m and 9.79-11.79°C respectively. This biotope was recorded from the canyon head and interfluve features in all canyons.

A4.6 Biotope descriptions for non listed habitats defined from the SW Approaches

cf. *Bathylasma* sp. and hydroid assemblage on bedrock

The biotope Bat.Hyd, identified as cluster r, was characterised by barnacles (cf. *Bathylasma* sp.) and Hydrozoa (bushy) associated with steep bedrock outcrop towards the base of Explorer canyon at a depth of 902-912 m and a temperature of 8.99-9°C. Bat.Hyd assemblage was only observed for a short period during a single camera-transect.

Bathylasma is a widespread bathyal species in the NE Atlantic (Gage 1986). A number of assemblages have been described from the region; Pfannkuche *et al*. (2004) describe a *Bathylasma* cf. *hirsutum* assemblage associated with drop stones between 636-650m water depth on a prominent escarpment feature in the Belgica mound province; however, Gage (1986) describes a *Bathylasma hirsutum* assemblage with the brachiopod *Dallina septigera* and *Macandrevia cranium* from rocky, high current areas on the Wyville-Thomson Ridge and the summit of the Anton Dohrn Seamount in a water depth band ranging from 200-700 m. He also noted the remains of plates of *Bathylasma hirsutum* covering the substratum of the floor of a gorge between the Wyville-Thomson Ridge and Ymir ridge and suggested this species may cover the walls of this gorge. Howell *et al*. (2010b) describe an assemblage characterised by large barnacles (noted as possibly *Bathylasma hirsutum*) and brachiopods (noted as possibly *Dallina septigera*) on the summit of the Anton Dohrn Seamount at *approx*. 600 m water depth.

Amphiuridae ophiuroids and cerianthid anemones on bioturbated mud/sand

The biotope Amp.Cer, identified as cluster al, was characterised by occasional cerianthid anemones and amphiuridae sp.1 ophiuroids on bioturbated mud and sand and was observed throughout the canyons over a wide depth range of 184-943 m and temperature of 9.59-11.69°C associated with the canyon head, flanks and was also observed on from one transect on the continental shelf. Note, this assemblage has not been previously described from the deep sea.

Annelids, hydroids and cerianthids on bedrock ledges

The biotope Unk.Cer, identified as cluster ac, was characterised by cerianthid anemones, annelid worms and hydroid species associated with bedrock ledges. Ophiuroid species and the squat lobster *Munida sarsi* were also commonly observed. The biotope was observed from both Dangaard and Explorer canyons from the canyon head and incised channels (canyon floor) associated with bedrock ledges over a depth range of 238-1070 m and a temperature of 8.36-11.51°C. This kind of biotope has not been previously described in the deep sea.

Cerianthids on sediment draped bedrock

The biotope Cer, identified as cluster x, was characterised by cerianthid anemones associated with areas of bedrock covered with a sand veneer – thus preventing the attachment of fauna and acting as a soft sediment habitat. The assemblage was observed on wide range of geomorphological features including canyon head, flank, amphitheatre rims and incised channels. It was observed from the three canyons over a water depth and temperature range of 360-1064 m and 8.98-11.3°C, respectively. This assemblage has not been previously described from the deep sea. This assemblage has a similar distribution to the ‘Cerianthid anemones on bioturbated mud/sand’ biotope.

Burrowing (*Amphiura* sp.) and surface dwelling ophiuroids on mud/sand

The biotope Oph, identified as cluster am, was characterised by surface dwelling ophiuroids associated with soft sediment (mud-sand). Burrowing ophiuroids (*Amphiura* sp.) were also identified as being characteristic of this biotope from video observations. The assemblage was found on the flanks, incised channels and amphitheatre rims; and occurred in the three canyons at water depths of 184-1094 m and temperatures of 7.67-11.69°C. This assemblage has not been previously described from the deep sea.

Serpulids and brachiopods on mixed substratum

The biotope Ser.Bra, identified as cluster ao, was associated with cobble and pebble substratum with serpulid polychaetes (Serpulidae sp. 1) and brachiopods (Brachiopoda sp. 1) attached to the hard substratum and squat lobsters (*Munida sarsi*) associated with the surrounding soft sediment. The assemblage was observed only on the smooth flank of Dangaard canyon between 691-764 m and over a temperature range of 10.1-10.5°C.

The Ser.Bra assemblage is similar to that described by Howell *et al*. (2010b) as 'brachiopods on mixed substrate' which was widely observed between 266-803m water depth on a number of features in UK waters. Narayanaswamy *et al*. (2006) also reported a similar assemblage from Anton Dohrn Seamount, where abundant brachiopods were associated with coarse sediment on the seamount summit.

Munida sarsi and *Leptometra celtica* on mixed substratum

The biotope Mun.Lep, identified as cluster aq, was associated with mixed and biogenic gravel (shell hash) substratum on the canyon head and interfluves features from all three canyons. It occurred over a wide depth and temperature range (183-792 m; 9.79-11.79°C) and was characterised by the crinoid *Leptometra celtica*, the squat lobster

Munida sarsi. This assemblage occurred on the interfluves between the mini-mounds features and was also associated with tributary gullies.

Leptometra celtica were more abundant at the canyon heads and on the edge of the flanks, which suggests they are positioning themselves within optimal conditions for feeding. The occurrence of *Leptometra celtica* has been reported by a number of authors; Lavaleye *et al*. (2002) reported abundant crinoids at 190 m from the NW Iberian Margin and 200m from the Goban Spur, and Flach *et al*. (1998) found the crinoid to be the dominant fauna at a station at 208m water depth from the continental Shelf (Goban Spur).

A5.1 Correlation tests of terrain parameter

	BPI_B	BPI_F	Slope	Aspect	Rugosity	Depth
BPI_F	0.94569					
Slope	0.14373	0.12512				
Aspect	0.00507	0.01409	0.01441			
Rugosity	0.10851	0.11036	0.91248	-0.044		
Depth	-0.15115	-0.13896	-0.15751	0.04189	-0.15742	
Temperature	0.08420	0.08937	0.07237	-0.07752	0.09657	**-0.97412**

Table 5.6: Persons correlation test of terrain parameters of Anton Dohrn Seamount. Depth and temperature show the highest correlation with a p = 0.97. BPI_B denotes broad Bathymetric Positioning Index and BPI_F, fine scale Bathymetric Positioning Index.

	BPI_B	BPI_F	Slope	Aspect	Rugosity	Depth
BPI_F	0.92896					
Slope	0.09457	0.12629				
Aspect	-0.00951	-0.02813	-0.06899			
Rugosity	0.07554	0.10135	0.87324	-0.05234		
Depth	0.03749	0.00063	-0.50165	-0.18523	-0.36864	
Temperature	0.05025	0.01341	-0.47588	-0.10959	-0.34691	**0.95827**

Table 5.7: Persons correlation test of terrain parameters of the SW Approaches. Depth and temperature show the highest correlation with a p = 0.95. BPI_B denotes broad scale Bathymetric Positioning Index and BPI_F, fine scale Bathymetric Positioning Index.

A5.2 Results from dredge model selection for VMEs of Anton Dohrn Seamount and the SW Approaches

Anton Dohrn Seamount

Lop.Por biotope (Predominantly dead, low-lying coral framework with encrusting sponges)

Model	(Int)	B sub	MesG	Aspect	B BPI	Depth	Slope	Side	df	logLik	AICc	delta	weight
128	-96.700	+	+	+	+	+	+	+	23	-198.628	444.3	0.00	0.510
64	-139.000	+	+	+	+	+		+	22	-200.162	444.4	0.11	0.482

Lop.Mad biotope (*Lophelia pertusa* reef)

Model	(Int)	MegG	MesG	Aspect	Depth	F BPI	Slope	Side	df	logLik	AICc	delta	weight
121	-2.323e+			+	+	+	+		20	-0.112	41.6	0.00	0.317
125	-3.983e+03		+	+	+	+	+		21	0.000	43.3	1.72	0.134
249	-2.345e+03			+	+	+	+	+	21	-0.058	43.5	1.92	0.121
61	-3.187e+03		+	+	+	+			21	-0.428	43.6	2.07	0.113

Lop.Oph (Predominantly dead, low-lying coral framework)

Model	(Int)	B sub	MegG	MesG	Aspect	B BPI	Depth	Slope	Side	df	logLik	AICc	delta	weight
127	-130.100		+	+	+	+	+	+		17	-211.091	457.3	0.00	0.207
111	-128.800		+	+	+		+	+		15	-213.697	458.4	1.13	0.118
255	-159.300		+	+	+	+	+	+	+	18	-210.697	458.5	1.17	0.115
247	-146.200		+	+		+	+	+	+	17	-211.800	458.7	1.45	0.101
119	-142.200		+	+		+	+	+		16	-212.796	458.8	1.50	0.098
239	-149.900		+	+	+	+	+	+	+	16	-213.248	459.6	2.28	0.066
231	-145.700		+	+			+	+	+	15	-214.253	459.7	2.41	0.062
103	-143.200		+	+			+	+		14	-215.389	459.8	2.55	0.058

Gor.Lop biotope (Gorgonian dominated coral garden)

Model	(Int)	B_sub	MesG	Aspect	B BPI	Depth	Slope	Side	df	logLik	AICc	delta	weight
31	-9520		+	+	+	+			14	- 0.389	28.4	0.00	0.575
32	-10160		+	+	+	+		+	15	- 0.327	30.4	1.93	0.219
63	-6965		+	+	+	+	+		15	-0.946	31.3	2.86	0.138

Lep.Ker biotope (Coral garden with bamboo corals and antipatharians on bedrock)

Model	(Int)	B_sub	MegG	MesG	Aspect	B BPI	Depth	Slope	Side	df	logLik	AICc	delta	weight
253	-139.9000			+	+	+	+	+	+	19	-17.462	197.6	0.00	0.338
254	-124.6000	+		+	+	+	+	+	+	24	-79.614	197.8	0.23	0.302
255	-96.3600		+	+	+	+	+	+	+	20	-79.462	199.6	2.06	0.120
256	-96.1200	+	+	+	+	+	+	+	+	25	-74.614	199.9	2.30	0.107
126	-125.3000	+		+	+	+	+	+		23	-76.590	200.5	2.93	0.078

Syr.Oph biotope (Xenophyophores and ophiuroids on mixed substratum)

Model	(Int)	B_sub	MegG	MesG	B BPI	Depth	Slope	Side	df	logLik	AICc	delta	weight
128	16.990	+	+	+	+	+	+	+	21	-95.566	233.6	0.00	0.741
120	1.901	+	+	+		+	+	+	20	-97.764	236.0	2.35	0.229

Syr.Cer biotope (Xenophyophores and caryophyllids on gravelly sand and mixed substratum)

Model	(Int)	B_sub	MegG	MesG	B BPI	Curvature	Depth	Slope	Side	Aspect	df	logLik	AICc	delta	weight
504	-2.859e+02	+	+	+	+	+	+	+	+		24	-19.727	88.0	0.00	0.626
502	-1.980e+02	+		+	+	+	+	+	+		24	-20.034	89.1	1.11	0.3

SW Approaches

Kop.Cer biotope (*Kophobelemnon stelliferum* and cerianthid assemblage on mud/muddy sand)

Model	(Int)	B_sub	MegG	MesG	Aspect	B BPI	Depth	df	logLik	AICc	delta	weight
60	-138.8000	+	+		+	+	+	17	-252.501	539.9	0.00	0.413
58	-5.7250	+			+	+	+	13	-257.060	540.9	0.94	0.258
62	-122.1000	+		+	+	+	+	22	-247.873	541.1	1.12	0.236

Lop.Hal biotope (Predominantly dead low-lying coral Framework)

Model	(Int)	B_sub	MegG	MesG	Aspect	B BPI	Depth	Slope	df	logLik	AICc	delta	weight
120	-922.700	+	+	+		+	+	+	26	-5.831	64.1	0.00	0.679
128	-999.700	+	+	+	+	+	+	+	27	-5.552	65.7	1.61	0.303

Lop.Mad biotope (*Lophelia pertusa* reef)

Model	(Int)	B_sub	MegG	MesG	Aspect	B BPI	Depth	Slope	df	logLik	AICc	delta	weight
117	-2721.000			+		+	+	+	15	-0.005	30.3	0.00	0.444
61	-3465.000			+	+	+	+		16	-0.047	32.2	1.94	0.168
119	-4500.000			+		+	+	+	16	-0.005	32.3	2.06	0.159

Oph.Mun biotope (Ophiuroids and *Munida sarsi* associated with coral rubble)

Model	(Int)	B_sub	MegG	MesG	Depth	F BPI	df	logLik	AICc	delta	weight
26	-137.300	+			+	+	9	-26.073	70.3	0.00	0.264
14	-155.100	+		+	+		17	-18.419	71.4	1.09	0.153
6	-129.100	+	+				16	-19.505	71.5	1.20	0.145
18	-137.500	+				+	8	-28.130	72.4	2.08	0.093
30	-154.500	+		+	+	+	18	-18.246	73.1	2.81	0.065

Appendix A5.3 Results of significant variables identified from GAM of biotopes from the SW Approaches and Anton Dohrn Seamount.

Anton Dohrn Seamount

Gor.Lop

	edf	Ref.df	Chi.sq	p-value	
B BPI	2.986	3.000	57.86	1.68e-12	***
Depth	2.850	2.978	33.21	2.82e-07	***
Aspect	2.731	2.945	55.39	5.18e-12	***

Lep.Ker

	Estimate	Std. Error	z value	p-value	
Bedrock	-1.620e+00	5.938e-01	-2.728	0.00636	**

	edf	Ref.df	Chi.sq	p-value	
B BPI	2.859	2.981	24.894	1.59e-05	***
Slope	2.320	2.658	6.182	0.08043	.
Aspect	2.806	2.961	3.622	0.29933	
Depth	1.842	1.979	11.803	0.00266	**

Lop.Por

	Estimate	Std. Error	z value	p-value	
Side	-4.056e+00	6.654e-01	-6.096	1.09e-09	***

	edf	Ref.df	Chi.sq	p-value	
Aspect	2.251	2.646	14.94	0.00127	**
B BPI	2.442	2.772	34.99	8.74e-08	***
Depth	3.000	3.000	111.32	< 2e-16	***

Lop.Mad

	Estimate	Std. Error	z value	p-value	
Radial ridge	1.645e+02	4.980e+01	3.303	0.000958	***
Cliff-top mounds	1.704e+02	4.748e+01	3.588	0.000333	***

	edf	Ref.df	Chi.sq	p-value	
Aspect	2.999	3.000	16.12	0.00107	**
Depth	2.389	2.697	13.04	0.00334	**
F BPI	2.613	2.864	9.89	0.01731	*

Lop.Oph

	Estimate	Std. Error	z value	p-value
Flute	6.199e+00	1.537e+00	4.032	5.52e-05 ***
Radial ridge	3.765e+00	1.053e+00	3.576	0.000348 ***

	edf	Ref.df	Chi.sq	p-value
B BPI	1.836	2.263	3.766	0.1851
Depth	2.750	2.939	56.769	2.6e-12 ***
Aspect	1.000	1.000	4.355	0.0369 *

Syr.Cer

	Estimate	Std. Error	z value	p-value
Flank	5.343e+01	2.262e+01	2.362	0.01818 *
Side	4.396e+01	2.207e+01	1.992	0.04638 *
Gravelly sand	2.012e+01	3.778e+00	5.325	1.01e-07 ***

	edf	Ref.df	Chi.sq	p-value
Depth	2.973	2.999	35.64	8.92e-08 ***
B BPI	2.894	2.990	10.37	0.0155 *
Slope	1.000	1.000	16.44	5.02e-05 ***

Syr.Oph

	Estimate	Std. Error	z value	p-value
Sandy gravel	4.408e+00	1.077e+00	4.091	4.30e-05 ***
Gravel	1.484e+00	5.923e-01	2.505	0.0123 *
Side1	-3.710e+00	7.825e-01	-4.741	2.13e-06 ***

	edf	Ref.df	Chi.sq	p-value
B BPI	1.000	1.000	3.766	0.05231 .
Depth	2.898	2.992	43.636	1.78e-09 ***
Slope	1.000	1.000	10.385	0.00127 **

<u>SW Approaches</u>

Kop.Cer

	Estimate	Std. Error	z value	p-value
Mud	4.792e+00	7.118e-01	6.733	1.67e-11 ***
Sand	3.856e+00	7.035e-01	5.481	4.22e-08 ***

	edf	Ref.df	Chi.sq	p-value
Depth	2.282	2.611	65.983	1.54e-14 ***
B BPI	2.893	2.991	36.772	5.08e-08 ***
Aspect	1.000	1.000	9.785	0.00176 **

Lop.Hal

	edf	Ref.df	Chi.sq	p-value
Depth	2.924	2.993	8.833	3.1e-6 ***

Slope	2.731	2.942	12.513	5.49e-4 ***
B BPI	1.000	1.000	5.495	1.914-5 ***

Lop.Mad

	edf	Ref.df	Chi.sq	p-value
B BPI	1.919	1.993	17.82	0.000134 ***
Slope	1.891	1.988	11.92	0.002544 **
Depth	1.944	1.997	21.73	1.9e-05 ***

Oph.Mun

	Estimate	Std. Error	z value	p-value
Mini-mounds	1.0005361	0.0142395	70.265	<2e-16 ***

	edf	Ref.df	Chi.sq	p-value
F BPI	1.859	1.980	8.862	0.00116 **